CHALMERS
UNIVERSITY OF TECHNOLOGY

Performance and filtration characteristics of floccular and aerobic granular sludge using dynamic membrane filtration

Master's thesis in Infrastructure and Environmental Engineering

NILOUFAR TABESH

Department of Architecture and Civil Engineering
CHALMERS UNIVERSITY OF TECHNOLOGY
Gothenburg, Sweden 2016
Master's Thesis BOMX60-16-04

CHALMERS
UNIVERSITY OF TECHNOLOGY

Department of Civil and Environmental Engineering
Division of Water Environment Technology
CHALMERS UNIVERSITY OF TECHNOLOGY
Master's Thesis BOMX60-16-04
Gothenburg, Sweden 2016

MASTER THESIS BOMX60-16-04

Performance and filtration characteristics of floccular and aerobic granular sludge using dynamic membrane filtration

Niloufar Tabesh

Department of Architecture and Civil Engineering

Division of Water Environment Technology

CHLAMER UNIVERSITY OF TECHNOLOGY

Gothenburg, Sweden, 2018

Performance and filtration characteristics of floccular and aerobic granular sludge using dynamic membrane filtration

Master's Thesis BOMX60-16-04

Department of Architecture and Civil Engineering

Division of Water Environment Technology

SE-41296 Gothenburg

Telephone + 46 (0)31- 772 1000

Department of Architecture and Civil Engineering

Gothenburg, Sweden, 2018

Cover:

A microscopic image on emergence of semi-granulated sludge in Reactor 2

Performance and Filtration Characteristics of Floccular and Aerobic Granular Sludge Using Dynamic Membrane Filtration

Niloufar Tabesh

Department of Architecture and Civil Engineering

Division of Water Environment Technology, Chalmers University of Technology

Abstract

Three laboratory scale column shaped sequencing batch reactors (SBRs) fed with acetate as a sole organic carbon source, were operated with floccular sludge (R1 and R2) and granular sludge (R3) during two time periods. Performance of these reactors in removing organic matter and nutrients was investigated.

In the first period, R2 and R3 were in operation for 295 and 162 days, respectively. In the second period, R1 and R3 were in operation for 108 and 43 days, respectively. The substrate loading rate ratios in the constructed feed stream were 20:3:1 for COD:N:P corresponding to concentrations of 757 mg/L, 112 mg/L and 38 mg/L for COD, N and P, respectively.

The acetate removal efficiency in all the reactors during both runs was above 99%. However, the average total nitrogen (TN) removal efficiency for R2 and R3 during the first run was 50% and 46 %. During the second run, the removal efficiency for R1 and R3 was 42% and 20%, respectively. The performance of all the reactors in removing phosphate was poor and except for R2 with 7%, the average measured phosphate removal efficiency for the other reactors was negative.

Filterability of three types of sludge suspension, floccular, semi-granular, and granular sludge was studied based on short membrane filtration tests on a 100 μm nylon mesh filter. The results showed that, the cake layer formed on the membrane surface was the main component of the total hydraulic resistance. Moreover, the cake layer resistance formed by floccular sludge and granular sludge had the highest and the lowest resistance, respectively.

Formation and performance of dynamic membrane as an alternative to conventional membrane filters were investigated by filtering the supernatant from the reactors operated during the first run.

The results from both reactors demonstrated the successful formation of dynamic membrane and also the sludge cake layer appeared to be a controlling resistance while pore blockage resistance was relatively small. However, dynamic membrane formed by granular sludge showed better performance in suspended solids rejection and it also provided permeate flux 1.5 times greater than that of floccular sludge.

Adsorption capacity of the cake layer formed by semi-granular and granular sludge was investigated by using kaolin suspension as a model compound. The findings showed that both sludge provided approximately the same permeate flux, however, the adsorption capacity of granular sludge was higher which leaded to almost two times higher removal efficiency than that of floccular sludge.

Key Words: wastewater treatment, granular sludge, floccular sludge, SBR, membrane filtration, dynamic membrane, cake layer resistance

Acknowledgement

First and foremost, deepest gratitude to my two supervisors, Britt-Marie Wilen and Oskar Modin, for being always patient and generous with their time, and whose guidance has made this master's thesis a rewarding experience. Without their help, fulfilment of this work was impossible

I would like to thank Mona Pålsson as the tests could have never been conducted without her supports.

My very special thanks to my family for their constant encouragement for quality education, perseverance and for constantly instilling in me motivation to carry on.

To my Reza, of course!

Table of Contents

Chapter 1 : Introduction **1**

1.1-Problem statement 1

1-2- Aim 3

1-3- Structure of the thesis 3

Chapter 2 : Literature review **5**

a) Biological wastewater treatment and the application of aerobic granulation ..... **Error! Bookmark not defined.**

2a.1.Wastewater treatment methods 5

2a.1.1. Physical unit operations 5

2a.1.2. Chemical processes 5

2a.1.3. Biological processes 5

2a.2.Activated sludge process 9

2a.3. Sequencing batch reactors 10

2a.4. Aerobic granulation 12

b) Dynamic membrane Filtration 27

2b.1.Definition of Filtration 27

2b.2. Membrane filtration process 27

2b.3. Membrane materials, modules and operation's modes 30

2b.4.Membrane bioreactors 33

2b.5. Mesh filters 35

2b.6.Dynamic membrane 36

2b.7.Membrane resistance 44

Chapter 3 : Materials and methods **47**

a) Materials and methodology 47

3a.1. Reactors setup 47

3a.2. Feed condition 49

3a.3. Experiments time schedule 51

3a.4. Cycle time 53

3a.5. Sludge wasting 55

3a.6. Granular sludge formation 55

3a.7. Analytical methods 56

3b. Membrane filtration 58

3b.1 Experimental setup 58

3b.2 Experiments 61
3b.3. Hydraulic Resistance Analysis 67
Chapter 4 : Results and Discussion 73
a) Aerobic granulation 73
4a.1. First run 73
4a.1.1. Sludge analysis 78
4a.1.2. Supernatant (effluent) analysis 82
4a.2. Second run 96
4a.2.1. Sludge analysis 98
4a.2.2. Supernatant (effluent) analysis 101
4a.3. pH records 113
b) Membrane filtration 115
4b.1. Cake layer resistance 115
4b.1.1. Floccular sludge 115
4b.1.2. Granular sludge 126
4b.2. Dynamic membrane formation 135
4b.2.1. Filtration of the supernatant from R2 (Floccular sludge) 135
4b.2.2. Filtration of the supernatant from R3 (granular sludge) 136
4b.3. Adsorption capacity 137
4b.3.1. Kaolin suspension 138
4b.3.2. Kaolin suspension and cake layer from R2 and R3 139
Chapter 5 : Conclusions 141
5.1. Aerobic granulation technology 141
5.2. Dynamic membrane technology 142
5.3. Future Works 142
Chapter 6 References 144
Chapter 7 : Attachments 153
7-1. Appendix I- Settling time alteration 153
7-2. Appendix II- Cycle studies 154
7-3. Appendix III- TMP vs flux records of floccular sludge (R2), first trial 156
7-4. Appendix IV- TMP vs flux records of floccular sludge (R2), second trial 159
7-5. Appendix V- TMP vs flux records of floccular sludge(R2), not promising results 163
7-6. Appendix VI- TMP vs flux records of granular sludge (R3), first trial 164
7-7. Appendix VII- TMP vs flux records of granular sludge (R3), second trial 169
7-8. Appendix VIII- Dynamic membrane development for supernatant from R2 171
7-9. Appendix IX- Dynamic membrane development for supernatant from R3 173

List of Tables

Table 2-1. Classes of membrane filtration processes 28
Table 3-1. Physical properties of the reactors 49
Table 3-2. Organic source recipe 50
Table 3-3 Nitrogen and phosphorous source recipe 50
Table 3-4. Trace elements source recipe 50
Table 3-5. Composition of the microelements solution 51
Table 3-6. Targeted load and theoretical concentration for the substrates in the influent 51
Table 3-7. Detailed information for the first run 52
Table 3-8. Detailed information for the second run 52
Table 3-9. Detailed information about the seed sludge 53
Table 3-10. Membrane's specifications 61
Table 3-11. Time Schedule of the cake layer resistance measurement 63
Table 3-12. An example of TMP and flux measurements to obtain membrane intrinsic resistance 69
Table 3-13. An example of TMP and flux measurements to obtain cake layer resistance 70
Table 3-14. An example of TMP and flux measurements to obtain pore blockage resistance ... 71
Table 4-1. Overall reactors' performance 113
Table 4-2. Total and cake layer resistance of the sludge from R2, first trial 119
Table 4-3. Total and cake layer resistance of the sludge from R2, second trial 124
Table 4-4. Total and cake layer resistance of the sludge R3, first trial 130
Table 4-5. Total and cake layer resistance of the sludge R3, second trial 134
Table 4-6. Filtration of supernatant from floccular sludge, R2 135
Table 4-7. Filtration of supernatant from granular sludge, R3 136
Table 4-8. Kaolin concentration vs absorbance at 400nm 138
Table 7-1. Settling time alteration plan for R3 in the first run 153
Table 7-2. Settling time alteration plan for R3 in the second run 153
Table 7-3. TMP and flux for clean membrane 156
Table 7-4. TMP and flux for 10 mL (60.48 mg) of sludge R2 156
Table 7-5. TMP and flux for 25 mL (151.2 mg) of sludge R2 157
Table 7-6. TMP and flux for 40 mL (242 mg) of sludge R2 157
Table 7-7. TMP and flux for 75 mL (573 mg) of sludge R2 with suction pump and pressure gauge 157
Table 7-8. TMP and flux for 100 mL (725 mg) of sludge R2 with suction pump and pressure gauge 158
Table 7-9. TMP and flux for 150 mL (942 mg) of sludge R2 with suction pump and pressure gauge 158
Table 7-10. TMP and flux for 300 mL of sludge R2 with suction pump and pressure gauge .. 159
Table 7-11. TMP and flux for measuring membrane intrinsic resistance 159
Table 7-12. TMP and flux for 20 mL (232 mg) of sludge R2 160
Table 7-13. TMP and flux for 40 mL (464 mg) of sludge R2 160
Table 7-14. TMP and flux for 75 mL (812 mg) of sludge R2 160

Table 7-15. TMP and flux for 100 mL (1160 mg) of sludge R2 160
Table 7-16. TMP and flux for 150 mL (1740 mg) of sludge R2 161
Table 7-17. TMP and flux for 200 mL (2320 mg) of sludge R2 161
Table 7-18. TMP and flux for 240 mL (2784 mg) of sludge R2 161
Table 7-19. TMP and flux for 300mL (3480 mg) of sludge R2 162
Table 7-20. TMP and flux for 350 mL (4060 mg) of sludge R2 162
Table 7-21. TMP and flux for 450 mL (5160 mg) of sludge R2 162
Table 7-22. TMP and flux for 500 mL (5960 mg) of sludge R2 163
Table 7-23. TMP and flux for measuring membrane intrinsic resistance 163
Table 7-24. TMP and flux for 50 mL (174 mg) of sludge R2 163
Table 7-25. TMP and flux for 100 ml (348 mg) of sludge R2 164
Table 7-26. TMP and flux for 125 mL (425 mg) of sludge, R2 164
Table 7-27. TMP and flux for measuring membrane intrinsic resistance 164
Table 7-28. TMP and flux for 25 mL (122 mg) of sludge, R3 165
Table 7-29. TMP and flux for 250 mL (1220 mg) of sludge, R3 165
Table 7-30. TMP and flux for 290 mL (1415 mg) of sludge, R3 165
Table 7-31. TMP and flux for 450 mL (2200 mg) of sludge, R3 166
Table 7-32. TMP and flux for 520 mL (2538 mg) of sludge, R3 166
Table 7-33. TMP and flux for 600 mL (2928 mg) of sludge, R3 166
Table 7-34. TMP and flux for 700 mL (3416 mg) of sludge, R3 167
Table 7-35. TMP and flux for 800 mL (3904 mg) of sludge, R3 168
Table 7-36. TMP and flux for 1000 mL (4880 mg) of sludge, R3 168
Table 7-37. TMP and flux for measuring membrane intrinsic resistance 169
Table 7-38. TMP and flux for 25 mL (73 mg) of sludge, R3 169
Table 7-39. TMP and flux for 250 mL (730 mg) of sludge, R3 170
Table 7-40. TMP and flux for 350 mL (1022 mg) of sludge, R3 170
Table 7-41. TMP and flux for 450 mL (1314 mg) of sludge, R3 170
Table 7-42. TMP and flux for 550 mL (1606 mg) of sludge, R3 170
Table 7-43. TMP and flux for 650 mL (1900 mg) of sludge, R3 171
Table 7-44. TMP and flux for measuring membrane intrinsic resistance 171
Table 7-45. Filtration of supernatant from R2, first trial May 20th 171
Table 7-46. Experiment's specifications, first trial May 20th 172
Table 7-47. Filtration of supernatant from R2, second trial May 24th 172
Table 7-48. Experiment's specifications, second trial May 24th 172
Table 7-49. Filtration of supernatant from R2, third trial May 30th 172
Table 7-50. Filtration of supernatant from R3, first trial, May 11th 173
Table 7-51. Experiment's specifications, first trial, May 11th 174
Table 7-52. Filtration of supernatant from R3, second trial, May 13th 174
Table 7-53. Experiment's specifications, second trial, May 13th 175
Table 7-54. Filtration of supernatant from R3, third trial, May 17th 175
Table 7-55. Experiment's specifications, third trial, May 17th 176
Table 7-56. TMP and flux for measuring membrane intrinsic resistance, fourth trial, June 3rd 176
Table 7-57. Filtration of supernatant from R3, fourth trial, June 3rd 176
Table 7-58. Experiment's specifications, fourth trial, June 3rd 177
Table 7-59. Filtration of supernatant from R3, fifth trial, June 7th 177

Table 7-60. Experiment's specifications, fifth trial, June 7th 178

Figure 2-1.Concentration profile of BOD and phosphorus during biological phosphorus removal 9
Figure 2-2. One Cycle Profile. 12
Figure 2-3. Aerobic granular sludge 14
Figure 2-4. Microbial Structure of A) sludge floc and B) aerobic granule 15
Figure 2-5. Image analysis of aerobic granules, a) glucose fed, b) acetate fed 19
Figure 2-6. Structure of aerobic granules formed at different feeding pattern, aerated fill from left to right, 0%, 33% and 66% 22
Figure 2-7. Granules structure at. (a) 20 min (b) 15 min (c) 10 min (d) 5 min settling time 24
Figure 2-8. Hierarchy of pressure driven membrane processes 29
Figure 2-9. Schematic figure of different filtration modes 32
Figure 2-10. MBRs: a) submerged b) side-stream 34
Figure 2-11. Dynamic Membrane 37
Figure 3-1. Schematic view of the system's layout 48
Figure 3-2. Schematic view of the reactors 49
Figure 3-3. Seed sludge from Hammargården WWTP 53
Figure 3-4. One cycle profile of R1 and R2 (floccular sludge) 54
Figure 3-5. One cycle profile of R3 (granular sludge) 54
Figure 3-6. Filtration set-up 59
Figure 3-7. Physical Characteristics of the filter column 60
Figure 3-8. Methodology for measuring cake layer resistance of the sludge in R2 and R3 63
Figure 3-9. Methodology to develop dynamic membrane using effluent from R2 and R3 64
Figure 3-10. Kaolin adsorption measurement test: Step 1 65
Figure 3-11. Kaolin adsorption measurement test: Step 2 65
Figure 3-12. Kaolin suspension (in the filter column) and the installations 66
Figure 3-13. TMP vs flux using clean membrane and tap water 69
Figure 3-14. TMP vs Flux using tap water and sludge layer developed on top of the membrane 70
Figure 3-15. An example of pore blockage resistance using a water rinsed membrane and tap water 71
Figure 4-1. From left to right: 1 day and 10 days after inoculation 74
Figure 4-2. Microscopic image of the seed sludge, first run 75
Figure 4-3. Fluffy surface granules, 90 days from inoculation 75
Figure 4-4. Settling time for R2 and R3 during the first 21 days of operation 76
Figure 4-5. Microscopic image after 14 days from the inoculation for R2 (left) and R3 (right) 76
Figure 4-6. Microscopic image after 21 days from the inoculation. R3 77
Figure 4-7. Microscopic image from R2 after 115 days from the inoculation 77
Figure 4-8. Microscopic image from R2 after 132 days from inoculation 78
Figure 4-9. MLSS and MLVSS concentration in R2 79
Figure 4-10. Change of MLVSS/MLSS ratio for R2 79
Figure 4-11. MLSS and MLVSS concentration in R3 80

Figure 4-12. Changes of MLVSS/MLSS ratio in R3 80
Figure 4-13. TSS and VSS of the supernatant from R2 83
Figure 4-14. VSS/TSS ratio for the supernatant from R2 83
Figure 4-15. TSS and VSS of the supernatant from R3 84
Figure 4-16. VSS/TSS ratio for the supernatant from R3 84
Figure 4-17. DOC concentration in the effluent from R2 86
Figure 4-18. DOC removal efficiency for R2 86
Figure 4-19. Acetate removal efficiency 87
Figure 4-20. DOC concentration in the effluent from R3 87
Figure 4-21. DOC removal efficiency for R3 88
Figure 4-22. Acetate removal efficiency for R3 88
Figure 4-23. Ammonium, nitrate and nitrite concentration in the effluent from R2 89
Figure 4-24. Total nitrogen removal efficiency for R2 90
Figure 4-25. Ammonium, nitrate and nitrite concentration in the effluent from R3 90
Figure 4-26. Total nitrogen removal efficiency for R3 91
Figure 4-27. Phosphate removal efficiency for R2 92
Figure 4-28. Phosphate removal efficiency for R3 93
Figure 4-29. Cycle analysis for R2 (aeration was started at 60' and turned off at 3h23') 94
Figure 4-30. Cycle analysis for R3 (aeration was started at 60' and turned off at 3h51') 95
Figure 4-31. Changes of settling time for R1 and R3 during the first 19 days of operation 97
Figure 4-32. Microscopic image of R1 after 21 days from inoculation 97
Figure 4-33. Microscopic image from R3 after 7 days from inoculation 98
Figure 4-34. Microscopic image from R3 after 15 days (left) and 21 days (right) from inoculation 98
Figure 4-35. MLSS and MLVSS concentration in R1 99
Figure 4-36. Changes of MLVSS/MLSS ratio for R1 99
Figure 4-37. MLSS and MLVSS concentration in R3 100
Figure 4-38. Changes of MLVSS/MLSS ratio for R3 100
Figure 4-39. TSS and VSS of the supernatant from R1 102
Figure 4-40. TSS and VSS of the supernatant from R3 102
Figure 4-41. VSS/TSS ratio for the supernatant from R1 103
Figure 4-42. VSS/TSS ratio for the supernatant from R3 103
Figure 4-43. DOC concentration in the effluent from R1 104
Figure 4-44. Acetate removal efficiency for R1 105
Figure 4-45. DOC concentration in the effluent from R3 105
Figure 4-46. Acetate removal efficiency for R3 106
Figure 4-47. Ammonium, nitrite and nitrate concentration in the effluent from R3 107
Figure 4-48. Total nitrogen removal efficiency for R3 107
Figure 4-49. Ammonium, nitrite and nitrate concentration in the effluent from R1 108
Figure 4-50. Total nitrogen removal efficiency for R1 108
Figure 4-51. Phosphate removal efficiency for R1 110
Figure 4-52. Phosphate Removal efficiency for R3 110
Figure 4-53. cycle study for R1(aeration was started at 60' and turned off at 3h23') 111
Figure 4-54. cycle analysis for R3 (aeration was started at 60' and turned off at 3h51') 112
Figure 4-55. A 9-day pH recording in June 2016 ..... **Error! Bookmark not defined.**
Figure 4-56. A one cycle pH recordings 114

Figure 4-57. TMP vs Flux for clean membrane and for different amount for sludge from R2 (first trial'9 118
Figure 4-58. Cake layer resistance for sludge per square meter of the membrane for R2 at first trail 119
Figure 4-59. TMP vs Flux for clean membrane and for different amount of sludge from R2 (second trial)..... 124
Figure 4-60. Cake layer resistance for sludge from R2 per square meter of the membrane (second trial)..... 125
Figure 4-61. TMP vs Flux for clean membrane and for different amount of sludge from R3 (first trial)..... 130
Figure 4-62. Cake layer resistance for sludge from R3 per square meter of the membrane (first trial)..... 131
Figure 4-63. TMP vs flux for different cake layer amount for sludge from R3, second trial ... 134
Figure 4-64. Filtration characteristics of the Supernatant from R2..... 136
Figure 4-65. Filtration characteristics of supernatant from R3 137
Figure 4-66. Calibration curve for kaolin suspension at 400 nm 138
Figure 4-67. Removal efficiency of kaolin suspension through clean membrane 139
Figure 4-68. Kaolin removal efficiencies with cake layer from R3..... 140
Figure 4-69. Kaolin removal efficiencies with cake layer from R2 140
Figure 7-1. Cycle study for R2 during the first run..... 154
Figure 7-2. Cycle study for R3 during the first run..... 155
Figure 7-3. Cycle study for R1 during the second run (aeration was started at 60' and turned off at 3h23')..... 155
Figure 7-4. Cycle study for R3 during the second run 156

TERMINOLOGY AND ABBREVIATIONS

Symbols

°C	Degree Celsius
μ(Pa.s)	Dynamic Viscosity of Water
mg/L	Milligram per litre
m^2	meter squared
m^3	meter cubic
L	Litre
m^3/s	Cubic meter per second
kPa	kilo Pascale
mL	millilitre
ρ	Density of Water
$kg/(m^3.d)$	Kilogram per cubic metre per day

Nomenclature

AOB	Ammonia-oxidizing bacteria
BOD (mg/L)	Biological oxygen demand, Measurement for organic matter
BSCOD (mg/L)	Biodegradable soluble chemical oxygen demand
COD (mg/L)	Chemical oxygen demand, Measurement for organic matter
DO	Dissolved oxygen
DOC (mg/L)	Dissolved Organic Carbon
EPS	Extracellular Polymeric Substance
LMH	Litre per square meter per hour
MBRs	Membrane Bioreactors
MLSS	Mixed Liquor Suspended Solids
MLVSS	Mixed Liquor Volatile Suspended Solids

N	Nitrogen
NOB	Nitrite-oxidizing Bacteria
OLR	Organic Loading Rate
P	Phosphorous
PAOs	Phosphate Accumulating Organisms
PHAs	Polyhydroxyalkanoates
Rb (m^{-1})	Pore blockage resistance
Rc (m^{-1})	Cake layer resistance
Rm (m^{-1})	membrane intrinsic resistance
Rt (m^{-1})	membrane total resistance
SBRs	Sequencing Batch Reactors
SEM	Scanning Electron Microscopy
SFDM	Self-Forming Dynamic Membrane
SND	Simultaneous Nitrification Denitrification
TMP (Pa)	Transmembrane pressure
TN (mg/L)	Total Nitrogen
TOC (mg/L)	Total Organic Carbon
TS (mg/L)	Total Solids
TSS (mg/L)	Total Suspended Solids
VFAs	Volatile Fatty Acids
VSS	Volatile Suspended Solids
WWTPs	Wastewater Treatment Plants

Chapter1: Introduction

1.1-Problem statement

Liquid and solid wastes production are inevitable in every community. Wastewater is liquid or water carried waste discharged by domestic residences, commercial properties, industrial and agricultural activities which is often combined with surface runoff, ground water and stormwater, hence it carries different type of contaminations (Tchobanoglous, et al., 2004).Once this polluted water is discharged to the environment without proper treatment, it makes nuisance to the environment. Moreover, wastewater contains pathogenic microorganisms which cause severe health problems (Tchobanoglous, et al., 2004). Thus, appropriate selection of treatment methods and processes is required to avoid possible risks to the environment and public health. To date, there are numerous methods to treat wastewater to different degrees and with respect to standards, regulations, and economic budget.

The conventional activated sludge process is an old method of treating domestic wastewater and is still very common in wastewater treatment plants (WWTPs) (Tchobanoglous, et al., 2004). Despite various optimizations and new configurations, this technology is still very energy demanding and many WWTPs are struggling with various sludge-water separation challenges and operational problems such as: slow settling sludge, poor microbial flocculation, low maximum hydraulic load to secondary clarifiers and high space requirement for clarifiers (Tchobanoglous, et al., 2004; de Bruin, et al., 2004; Persson, 2015).

Aerobic granular sludge is a novel and promising technology introduced recently as a modification to conventional activated sludge (de Bruin, et al., 2004). Aerobic granule is a class of microbial aggregation with dense and strong structure which favours high biomass concentration in the reactor, excellent settling properties and good ability to withstand high organic load and shock loadings (Li, et al., 2014). Possibility to design

compact systems with higher loading rate and lower operational and construction costs have made this system superior to conventional activated sludge (Li, et al., 2014). De Bruin et al., have shown that WWTPs operating with granular sludge have 25% lower footprint and 7-17% lower costs (de Bruin, et al., 2004). Comparing to conventional floccular sludge, aerobic granules have regular nearly round shape and more compact structure (Gao, et al., 2011). This technology is proved to be successfully achieved through sequencing batch reactors (SBRs) since they offer suitable environmental conditions such as periodic feast and famine condition for microorganisms to become densely packed (de Bruin, et al., 2004).

Increasingly stringent discharge and reuse requirements in many developed countries like Sweden, have forced WWTPs to use advanced treatment technologies.

Membrane filtration and specifically membrane bioreactors (MBRs) have emerged as significant innovations in advanced water/wastewater treatment and reclamation. They are suitable options for being coupled with other processes and/or upgrading the current WWTPs systems (Tchobanoglous, et al., 2004). Moreover, independency on requiring further additives or chemicals for producing high quality product, requiring less space and man labour have made these technologies even more attractive than the competing technologies (Basile, et al., 2015).

Implementation of membrane filtration and MBRs has been proved to be effective in removing residual constituents from treated wastewater. However, they were not widely embraced due to high membrane costs and energy demanding, prone to fouling and inadequate scientific knowledge about them (US EPA, 2005). Therefore, adaptation of these technologies with more cost effective membranes and comparable performance seems an attractive solution.

A very promising alternative for MBRs is dynamic membrane filtration which is the focus of the present research. Dynamic membrane filtration makes the use of a physical barrier usually of a cheap material as a support layer to form a secondary membrane on top of it by deposition of particles and feed stream contents (Ersahin, et al., 2012). Due to the benefits from using coarse and cheap material membranes, this technology is less costly and need less fouling control compared to conventional MBRs (Ersan & Erguder, 2014).

1-2- Aim

The main aim of this project is to compare the filtration properties of aerobic granular sludge and activated sludge cultivated in laboratory scale sequencing batch reactors. The objectives of the present work are as follows. First, planning, starting-up and running laboratory scale SBRs. Second, comparing the growth and performance of aerobic granular and floccular sludge (conventional activated sludge) in treating synthetic wastewater and finally, investigating the short-term filtration characteristics of the aforementioned sludge using a dynamic membrane filtration process. In order to accomplish these objectives, the following research questions should be answered.

1- What are the efficiencies of floccular sludge and aerobic granular sludge in removing organic matter, (COD), ammonium ($N\text{-}NH_4^+$), and phosphate (PO_4^{3-}) from the synthetic wastewater in SBRs?
2- What is the cake layer resistance of aerobic granular sludge and floccular sludge using 100 µm nylon mesh filter?
3- What is the cake layer resistance of the supernatant from floccular sludge and aerobic granular sludge reactors using 100 µm nylon mesh filter?
4- What is the adsorption capacity of the cake layer formed by floccular sludge and aerobic granular sludge using concentrated kaolin solution and 100 µm nylon mesh filter?

1-3- Structure of the thesis

This master thesis was carried out as a part of a research project running at the Department of Civil and Environmental Engineering, Division of Water Environment Technology at Chalmers University of Technology. The thesis is organized in monograph format and is prepared in 5 chapters. Chapter 2 outlines the existing literature for general understanding of the main topics of the thesis this and is divided in two sections. The first section, namely ‘a’ covers the fundamentals and a literature review about aerobic granules. The second section, namely ‘b’ covers the literature about the dynamic membrane filtration. Subsequently, the materials and methods used in this work are outlined in Chapter 3. This

chapter is constructed in two sections. Section ‘a’ covers the materials and methods in the reactors’ part while section ‘b’ covers the materials and methods in the dynamic membrane filtration part.

The results of the tests are pointed out and discussed in Chapter 4. This chapter is also structured in two parts. Part ‘a’ and part ‘b’ are dedicated to the main findings and results on the reactors and the dynamic membrane filtration parts, respectively. Finally, Chapter 5 brings the thesis to the conclusion and outlines directions for future research.

Chapter2: Literature review

General background information is gathered in this chapter and presented in two parts. Part ‘a’ covers background information on various wastewater treatment methods as well as aerobic granules. while, part ‘b’ deals with background information on dynamic membrane filtration.

a) Wastewater treatment and aerobic granules

2a.1.Wastewater treatment methods

2a.1.1. Physical unit operations

When the operations used to treat the wastewater are brought about by using naturally occurring forces, it is called physical unit operation (Tchobanoglous, et al., 2004). During physical treatment, the chemical composition of the substance in the wastewater does not change. Some of the most commonly used physical operation units in WWTPs are, barriers such as bar racks and screens, sedimentation, membrane filtration, and aeration (Tchobanoglous, et al., 2004).

2a.1.2. Chemical processes

Chemical processes are treatment processes or technologies utilizing chemical reactions to treat the wastewater. Some of the most common chemical processes are chemical coagulation, disinfection and ion exchange (Tchobanoglous, et al., 2004).

2a.1.3. Biological processes

In biological treatment processes, transforming or removing organic or inorganic (such as nutrients) constituents is done by a variety of microorganisms but principally bacteria (Tchobanoglous, et al., 2004). Microorganisms use organic pollutions as their food source and convert them to simple products such as H_2O and CO_2. Depending on the microbial metabolisms, biological processes are classified into aerobic, anaerobic, anoxic or combined processes. Conventional activated sludge and SBRs are two well-known examples of biological processes (Tchobanoglous, et al., 2004).

Brief explanation about basic principles behind biological nutrient removal are presented below as nutrient removal has been studied in this work.

2a.1.3.1. Biological nutrient removal from wastewater

The need for treatment of wastewater from nutrients is due to the potential environmental and health problems they may cause. DO concentration depletion, toxicity of aquatic life, and eutrophication of water bodies are some examples of adverse environmental effects caused by discharge of nutrient rich wastewater to the environment (Tchobanoglous, et al., 2004). Below, brief explanations about biological nitrogen and phosphorous removal are provided.

2a.1.3.1.1. Biological nitrification and denitrification

Nitrogen in the wastewater is mostly present in the form of ammonium and to remove it biologically several reactions and different types of bacteria are required (Tchobanoglous, et al., 2004). The biological method of removing nitrogen comprises of nitrification and denitrification (Tchobanoglous, et al., 2004). Nitrification is a two-step process in which ammonium (NH_4-N) is oxidized to nitrite, NO_2-N, and then from nitrite to nitrate, NO_3-N under aerobic condition (Tchobanoglous, et al., 2004). Ammonium oxidation to nitrite is done by ammonium oxidizing bacteria (AOB) and nitrite oxidation to nitrate is done by another group of bacteria, nitrite oxidizing bacteria (NOB) (Tchobanoglous, et al., 2004). Eqs (1) to (2) show the reactions during nitrification.

$$NH_4^+ + 1.5O_2 \rightarrow NO_2^- + H_2O + 2H^+ \qquad \text{Eq}(1)$$

$$NO_2^- + 0.5O_2 \rightarrow NO_3^- \qquad \text{Eq}(2)$$

In addition to oxygen, pH, un-ionized ammonia, metals and toxic materials, and alkalinity may affect the process (Tchobanoglous, et al., 2004). For instance, the nitrification rate at pH around 5.8 is almost 20% of its rate at pH 7 (Tchobanoglous, et al., 2004). The optimum pH for nitrification is reported in the range of 7.5-8.5 (Leong, et al., 2016). Ammonium oxidation is reported to be completely inhibited at 0.10 mg/L of copper, 0.25 mg/L of nickel and 0.25 mg/L of chromium (Tchobanoglous, et al., 2004).

During biological denitrification, nitrite and nitrate are oxidized to nitrogen gas under anoxic condition meaning that nitrite and nitrate act as electron acceptor instead of oxygen

(Tchobanoglous, et al., 2004). Eq. (3) shows the biological reactions during denitrification (Tchobanoglous, et al., 2004).

$$NO_3^- \rightarrow NO_2^- \rightarrow NO \rightarrow N_2O \rightarrow N_2 \qquad Eq(3)$$

During denitrification, alkalinity is produced and therefore, pH is generally elevated while during nitrification, the pH is decreasing (Tchobanoglous, et al., 2004).

WWTPs often use processes enabling simultaneous nitrification and denitrification (SND). Because nitrification and denitrification require different levels of oxygen and different chemical environments, only specific bacteria are capable to survive at these conditions. At SND, the bacteria strains do the denitrification and nitrification in flocs' interior and at the flocs' exterior respectively (Waltz, 2009). A well-known process which provides the appropriate environment for growth of bacteria capable of SND is sequencing batch reactors (SBRs) (Waltz, 2009).

2a.1.3.1.2. Biological phosphorous removal

Phosphorous is the key controlling nutrient in waterways and the main cause of eutrophication (over-nutrients enrichment) of the surface waters. It has been proved that a little anthropogenic addition of phosphorous can trigger algal growth (Tchobanoglous, et al., 2004; Sathasivan, n.d.). Excess growth of algae not only put the aquatic life into danger but also it causes an increase in disinfectant dosage in water treatment plants (Sathasivan, 2014). Therefore, appropriate removal of phosphorus from wastewater is necessary. Currently, there are two basic methods for removing phosphorous; chemical processes and biological processes (Tchobanoglous, et al., 2004). In contrast to nitrogen removal which is mostly accomplished by biological processes, the phosphorous removal is achieved mainly by chemical processes (Sathasivan, 2014). In general, the chemical process achieves higher phosphorous removal but, high sludge production, high chemical costs, and environmental concerns have shifted the tendency towards biological processes (Sathasivan, 2014).

Biological phosphorous removal is achieved by incorporating the phosphate into cell biomass, TSS, and subsequent removal of it from the system by sludge wasting. The basic principle underlying biological phosphorus removal is to encourage specific type of microorganism, Polyphosphate accumulating organisms (PAOs) to uptake the dissolved

phosphorus from the influent and store it as polyphosphate in their cells by subjecting them into cyclic aerobic/anaerobic and anoxic phase (Tchobanoglous, et al., 2004; Sathasivan, n.d.).

Under the anerobic phase, when the organic carbon source is high, PAOs use their polyphosphate and glycogen supplies to obtain energy to assimilate the fermentation of the easily biodegradable solubel organic carbon source (BSCOD) such as volatile fatty acids (VFAs). Then they store VFAs within their cells as polymeric carbon namely Polyhydroxyalkanoates (PHAs). The required energy for production of PHAs at this stage is brought about from degradation of prevoiusly stored inter-cellular glycogen and polyphosphate; thus, their glycogen and polyphospahte supplies decrease (Tchobanoglous, et al., 2004; Helness, 2007). Simoultaneouslly, PAOs decompose the stored intercelluar polyphosphate to simple orthophosphate and release them to the mixed liquor (Tchobanoglous, et al., 2004; Wisconsin Department of Natural Resources, 2009; Sathasivan, n.d.). As a result, the concentration of phosphorus in the mixed liquor increases.

During the aerobic phase, PAOs use PHA as a carbon and enery source for cell growth. Also they use a portion of the energy released in anaerobic phase together with orthophosphate from the mixed liquor to replenish their intercelluar polyphophate and glycogen supplies. Meanwhile orthophosphorus is taken up from the mixed liquor. In this phase, PAOs take up phosphate more than released during the anaerobic phase. Finally phosphate is removed from the system by sludge wasting (Lee, et al., 2001; Helness, 2007; Wisconsin Department of Natural Resources, 2009).

In Figure 0-1, the schematic concentration profile of BOD and phophorus during biological phosphorous removal is provided.

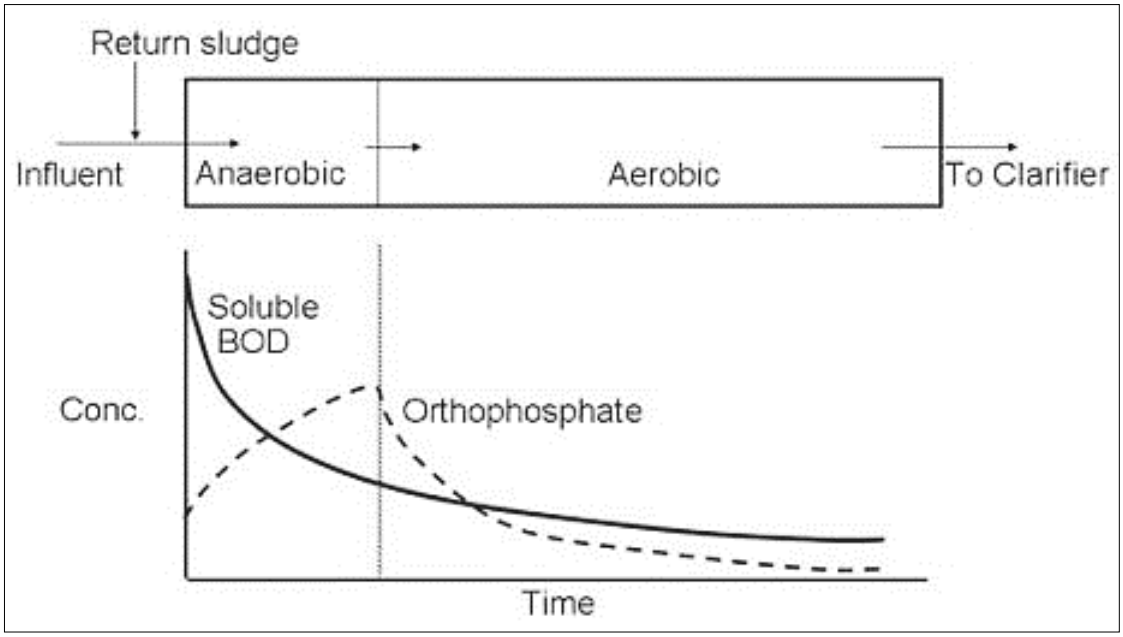

Figure 0-1.Concentration profile of BOD and phosphorus during biological phosphorus removal (Wisconsin Department of Natural Resources, 2009)

2a.2.Activated sludge process

Biological treatment technologies have been employed in WWTPs almost over a century. Among many different processes, activated sludge is the oldest and still the most dominating method (Tchobanoglous, et al., 2004). The very early and basic activated sludge process facility was constructed in 1914 to alleviate the smell, remove organic matter form the wastewater and to promote the aesthetic situation (Persson, 2015). A basic activated sludge process is comprised of the three following components: (1) An aerated basin in which microorganism which are responsible for treating wastewater are kept in suspension form; (2) a gravity sedimentation tank for liquid/solids separation; and (3) a recycling line to return a portion of the solids removed in sedimentation tank to the aerated basin. Since the returned sludge contains high density of active biomass and microorganisms, this process is called 'Activated sludge' (Stypka, 1998; Tchobanoglous, et al., 2004). The end products of the sedimentation tank are treated water and sludge and it should be emphasized that the overall efficiency of this technology is to a large extent dependent on solids/liquid separation in sedimentation tanks (Stypka, 1998).

The main mechanism underlying activated sludge process is bio-flocculation which is resulted from biological degradation of organic matter present in raw wastewater and growth of microbial cells in flocculent mode (Tchobanoglous, et al., 2004). The structural composition of activated sludge flocs is comprised of microorganisms (most often bacteria), organic matter and inorganic matter such as cations and anions (Park, 2007). The effectiveness of this bio-flocculation governs the liquid/solids separation in sedimentation tanks and the performance of this separation governs the overall quality of the effluent (Stypka, 1998).

The need for higher quality effluent and more efficient nitrogen and phosphorus removal, increased knowledge about microbial processes and underlying mechanisms and the ever need to cut down the capital and operation costs, resulted in various design and process evolution in conventional activated sludge processes (Tchobanoglous, et al., 2004). One of these new configurations is sequencing batch reactors which will be discussed further in the next section.

2a.3. Sequencing batch reactors

Sequencing batch reactor (SBR) system is one variation of activated sludge process at which all treatment processes including sludge separation take place in a single reactor. In other words, SBR is no more than activated sludge plants operates in time rather than space (US EPA, 1999).

Having great process flexibility in terms of cycle time and operation, suitability for treating wastewater with high variations in loads and volumes such as landfill leachate, possibility to have aerobic, anaerobic and anoxic phase in one single unit, relatively small footprint and suitability to couple with advanced treatment methods such as membrane filtration, are some advantages of SBRs over conventional activated sludge process (US EPA, 1999; Kennedy & Lentz, 2000).

Operation of SBR is based on fill and draw principle and cyclic mode. Each cycle of SBR is divided into five identical periods: Fill, React, Settle, Decant and Idle. Below short explanations for each of the operational steps are given.

Fill: Depending on the aeration and mixing conditions, there are several types of fill and React periods (IWA, 2013). During the fill phase, the biomass in the tank remained from the previous cycle is provided with the influent wastewater to start the biochemical reactions. Depending on the type of substrate needed to be removed this phase can be either aerated (aerators are on), mixed (mixers are on and aerators are off) or static (mixers and aerators are off). The latter is normally used when production of biomass with good settling properties and also selection for slow growing microorganisms such as PAOs are desired (de Kreuk & Loosdrecht, 2004; NEIWPCC, 2005).

Many studies have recommended not to couple static fill with aeration or mixing (aerobic -pulse feeding) since static fill helps flocculent bacteria to grow much faster, overcome filamentous bacteria and prevent from sludge bulking. Also, static fill results in more stable bio-aggregates (de Kreuk & Loosdrecht, 2004; Vigneswaran, et al., n.d.). Duration of the fill phase is varied from an almost instantaneous fill to continuous fill throughout the whole cycle (IWA, 2013).

React: When the reactor is filled with wastewater, it enters the react phase. The aim of this stage is for further polishing the wastewater and completing the reactions that began in the fill phase (US EPA, 1999). During this period biomass in the reactor consumes organic substrate and ammonium under controlled environmental condition (Tchobanoglous, et al., 2004). Although this phase is normally associated with vigorous aeration, depending on the desired level of dissolved oxygen concentration in the tank, this phase can be aerated or only be mixed. Duration of this phase can be in order of 15 minutes to more than 50 % of the whole cycle duration (Vigneswaran, et al., n.d.). Long aeration phase (usually more than 4 hours) is practiced when high level of nitrification is required. if denitrification is also desired intermittent aeration will be used. It means that aerators are turned off to let the reactor enter the anoxic phase (Vigneswaran, et al., n.d.).

Settle: In this phase the separation of sludge and treated effluent take place under quiescent condition, no feed stream no aeration and mixing are working. The settled sludge forms a distinct interface with the clear supernatant, this sludge mass is called sludge blanket (NEIWPCC, 2005) and the duration of this phase is dependent on sludge properties.

Decant: Once the settle phase is complete, the supernatant is drawn from the reactor. Duration of this phase can be varied from 3% up to 30% of the total cycle time (IWA, 2013; Vigneswaran, et al., n.d.). A simple pipe fixed at the predetermined level operated with valve or pumps can be used as a simple withdrawal mechanism (NEIWPCC, 2005).

Idle: The period between decant and fill phase is called idle and this phase can be effectively used for sludge wasting (IWA, 2013). However, it can be eliminated and sludge wasting can be done form the mixed liquor during the react phase (Vigneswaran, et al., n.d.). Figure 0-2 illustrates the schematic view of one cycle of SBR operation.

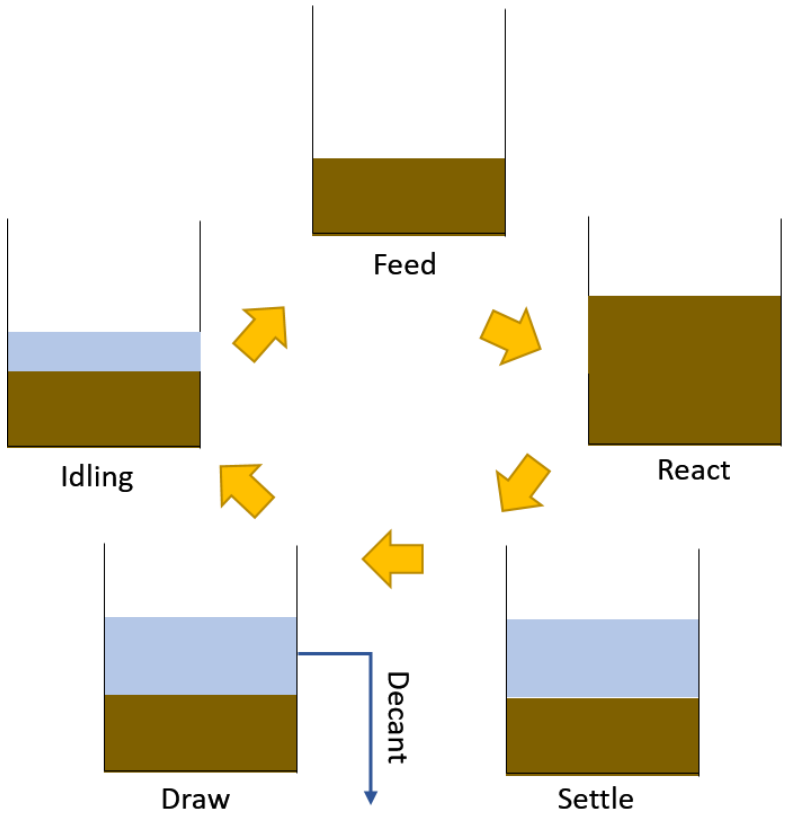

Figure 0-2. One cycle profile of SBR

2a.4. Aerobic granulation

An ever-increasing trend in the number of inhabitants in urban area has forced WWTPs to upgrade their existing systems or to build new ones in order to cope with the proportional increase in the amount of wastewater production. But in some areas, the available land is limited and the WWTPs have to go for alternatives that are as compact

as possible which in many cases are expensive and require advanced equipment and highly trained operators.

One economically feasible alternative is to improve the settleability of the activated sludge flocs for minimizing the surface area of the clarifiers. Aerobic granule technology is one of these alternatives.

Granular sludge is a special type of biofilm at which self-immobilized microorganisms allow the accumulation of high concentration of active biomass with very dense and compact structure (Abdullah, et al., 2011). Thus, granular sludge has higher settling velocity (typically three times more than that of floccular sludge). These features enable the more compact system with higher biomass concentration and more resilient against high hydraulic loads without biomass wash out (Adav & Lee, 2008; Castro-Barros, 2013). Granular sludge technology was first practiced for anaerobic industrial wastewater treatment process (Winkler, 2012). However, long start-up period, relatively high operation temperature, suitability only for organic removal from low strength wastewater, and no nutrient removal limit its application (Oh, no date). These weaknesses were overcome by development of aerobic granule technology in an Aerobic Up-flow Sludge Blanket system by Mishima and Nakamura in the early 1990's (Campos, et al., 2009; Castro-Barros, 2013). As the main focus of this thesis is aerobic granular sludge, the rest

of the text will deal only with aerobic granules. Aerobic granular sludge that was developed in this work is shown in Figure 0-3

Figure 0-3. Aerobic granular sludge

Aerobic granule can withstand organic loading rate from 2.5 to nearly 15 kg COD/(m^3.d) (Oh, no date) and they are suitable option for treating industrial wastewater as well as domestic wastewater (Campos, et al., 2009; Castro-Barros, 2013). For instance, Abdullah et al., (2011) investigated the feasibility of aerobic granules to treat palm oil mill effluent from an oil mill plant. The results showed that aerobic granules could treat COD, ammonia and colour up to 91.1%, 97,7% and, 66% respectively (Abdullah, et al.,

2011).Other advantages of aerobic granules are referred to their structure. In aerobic granules, maximum surface area per volume is obtained, moreover, each granule consists of several layers at which wide and diverse species of microorganisms are present (de-Kreuk & van-Loosdrecht, 2004; Oh, n.d.). Figure 0-4 shows the microbial distributions in an activated sludge floc and an aerobic granule.

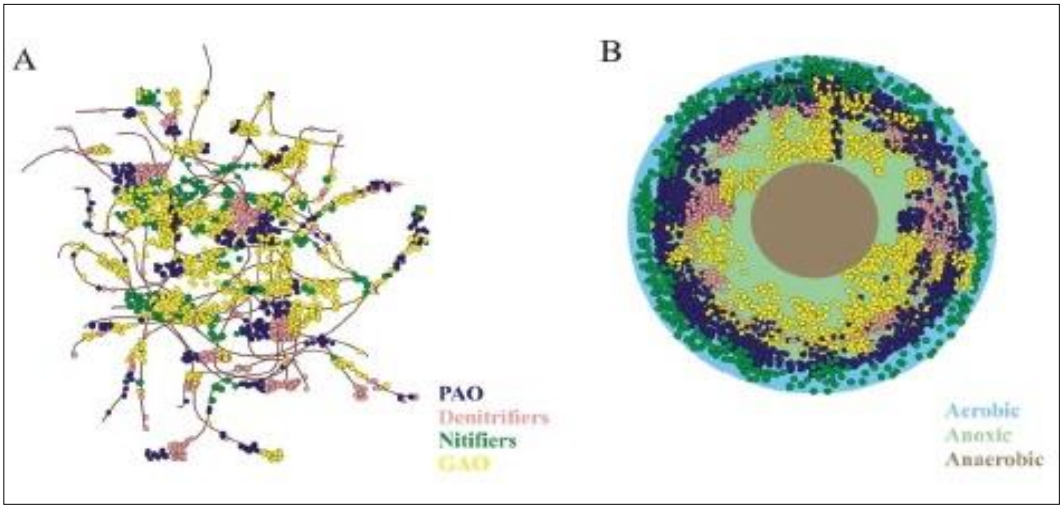

Figure 0-4. Microbial Structure of A) sludge floc and B) aerobic granule (Winkler, 2012). Reprinted with permission

Since biological nitrogen and phosphorous removal require alternate aerobic, anaerobic and anoxic conditions, WWTPs can benefit from aerobic granules by having all the reactions and conversions (aerobic, anaerobic and anoxic) in one single granule and in one-unit operation (Winkler, 2012). One example of this technology is the Nereda® process which offers an energy efficient, chemical free optimized SBR process to biologically remove organic matter and nutrients from industrial and domestic wastewater. Thanks to unique features of aerobic granules, the Nereda® process could achieve high simultaneous aerobic, anoxic and anaerobic biological processes achieved in just one effective aeration step (Royal HaskoningDHV, 2013).

2a.4.1. Characteristics of aerobic granular and floccular sludge

2a.4.1.1. Extracellular polymeric substances

Extracellular polymeric substances (EPS) are large polymeric molecules secreted by microorganisms (Xuan, et al., 2010) and together with cells they form activated sludge flocs or bio-aggregates such as biofilms and aerobic granules (Adav, et al., 2008; Zhao,

et al., 2016). EPS are located inside or outside of the bacterial cells' surface and determine the physiochemical properties of microbial aggregates (Wang, et al., 2005; Park, 2007). Chemical composition of EPS are polysaccharides, extracellular proteins, nucleic acids, humic acid, and some organic and inorganic components (Xuan, et al., 2010). Approximately 70 to 80 % of the EPS contents are polysaccharides and proteins (Zhao, et al., 2016). By changing the surface charge and reducing the repulsive force between adjacent cells, EPS promotes sludge flocculation and dewatering properties (Tay, et al., 2001a; Wang, et al., 2005; Adav & Lee, 2008; Sam & Dulekgurgen, 2015). In addition, by forming a gel-like network and cohesion and adhesion of microorganisms, EPS together with divalent ions play crucial roles in the network integrity and the mechanical stability (stability of aerobic granules against hydrodynamic shear force (Awang & Shaaban, 2016)) of aerobic granules (Wang, et al., 2005; Adav & Lee, 2008; Konczak, et al., 2014).

2a.4.1.2. Cell surface hydrophobicity

One of the most important factor which governs the adhesion of the bacterial cells to each other is the cell surface hydrophobicity (Gao, et al., 2011). Studies have shown that as the cells' hydrophobicity increases, the ability of the cells to stick together and to form bio-aggregates (activated sludge flocs or granules) increase (Zita & Hermansson, 1996; Zita & Hermansson, 1997). Cell surface hydrophobicity of aerobic granular sludge is two times higher than that of activated sludge (Oh, no date). Also for aerobic granules the distribution of cell surface hyrophobicity is not distributed uniformly throghout the core and the shell. Wang et al., have reported that the cell surface hyrophobicity of aerobic granules is much higher at the outer shell than in the core (Wang, et al., 2005).

2a.4.1.3. Specific gravity and water content

Due to higher microbial density, specific gravity of granular sludge is higher than that of floccular sludge. At the beginning of the inoculation and during the adaptive stage, the specific gravity increases slowly but once the aerobic granules are appeared and inter particle bridges are stablished, a sharp increase in specific gravity is observed (Zhao, et al., 2016).

Water content of aerobic granules is around 94%-97%, while that of floccular sludge is around 99%. (Zhao, et al., 2016).

2a.4.1.4. Sludge volume index

In wastewater treatment, the quality of the treated water is highly dependent on how well the biomass is separated from the treated water or how well the sludge settleability is. On the other hand, the biomass settling ability is highly related to sludge flocs structure and presence of filamentous bacteria (Mesquita, et al., 2011). In wastewater engineering, Sludge Volume Index known as SVI is commonly used to show the tendency of sludge to settle or to thicken (Qin, et al., 2004). SVI is the volume in millilitres occupied by one gram of a suspension after 30 minutes of settling (Wilen, 1995) and it is calculated by using Eq. (4) (APHA, 1995).

$$\mathrm{SVI}\left(\frac{\mathrm{mL}}{\mathrm{g}}\right) = \frac{\text{Settled sludge volume after 30 minutes}\left(\frac{\mathrm{mL}}{\mathrm{L}}\right) \times 1000\left(\frac{\mathrm{mg}}{\mathrm{g}}\right)}{\text{Suspended solids}\left(\frac{\mathrm{mg}}{\mathrm{L}}\right)} \qquad \mathrm{Eq}(4)$$

SVI is not a scientific parameter and it does not give any information about the composition of sludge however, it is one of the most practical process control parameter which gives a quick overview about the sudden changes in the sludge's settling properties (Wilen, 1995).

The typical SVI range for a well operated activated sludge process is between 50-150 mL/g. High value for SVI (in the range of 150 mL/g) means poor settleable sludge which is usually the sign of one or multiple of the following problems: an imbalance between filamentous and floc forming organisms due to the excess growth of the filamentous bacteria, too high or too low dissolved oxygen concentration, sludge overloading and, inappropriate reactor shape (Wilen, 1995; Stypka, 1998; Janczukowicz, et al., 2001).

High SVI is called sludge bulking and it is the most common unfavourable situation in activated sludge operation (Wilen, 1995; Janczukowicz, et al., 2001). Sometimes, as it has been also observed during this project, sludge with good settling properties rises up and float to the surface, this phenomenon is different form sludge bulking and it is mainly due to denitrification in which nitrogen gas is produced from conversion of nitrite and nitrate (Tchobanoglous, et al., 2004). The produced nitrogen bubbles are entrapped in the sludge layer and stick to the sludge flocs. As denitrification is proceeding, the nitrogen gas concentration is increasing and when the accumulated nitrogen gas reaches a critical

concentration, the sludge flocs become buoyant and rise to the surface (Tchobanoglous, et al., 2004).

Aerobic granular sludge has SVI value, typically between 22-65 mL/g (Toh, et al., 2002; Zhao, et al., 2016), while the conventional activated sludge usually has SVI greater than 120 mL/g (Toh, et al., 2002).

2a.4.2. Aerobic granulation

Aerobic granulation is a gradual process starting with seeding sludge, developing into compact aggregates and then into aerobic granules and finally into mature aerobic granules (Tay, et al., 2001a). Thus, the formation and morphology of aerobic granules are very complicated and to date, the exact mechanism(s) underlying them is(are) not fully understood. Until now, research on aerobic granulation has primary been carried out in SBRs (Awang & Shaaban, 2016). This is due to cyclic configuration, flexible feeding pattern condition and exchange ratio of this method (de Bruin, et al., 2004). However, there are several hydraulic, operational and environmental factors affecting granules formation as well as the morphology of the aerobic granules (Gao, et al., 2011). Seeding sludge, substrate concentration, presence of different chemicals, organic loading rate, feeding pattern, reactor design, settling time, feast-famine regime, air intensity, and exchange ratio are some common influential parameters (Tay, et al., 2001c; Ahmed, et al., 2007; Bindhu & Madhu, 2013; Oh, n.d.). These factors are discussed in the following.

2a.4.2.1. Seed sludge

In 2014, Ersan and Erguder investigated the effect of two seed sludge types; conventional activated sludge and membrane bioreactor sludge on the aerobic granules performance and characteristics. The results revealed that the aerobic granules formed by the membrane bioreactor (MBR) sludge had greater size, better settleabiliy and biomass retention, and higher performance to treat high organic loading rate (Ersan & Erguder, 2014). They have also recommended the usage of the MBR sludge to decrease the start-up duration.

Li et al., (2015) conducted a research to study the effect of adding dry sewage sludge micropowder on the formation and characteristics of the aerobic granules. The results showed that adding micropowder accelerated the aerobic granules formation and controlled the formation of the filamentous bacteria to great extent (Li, et al., 2015)

2a.4.2.2. Feed composition and organic loading rate (OLR)

As previously mentioned, aerobic granules can be cultured successfully in SBRs fed with a variety of wastewater both real and synthetic. For instance, aerobic granules can be developed using, glucose, acetate, ethanol or phenol as a sole organic source (Castro-Barros, 2013).

Substrate components and organic loading rate have great influence on the formation and characteristics of aerobic granules (Oh, no date). In 2001, Toy et al., investigated the effect of glucose and acetate as two separate organic sources on the structure of aerobic granules. They have found that aerobic granules fed with glucose had fluffier and irregular outer shape dominated with filamentous bacteria while acetate fed granules had more regular, round outer surface (Tay, et al., 2001a). **Error! Reference source not found.** shows aerobic granules evolved by glucose and acetate solution.

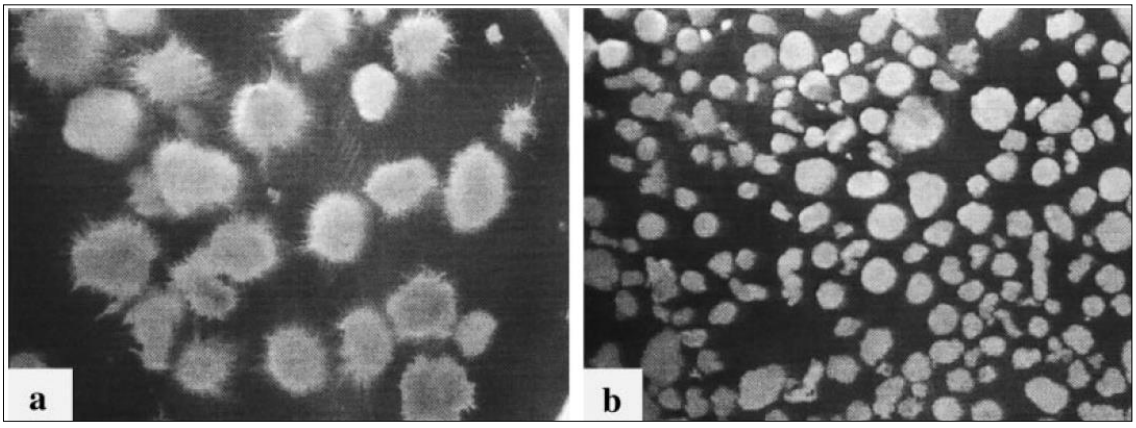

Figure 0-5. Image analysis of aerobic granules, a) glucose fed, b) acetate fed (Tay, et al., 2001a). Reprinted with Permission.

Another factor which has significant effects on any biological processes such as the aerobic granules formation is organic loading rate (Bindhu and Madhu, 2013).

Aerobic granular sludge technology is suitable for low to high organic loading rates (OLRs), from 2 up to 15 kg/(m^3.d) of COD wastewater (Oh, no date). However, with OLR below 2 kg COD/(m^3.d), the aerobic granules formation is difficult (Tay, et al., 2004). Another study done by Bindhu and Madhu 2013, showed that the aerobic granules sludge can be developed successfully at OLR of 3, 6 and 9 kg COD/(m^3.d) but the best performance in terms of higher COD removal and better SVI was achieved with OLR of

6 kg COD/(m^3.d) (Bindhu and Madhu, 2013). Also at OLR higher than 9 kg COD/(m^3.d) disintegration of granules in acetate feed reactors was observed (Moy, et al., 2002).

In a research conducted by Moy et al., in 2002, the effect of different OLRs on the structure of acetate feed and glucose feed granules were studied. The results showed that glucose fed granules had looser and fluffier structure than that of acetate fed granules. Filamentous bacteria were also dominated in glucose feed reactors. They also showed that at similar OLR, aerobic granules cultivated with glucose had lower settling velocity than granules cultivated by acetate (Moy, et al., 2002). In 2003, Liu et al., demonstrated the possibility of aerobic granules formation under variety of OLR (from 500 to 3000 mg/L COD). They have found that formation of aerobic granules is independent of the substrate concentration however, higher substrate concentration results in bigger aerobic granules (Liu et al., 2003). Similar results were also found by Liu and Tay (2004). They have increased the ORL from 3 to 9 kg COD/(m^3.d) and observed that the mean size of the aerobic granules has increased form 1.6 mm to 1.9mm (Liu and Tay, 2004).

In 2006, van-Loosdrecht and de-Kreuk investigated the feasibility of aerobic granules formation using real domestic wastewater with OLR of 1 kg COD/(m^3.d) (de-Kreuk and van-Loosdrecht, 2006). The results demonstrated that for aerobic granules to be formed under real and low strength wastewater, short cycle time, relatively long start-up time and concentrated wastewater are crucial (de-Kreuk & va-Loosdrecht, 2006). In terms of sludge characteristics, the results indicated that the granules formed by real wastewater are more heterogeneous than granules grown by synthetic wastewater (de-Kreuk and van-Loosdrecht, 2006). Liu et al., (2003) investigated the effect of substrate concentration, here COD, on cell surface hydrophobicity. It was found that the cell surface hydrophobicity of the aerobic granules increased to 71% for reactor fed with 500 mg/L COD, to 86% for reactor fed with 1000 mg/L COD and to 78% and 79% for reactors fed with 2000 and 3000 mg/L COD, respectively (Liu, et al., 2003).

2a.4.2.3. Feeding pattern and feast/famine regime

One of the unique features of SBRs which promotes the aerobic granules formation is operating in cyclic configuration or in other words, submitting the microorganisms into periodic feast and famine phase (Tay, et al., 2006). When microorganisms face to these situations, bio-aggregation is an effective way to survive during starvation phase. These

conditions also increase the hydrophobicity of the bacteria and facilitate the ability of bacteria to aggregate and to form granules (Zita and Hermansson, 1997; Bathe, et al., 2005; Tay, et al., 2006; Ni, 2012).

There are various definitions for feast/famine regime and researchers have agreed that by the feast/famine regime one means variation of substrate concentration in the reactor volume (Bathe, et al., 2005). During feast period, when a huge amount of organic matter enters the reactor in the short periods of time, microorganisms start to oxidize the organic matter quickly and store it in their cells as VFA, PHA and during the famine period, the bacteria grow on the stored compounds (Val del Rio, et al., 2013).

However, the duration of feast and famine period must be carefully selected. Starvation below 30 minutes has no significant effect on aerobic granules and very long starvation period leads to high energy consumption and low reactor capacity (Tay, et al., 2006; Val del Rio, et al., 2013).

Feeding pattern is also proved to have critical role on the formation and structure of the aerobic granules (McSwain, et al., 2004) as well as COD and nitrogen removal efficiency (Mosquera-Corral, et al., 2005). Many researchers have shown that to promote aerobic granules, short feeding period must be selected in order to make a feat and famine regime condition for the microorganisms (Campos, et al., 2009).

Long feeding time leads to constant smaller COD load entering to the reactor. Therefore, the organic substrate for instance, acetate is oxidized by heterotrophic organisms at the outer layer of the aerobic granules while in the inner layers where oxygen can penetrate and substrates cannot, autotrophic organisms oxidize ammonia. This condition results to have high nitrification and COD removal but no denitrification (Mosquera-Corral, et al., 2005). Also by increasing the organic substrate concentration to a level which enable it to penetrate to the inner layer, heterotrophic organisms will outcompete ammonia oxidizing bacteria and in this case even nitrification is interrupted (Mosquera-Corral, et al., 2005). However, there are some studies which recommend elongated anaerobic feeding pattern to select slow growing microorganisms such as PAOs for promoting biological phosphorus removal (Winkler, 2012).

de-Kreuk et al., have shown that using aerobic pulse feeding pattern does not contribute to stable aerobic granules at low dissolved oxygen concentration. The results showed that by decreasing DO concentration from 100% to 40% nitrification was improved while aerobic granules were disintegrated. They have recommended that in order to have high simultaneous COD, nitrogen and phosphate removal, the growth rate of slow-growing microorganisms such as PAOs should be maximized by providing anaerobic substrate feeding pattern at low dissolved oxygen concentration (de-Kreuk and van-Loosdrecht, 2004). Also, they have pointed out that long feeding pattern followed by an anoxic phase will improve nitrogen and phosphorus removal without affecting the properties of the aerobic granules (de-Kreuk and van-Loosdrecht, 2004).

McSwain et al., (2004) investigated the effect of feeding pattern on the aerobic granules properties. They have run three parallel SBRs which were similar in everything except for feeding pattern. As it is seen in Figure 0-6, aerobic granulation happened in all the reactors but the reactor which received instant feed had more compact and smoother outer surface aerobic granules. The other two reactors which received elongated aerobic feed developed fluffier aerobic granules dominated by filamentous bacteria (McSwain, et al., 2004).

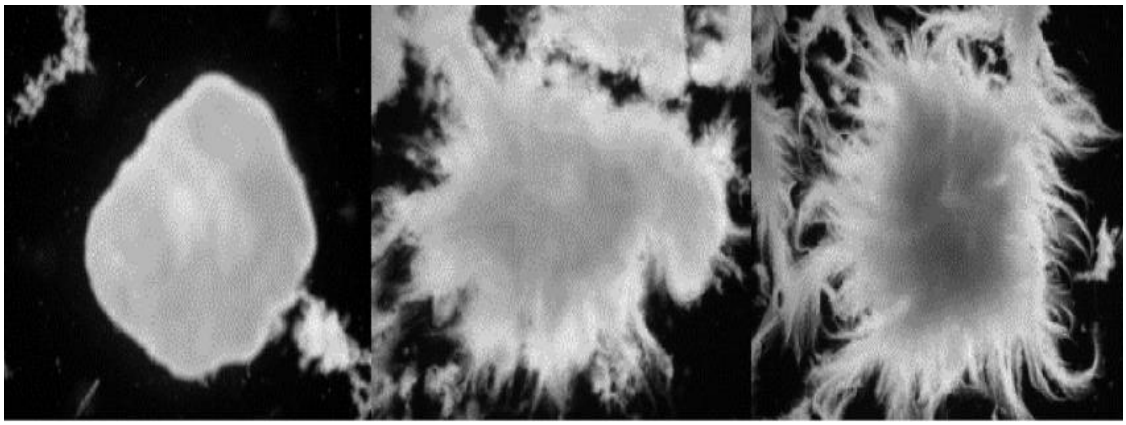

Figure 0-6. Structure of aerobic granules formed at different feeding pattern, aerated fill from left to right, 0%, 33% and 66% (McSwain, et al., 2004). Reprinted with permission.

2a.4.2.4 Reactor configuration and design

To date, many studies on aerobic granules formation have been conducted in column type reactors (Liu & Tay, 2004; Castro-Barros, 2013). This is because of the effect of reactor configuration on the relation between flow pattern and microbial aggregation. Column

type reactors and complete mixed tank reactors have totally different hydrodynamic behaviour; thus, they have different effect on the relation between the liquid and the microbial community in the tank (Liu & Tay, 2004). Column type reactors produce more homogenous circular air and liquid flows in the reactor and apparently circular flow causes the microbial aggregated to adapt a regular granular shape. Therefore, column type SBRs are preferable for granulation (Liu & Tay, 2004).

Reactor height to diameter (H/D) is another influential parameter on the aerobic granules formation (Awang and Shaaban, 2016). Until now extensive successful aerobic granules formation were reported in SBRs using H/D ratio of greater than 10, since high H/D ratios, reduce the start-up time for the formation of mature aerobic granules (Awang and Shaaban, 2016). A review by Liu and Tay (2002) stated that high ratios of H/D provide better hydraulic situation for the microbial aggregation (Liu and Tay, 2002). In contrast, Kong et al., (2009) by conducting a research concluded that the reactor's H/D ratio does not have effect on aerobic granules properties such as: formation, microbial community and physical characteristics (Kong, et al., 2009). In 2016, Awang and Shaaban investigated the performance of two SBRs with different H/D ratios but with the same working volume and substrate concentration. The results showed that the reactor with H/D ratio of four develop mature granules after 90 days while the reactor with H/D ratio of 11.3 developed aerobic granules after 50 days (Awang and Shaaban, 2016).

2a.4.2.5 Settling time

In SBR, time allocated for settling the sludge in one important factor which promotes the formation of aerobic granules (Campos, et al., 2009). When the SBR is working in long settling time, light and slow settling flocs are allowed to remain and grow in the reactor leading to the failure of the granules formation (Campos, et al., 2009). In contrast, using short settling time allows the fast settling and heavy sludge particles to remain and grow in the reactor and poorly settling sludge flocs to be washed out. Thus, resulting in the aerobic granules formation (Campos, et al., 2009). In 2004, Qin et al., conducted a research investigating the effect of the settling time ranging from 20 to 5 minutes on the

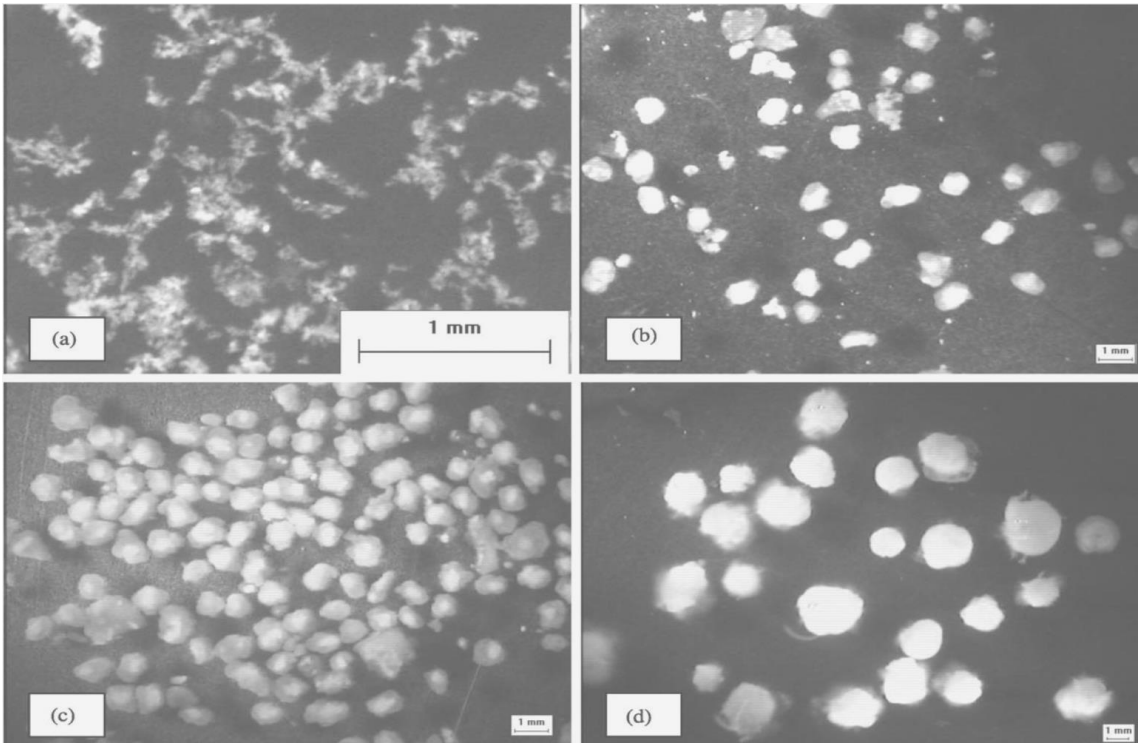

Figure 0-7. Granules structure at. (a) 20 min (b) 15 min (c) 10 min (d) 5 min settling time (Qin, et al., 2004). Reprinted with permission.

formation and characteristics of aerobic granules. The study proved that granules sludge only form when the settling time is shorter than 15 minutes (Qin, et al., 2004). In addition, a clear correlation between the sludge washout rate and the settling time was obtained. Meaning that the higher the settling time, the lower the rate of sludge discharge (Qin, et al., 2004). Another finding of this study was the effect of short settling time on compactness of the granules structures (Qin, et al., 2004). Figure 0-7 shows the shape and the structure of aerobic granules at different settling time.

2a.4.2.6. Hydrodynamic shear force and dissolved oxygen concentration

Another factor that has great influence on aerobic granules formation, characteristics and settling velocity is hydrodynamic shear force (Oh, no date). In SBR, the hydrodynamic turbulence which is caused by the up-flow aeration is considered as shear force (Tay, et al., 2001c). Shear force is usually present in superficial up-flow air velocity (Tay, et al., 2001b). It is proved that applying high shear force (minimum 1.2 cm/s in superficial up-flow air velocity) in SBR favours the condition for aerobic granules formation (Liu and Tay, 2004). Also, high shear force has positive impact on the density and strength of aerobic granules (Tay, et al., 2001c). A study carried out by Tay et al, in 2001, has shown

that at very low aeration rate (0.008 m/s) no aerobic granules were formed. In contrast, regular, clear outer shape aerobic granules were formed at aeration rate approximately 0.025 m/s (Tay, et al., 2001b). van-Loosdrecht et al., indicated the dependency of the aerobic granules structure on shear forces by showing that low shear stress contributes to formation of irregular, highly heterogeneous, low density with high pores and protuberance granules (van-Loosdrecht, et al., 1995).

Oxygen concentration is of great importance for initiation and continuation of many biological processes such as COD removal, SND and phosphorus removal (de Kreuk and Loosdrecht, 2004). To date there are several successful aerobic granules formation under periodic feast/famine regime in SBRs operated at very high oxygen concentration since developing aerobic granules at low oxygen saturation normally results to easily breakable, instable, filamentous- dominant aerobic granules (de-Kreuk, et al., 2005; Mosquera-Corral, et al., 2005). However, the main purposes of developing aerobic granules were to have a more energy efficient system as well as having a single unit with simultaneous COD, SND and phosphate removal. Therefore, these purposes will not be obtained if the SBRs have to operate at very high dissolved oxygen concentration. In other words, for benefitting from aerobic granules to the fullest oxygen concentration must be optimized (de-Bruin, et al., 2004; de-Kreuk, et al., 2005; Mosquera-Corral, et al., 2005). A study conducted by van-Loosdrecht and de-Kreuk has revealed that low dissolved oxygen concentration together with anaerobic feeding provide a favourable condition for PAOs thus improving phosphate removal (de-Kreuk and van-Loosdrecht, 2004). They could also successfully obtain simultaneous COD, N and P removal at dissolved oxygen saturation of only 20% (de-Kreuk, et al., 2005). Another researcher showed that by decreasing the oxygen concentration from 100% to 50% the nitrification decreased to 47% but since the denitrification efficiency increased dramatically, the overall nitrogen removal efficiency was increased (Mosquera-Corral, et al., 2005).

2a.4.2.7 Other factors

The concentration of alkalinity in the influent and the pH in the reactor are important parameter having great influence on morphology and formation of aerobic granules. In 2007, Xiao and colleagues made a study on the effect of alkalinity on properties of the aerobic granules which were cultivated in SBR fed with glucose as carbon source. They have found that feed stream with low alkalinity (28.7 mg/L $CaCO_3$) results in big size,

loose, irregular structure and fluffy aerobic granules dominated by fungi. In contrast, the reactor which received high alkalinity content (301 mg $CaCO_3$) developed medium sized, dense and compact granules with well-defined surface (Xiao, et al., 2008). Soltanzadeh et al., (2015) have obtained similar results. They have investigated two SBRs one operated with low influent alkalinity and neutral pH and the other one operated with high alkalinity influent and acidic pH. The results showed that in the reactor with high alkalinity adjusted with neutral pH, the aerobic granules were formed in the third week of operation with a good bacterial diversity. In contrast, the reactor which received low alkalinity influent and low pH develop bigger sized aerobic granules after only one week from the start-up, however, on the third week this reactor was dominated with mass growth of fungi (Soltanzadeh, et al., 2015). In 2016, Leong et al, investigated the aerobic granules formation using low pH and low alkalinity feed stream. The aerobic granules formed under this condition required relatively long formation time (166 days after the start-up) and they had lower density and lower long-term stability (Leong, et al., 2016). In addition, utilizing low pH and low alkalinity for aerobic granulation, resulted in limited nitrification and denitrification (Leong, et al., 2016). According to the findings above, it can be concluded that for reducing the aerobic granules formation time, one option is to provide acidic situation in the reactor while increasing the influent alkalinity. Since the acidic environment encourages the growth of fungi while this environment is not suitable for bacteria (Soltanzadeh, et al., 2015). However, it is evidence that fungi-rich aerobic granules will lose their superior performance over bacterial-rich aerobic granules in the long-term operation (Soltanzadeh, et al., 2015).

Another important influential factor in aerobic granules formation is presence of divalent cations specially Ca^{+2} and Mg^{+2} (Konczak, et al., 2014; Liu, et al., 2010). EPS and divalent cations play as a cementing agent and connect individual cells and form a three-dimensional structure, aerobic granules (Konczak, et al., 2014). Aerobic granules cultivation time with wastewater rich in Ca^{2+} is quite fast (almost half) and the formed aerobic granules appeared to be more rigid with higher strength and better settling properties (Liu, et al., 2010). A study by Liu et al., (2010) has revealed that augmentation with Mg^{2+} at the concentration of 40 mg/L results in aerobic granules rich in microbial diversity comparing to augmentation with Ca^{2+} at the same concentrations (Liu, et al., 2010). However, the both cations significantly reduced the granulation time from 32 days

to 18 days, and promoted the physical characteristics of the granules (Liu, et al., 2010). In addition to Mg^{2+} and Ca^{2+}, Fe^{2+} and Cu^{2+} are some other metals cations playing crucial role is aerobic granules formation (Zheng, et al., 2010; Konczak, et al., 2014). For instance, Konczak et al., (2014) have proved that the most compact and stable forms of aerobic granules is achieved only when all the metal cations include Ca^{2+}, Mg^{+2} and Fe^{+2} are present (Konczak, et al., 2014). The researchers have found that the concentration Cu^{2+} plays slightly different roles on morphology, EPS and physical structure of aerobic granules (Zheng, et al., 2010). They have found that when the Cu^{2+} concentration lies between 0.5-5 mg/L, stable MLSS, high settleable aerobic granules with low SVI and high specific gravity could obtain (Zheng, et al., 2010). But as the concentration of Cu^{2+} increase to the range of 20-50 mg/L, the aerobic granules become fluffier and looser with domination of filamentous bacteria (Zheng, et al., 2010). Also disintegration of aerobic granules was observed at the concentration of 50 mg/L (Zheng, et al., 2010).

b) Dynamic membrane Filtration

Membrane filtration is a novel, advanced technology introduced recently to increase the quality of treated water from conventional secondary treatment processes (Tchobanoglous, et al., 2004). This section marked as ‘b’ deals with literature review about membrane filtration in general and on dynamic membrane filtration in detail.

2b.1.Definition of Filtration

In wastewater treatment technology, the term filtration can be defined as the process of removing solids or gases from the water stream by passing it through the porous medium, thus; solids and ions larger than the filter pore size would remain on the filter. This method is called filtration and the mechanism in most cases is size exclusion or sieving (Allhands, 2005).

2b.2. Membrane filtration process

Membrane processes are pressure driven or vacuum driven filtration processes for separating substances from the feed stream by using an engineered barrier. The primary mechanism behind membrane filtration is size exclusion (US EPA, 2005). Some of the most common terms in membrane filtration are explained in the following.

2b.2.1. Membrane

Membrane is a thin layer, usually with the thickness of about 0.2-0.25 µm (Tchobanoglous, et al., 2004), of semi-permeable barrier that selectively allows the passage of some components of the feed stream (permeate or filtrate) while rejecting the passage of others which is called concentrate or retentate (US EPA, 2005). Depending on the membrane pore size and operating pressure, membrane filtration processes are classified into microfiltration (MF), ultrafiltration (UF), nanofiltration (NF) and reverse osmosis (RO). MF and UF membranes are usually called low pressure membranes while the other two are known as high pressure membranes (Wilf, 2007). Table 0-1 lists the common membrane pore size and operating pressure of various membrane filtration. In Figure 0-8 the hierarchy of conventional membranes is illustrated.

Table 0-1. Classes of membrane filtration processes (US EPA, 2005)

	Pore size	Operating pressure	Mechanism of removal
Microfiltration	0.1-10 µm	100-400 kPa	Size exclusion
Ultrafiltration	0.005-0.1 µm	200-700 kPa	Size exclusion
Nanofiltration	Less than 0.001 µm	600-1000 kPa	Mass transfer
Reverse osmosis	Non porous		Mass transfer/reverse osmosis

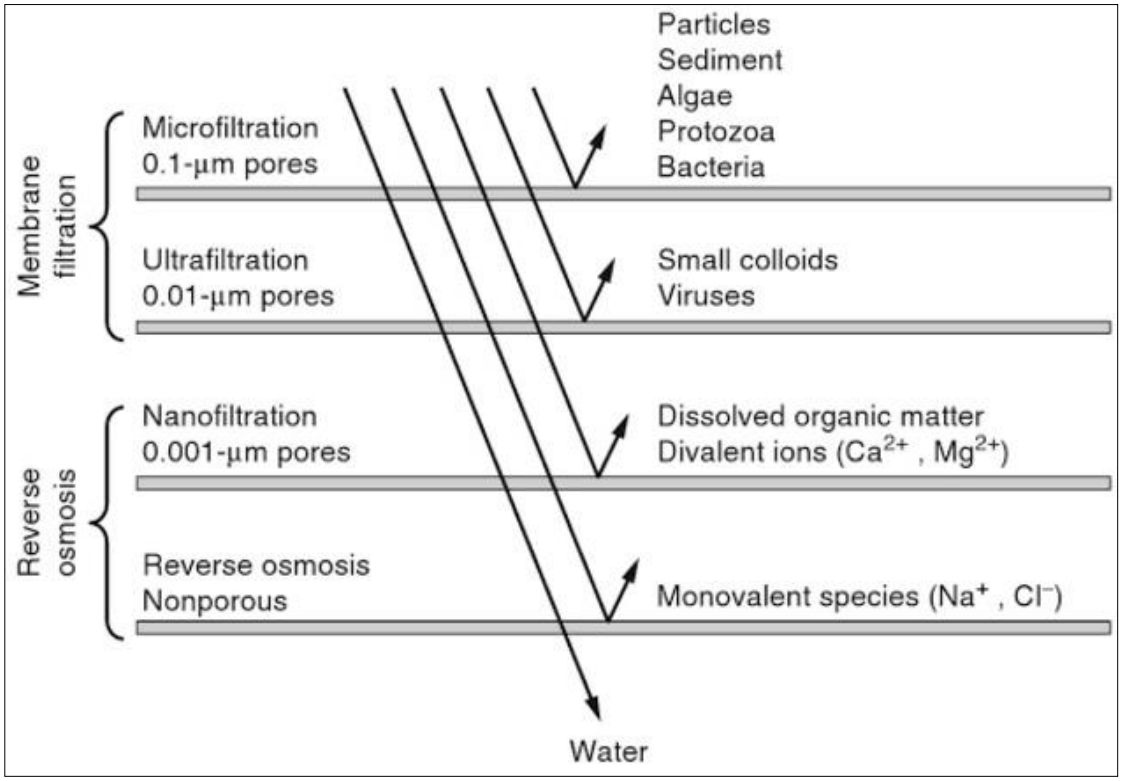

Figure 0-8. Hierarchy of pressure driven membrane processes (Crittenden, et al., 2012). Reprinted with permission.

2b.2.2. Permeate flux

The permeate flow per unit membrane area is called permeate flux (US EPA, 2005) and it is often presented in litre per square meter per unit of hour (LMH).

2b.2.3. Transmembrane pressure

The pressure gradient through the membrane filter is called transmembrane pressure (TMP), i.e., the difference in the average pressure between the feed/concentrate and the filtrate. TMP can be calculated using Eq. (5) (US EPA, 2005).

$$\mathrm{TMP} = \frac{P_f + P_c}{2} - P_p \qquad \mathrm{Eq}(5)$$

Where, TMP is transmembrane pressure (Pa), P_f is the pressure in the feed stream (Pa), P_c is the concentrate pressure (Pa) and Pp is the filtrate pressure (Pa). For UF/MF and coarse membranes, the feed stream pressure and the concentrate pressure are almost equal (US EPA, 2005).

2b.2.4. Membrane total and open surface area

The membrane total surface area is the area that is exposed to the water flow including both membrane holes, openings and structure. But the membrane open surface area is the area of the open space only. Open area is usually expressed as percentage of total surface area (US EPA, 2005).

2b.2.5. Membrane degree

The term which is used to describe the nominal membrane degree is the shortest linear distance across the single opening and it is usually given in micron or inches (Allhands, 2005).

2b.3. Membrane materials, modules and operation's modes

2b.3.1. Membrane materials

Membrane material refers to the substance(s) from which the membrane is made and the membrane material properties will dictate the size exclusion capacity of the membrane (US EPA, 2005). Most commercial membrane filters are manufactured as flat sheets, fine hollow-fiber and tubular forms and created from wide variety of organic and inorganic materials (Tchobanoglous, et al., 2004).

Beside economic justification, the membrane's material should have high porosity, good chlorine and oxidant tolrance, wide range of pH tolerance(US EPA, 2005; Wilf, 2007). Also due to the fact that most interaction between the membrane and foulants are hydrophobic in nature, hydrophilic membrane are preferred (Radjenovic, et al., 2008).

Membrane mechanical strength is also of major importance since high mechanical strength allows the membrane to withstand higher TMP and gives it more operational flexibility. (Pennsylvania Department of Environmental Protection, no date).

The most commercially utilized membranes' materials for drinking water production are organic, specifically synthetic polymers because of their economic justification. But other type of inorganic materials such as ceramic and metallic membranes are available (Pennsylvania Department of Environmental Protection, n.d.; Tchobanoglous, et al., 2004).

The main problem associated with membranes made of polymeric materials is that they are hydrophobic and hydrophobic membranes are more prone to fouling (Radjenovic, et al., 2008).

2b.3.2. Membrane operations and modes

Membrane filtration can be operated basically in two modes: dead-end filtration and cross flow filtration (US EPA, 2005).

In dead-end filtration mode, known as direct flow filtration, the feed stream movement is perpendicular to the surface of the membrane. As the water flows through the membrane, particles larger than membrane pores will stay behind the membrane. Accumulation of particles behind the membrane results in gradual increase of resistance to flow and ultimately membrane fouling (Evenblij, 2006).

In cross flow filtration also known as tangential flow filtration, the feed stream flow is parallel to the membrane surface. The pressure difference along the membrane moves the particles smaller than the pore size through the membrane while larger particles will deposit on the membrane surface. Later on, this parallel motion of the flow, sweeps the accumulated particles on the membrane surface and keeps the membrane from fouling. For feed stream with high amount of filterable matter, cross flow filtration provides stable filtration rate (US EPA, 2001). Figure 0-9 provides a schematic figure of dead end filtration and cross flow filtration.

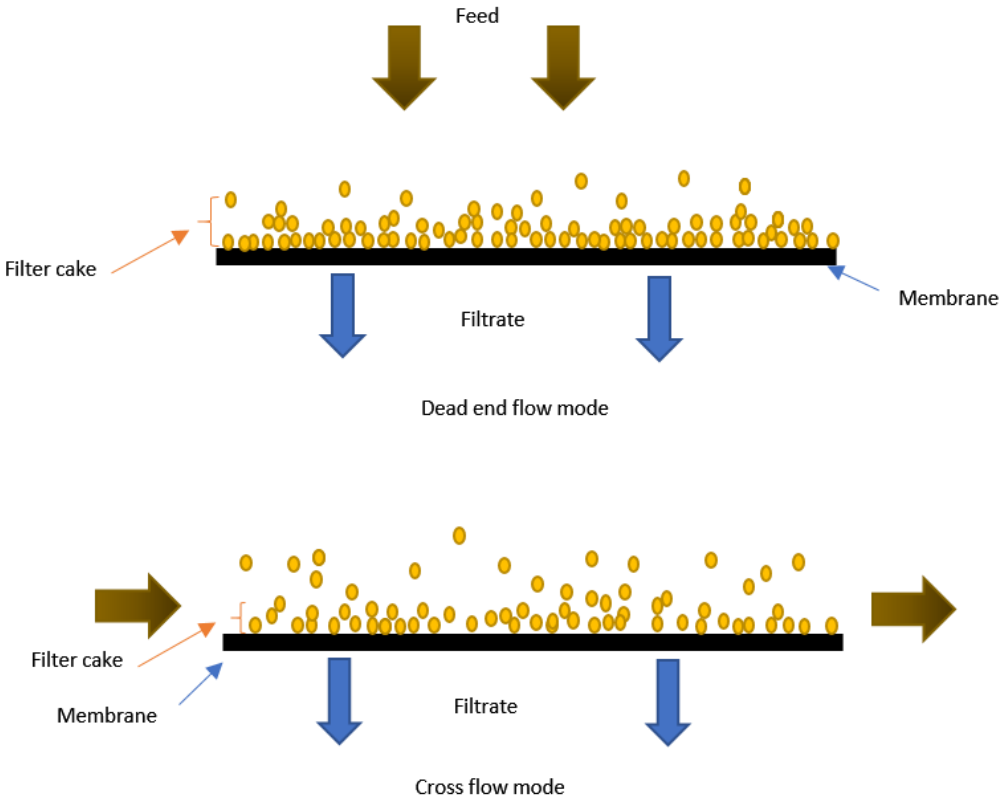

Figure 0-9. Schematic figure of different filtration modes

Normally in dead end filtration, the feed stream passes through the membrane once, while in cross flow filtration, what that does not pass through the membrane is blended with the incoming feed stream and recirculated back to the feed reservoir and passed along the membrane several times. Thus, from an economic point of view, dead end filtration seems to be more cost effective. However, cross flow filtration has better ability to handle wide variations to particle size and solids concentration and it produces permeate with higher rate and quality (Bhave, 1996; US EPA, 2001)

Xu-Jiang et al (1995), have conducted a research to investigate the cake characteristics of cross flow and dead end microfiltration using tar suspension (Xu-Jiang, et al., 1995). They have found that the cake formed in cross flow mode is more permeable and has higher compressibility than that of dead end filtration (Xu-Jiang, et al., 1995).

The choice of the membrane and the system configuration are based on minimizing membrane fouling, and operation costs while optimizing the performance. For having the most appropriate membrane filtration, the following aspects must be taken into account:

membrane pore size, material and shape, and operation mode (Tchobanoglous, et al., 2004; de Amorim & Ramos, 2006).

2b.4.Membrane bioreactors

2b.4.1. Membrane bioreactor history and configurations

Membrane bioreactor technology (MBRs) is an elegant combination of activated sludge process with membrane filtration, and it is an attractive alternative where the land is scarce and/or demand on quality of the effluent exceeds the capability of conventional treatment processes (Radjenovic, et al., 2008). MBRs have been successfully tested and applied both in pilot plant and full scale for treating wastewater from small community, landfill leachate, industrial, and agricultural activities (Cicek, 2002).

The main difference between MBRs and conventional activated sludge process is that, in conventional activated sludge the biomass separation from treated water takes place in secondary clarifiers while, in MBRs, the solids/liquids separation is accomplished by membranes (especially micro/ultra) instead of secondary sedimentation tanks. Depending on the location of the membrane relative to the bioreactor, MBRs are divided in two configurations: Side-stream and Submerged, see Figure 0-10.

The very early commercialized MBRs were developed in the late 1960s and they were based on Side-stream configuration. In this configuration, the membrane is fixed outside the bioreactor and the sludge from the bioreactor is pumped through the membrane either in cross flow mode or direct mode. The retentate is then recycled back to the bioreactor. In this configuration, pumping of the sludge through the membrane breaks up the sludge flocs and increases the fine particles and fouling materials in the feed stream (Radjenovic, et al., 2008). Therefore, it operates at higher TMP, usually around 4 bar.

Because of the energy dissipation, suppressing membrane fouling, and high costs, application of this configuration in industrial scale remained limited (Pabby, et al., 2008). However, this configuration produces higher permeate flux (50-100 LMH) and it is more applicable to retrofit to the existing processes (Pabby, et al., 2008; Radjenovic, et al., 2008).

Submerged MBRs are more recent configuration in which the membrane is immerse directly inside the bioreactors. The required TMP is provided either by water level difference between the bioreactor and the effluent port or by suction pump (Kiso, et al., 2000; Basile, et al., 2015). The permeate flux from this configuration is between 20-50 LMH and TMP is between 0.2-0.5 bar (Radjenovic, et al., 2008; Gupta, et al., 2008). In contrast to side-stream configuration, implementation of the submerged MBRs at full industrial scale requires less cost and energy as there is no need for the recycle pump (Gupta, et al., 2008).

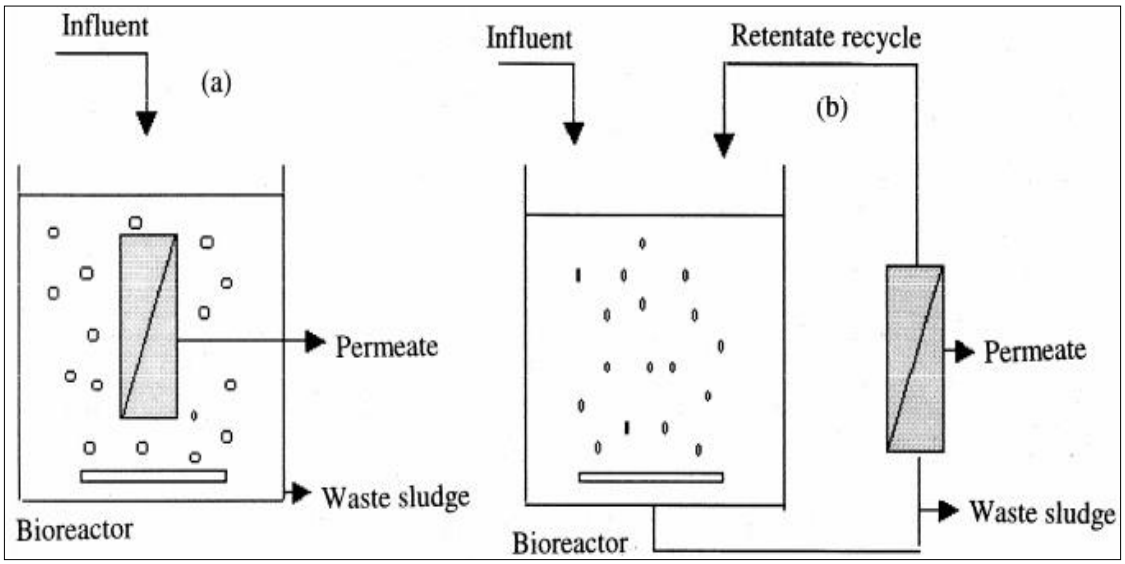

Figure 0-10. MBRs: a) submerged b) side-stream (Gupta, et al., 2008) CC-BY.

In order to prevent membrane fouling, tangential velocities (shear force) over the membrane surface should be provided either by aeration or by pumping. Submerged configuration employs aeration system to provide oxygen for biological processes and to mitigate fouling by constantly scouring the membrane surface (Wu and He, 2012). In side-stream configuration this shear force is provided by pumping (Radjenovic, et al., 2008).

2b.4.2. Membrane bioreactor fouling

Improved effluent quality, free of bacteria and pathogens, low foot print, less sludge production, high sludge retention time, and high organic loading rate are some striking advantages of MBRs over many conventional biological wastewater treatment processes

(Ersahin, et al., 2012; Cicek, 2002). However, despite of introducing many modifications to aeration system, the membrane fouling is still the main obstacle in widespread use of MBRs (Gupta, et al., 2008). There has been done a lot of research on fouling and how to mitigate it. For instance, in 2012, Wu and He, investigated the effect of intermittent and intensive aeration in fouling of a submerged MBR. The results showed that cyclic aeration provides less irreversible fouling and intensive aeration will break apart activated sludge flocs into soluble particles and colloids thus increasing the internal fouling, pore blockage, of the membrane (Wu and He, 2012).

Researchers even investigated the use of attached growth microorganisms on submerged MBRs operated with 0.1 µm hollow fiber membrane in fouling reduction. The results showed that both kinds of growth conditions could reject COD and NH_4-N up to 98% and 95% respectively. But surprisingly, the rate of membrane fouling was7 times higher than that of suspended growth (Lee, et al., 2001).

Membrane fouling is a very complicated phenomenon that many variables and parameters are causing it. A brief explanation about membrane fouling and its different components are provided in section 2b.7.

In spite of having distinct advantages over conventional activated sludge; low permeate flux, high membrane and energy costs together with unavoidable membrane fouling have necessitated the further development in MBR technology (Kiso, et al., 2000). One of these improvement is using coarser membrane known as mesh filters instead of MF/UF membranes which can significantly reduce the costs and frequent needs of backwash and chemical cleaning (Basile, et al., 2015). Since the focus of this work is on mesh filters, the rest of the text is dedicated to mesh filters.

2b.5. Mesh filters

Using coarse cheap filters instead of conventional UF/MF membranes is one modification in MBR technology which has great influence on saving costs and energy since their costs are several orders of magnitude lower than conventional membrane filters and also they do not require high pressure to drive the filtration (Kiso, et al., 2000; Li, et al., 2012). Examples of these coarse filters are: nylon mesh, stainless steel mesh, woven and

nonwoven fabrics. Mesh filters have relatively large pore size in the range of 10-200 µm, thus, MBRs equipped with mesh filters have higher filtration flux with lower trans-filter pressure (TFP) (Li, et al., 2012). Although losing a bit effluent quality, this technology still competes with common treatment processes (Fuchs, et al., 2005). In 2000, Kiso et al., investigated the performance of MBR equipped with 100-micron Nylon mesh for treating a domestic wastewater with SS up to 11500 mg/L. The results showed that the mesh filter together with the formed sludge layer could effectively reduce SS and BOD from the feed stream to less than 1.5 mg/L and 5 mg/L respectively (Kiso, et al., 2000). Fuchs et al, have obtained a permeate with flux of 150 L/(m^2.h), SS concentration below 12 mg/L, BOD_5 lower than 5 mg/L and COD between 24-45 mg/L in bioreactor operated with 30 µm nylon mesh filter (Fuchs, et al., 2005). One unique feature about the mesh filters is that they do not themselves act as a real membrane, instead the bio-cake layer which has developed on top of them plays the role of a real membrane. This feature was the basic principle behind dynamic membrane filtration (Li, et al., 2012).

2b.6.Dynamic membrane

2b.6.1. Overview

High capital and energy costs, prone to membrane fouling, and low permeate flux have restricted the dominancy of MBRs. To overcome these limitations many endeavours have been made, e.g., changing the operation condition, using gravity driven to reduce the high energy costs, and also using cheap filtration materials as a substitute for expensive membranes (Zhang, et al., 2014). Among those alternatives, dynamic membrane has been successfully proved to be successfully applicable in liquid/solids separation process to produce permeate at high flux without losing the quality (Wu, et al., 2005; Ersahin, et al., 2012; Fan and Huang, 2002).

The basic mechanism in dynamic membrane filtration is developing a ‘secondary’ membrane on top of the primary membrane, which in most cases are mesh filters (Kiso, et al., 2005). When the feed stream containing fine particles such as activated sludge flocs and microbial cells is passed through the membrane, a bio-cake layer is instantly formed on top of the membrane surface (Kiso, et al., 2005) which can be dynamically rebuild and removed with water or air flushing during backwash (Wu, et al., 2005; Zhang, et al.,

2014). This bio-cake layer has micropores and microstructure channels (Jun, et al., 2007; Huang, et al., 2013) and acts as an actual filter and does the most physical interception while, the real membrane acts only as a support layer for it (Ersahin, et al., 2012). Figure 0-11 shows a schematic view of the formed dynamic membrane on the support layer.

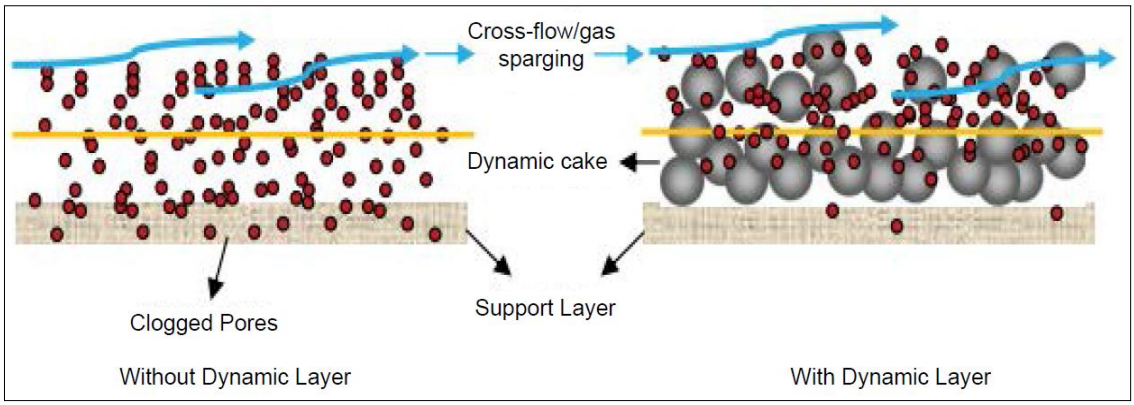

Figure 0-11. Dynamic Membrane (Ersahin, et al., 2012). Reprinted with permission

The filtration characteristic and capacity of the formed bio-cake layer is highly dependent on the concentration of the sludge, properties of the membrane filter itself, hydrodynamic conditions, TMP and operating conditions (Li, et al., 2012; Ersahin, et al., 2012).

The formed bio-cake is composed of a sludge cake layer and gel layer (Fan and Huang, 2002). The sludge cake layer is formed shortly after initiation of the filtartion process and its thickness is increasing over time from a few milimiters to several centimiters (Yamagiwa, et al., 1991; Wu, et al., 2005; Kiso, et al., 2005). But, the thikness of the cake layer is not equal over the entire membrane surface since the particles do not distribute and deposit uniformlly (Buetehorn, et al., 2011). Morphology and internal micostructure of the cake layer can be studied by various techniques such as Scanning electron microscpoy (SEM), atomic force microscopy (AFM), and static light scattering (SLS) (Meng, et al., 2005).

The formation of cake layer on the membrane surface is divided in three stages; pore blocking at the beginning of the filtration, cake formation and cake compression (Meng, et al., 2005). It is reported by many researchers that the main component of the hydraulic resistance is due to cake layer formation (Chu & Li, 2006; Jun, et al., 2007) and the rapid jump in TMP is due to the last two stages (Meng, et al., 2005).

In contrast, gel layer is formed gradually within the pores of the membrane and it is due to adhesion of organisms and soluble components of the sludge to the fabrics of the membrane. Since it has more sticky components, gel layer is more difficult to be removed by water or air flushing, thus; chemical agent should be used (Wu, et al., 2005; Motosic, et al., 2008; Wu and He, 2012; Hong, et al., 2014).

Hong et al., (2014) have showed that the gel layer hydraulic resistance is 100 times higher than cake layer resistance on 0.3µm polyvinylidene fluoride membrane (Hong, et al., 2014). Gel layer accumulation within the pores of the mesh filters in the long term operation causes irreversible pore blocking fouling which even after chemical cleaning is still remained (Jun, et al., 2007; Wu and He, 2012). However, Fan and Huang reported that gel layer has critical role in improving the permeability of the cake layer during the early stage of its formation by making the support layer more hyrophilic (Fan & Huang, 2002).

Support layer in dynamic membrane filtration are mostly coarse sized membrane of different cheap materials such as woven and non-woven fabrics, stainless steel meshes and ceramic membranes (Ersahin, et al., 2012; Zhang, et al., 2014). The reasons for choosing these materials are: providing higher flux at lower TMP in a more cost beneficial way, easier cleaning and good anifouling properties (Poostchi, et al., 2015). However, there are several examples of successful formation of dynamic membrane on MF/UF membranes. For instance: dynamic membrane filtration application with MF/UF were investigated in drinking water facilities to remove some patogenic microorganisms. The results showed that the virus and other patogenic microorganisms removal are not solely dependent on the membrane pore size, instead the formation of dynamic cake layer on the membrane surface plays an important role in rejection of microorganisms (US EPA, 2001). More detailed investigation revealed that the virus removal by dynamic membrane is due to size exclusion and adsorption to particles in the cake layer (US EPA, 2001).

Dynamic membranes are created in two different ways; self -formed dynamic membrane (SFDM) and pre-coated dynamic membrane (Ersahin, et al., 2012; Poostchi, et al., 2015).

In SFDM the cake layer is formed by the colloids and/or high weight organics and other substances which are present in the feed stream (Ersahin, et al., 2012).

Pre-coated dynamic membrane is formed by passing a solution of one or more specific colloidal solution through the surface of the membrane (Ersahin, et al., 2012). Disadvantages of this form over SFDM is the dependency on extra materials and additives. Examples of these material are bio-diatomite, kaolinite, bio-enhanced powder activated carbon and hydrous metal oxides specially zirconium (Chu, et al., 2012; Ersahin, et al., 2014; Poostchi, et al., 2015). Chu et al., (2012) investigated the effect of bio-diotomite on purifying surface water. The test results demonstrated that bio-diotomite could provide permeate with turbidity around 0.11 – 0.25 NTU and high permeate flux (200-300 LMH) under water head difference of less than 70 cm (Chu, et al., 2012). They have also obtained satisfactory results for bacteria and coliform removal (Chu, et al., 2012).

2b.6.2. Dynamic membrane history

Dynamic membrane filtration was first introduced by some researchers at Oak Ridge laboratory in Tennessee who successfully formed a compact, thin and high permeable self-filtering layer by exposing the membrane to the passage of solution containing zirconium oxychloride for rejection of salts from pressurized feed stream (Ersahin, et al., 2012; Zhang, et al., 2014). Because dynamic membranes had provided satisfactory permeate flux and long service life for the support material on desalination of water, they became very attractive shortly after their introduction (Zhang, et al., 2014). However, later on, due to their limited salt rejection efficiency, they did not become widely spread and popularized in this field (Zhang, et al., 2014; Groves, et al., 1983). In 1980s the application of dynamic membrane were centred toward indutrial effluents such as food industry effluents, textile printing and dyeing effluents (Zhang, et al., 2014). Advantages of using dynamic membrane filtration for industrial effluents are, high permeate flux, lower modul costs, less fouling problems, higher mechnical stability and durability of support layer at high operation temperature and under wide range of pH (Groves, et al., 1983). In 1983, a group of researchers investigated the performance of dynamically formed membrane on a 0.5 µm stainless steel mesh and fiber glass membrane tube on varoius idustrial wastewaters. The results showed a limited decline in membrane flux and 90% of TOC and 95% of TS removal from polymer manufacturing effluent (Groves, et al., 1983). Another study was carried out on the performance of dual layer dynamic membrane in removing colloidal dyestuff, acetic acid, alkali and organic auxiliary

chemicals from four different dyeing effluents with the temperature between 60-75°C, pH in the range of 4-9, colour in the range of 2000-10000 coulur unit and TS in the range of 300-4500 mg/L. The results showed an average of 98% colour removal, 45% of acetic acid removal and almost 70% of TS removal (Groves, et al., 1983).

The first application of DM in treating aerobic domestic wastewater treatment was reported by Yamagiwas and some other researchers who sucessfully formed a dynamic membrane on a ceramic MF membrane. The cake layer formed on the membrane could reduce TOC with more than 70%. They also recommended the further application of dynamic membrane in treating domestic and agricultural wastewater (Yamagiwa, et al., 1991). Later on, the same researchers obtained 95% TOC by forming a dynamic cake layer on a UF membrane. The results of their experiments indicated that the cake layer plays a major role in SS rejection and carbon removal (Yamagiwa, et al., 1994).

In 2000, Kiso et al., successfully formed a dynamic membrane on 100µm nylon mesh feeding with synthetic domestic wastewater. The permeate from dynamic membrane had SS lower than 10 mg/L while the influent had SS up to 11500 mg/L. In addition, the dynamic membrane could effectively remove the BOD from the feed stream to lower than 5 mg/L (Kiso, et al., 2000).

Seo et al., (2002) investigated the performance of non-woven fabric filters installed in a submerged MBRs treating domestic wastewater. The SS, COD, TN and TP removal effeciency were 93.5%, 91.6%, 66% and 23% respectively (Seo, et al., 2002).

Fan and Huang (2002) have investigated the performance of gravity driven SFDM in treating real wastewater. They developed a cake layer on a 100 µm Dacron mesh material coupled with submerged MBR at a very low TMP (less than 5 cm of water head drop). The results have shown a successful COD and NH_3-N removal by 84.2% and 98.03% respectively (Fan and Huang, 2002). In addition, they have proved that the SFDM is composed of two components; gel layer and cake layer (Fan and Huang, 2002).

In 2005, Kiso et al have successfully formed dynamic membrane within only 5 minutes on a 100µm mesh filter in a gravity driven mesh bioreactor coupled with SBR (Kiso, et al., 2005). The obtained results proved that the dynamic membrane could effectively separate sludge particles (SS concentration of 10 mg/L in the filtrate within 5 minutes).

After roughly 55 minutes the SS concentration in the permeate reached to 1 mg/L. Moreover, high TN removal efficiency under intermittent aeration were achieved. It was also found that the increase in pH of the biomass in SBR results in higher filtration time (Kiso, et al., 2005). Li et al., (2012) conducted a short-term filtration research study on a 80 µm nylon mesh filter operated under dead end filtration and gravity driven mode. Dynamic membrane formed only 23 minutes after the filtration has started and the total resistance was 1.51×10^{9} m^{-1}. The membrane resistance analysis revealed that the cake layer resistance was responsible for 87.5%, pore blocking for 7.5% and the mesh filter itself was 5% of the total resistance (Li, et al., 2012). They have also concluded that for optimizing the formation of dynamic membrane it is important to have high stirring rate, high MLSS and low TMP (Li, et al., 2012).

Chu and some other researches (2014) have investigated the formation and characteristics of dynamic membrane filtration on a 38µm stainless steel using municipal wastewater. The results showed that dynamic membrane could provide permeate flux as high as 75 LMH while keeping the permeate quality at an acceptable level. During the study, dynamic membrane showed excellent particle rejection efficiency by providing permeate with turbidity below 9 NTU and SS around zero (Chu, et al., 2014). The Particle size distribution analysis of the cake layer showed a hierarchical structure with the increase from the top cake layer to the middle cake layer with the biggest particle size found in bottom cake layer (Chu, et al., 2014).

To date, much of the studies done on the application of dynamic membrane in domestic wastewater treatment were centred mainly on aerobic processes and much less is done on anaerobic processes. Since anaerobic processes are not the target of this mater project, only a little effort were put on reviewing available literature on the application of dynamic membrane in anaerobic wastewater treatment processes.

The applicability of dynamic membrane in anaerobic MBRs at different SRTs was also investigated by Ersahin et al. The results of their study showed that at SRT of 60 days, the membrane resistance was much higher than that of SRT of 40 days due to higher content of the gel layer. Also, the COD removal efficiency for both SRTs were the same and around 99% (Ersahin, et al., 2014).

2b.6.3. Parameters affecting the performance of dynamic membranes

There are several parameters which have critical role on performance of dynamic membranes. Some of these parameters are: membrane material and pore size, sludge properties and operation conditions (Jun, et al., 2007; Ahmed, et al., 2007; Duan, et al., 2011; Ersahin, et al., 2012; Ersahin, et al., 2013)

Dynamic membrane is about formation of a cake layer on a support layer and an effective formation of the cake layer is dependent on the retention of the particles on the surface of the support layer (Ersahin, et al., 2013). The material of support layer should have enough mechanical strength and wide range of pH tolerance to withstand the operating pressure as well as high fluctuation in pH and temperature (Ersahin, et al., 2012). Ersahin et al., (2013) have found that mono-monofilament filter cloth was more suitable for cake layer formation that staple filters (Ersahin, et al., 2013) Sludge type and characteristics of the sludge flocs are identified as other important parameters having direct impact not only on formation of dynamic membrane but also on total hydraulic resistance of the membrane (Fuchs, et al., 2005; Zhu, et al., 2006; Jun, et al., 2007). Aerobic granular sludge usually provides more permeable cake layer with lower resistance than that of floccular sludge. Also, membrane hydrophobicity/hydrophilicity, surface charge and roughness influence the cake layer formation and permeate quality. It is believed that membrane with negative charge are preferable (Shan, 2004). Membrane with smooth surface will trap fewer particles than membrane with more rough and more topographic surface. Thereofer, smoother membrane are less prone to fouling (Shan, 2004).

The morphological characteristics of the biomass is identified as of great importance in dynamic membrane formation. Floccular sludge has higher EPS content and are stickier than granular sludge therefore, the cake layer formed by them is more compact and has higher resistance against the flow. (Jun, et al., 2007; Jing-Feng, et al., 2012). June et al., investigated the filtration characteristics of aerobic granular sludge and activated sludge by running short term filtration tests on a 0.1µm fiber hollow membrane. The results indicated that the cake layer formed by aerobic granular sludge had higher permeability which lead to a permeate flux twice as great as that of activated sludge. The total hydraulic resistance for aerobic granular and floccular sludge were 16.91 and 8.75 m^{-1} respectively. The have also found that the cake layer resistance with 72.68% was the main component

of the total resistance. The main components of membrane fouling were proteins and polysaccharide materials which are mainly found in gel layer (Jun, et al., 2007). Other findings also proved that dynamic membrane formed by aerobic granular sludge had better permeability and more effective in membrane fouling reduction (Jing-Feng, et al., 2012).

Membrane pore size has also proved to have significant role in determination of permeate flux and the overall removal efficiency of the dynamic membrane, therefore, appropriate selection of the membrane pore size and the particle size of the dynamic membrane forming material are crucial (Ersahin, et al., 2012). It should be noted that since support materials have pore size greater than UF/MF membranes, permeate with higher turbidity at the initial stages of the filtration is normal (Ersahin, et al., 2012).

Wu et al investigated the filtration performance of dynamic membrane formed on 15, 65 and 100 μm Dacron meshes under TMP in the range of 15-65 mmH_2O. The results showed that the effluent turbidity from the three mesh filters is function of time and not the membrane pore size, and that the effluent turbidity decreased with the increase of time at a constant TMP. Permeate flux decreased very sharply at the initial stage of the filtration and then stabilized at a constant value. The highest permeate flux was observed in 100 μm mesh filter and the lowest in 15 μm mesh filer due to formation of gel layer. Therefore, it was expected to get the highest resistance for 15 μm mesh filters. Fortunately, the tests result met the expectation and the highest recorded resistance was obtained for the 15 μm mesh filter. The total hydraulic resistances were in the range of 10^9~10^{10} m^{-1} and for all the membranes, regardless of their pore size, the main resistance's component was cake layer (Wu, et al., no date)

Kiso et al., (2000) have investigated the filtration properties and effluent qualities of dynamic membrane formed on three nylon meshes with the pore size of 100, 200 and 500 μm. The SS concentration of the permeate was less than 10 mg/L for 100 μm and almost 100 mg/L for the other two. This result indicated that the membrane pore size had significant effect on the performance of the dynamic membrane filtration (Kiso, et al., 2000).

The MLSS concentration in the feed stream is also proved to have important role on formation and performance of the dynamic membrane. It is reported that high MLSS

results in fast cake layer formation (Fuchs, et al., 2005; Fuchs, et al., 2005; Chu and Li, 2006; Ersahin, et al., 2013). Fuchs et al., (2005) have found that at MLSS concentration above 7000 mg/L, the SS concentration in the permeate is more than twice as high as that of 4000 mg/L. In addition, higher MLSS lead to higher pore blocking behaviour of the mesh filter (Fuchs, et al., 2005). Later on, Chu and Li (2006) successfully formed a dynamic membrane on an industrial filter cloth in submerged MBRs operated with real wastewater. The results of their study revealed that the higher concentration of MLSS in the reactor can help and increase the formation of the cake layer but at the same time, deteriorating the permeate quality in terms of SS. The best performance and highest SS rejection was obtained at MLSS concentration less than 6000 mg/L (Chu and Li, 2006). But, there are some research showing the higher SS rejection in the permeate at very high MLSS concentration (Ersahin, et al., 2013).

Aeration rate, hydraulic retention time, shear forces, SRT and F/M ratio are also important parameters which should be taken into account for having proper installations and operations since these parameters can significantly change the biomass characteristics (Fuchs, et al., 2005; Ahmed, et al., 2007; Duan, et al., 2011; Yu, et al., 2016). Fuchs et al., (2005) have found that the increase in F/M ratio results in an increase in size of sludge flocs which finally contributed to higher SS and COD removal (Fuchs, et al., 2005). Also, they have found that higher aeration rate resulted in elevated SS concentration in the effluent (Fuchs, et al., 2005).

In 2011, Duan et al., have reported that the increase in SRT resulted in reduction of EPS and protein content of the activated sludge flocs (Duan, et al., 2011). However, by increasing the SRT, the type and the amount of microorganisms on the surface of dynamic membrane were more abundant. They have also reported that by increasing the SRT, the particle size distribution in the mixed liquor and dynamic membrane had decreasing trend (Duan, et al., 2011).

2b.7.Membrane resistance

When the particles of different size deposit on the membrane surface they form a layer. This built -up layer diminishes the permeate flux and increase the TMP over time and necessitates the periodic physical and chemical membrane cleaning (Shan, 2004; Field,

2010; Ersahin, et al., 2013). This loss of permeability is called fouling and it is a critical operational problem for membrane filtrations which may deteriorate the overall performance of them (Shan, 2004). In general, membrane fouling is caused first by, pore blocking fouling followed by cake layer formation. But in detail, main causes of membrane fouling are (Radjenovic, et al., 2008): (1)- growth of biofilm on the membrane surface, (2)-adsorption of macromolecules and colloids, (3)- precipitation of inorganic matter, and (4)-aging of the membrane.

There are various theories about membrane fouling among which resistance-in series is the most common and simplest one for low pressure membranes (Lee, et al., 2001). According to this theory, flux declination is caused by series of resistance, namely, membrane intrinsic resistance (Rm), cake layer resistance (Rc) and pore blockage resistance (Rb). The sum of these three components is called total hydraulic resistance (Buetehorn, et al., 2011). Studying the fouling mechanisms and membrane resistance in detail were not in the scope of this project, therefore, only short explanations of the resistance components are provided in the following text.

The membrane intrinsic resistance is dependent on the membrane material, membrane thickness, roughness, membrane pore size, porosity and some other morphological features (Shan, 2004). There are also several mathematical equations attempt to relate these parameters to the membrane resistance (Shan, 2004).

Cake layer resistance is due to the deposition of particles that can grow layer by layer on the membrane surface. it is reported that the physical and structural properties of the cake layer such as thickness, density, water content, and compressibility have major effect on membrane performance (Buetehorn, et al., 2011). For dynamic membranes and other low pressure membranes, the cake layer is the main component of the resistance (Shan, 2004; Jun, et al., 2007; Wu and He, 2012). This kind of fouling is good in a way that it blocks the passage of fine particles and colloids and reduce the pore blockage fouling of the membrane (Kiso, et al., 2000). In addition, cake layer fouling can be easily controlled by providing air bubbles in the bioreactor since these particles are large and they attach to the surface loosely (Wu and He, 2012).

In contrast, fine particles tend to form a more compact sludge layer which is very sticky and is not even removed by intensive aeration (Wu and He, 2012). Pore blocking

resistance is due to attachment and adsorption of these particle on the membrane surface and in the membrane pores (Radjenovic, et al., 2008). Therefore, sludge characteristics such as particle size, particle size distribution have effects on pore blocking resistance (Buetehorn, et al., 2011). Pore blocking resistance can be classified into reversible pore blocking Rb_{re} and irreversible pore blocking Rb_{ire} (Jiang, et al., 2008).

Chapter3: Materials and methods

This chapter deals with the materials and methodologies used during this work and it is structured in two sections. The first section, namely 'a' covers all the protocols and procedures for reactor design and run while, the second section, namely 'b' deals with the materials and methods for filtration part.

a) Materials and methodology for reactors' run

3a.1. Reactors setup

To investigate the performance of the aerobic granular sludge and compare its performance with that of floccular sludge, the seed sludge in one reactor was changed to form the aerobic granules while in the other reactor, the seed sludge was kept as the conventional floccular sludge.

To run the experiments, three parallel laboratory scale cylindrical column type SBRs were used. These reactors were previously designed and used in Water Environment and Chemistry Lab at Chalmers University of Technology. Influent was fed to the reactors from storage buckets at the loading rate of 2, 0.3, and 0.1 kg /(m^3.d) for COD, N, and P respectively.

The feed stream was introduced through the port located at the bottom of the reactors. The effluent was discharged from the outlet port located at approximately the middle height of the column resulting in volumetric exchange ratio of 0.43. Volumetric exchange ratio is ratio between the volume of treated water per cycle to the maximum reactor volume. After completion of each cycle, 1.30 L of water is withdrawn from each reactor while the total volume of water in the reactor is 3 L. Therefore, the volumetric exchange ratio is 0.43. Figure 0-1 shows a schematic view of the experiments' setup. A schematic view of the reactors is depicted in Figure 0-2 and physical properties of the reactors are listed in Table 0-1. The three reactors, R1, R2 and R3 were operated at identical conditions.

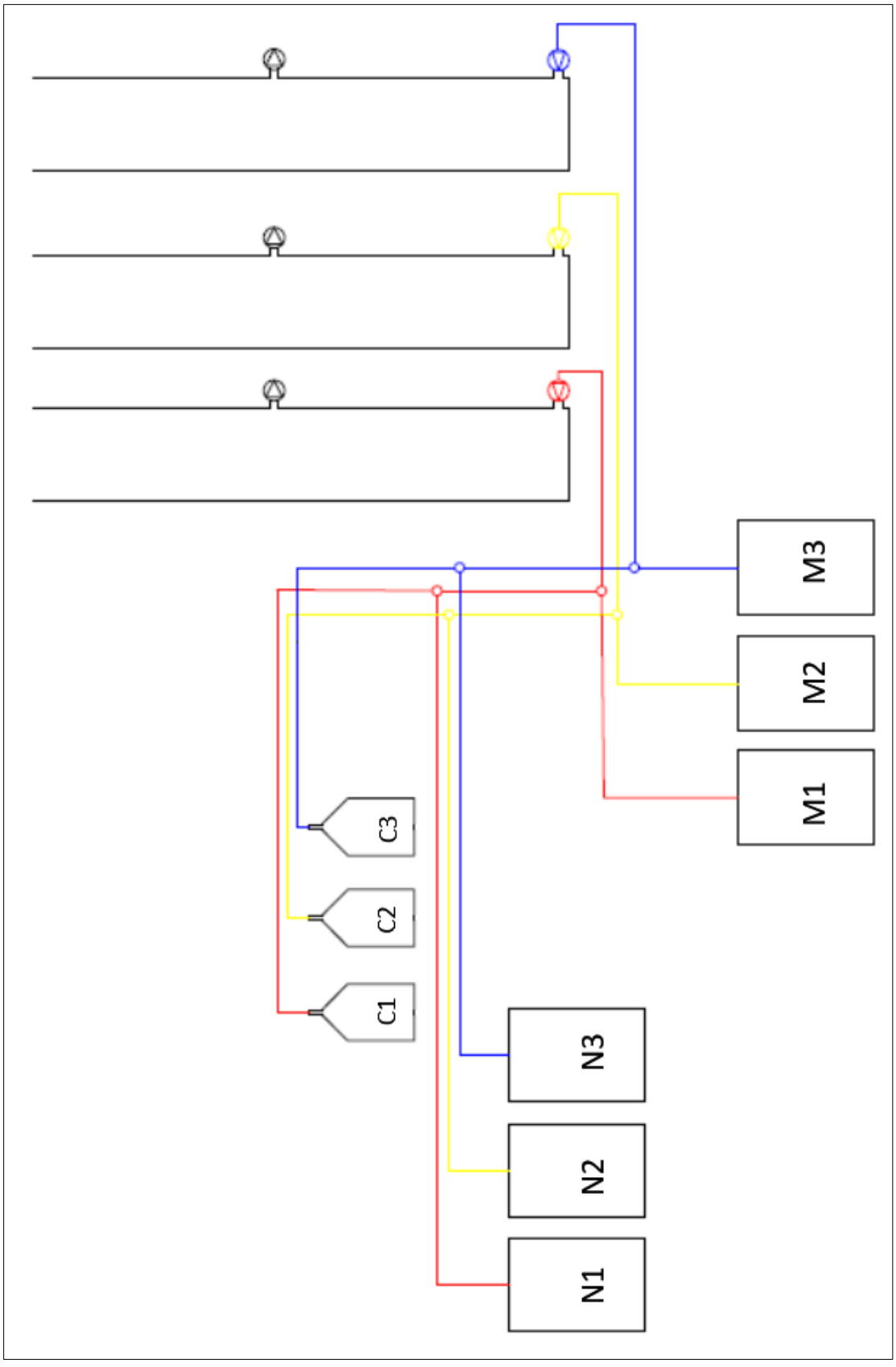

Figure 0-1. Schematic view of the system's layout

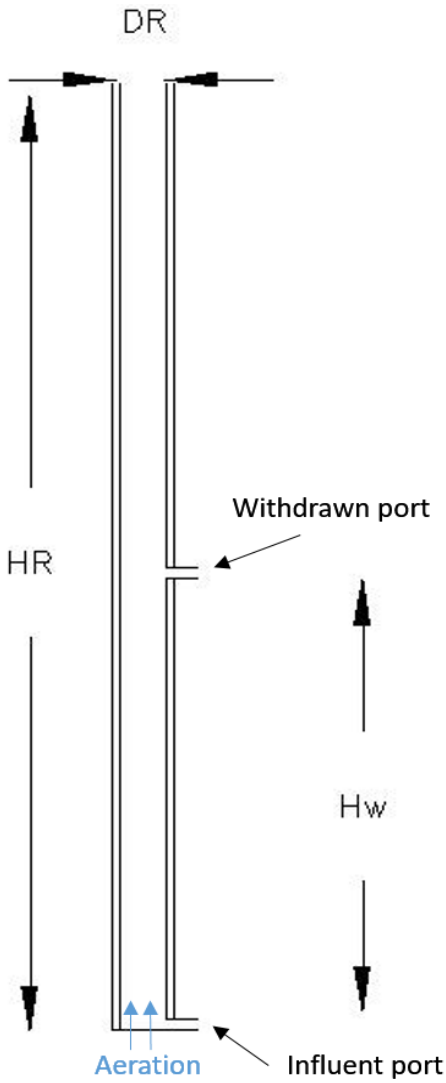

Figure 0-2. Schematic view of the reactors

Table 0-1. Physical properties of the reactors

Parameter	Value
Total Height (H_R)	1.32m
Internal Diameter(DR)	6 cm
Withdrawn Port Height (Hw)	63 cm
Exchange Ratio	0.43
Working Volume	3 L
Material	Acrylic glass

3a.2. Feed condition

The feed solution was comprised of nitrogen and phosphorous sources, organic source, micronutrients, and trace element source. The main sources of nitrogen and phosphorous were ammonium chloride and potassium dihydrogen phosphate. But from June 2016, due to some problems with the pH in the feed, another form of phosphate, dipotassium hydrogen phosphate, was also added. The nitrogen and phosphorous source solutions, N1-N3, were stored in the same bucket at the temperature of 4°C in the buckets of 30 litres. During the feeding phase, the substrate solution (nutrient source) was pumped into the reactor at the flow rate of 129 mL per minute and for a period of 5 minutes. The

micronutrient solutions, M1-M3 were prepared and stored in buckets of 30 litres and were kept in room temperature. The composition of microelement solution was referred to Tay et al. (2001a). The feeding phase and inflow rate to the reactor for the micronutrient source is the same as nutrient source. The only carbon source was sodium acetate solutions which were stored in the bottle of 2 litres, C1-C3. To avoid the degradation of the carbon source, they were kept separately from the other feed sources. During feeding phase, sodium acetate was pumped into the reactor with the flow of 6 mL per minute and for a period of 5 minutes.

Studies in the literature has shown that acetate as carbon source gives less filamentous growth and also favours biological phosphorous removing microorganisms. Table 0-2 to Table 0-6 show the composition of the feed stream.

Table 0-2. Organic source recipe

Organic Source	Final amount in 2 L (g)	Inlet concentration (mg/L)
CH_3COONa	85.5	972

Table 0-3 Nitrogen and phosphorous source recipe

Nutrients Source	Amount in 30 L (g)	Inlet concentration (mg/L)
NH_4CL	26.63	112.38 as TN
K_2HPO_4	8.37	37.62 as phosphorous
KH_2PO_4	3.39	

Table 0-4. Trace elements source recipe

Trace Elements	Stock Concentration (g/L)	Volume in 30 L (mL)	Inlet concentration (mg/L)
Microelement solution	-	30	
$FeSO_4.7H_2O$	0.012	25	4.88
$MgSO_4.7H_2O$	0.030	25	12.21
$CaCl_2$	0.030	26.2	12.8

Table 0-5. Composition of the microelements solution (Tay, et al., 2001a)

Microelement solution	Stock Concentration (g/L)	Amount in1 L (mL)	Inlet concentration (mg/L)
H_3BO_3	0.5	1.5	0.00036
$ZnCl_2$	0.5	1	0.00024
$CuCl_2.2H_2O$	0.038	1	0.00001
$MnSO_4.H_2O$	0.5	1	0.00024
$AlCl_3$	0.5	1	0.00024
$CoCl_2.6H_2O$	0.5	1	0.00024
$NiCl_2$	0.5	1	0.00024
$(NH_4)_6MO_7O_{24}.4H_2O$	0.5	1	0.00024

The targeted loads for COD, N and P and their theoretical concentration in the feed stream are listed in Table 0-6.

Table 0-6. Targeted load and theoretical concentration for the substrates in the influent

Substrate	Targeted load ($kg/m^3.d$)	Theoretical concentration (mg/L)
COD	2	757
N	0.3	112
P	0.1	38

3a.3. Experiments time schedule

The experiments were started from January 2016 and since the middle of the experiments the granules were dominated and covered by filamentous bacteria, the experiments were conducted in two periods. The first period was from January to July 2016 and the reactors were cultivated with seed sludge 1. The second period was from July 2016-September

2016 and the reactors were seeded with the seed sludge 2. The feed stream composition and the reactors operation were similar for both runs and only the seed sludge characteristics differed.

The seed sludge for both periods was obtained from the aeration tank of the activated sludge process from Hammargårds wastewater treatment plant located at Kungsbacka municipality. The reactors were then started up the same day. More detailed information about the operational conditions in each period is provided in Table 0-7 and Table 0-8.

Table 0-7. Detailed information for the first run

First period (seed sludge 1)			
Reactors in operation	Targeted sludge type	Date of start-up	Date of shut down
R2	Flocculated	Feb 2nd 2016	ongoing
R3	Granulated	Feb 2nd 2016	July 15th 2016

Table 0-8. Detailed information for the second run

Second period (seed sludge 2)			
Reactors in operation	Targeted sludge type	Date of start-up	Date of shut down
R1	Flocculated	July 5th 2016	October 18th 2016
R3	Granulated	July 5th 2016	September 9th 2016

The seed sludge particles were initially tiny and had relatively black colour before inoculation. But once it was poured in the reactors and aerated the colour was started to change from black to dark brown and finally to light brown. Figure 0-3 shows the picture of the seed sludge. More detailed information about the seed sludge characteristics are listed in Table 0-9.

Figure 0-3. Seed sludge from Hammargården WWTP

Table 0-9. Detailed information about the seed sludge

	Seed sludge 1 (2016.02.02)	Seed sludge 2 (2016.07.05)
T.S.S (mg/L)	4170	2720
VSS (mg/L)	3180	2260
SVI_{30} (mL/g)	80.33	84.5
MLVSS/MLSS	0.76	0.83

3a.4. Cycle time

In this work, all the reactors were operated in successive cycle of 4 hours, 6 cycles per day and comprehended feeding period of 5 minutes. The only difference was the aeration time. R1 and R2 which were targeting development of floccular sludge had aeration time of 143 minutes while R3 which was targeted to grow granular sludge had longer aeration time and shorter settling time. R1 and R2 had 30 minutes of setting time while R3 had variable settling time from 30 minutes at the beginning to 2 minutes at the end. Figure

0-4 and Figure 0-5 illustrate the phases' duration of one cycle operation for each of the reactors.

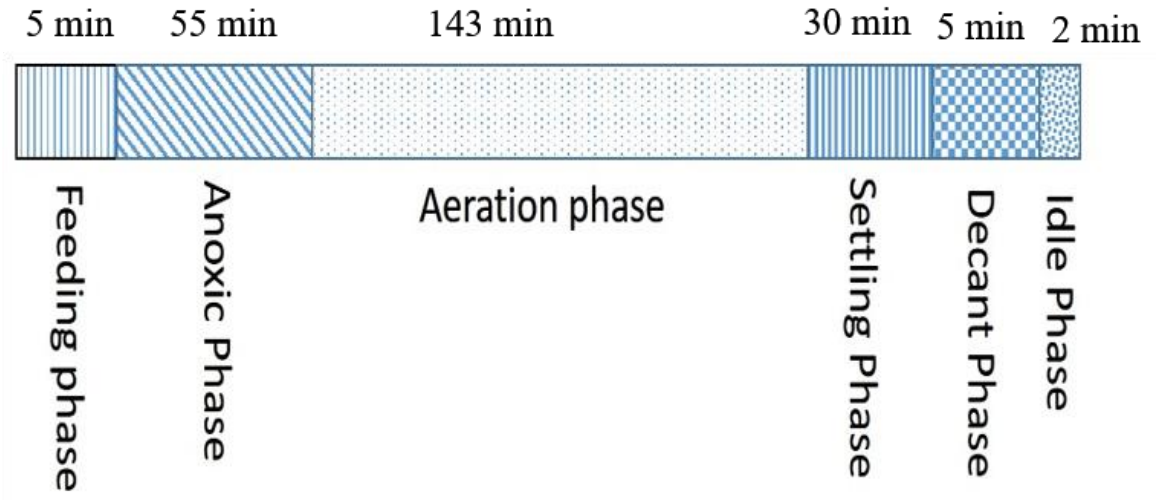

Figure 0-4. One cycle profile of R1 and R2 (floccular sludge)

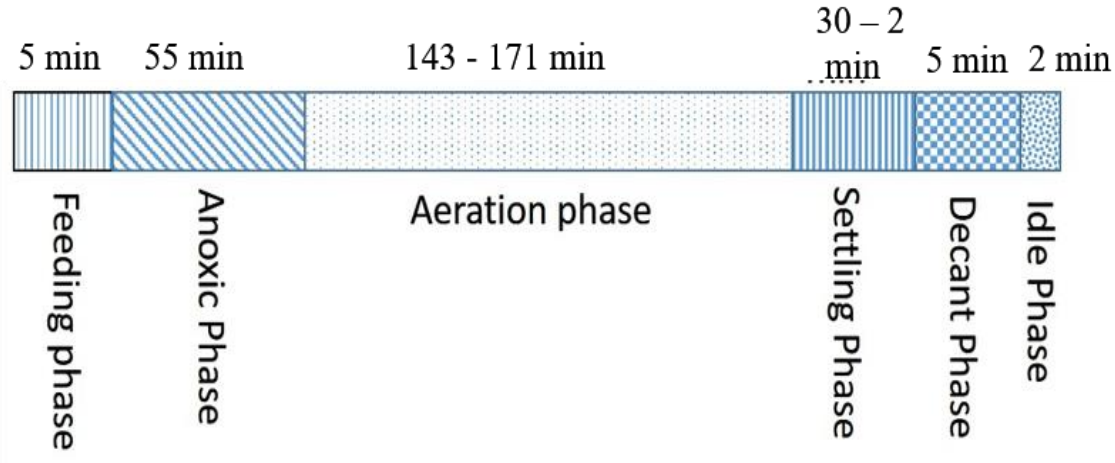

Figure 0-5. One cycle profile of R3 (granular sludge)

The substrate (feed stream) was supplied in a short period of time for allowing the SND and also the motivation for having static fill followed by and anoxic phase was to favouring the condition for slow-growing microorganisms such as PAOs and ensuring the simultaneous COD, nitrogen and phosphate removal situation. The volume and rate of influent and effluent during static feed and decant phase were controlled by peristaltic pumps. The aeration during react phase was accomplished by fine air bubble through a circular porous stone with diameter of 5 cm installed at the bottom of each rector. The air flow was supplied to the system by an air pump with the superficial up-flow air velocity of 1.5 cm/s.

3a.5. Sludge wasting

In SBRs, sludge wasting can be done either in react phase or idle phase (IWA, 2013). In this project, the sludge wasting was done near the end of aeration phase from mixed liquor to simply maintain the sludge age. Every day, from Monday to Friday, 100 mL of sludge was taken out from each reactor approximately in the last 30 minutes of the aeration phase. Sludge withdrawal both for sampling and wasting, conducted at equal amount from different height of the reactor. The reason for this is to have a good representative sample of the microbial community present in the reactors and also because of the PAOs bacteria are bigger and denser and they have the advantages of living at the bottom of the reactor, therefore, if the samples and sludge wasting happen only within the bottom of the reactor, then the phosphate removal will be deteriorated (Winkler, 2012).

3a.6. Granular sludge formation

For generating granular sludge and successfully applying the aerobic granular technology in laboratory scale the fulfilments of the following conditions were ensured.

- Conversion of rapidly biodegradable substrates into slowly biodegradable stored substrate by applying a feast/famine regime
- Selection of rapid settling aerobic granules by shortening the settling times
- Sufficiently high aeration rate during aeration phase

The straightforward approach for aerobic granules formation in SBRs is shortening the settling time (de-Kreuk & van-Loosdrecht, 2004). Therefore, in this project the same approach was done. During the first run, R2 and R3 had the same aeration time and settling time as in the beginning of the experiment. However, the settling time in R3 was decreased gradually to 2 minutes by increasing the aeration time. This helps select for high settling microorganisms. The detailed information on settling time alteration for both runs are found in Appendix Ⅰ.

3a.7. Analytical methods

For evaluating the performance of the reactors, several tests were carried out both on the sludge and on the effluent. All the tests were run according to standard methods. In the following section, more detailed information about the type of the tests, and machines which were used are given.

3a.7.1. Sludge analysis

For collecting samples, 100 ml of the sludge was taken during the aeration phase twice per week and the following tests were carried out on it. For having a good and representative sample, the sample was taken from top, bottom and middle of the reactor and thoroughly mixed before analysis.

- MLSS/MLVSS

Mixed liquor suspended solids (MLSS) was measured to determine the concentration of total suspended solids of the sludge in the reactors. Since MLSS includes inorganic and non-biological matter in addition to biomass or organic matter, mixed liquor volatile suspended solids (MLVSS) was also measured to determine the organic fraction of the activated sludge in the reactor. Both MLSS and MLVSS were measured according to standard method (APHA, 1995). For more clarification, an example of calculating MLSS and MLVSS is given below.

Weight of filter + tray (g)	**Weight of filter + tray+ sample after 105°C (g)**	**Weight of filter + tray + sample after 550°C (g)**	**Sample Volume(mL)**
1.7179	1.7611	1.7249	5

$$MLSS = \frac{(1.7611 - 1.7179) \times 10^6}{5} = 8640\ \frac{mg}{L}$$

$$MLVSS = \frac{(1.7611 - 1.7249) \times 10^6}{5} = 7240\ \frac{mg}{L}$$

The filter which was used for SS tests was Whatman Glass Microfiber grade GF/A with the 1.6 µm pore size.

3a.7.2. Effluent analysis

Two times per week, sufficient amount of effluent was collected from the reactors, from the same phase as the sludge were taken, and the samples were analysed on total and volatile suspended solids. For having precise result, the tests were carried out immediately after that the samples were collected.

- TSS/VSS

Total suspended solids (TSS) and volatile suspended solids (VSS) were measured according to standard methods (APHA, 1995) During these tests, sometime happened that the TSS concentration in the effluent gave negative results which indicate an error in calculation or weighing. Therefore, to prevent this, these tests were duplicated.

- Ion Chromatography

For measuring the concentration of some anions and cations such as NO^-_3, NO^-_2, PO_4^{3-}, CH_3COO^- and NH^+_4, the Thermo Scientific Dionex ICS-900 series ion chromatograph was used. Prior to putting samples into the machine, the samples were filtered through 0.2 µm syringe filters and diluted to the ratio of 1:10 with milli-Q water.

- TOC/TN

Total Organic carbon and total nitrogen in the effluent samples were measured by Shimadzu TOC-V_{CPH} machine with an ASI-V autosampler. Prior to putting samples into the machine, the samples were filtered through 0.2 µm syringe filters. Therefore, the measurement for organic carbon is only the dissolved fraction (DOC).

- pH

The continuous pH recording was achieved by means of pH electrodes extended deep into the reactor and connected to the computer using PicoLog® data logging software. Frequently, for getting the more accurate reading and checking the performance of the pH electrodes, portable pH meter was used.

3a.7.3. Cycle analysis

Cycle analysis was performed to better understanding the reduction of different substrate at different phases of a single cycle. The cycle analysis was performed once on the 14th of June the first run when R2 and R3 were in operation and once on the 15th of September for R1 and R3 which were started later.

For running the cycle analysis, the samples were taken from the reactors as follows. During the anoxic phase and the first 30 minutes of aeration phase, samples were taken every 10 minutes and the rest of the cycle, samples were taken every 30 minutes. Later on, the samples were analysed for TOC and other anion and cation concentrations. For determining their concentration, IC test was performed. The IC samples were prepared as explained in section 3a.7.2.

b) Materials and methodology for filtration part

3b. Membrane filtration

To compare the filtration characteristics of the aerobic granular sludge and floccular sludge, short term filtration tests were conducted. The results obtained from these short-term tests can later be used as a baseline for future research. Short term filtration means that the tests were stopped when the membrane was clogged. Therefore, periodic backwash and chemical cleanings are not included in these tests.

3b.1 Experimental setup

The experimental setup seen in Figure 0-6 was installed at Chalmers Water Environment Chemistry lab. The setup consisted of a filter column, a one layer 100 µm Nylon disc membrane, pipes and pumps for carrying the feed stream and the permeate. The filter column was equipped with the overflow port to recirculate the feed stream between the storage bucket and the filter column. Figure 0-7 shows physical characteristics of the filter column and

Table *0-10* lists some of the mesh filter's properties.

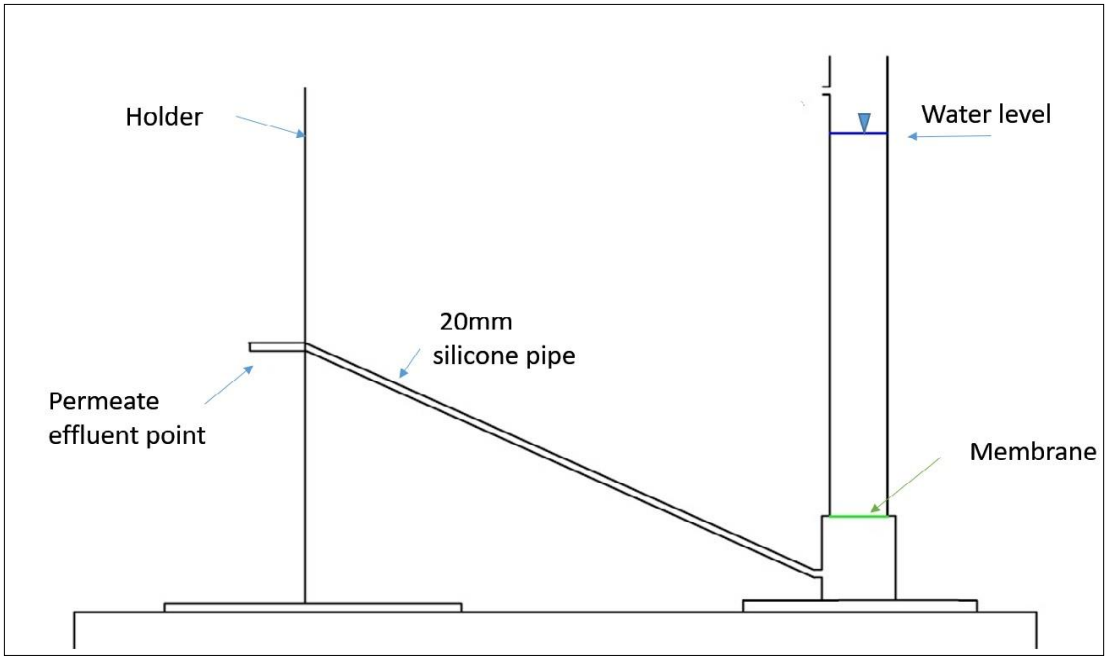

Figure 0-6. Filtration set-up

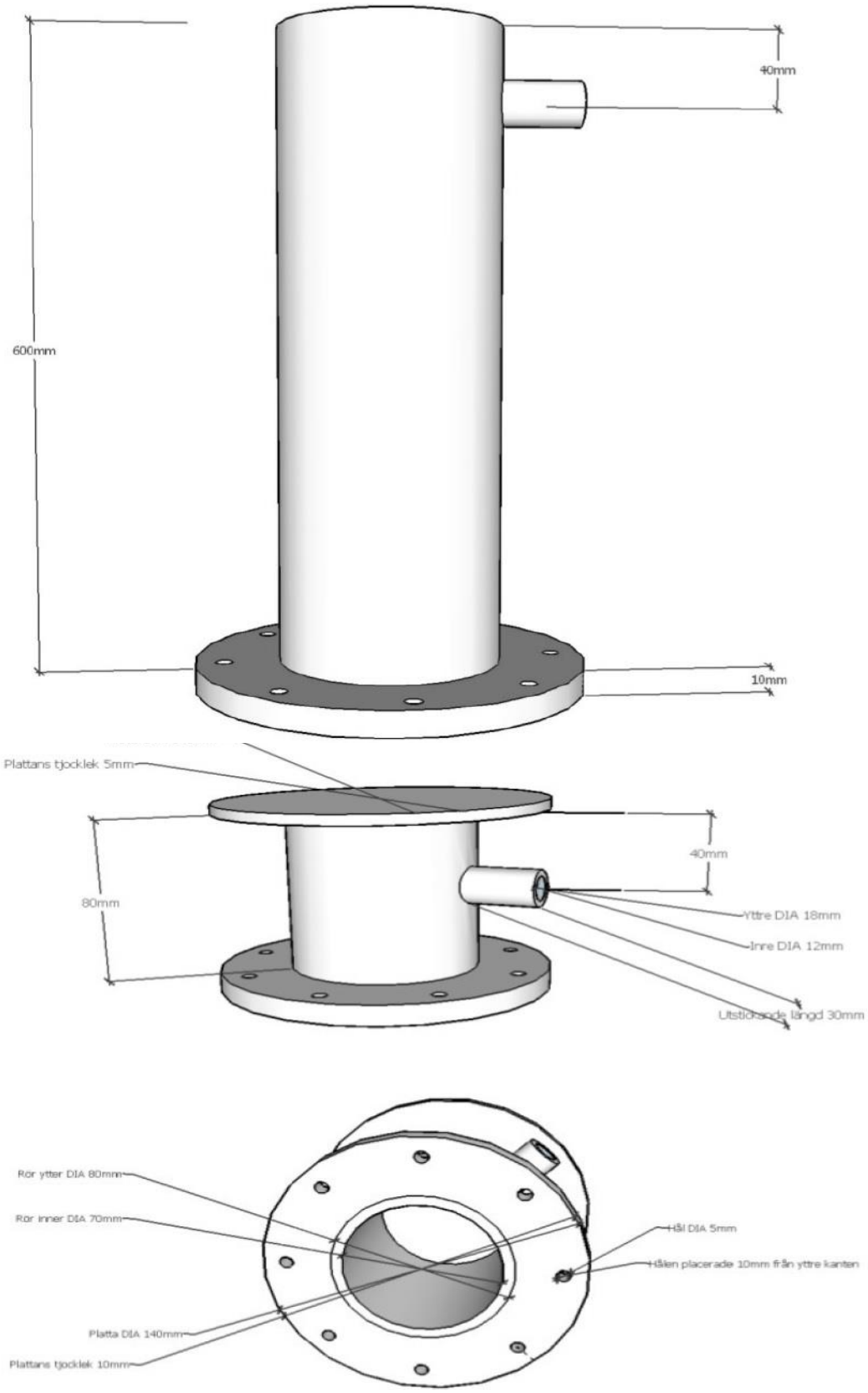

Figure 0-7. Physical Characteristics of the filter column

Table 0-10. Membrane's specifications

Brand name	Spectra/Mesh by SPECTRUM©
Filter code	145908
Filtration area (m^2)	0.0038
Filter diameter(mm)/ Open area (%)	90, / 47%
Filter material	Woven nylon
Water affinity/pH resistance	Hydrophilic/pH:3-10

3b.2 Experiments

The filtrations tests carried out in this project are divided in to three series of experiment and each of them was run in duplicate or triplicate.

1. Filtration of the sludge in R2 and R3
2. Filtration of the effluent from R2 and R3
3. Filtration of concentrated kaolin suspension using sludge from R2 and R3

Prior to initiating any tests, the membrane was thoroughly rinsed with deionitzed water and soaked in deionized water for 12 hours. This preparation was done for removing possible contamination and for prohibiting the membrane to adsorb any filtration water. All the above tests, as well as duplicate tests, a new mesh was used. This was done to avoid the influence of possible remaining foulants from previous filtration test. Also, some operation conditions were assumed to be constant for all the experiments, these conditions are as follow

1- The average room temperature in the lab was assumed to be 20 °C

2- Dynamic viscosity of water (μ) at 20 was assumed to be 1.002 Pa.s

3- Density of water (ρ) is assumed to be 1000 kg/m^3

4- Gravitational acceleration, g, is assumed to be 9.81 m/s^2

5- Except in experiments using kaolin solution, all the other experiments were run without applying stirrer to avoid detachment of the cake layer from the membrane surface.

Almost all the filtration tests were carried out in gravity driven mode and a few of them were run by using suction pump. For filtration tests in gravity-driven mode, the TMP was recorded by measuring the water head difference between both sides of the membrane. The filtration rate was obtained by numerically dividing volume by the time. In the following text a comprehensive explanation about the methodology and materials for each of the tests are given.

3b.2.1. Filtration of the sludge in R2 and R3: methodology and affiliated equipment

The main aim of this test was to measure the cake layer resistance of the two kinds of sludge, floccular and granular sludge. Thus, a known volume of sludge was taken out from the reactors and diluted by the ratio of 2:1 with tap water. Later on, a known volume of this suspension was filtered through the membrane and the TMP and permeate flux were recorded. To check the reasonability of the results each tests were repeated again some months later. However, during the repetition of the tests, the sludge in R2 had become semi-floccular form and the sludge in R3 had been dominated by fungi. The 5-step procedure of conducting this test is provided in Figure 0-8. The procedure to calculate the resistance' components are provided in section 3b.3.

..

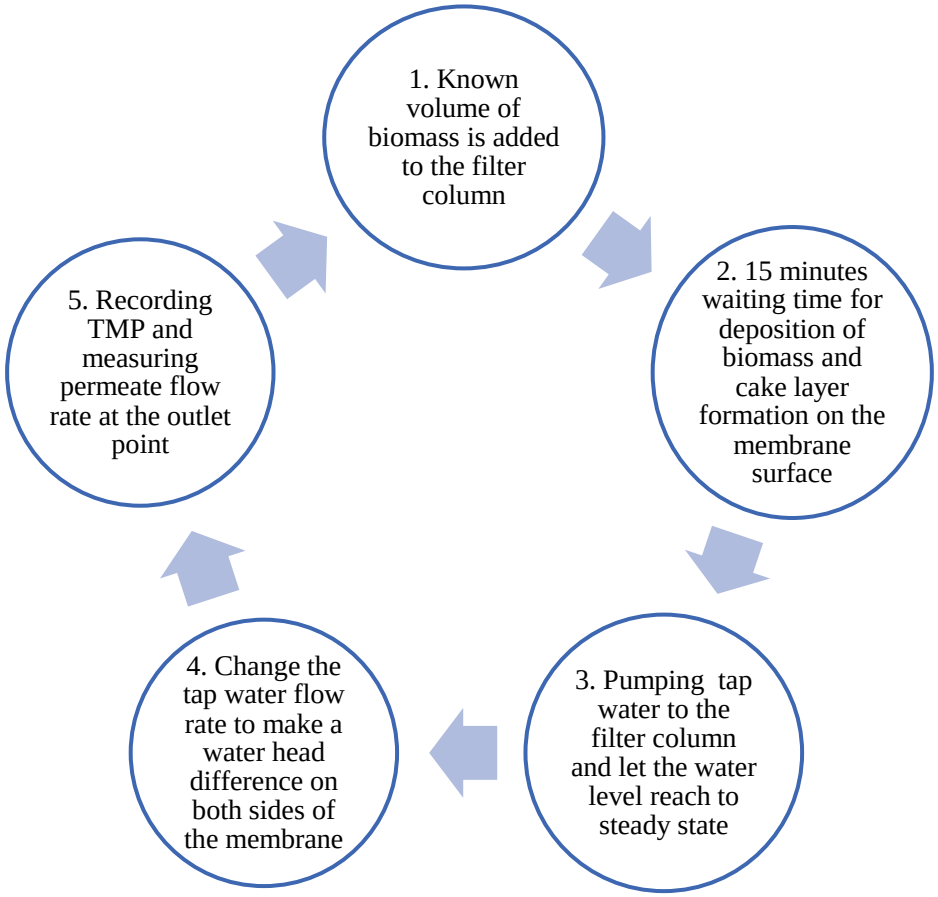

Figure 0-8. Methodology for measuring cake layer resistance of the sludge in R2 and R3

It should be noted that this cycle was stopped when the membrane clogged and the permeate flux through the membrane was negligible. More detailed information about the time schedule of this test can be found in Table 0-11.

Table 0-11. Time Schedule of the cake layer resistance measurement

	First run	**Second run**
R2 (floccular sludge)	April 18th 2016	June 20th 2016
R3 (granular sludge)	April 25th 2016	June 27th 2016

3b.2.2. Filtration of the effluents from R2 and R3: methodology and affiliated equipment

As it was mentioned previously, when a solution containing activated sludge flocs passes through the membrane, some of these particles and colloids will deposit on the membrane surface and some will partially block the membrane voids, thus, gradually a sludge layer is formed on top of the membrane, dynamic membrane. This cake layer later on acts as a real filter. The aim of this batch of testes were to develop a dynamic membrane on top of the membrane and also investigate the efficiency of this dynamic membrane in removing turbidity causing particles. The feed solution from the bucket was carried to the filter column by means of a Heidolph® peristaltic pump and the turbidity in the feed stream and permeate were measure by a portable turbidity meter, Hach® DR-890 and 10 mL sample cells.

Below the methodology of this test is depicted, Figure 0-9.

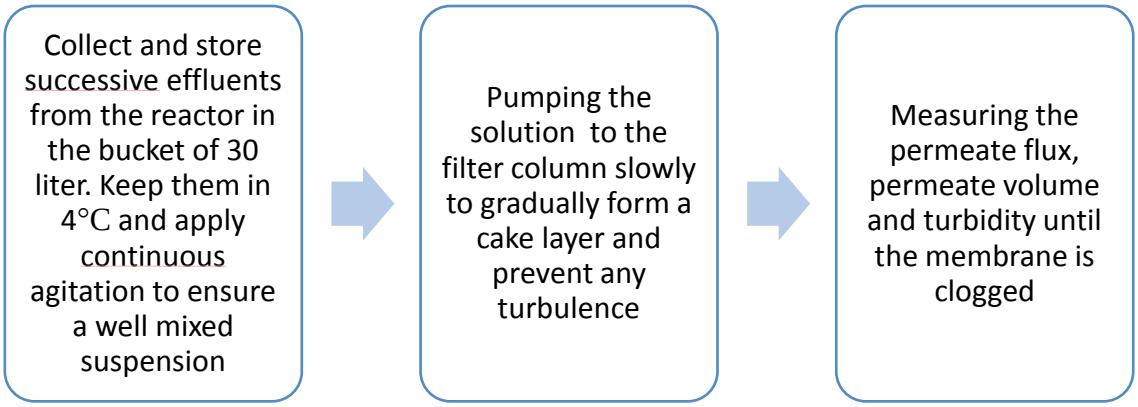

Figure 0-9. Methodology to develop dynamic membrane using effluent from

This batch of tests was run several times to form a reasonable dynamic membrane. Below is the time schedule for the tests. All the tests were performed in the year 2016. Chapter 4 outlines the best results and the rest can be found in the appendix section.

	First run	Second run	Third run	Fourth run	Fifths run
R2	May 20th	May 24th	May 30th	-	-
R3	May 11th	May 13th	May 17th	June 3rd	June 7th

3b.2.3. Filtration of concentrated kaolin suspension using sludge from R2 and R3

The main motivation behind conducting this series of experiment was to understand the adsorption capacity of the sludge cake layer. Therefore, kaolin was chosen as the model compound and a methodology was proposed for running the batch tests. Below, in Figure 0-10 and Figure 0-11, the 2-step procedure for performing this series of experiments are given. Also, the procedure for selecting the appropriate kaolin suspension concentration is explained later on in this section.

Kaolin particles tend to settle quite fast and deposit in the pipes and at the bottom of the filter column, to avoid this, the kaolin solution in the storage bucket was constantly mixed with mechanical mixer. Also, the filter column was placed on top of a stirrer and a magnetic stirred was put at the bottom end of the filter column. Figure 0-12. Kaolin suspension (in the filter column) and the installations Figure 0-12 shows the installation for these experiments.

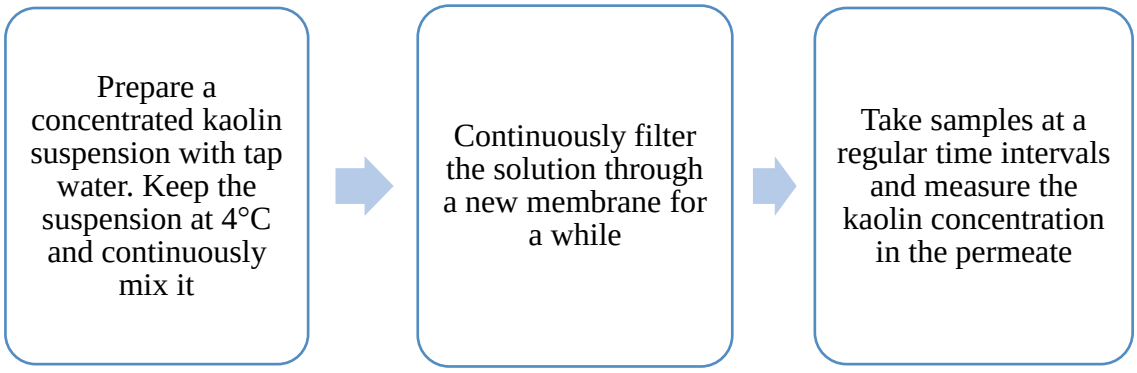

Figure 0-10. Kaolin adsorption measurement test: Step 1

.

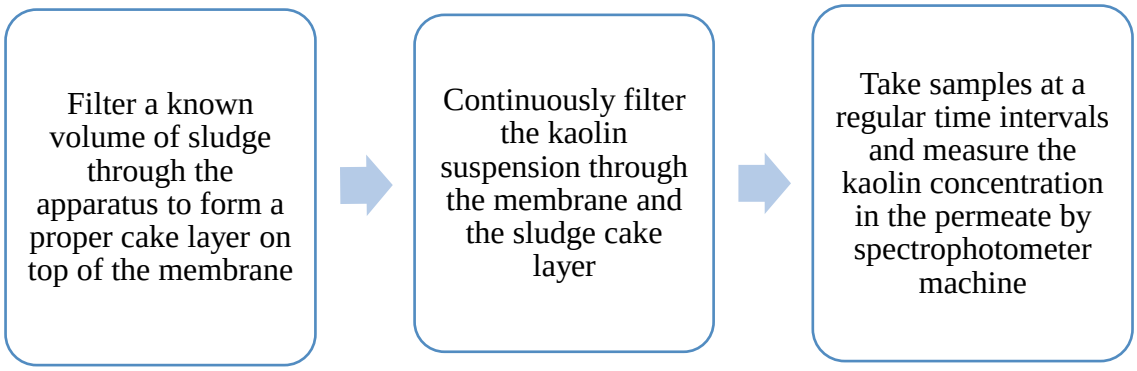

Figure 0-11. Kaolin adsorption measurement test: Step 2

Figure 0-12. Kaolin suspension (in the filter column) and the installations

For preparing the kaolin suspension the following steps were completed.

- Find the optimum wavelength using absorption Spectrum

Optimum wavelength is wavelength at which the absorption is maximum. To find that, a stock solution of kaolin was prepared and by dilution, several concentrations of kaolin suspensions were prepared. The absorbance of each sample was measured at different wavelength by a Shimazdu UV-1800 Spectrophotometer. Later, absorption spectrum (absorbance vs wavelength graph) was plotted and the best wavelength at which the absorbance is near to 1 was chosen. Here, 400 nm.

- Find the optimum concentration

The optimum concentration is the concentration at which the absorption is close to one. Therefore, several concentrations of kaolin solution were prepared and their absorption at 400 nm wavelength were measured.

- Find the relation between concentration and absorbance

The substance's concentration and its absorbance are proportional. According to the Beer's law, there is a simple and straight relationship between the substance's concentration and its absorbance especially at low concentrations. The Beer's law makes it possible to determine the concentration of a sample by simply measuring the sample's absorbance at that specific wavelength (here 400 nm). This is done by plotting the calibration curve and best-fit line for the concentration vs absorbance. The linear equation for the best-fit line is the one which is used to determine the unknown concentration.

Based on the above explanation, a batch kaolin suspension was prepared and by dilution different concentration were prepared and stored in 15 mL yellow falcon tube. Then the absorbance of each sample was measured at 400 nm wavelength.

3b.3. Hydraulic resistance analysis

The basis for analysis of the total hydraulic resistance against the flow is Darcy's law (Grenier, et al., 2008) and it can be calculated using Eqs. (6) to (10) (Li, et al., 2012).

$$TMP = \mu * J * R_t \quad \text{Eq(6)}$$

$$R_t = R_m + R_b + R_c \quad \text{Eq(7)}$$

$$TMP = \rho * g * \Delta H \quad \text{Eq(8)}$$

$$J = \frac{Q}{A} \quad \text{Eq(9)}$$

$$A = 0.25 \times \pi D^2 \quad \text{Eq(10)}$$

Where in Eq. (6), TMP is pressure gradient or transmembrane pressure (Pa), μ is dynamic viscosity of permeate (here it is water) at the operation temperature, Rt is total hydraulic resistance against the flow (m^{-1}) and J is the permeate flux ($m^3/m^2.s$) that can be calculated using Eq. (9). Total hydraulic resistance itself is comprised of three different components which can be calculated by Eq. (7). In this equation, Rm is the membrane intrinsic

resistance, Rb is pore blocking resistance and Rc is cake layer resistance. In Eq. (8), ρ is the density of water (kg/m^3) which is assumed to be 1000 for all the tests. ΔH is the water height difference between the filter column and effluent port (m) and g is the gravitational acceleration (m/s^2). In Eq. (9), Q is the flow of the permeate in m^3/s and A is the total membrane area (m^2). Total membrane area can be calculated using Eq. (10) in which A is the membrane surface area (m^2), and D is the membrane diameter (m). Therefore, according to the above equations the individual fractions of filtration resistance (Rm, Rb and Rc) can be estimated. Below the experimental procedure to determine each resistance components are provided.

3b.3.1. Membrane intrinsic resistance

Membrane intrinsic resistance, Rm, was estimated by measuring the steady state flux of deionized water under a given TMP. Deionized water was continuously passed through a clean and new membrane and the water height difference between the filter column and the effluent port was recorded to obtain transmembrane pressure (Eq.8). Also, the permeate flow at the effluent port was recorded to obtain the permeate flux (Eq.9).

3b.3.2. Pore blocking resistance

For measuring the pore blocking resistance, Rb, the fouled mesh was flushed with deionized water and cleaned with the soft sponge (here it refers as water rinsed membrane). Then deionized water was filtered through the water rinsed membrane and the resistance was calculated using Eqs. (6) to (7). The calculated resistance is Rm+Rb, therefore, by subtracting the membrane intrinsic resistance from the calculate resistance, the pore blocking resistance could be obtained.

3b.3.3. Cake layer resistance

Cake layer resistance was briefly explained above. But for more clarification on how the experiments conducted and how the resistance components calculated, following examples are provided. The membrane used in the following examples was not replaced with another one.

- Example of membrane intrinsic resistance

For more clarification, examples of membrane intrinsic resistance and cake layer resistance measurements are provided.

Table 0-12. An example of TMP and flux measurements to obtain membrane intrinsic resistance

ΔH (cm)	Flow (mL/s)	TMP (kPa)	Flux ($m^3/m^2.s$)
0	0	0	0
12.3	114.29	1.206	0.030
18.5	170.10	1.814	0.0447
8	85	0.784	0.0223
5	24.32	0.490	0.0064
17	166.27	1.667	0.0437
6	57.80	0.588	0.0152

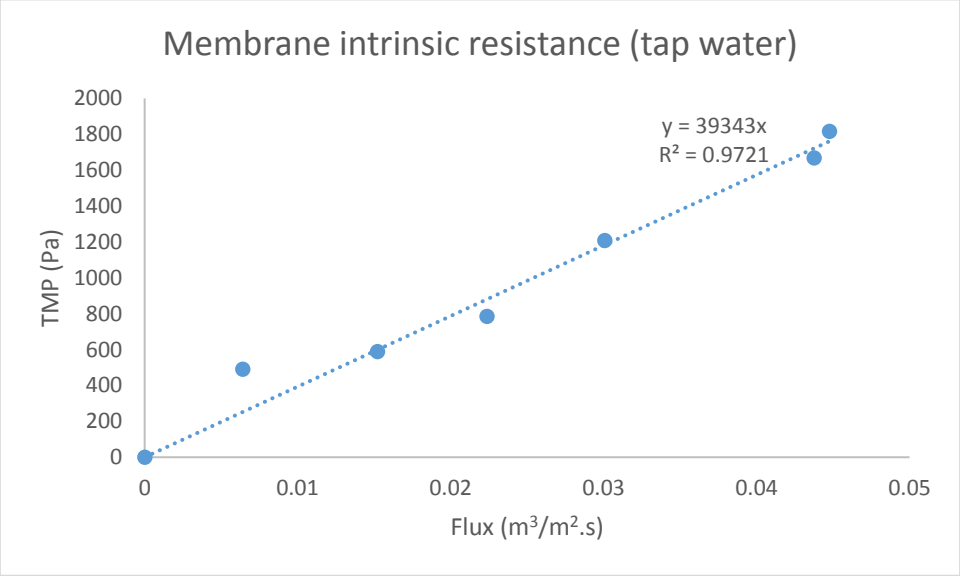

Figure 0-13. TMP vs flux using clean membrane and tap water

According to the graph above, y represents TMP, *x* represents the permeate flux, J, and the slope of the line is 39343 which is equal to μ×Rt. Since only tap water is used and the membrane was new, the only resistance against the flow is Rm. In other words, the term Rt in Eq. (6) has only one component which is Rm.

$$\frac{TMP}{J} = \frac{y}{x} = \mu \times Rm = 39343$$

$$Rm = \frac{39343}{\mu} = \frac{39343 \times 1000}{1.002} = 3.926 \times 10^7\ m^{-1}$$

- Example of cake layer resistance

An example of calculating the cake layer resistance is given in Table 0-13 and Figure 0-14

Table 0-13. An example of TMP and flux measurements to obtain cake layer resistance

ΔH (cm)	Flow (mL/s)	TMP (kPa)	Flux ($m^3/m^2.s$)
5.5	40	0.539	0.0105
11.5	101.98	1.128	0.027
8.5	93.75	0.833	0.0246
18	159.81	1.765	0.0420
23	159.79	2.256	0.0420

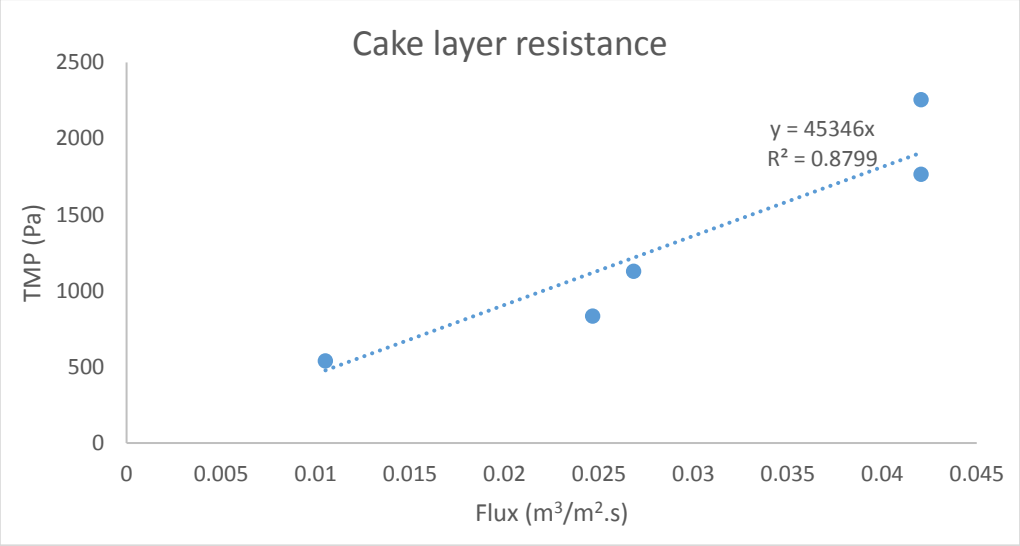

Figure 0-14. TMP vs Flux using tap water and sludge layer developed on top of the membrane

According to Figure 0-14, Y represents TMP, X represents for permeate flux and 45346 represents μ×Rt. This time, Rt has two components, Rm which was calculated before and Rc which is going to be calculated.

$$\frac{\text{TMP}}{\text{J}} = \frac{\text{Y}}{\text{x}} = \mu \times \text{Rt} = 45346$$

$$\text{Rt} = 45346 \times \frac{1000}{1.002} = 4.52 \times 10^7$$

$$\text{Rt} = \text{Rm} + \text{Rc}$$

$$Rc = (4.52 \times 10^7) - (3.926 \times 10^7) = 0.6 \times 10^7 \ m^{-1}$$

- Example of Pore blocking resistance

Table 0-14 lists one of the experiments done to measure the pore blockage resistance.

Table 0-14. An example of TMP and flux measurements to obtain pore blockage resistance

ΔH (cm)	Flow (mL/s)	TMP (kPa)	Flux ($m^3/m^2.s$)
0	0	0	0
6.37	46.43	0.624	0.0122
4.87	9.02	0.477	0.0023
5.87	28.83	0.575	0.0075
8.77	87.35	0.860	0.0229
13.27	121.39	1.301	0.0320
15.77	139.92	1.547	0.0368

TMP vs flux graph is depicted in Figure 0-15: The equation of the best fit line, gives the pore blockage resistance.

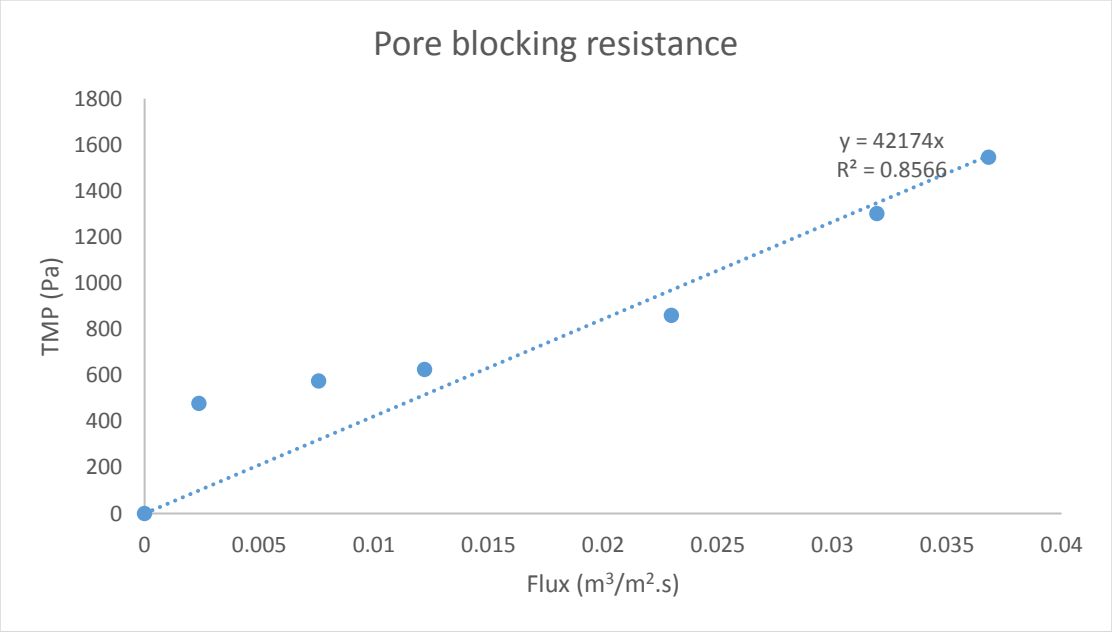

Figure 0-15. An example of pore blockage resistance using a water rinsed membrane and tap water

$$\frac{TMP}{J} = \frac{Y}{x} = \mu \times Rt = 42174$$

$$\mathrm{Rt} = 42174 \times \frac{1000}{1.002} = 4.2 \times 10^7$$

$$\mathrm{Rt} = \mathrm{Rm} + \mathrm{Rb}$$

$$\mathrm{Rb} = (4.2 \times 10^7) - (3.9 \times 10^7) = 0.3 \times 10^7 \ \ m^{-1}$$

Chapter4: Results and discussion

The main results and findings are outlined and discussed in this chapter. This chapter is structured in two parts. Part 'a' covers results and discussions in the aerobic granulation and part 'b' covers that of membrane filtration tests.

a) Aerobic granulation

The aerobic granulation experiments were started in February 2016 and continued to December 2016. The experiments were run in two parts. In the following section, the results from the first run are presented and discussed.

4a.1. First run

The first run was initiated on 2nd February 2016 and only R2 and R3 were in operation. From this date, R2 was in operation for 295 days (until November 22nd) and R3 for 162 days (when the reactor was shut down in 12th of July 2016).

The reactors were inoculated with the dark brown activated sludge from the WWTP (see Figure 0-3, and Figure 0-2) and after approximately 10 days from the inoculation, the dark brown flocs became lighter in colour, see Figure 0-1.

During the initial stages of the operation, white foam was observed on top of R3 and disappeared after a few weeks. Moreover, the activated sludge flocs in R3 became denser under longer aeration time, probably due to bridging between EPS, microbial cells, and ions. After five weeks from the inoculation, small white granules were observed in R3 with the simultaneous presence of floccular sludge. Microscopic observations were done frequently to monitor the progress of granulation and to detect the presence of filamentous bacteria in the reactor. From observations both in the reactor and under the microscope, spherical filamentous surface aerobic granules were found after 90 days form the start-up, see Figure 0-3. In general, the aerobic granules dominated by filamentous bacteria have spherical structure and fluffy surface while typical granules have a clear round

surface. More microscopic observations from the reactors are provided in Figure 0-5 to Figure 0-8. The observation of spherical structured granules is in accordance with the theory and findings of other researches. However, the presence of filamentous bacteria was not expected.

For promoting aerobic granules in R3, the settling time in this reactor was reduced stepwise from 30 minutes to two minutes over a 21 days period. After this period, the settling time remained unchanged at the value of two minutes.

Settling time for R2 remained constant at 30 minutes during the whole experiments for keeping the sludge in floccular form. Figure 0-4 shows the changes of settling times for both reactors.

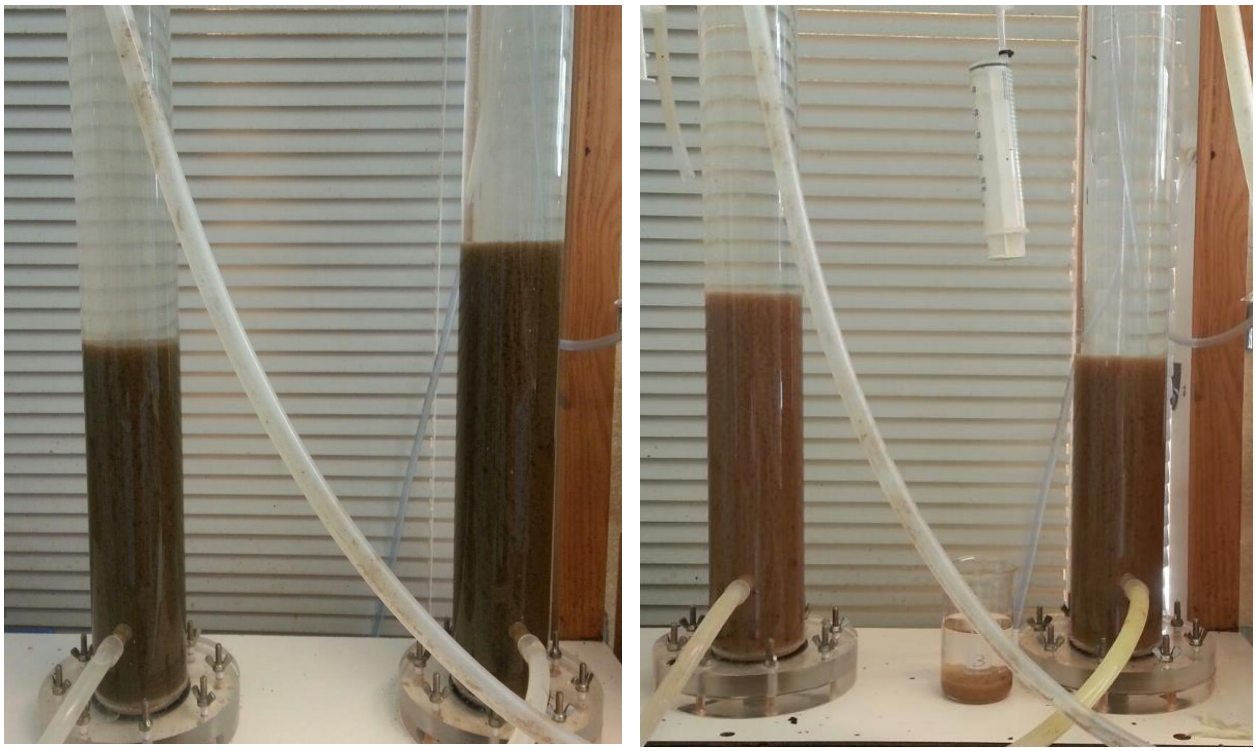

Figure 0-1. From left to right: 1 day and 10 days after inoculation

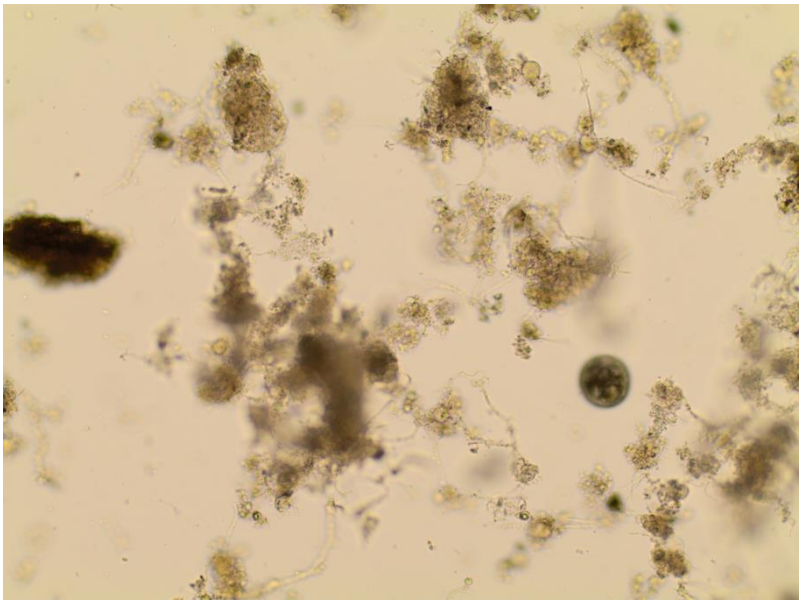

Figure 0-2. Microscopic image of the seed sludge, first run

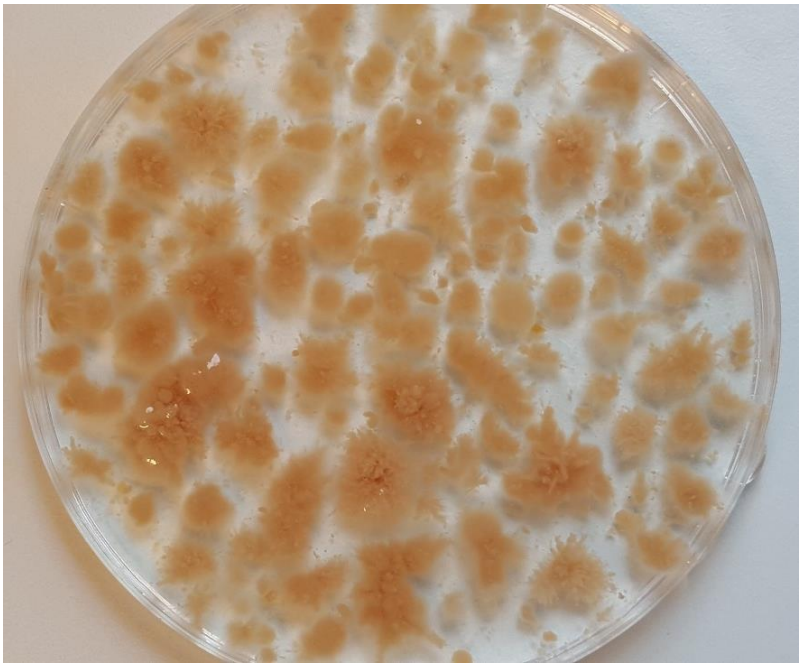

Figure 0-3. Fluffy surface granules, 90 days from inoculation

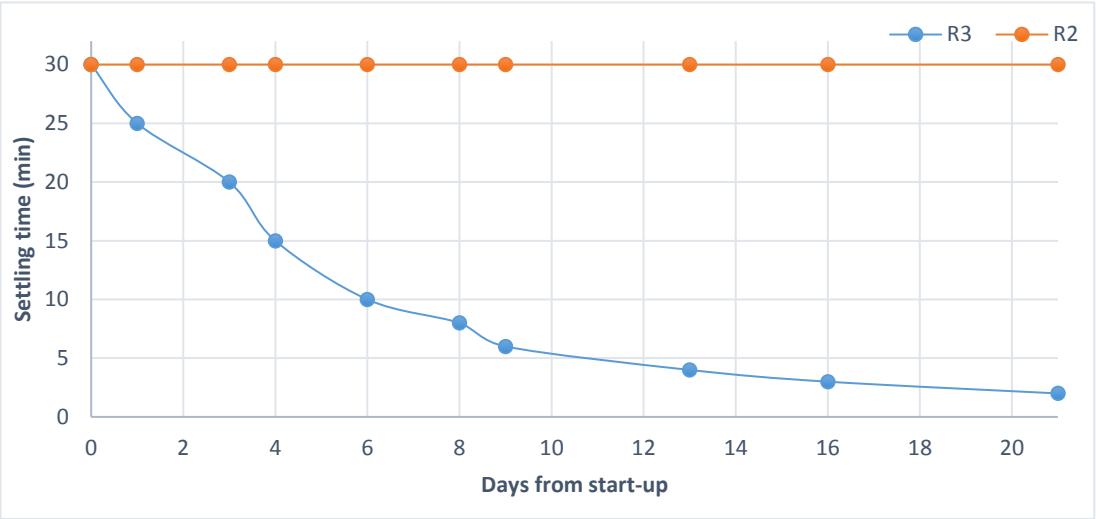

Figure 0-4. Settling time for R2 and R3 during the first 21 days of operation

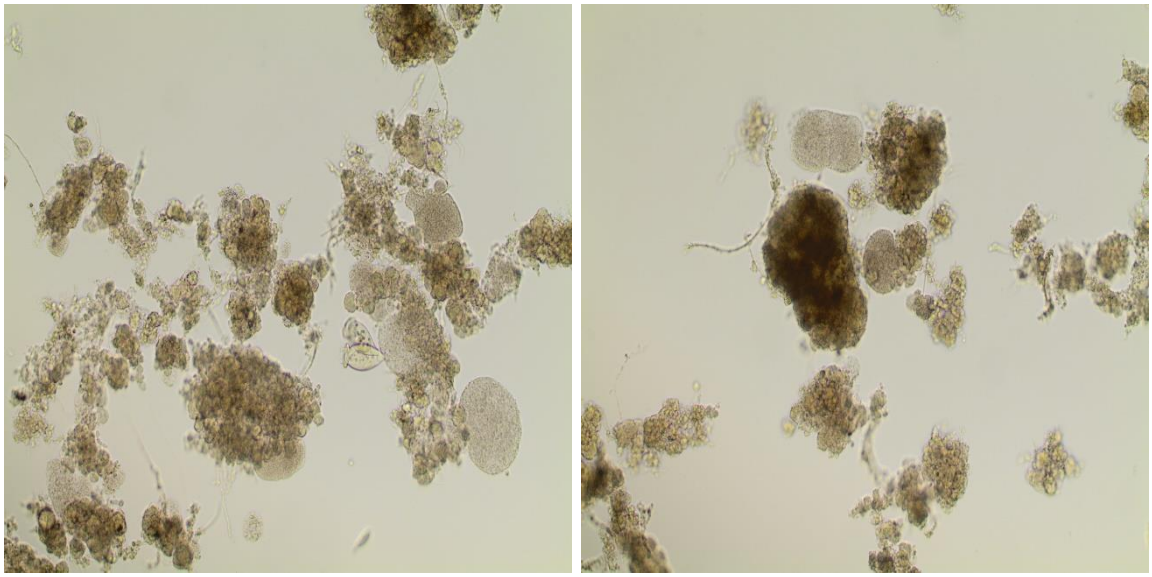

Figure 0-5. Microscopic image after 14 days from the inoculation for R2 (left) and R3 (right)

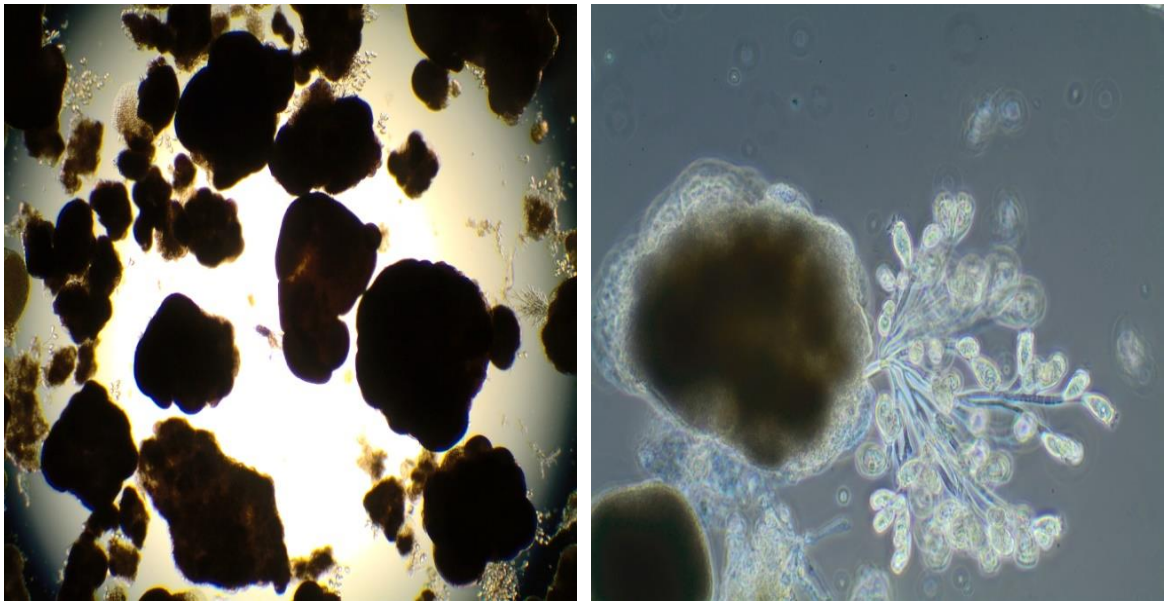

Figure 0-6. Microscopic image from R3 after 21 days from the inoculation.

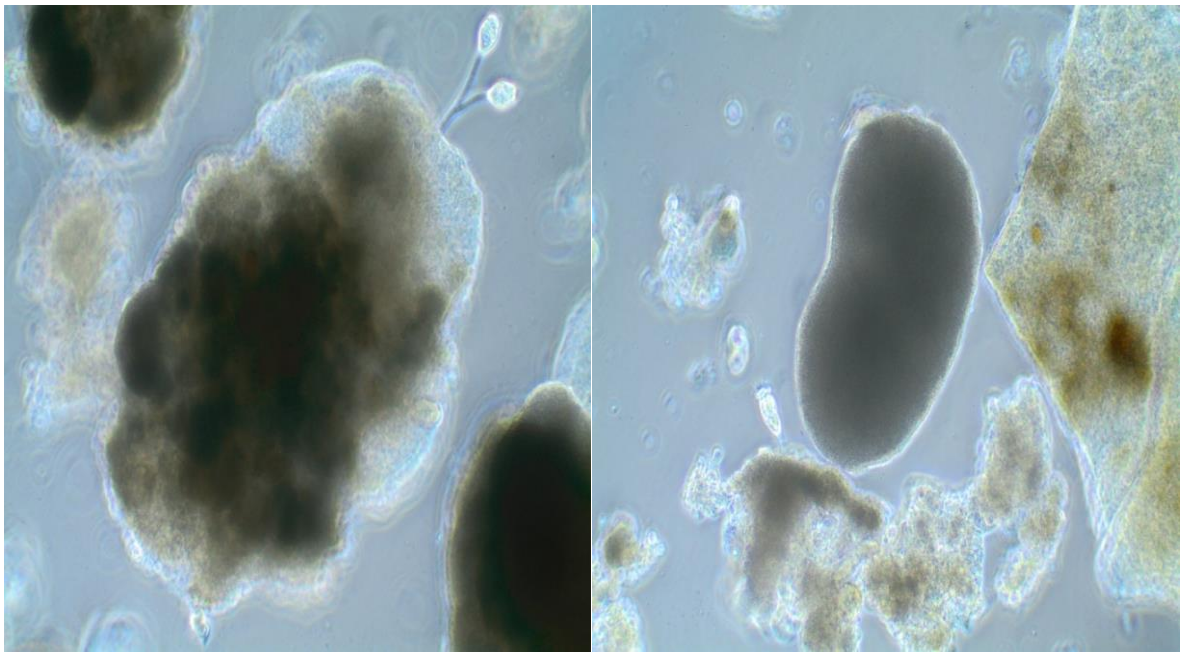

Figure 0-7. Microscopic image from R2 after 115 days from the inoculation

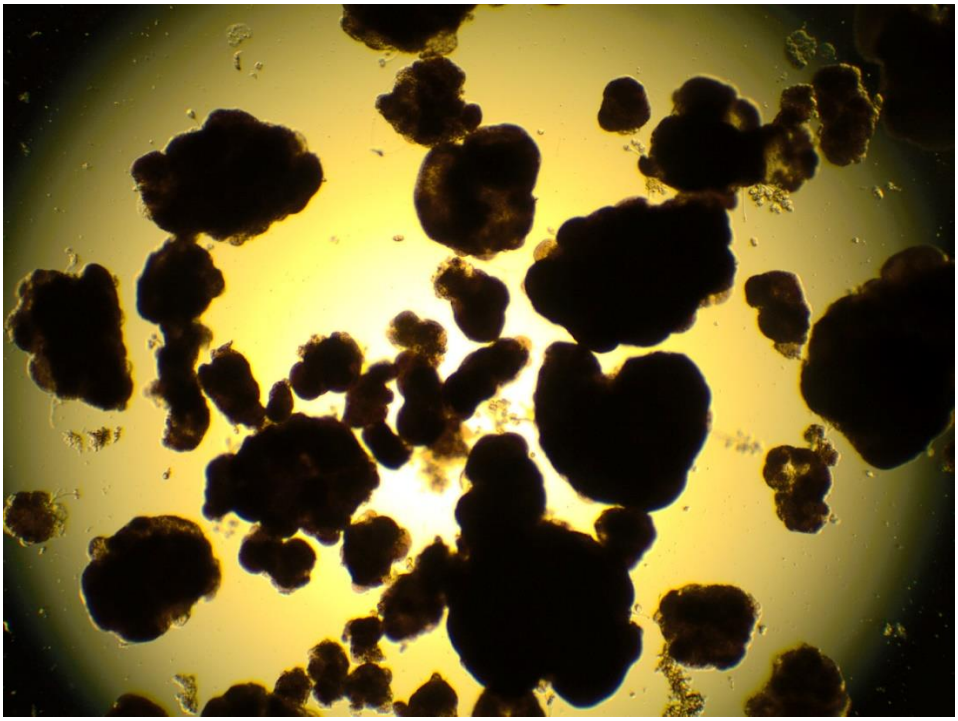

Figure 0-8. Microscopic image from R2 after 132 days from inoculation

4a.1.1. Sludge analysis

4a.1.1.1. Mixed Liquor Suspended Solids and Mixed Liquor Volatile Suspended Solids

The TSS and VSS of the mixed liquor and the MLVSS to MLSS ratios for the reactors are depicted in Figure 0-9 to Figure 0-12.

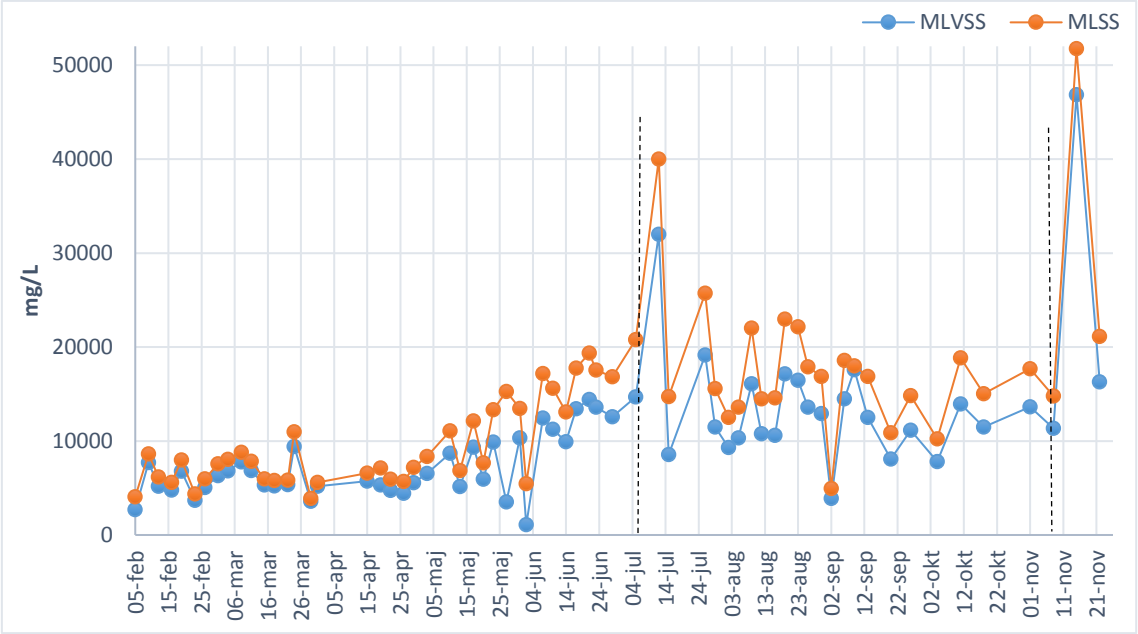

Figure 0-9. MLSS and MLVSS concentration in R2

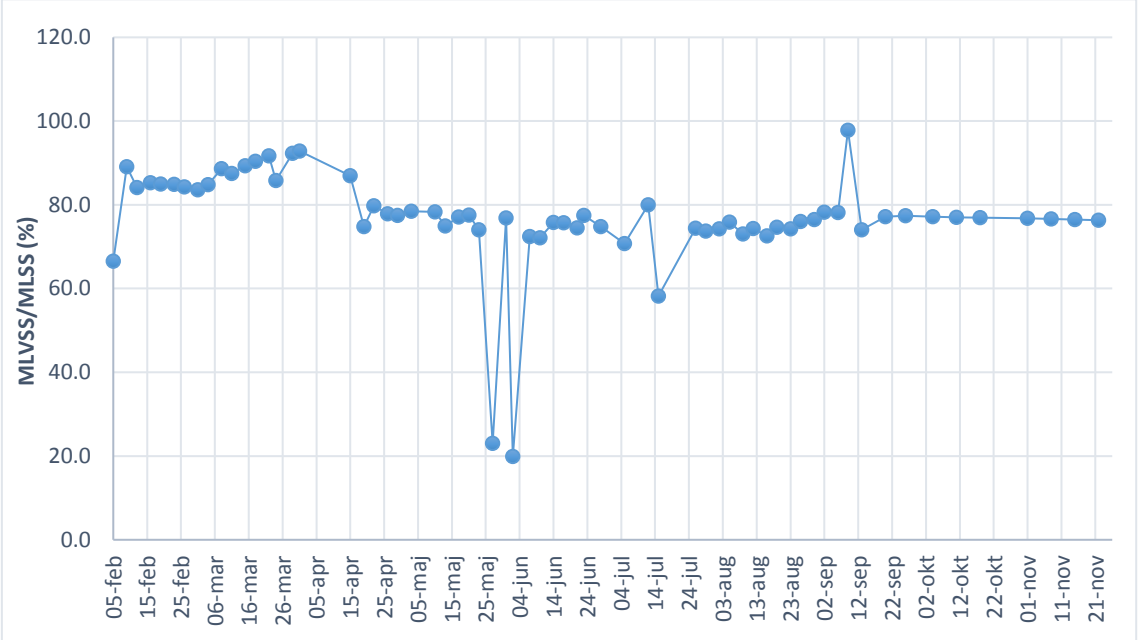

Figure 0-10. Change of MLVSS/MLSS ratio for R2

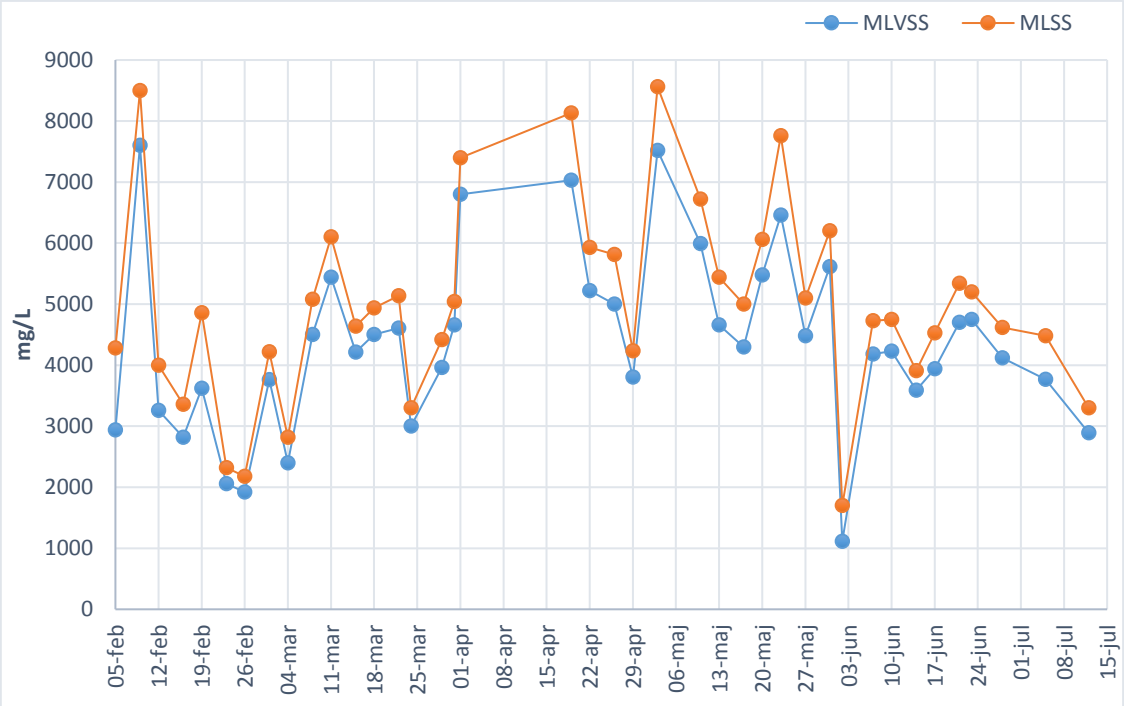

Figure 0-11. MLSS and MLVSS concentration in R3

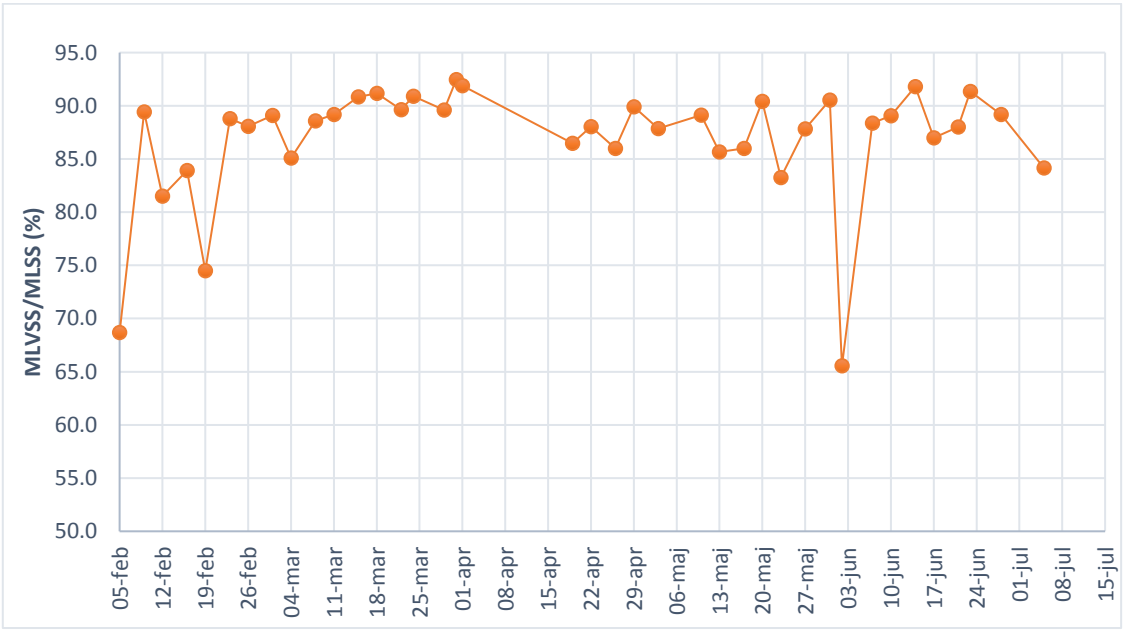

Figure 0-12. Changes of MLVSS/MLSS ratio in R3

According to Figure 0-9, the MLSS concentration in R2 was relatively stable until May. From May to July 12th, the biomass concentration underwent a gradual increase until it reached to a level of 40000 mg/L. The sludge in this reactor was in floccular form from

the beginning of the operation, however from May, the sludge flocs became semi-granulated and the morphology had changed.

After July 12th, the biomass concentration in the reactor dropped sharply, probably because of a great amount of sludge was removed from the reactor for use in membrane filtration experiments. From 15th of July to 8th of November, the biomass concentration in the reactor experienced a relatively stable condition at the average value of 16200 mg/L. On 15th of November there was a jump in the biomass concentration to 51000 mg/L. The exact reason(s) for this jump is(are) not fully understood, but it is probably related to inhomogeneous sampling.

MLVSS is the active part of MLSS which represents the concentration of the microorganisms in the bioreactor. For a common domestic wastewater, the MLVSS to MLSS ratio is typically between 0.75-0.9 (Tchobanoglous, et al., 2004). For R2, at the beginning of the inoculation, the MLVSS/MLSS ratio was around 78%, see Figure 0-10. After two weeks of acclimation, the ratio increased to almost 90%. From that time the MLVSS/MLSS ratio was almost constant and stable until July 12th at which it faced a sudden jump to 210%. The average value of MLVS/MLSS ratio during the whole experiment was 77.1% which were in accordance to the value obtained by similar research and available references. During the experiments, there were some strange points at which the ratios were either above 1 or below 0 and can be the signs of an error in sampling or weighing.

The accuracy and reasonability of the results were validated by calculating standard deviation and coefficient of variations of the data. The standard deviation and coefficient of variation were 12 and 15% respectively. According to these values, the results are in an acceptable range and those strange measurements may happen due to some operator's error during sampling or weighing.

Comparing the MLSS in R2 and R3, Figure 0-11, from February 5- 23, reveals that R3 underwent an intensive fluctuation trend while that of R2 had stable increasing trend. The reason is due to the decrease of the settling time in R3 during this period and consequently the biomass wash-out from the system. The biomass washout was so severe that the sludge concentration dropped below the seed sludge concentration. Although this fluctuating trend in normal during the first few weeks of granulation (Abdullah, et al.,

2011), by adjusting the cycle operation and allowing the longer settling time at the early stages of granulation, better granules can be achieved.

From February 26th until 3rd of May, the MLSS concentration in R3 increased gradually and reached to its maximum value of 8560 mg/L. After this point, the MLSS concertation showed a fluctuating trend probably due to extensive sludge removal for conducting filtration tests. The reason for a sudden decrease on 2nd of June is due to taking improper sample volume to filter through the Wathman filters. In most of the measurements, to ensure the complete filtering, only 5 mL of samples were filtered. But on 2nd of June, 7 mL of the sample was filtered and analysed. The too low values for the results on this day, indicates that the 7 mL sample volume was too high for appropriate filtration.

Like R2, MLVSS in R3 exhibited the similar tendency as MLSS. But, the MLVSS/MLSS ratio for R3 had a more stable and uniform trend. This stable trend is the indication of a good biomass acclimation in the reactor (Abdullah, et al., 2011). The MLVSS/MLSS ratio at the beginning of the experiment was almost 68% and only after two weeks from acclimation, it reached to approximately 90% which is the sign of the new biomass formation. The average value for MLVSS/MLSS for R3 during the whole experiment was 87% and the standard deviation and coefficient of variation were 5.6 and 6.43% respectively.

MLSS concentration in R3 is lower than that of R2 and it is because of the shorter settling time in this reactor, this finding is in agreement with the finding of Szabo et al. (Szabo, et al., 2016)

4a.1.2. Supernatant (effluent) analysis

4a.1.2.1. Total Suspend Solids and Volatile Suspended Solids

TSS, VSS, and the ratio of them for the supernatant from the reactors are illustrated in the Figure 0-13 to Figure 0-16.

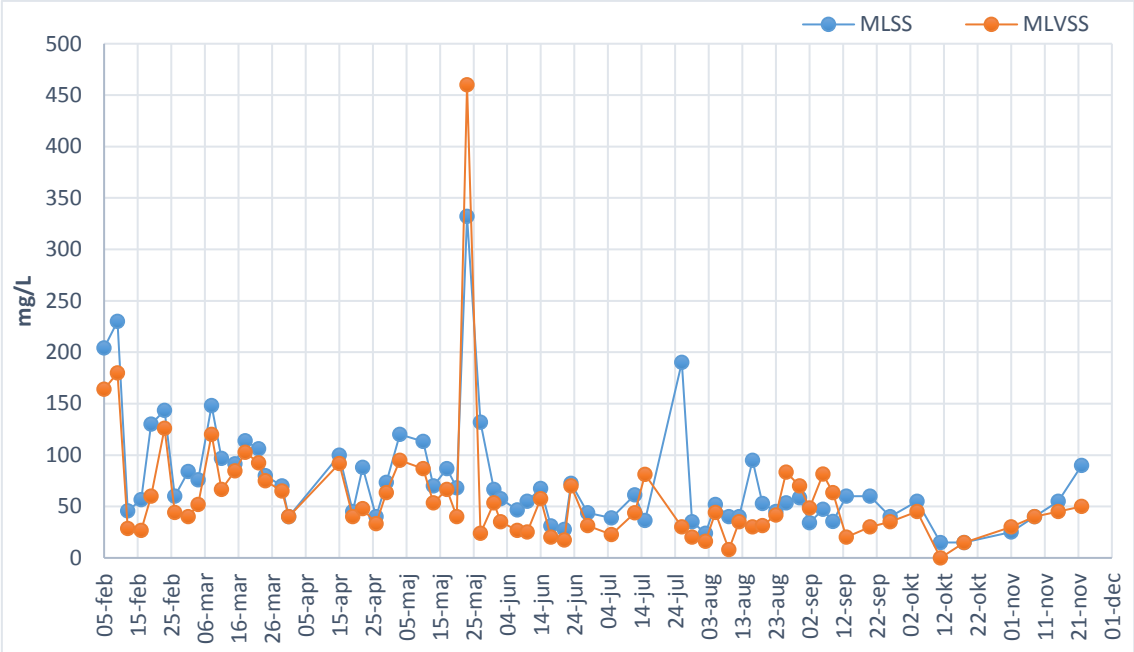

Figure 0-13. TSS and VSS of the supernatant from R2

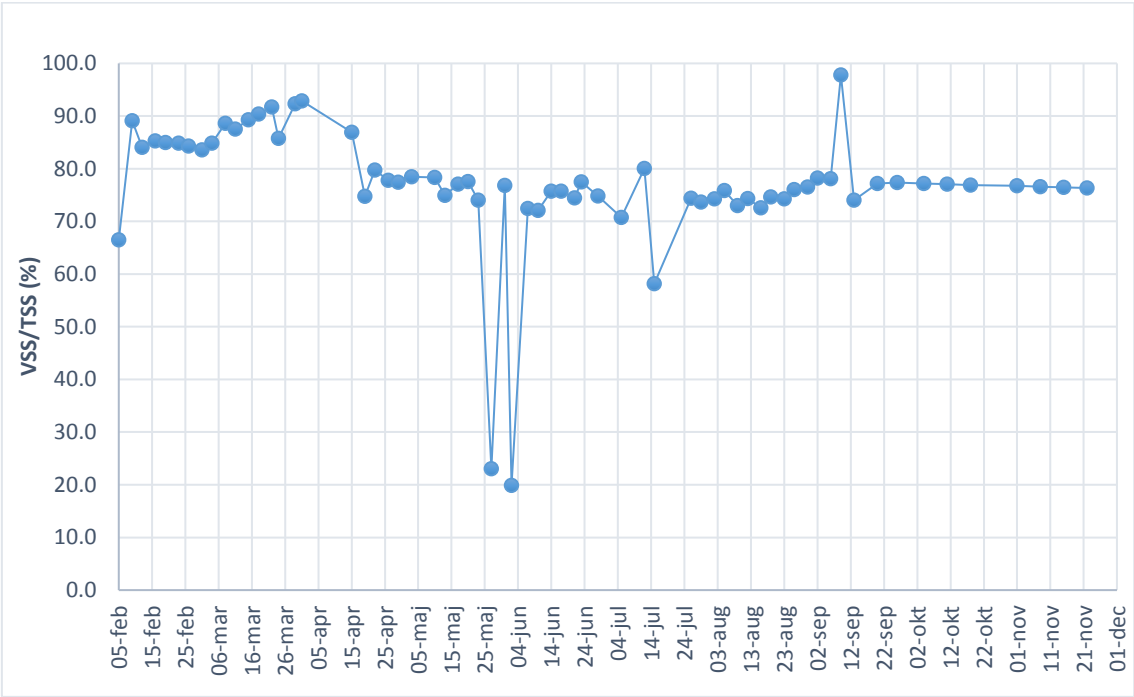

Figure 0-14. VSS/TSS ratio for the supernatant from R2

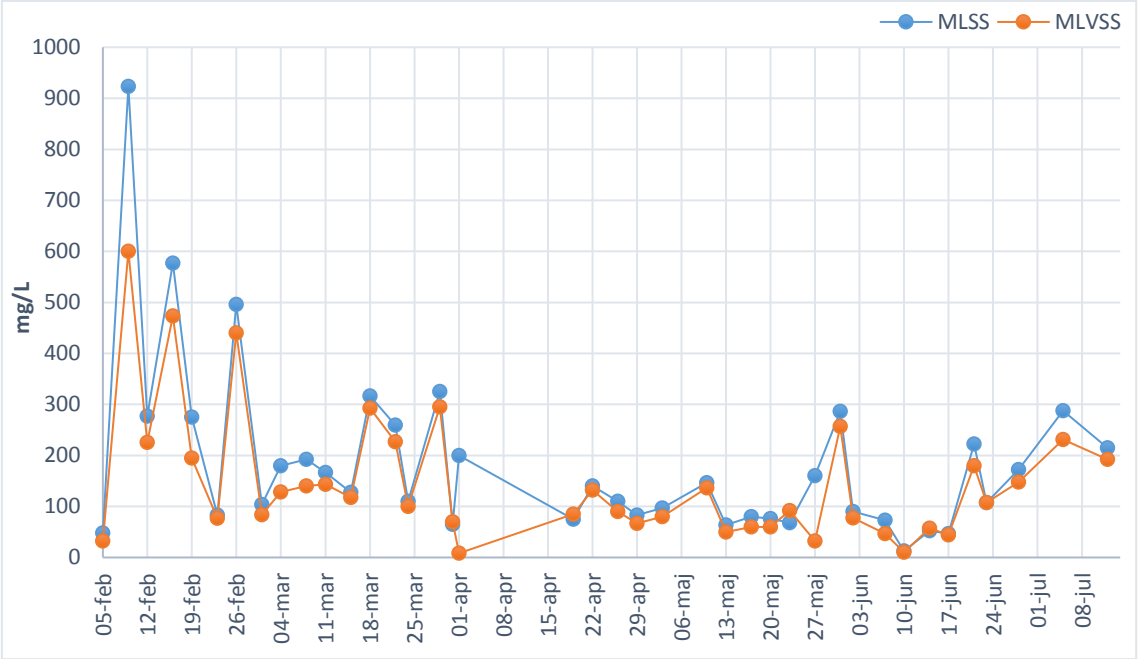

Figure 0-15. TSS and VSS of the supernatant from R3

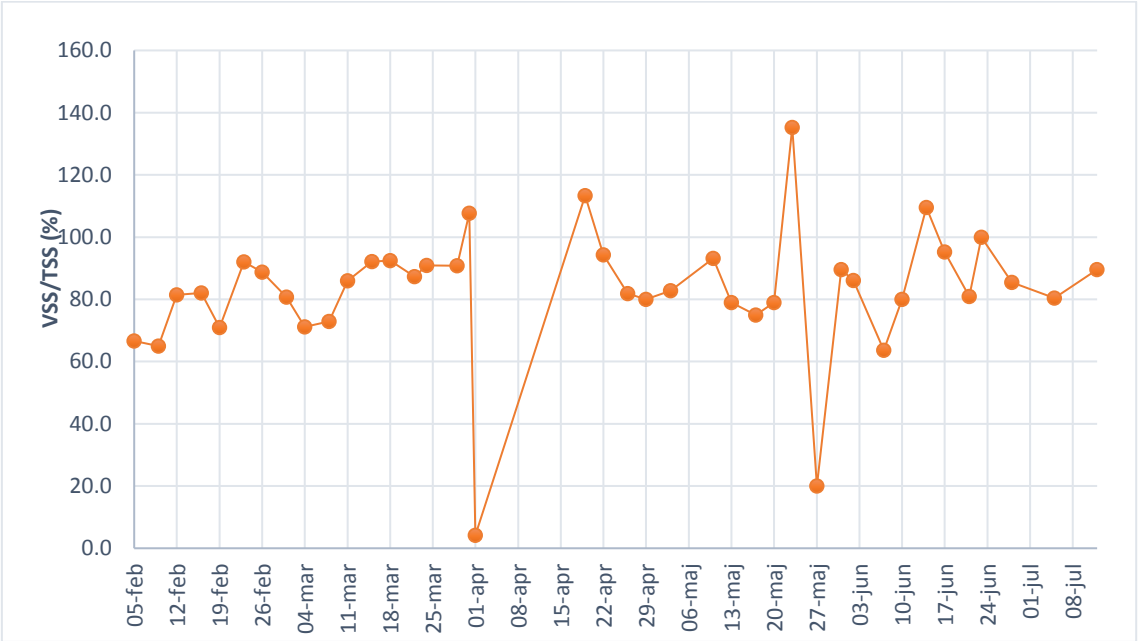

Figure 0-16. VSS/TSS ratio for the supernatant from R3

According to Figure 0-13, the TSS in the effluent from R2 experienced a sharp decrease from 200 mg/L on February 5th to almost 30 mg/L on February 12th. After that, the performance of the reactor stabilized and the average TSS in the effluent reached to below 75 mg/L. This result is in full agreement with the similar studies.

According to Figure 0-15, the TSS and VSS in the effluent from R3, underwent almost a similar fluctuating trend during the first three weeks of the acclimation. This ups and downs are due to the biomass washout from the reactor because of shortening the settling time. After this period, the reactor operation stabilized and the TSS concentration in the effluent reached the average of 150 mg/L which is slightly higher than the results obtained by Rocktäschel et al (Rocktäschel, et al., 2015). Also, according to the EU directive 91/27/EEC the TSS in the effluent from WWTP should not exceed 60 mg/L prior to discharge to the environment. For our case and with the assumption that the effluent is going to be discharged to the environment without further treatment, the EU directive requirement has not been met (EC, 1991). Also by comparing the TSS in the effluent from R2 and R3, it is obvious that floccular sludge had better performance in removing suspended solids.

The MLVSS/MLSS ratio for R3 had a gradual increase during the first three weeks of inoculation. Usually, high amount of VSS in the effluent is the sign of insufficient settling time (EBS, 2016). Since during the first three weeks the settling time was changed therefore, the results are reasonable. The same as for the biomass in the reactor, there are a few points at which MLVSS/MLSS ratio is either higher that 100% or very close to 0 which for both cases it is impossible. The average MLVSS/MLSS for the supernatant from R3 is 83% which means that there are still some biodegradable materials in the effluent.

4a.1.2.2. Organic Carbon Removal

The concentration of DOC (filtered TOC) discharged with the supernatant from the reactors are illustrated in Figure 0-17 and Figure 0-20. Also the DOC and the acetate removal efficiencies are depicted in Figure 0-18, Figure 0-19, Figure 0-21 and Figure 0-22. To obtain the COD removal efficiencies, the correlation between acetate and COD must be calculated (1g of sodium acetate contains almost 0.78g of COD).

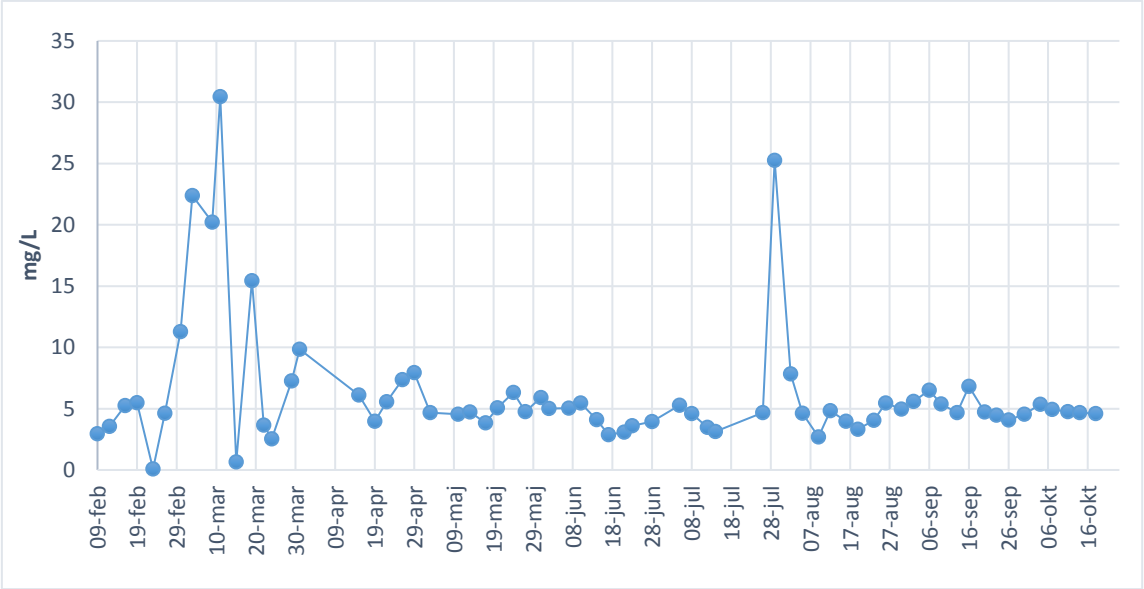

Figure 0-17. DOC concentration in the effluent from R2

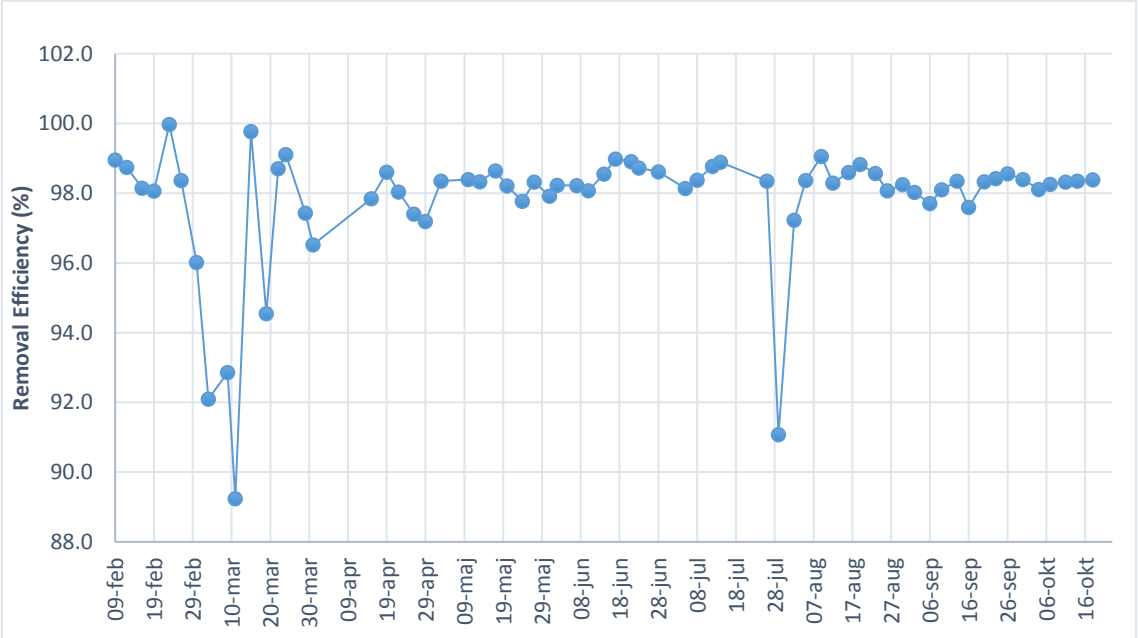

Figure 0-18. DOC removal efficiency for R2

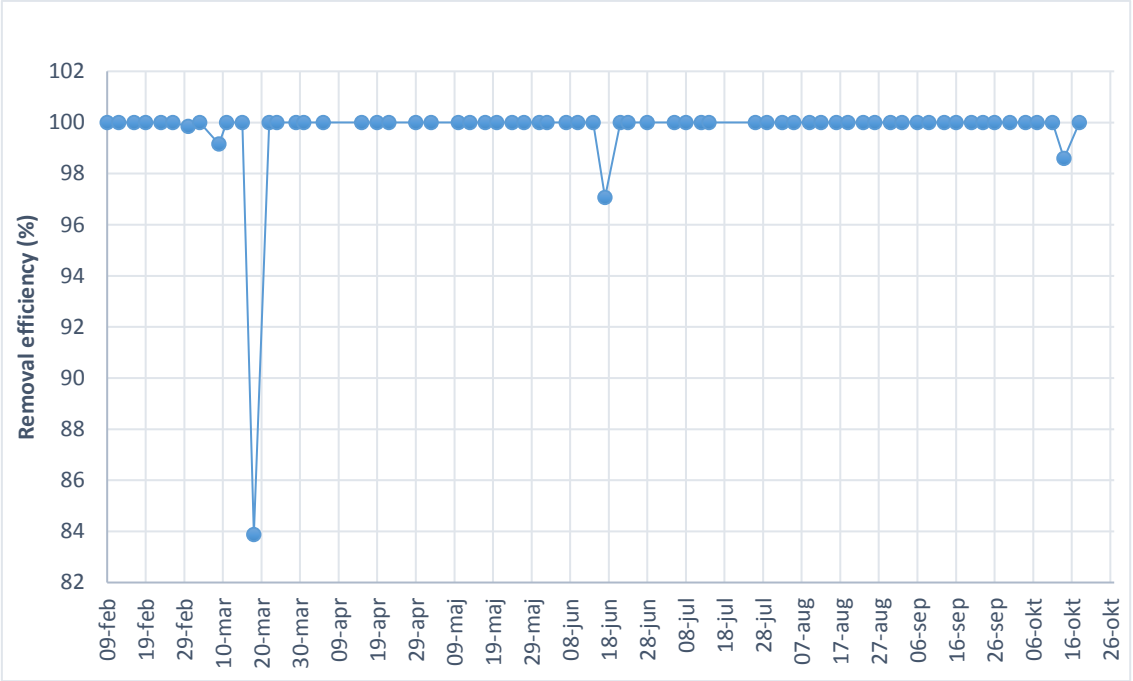

Figure 0-19. Acetate removal efficiency

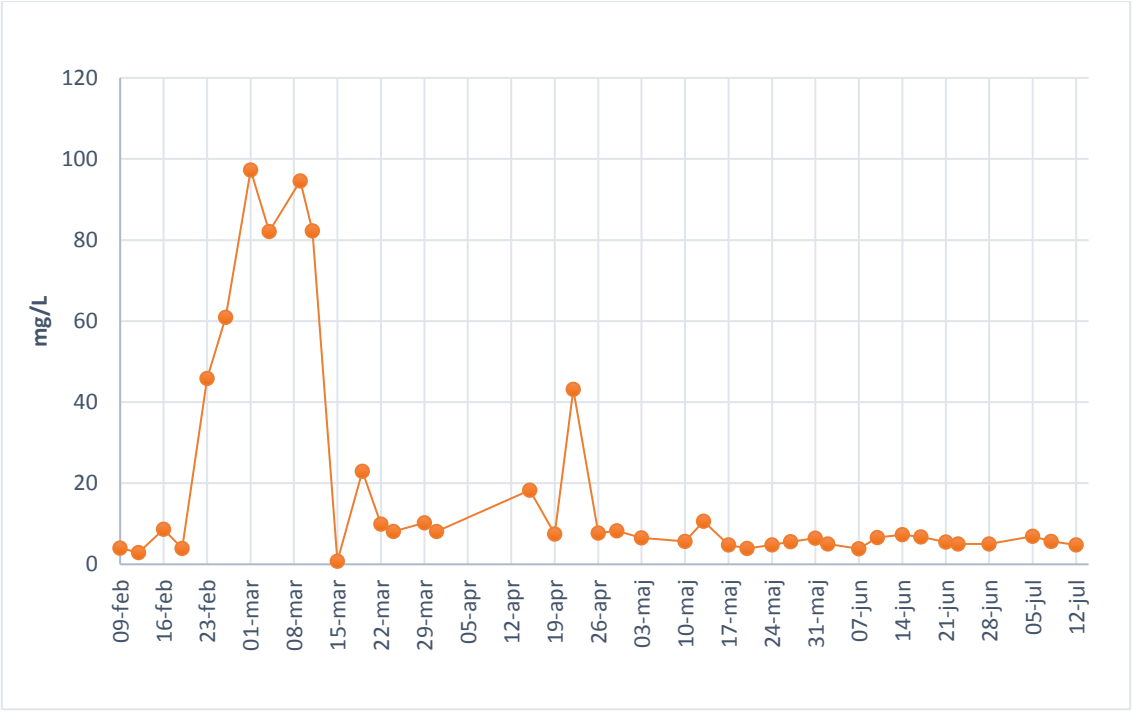

Figure 0-20. DOC concentration in the effluent from R3

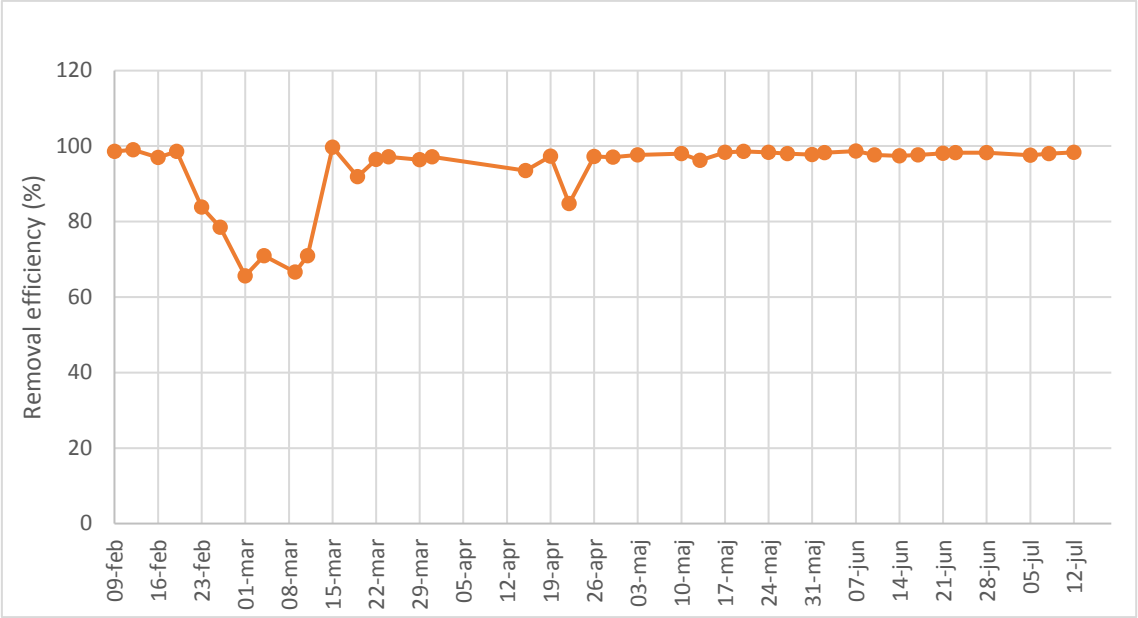

Figure 0-21. DOC removal efficiency for R3

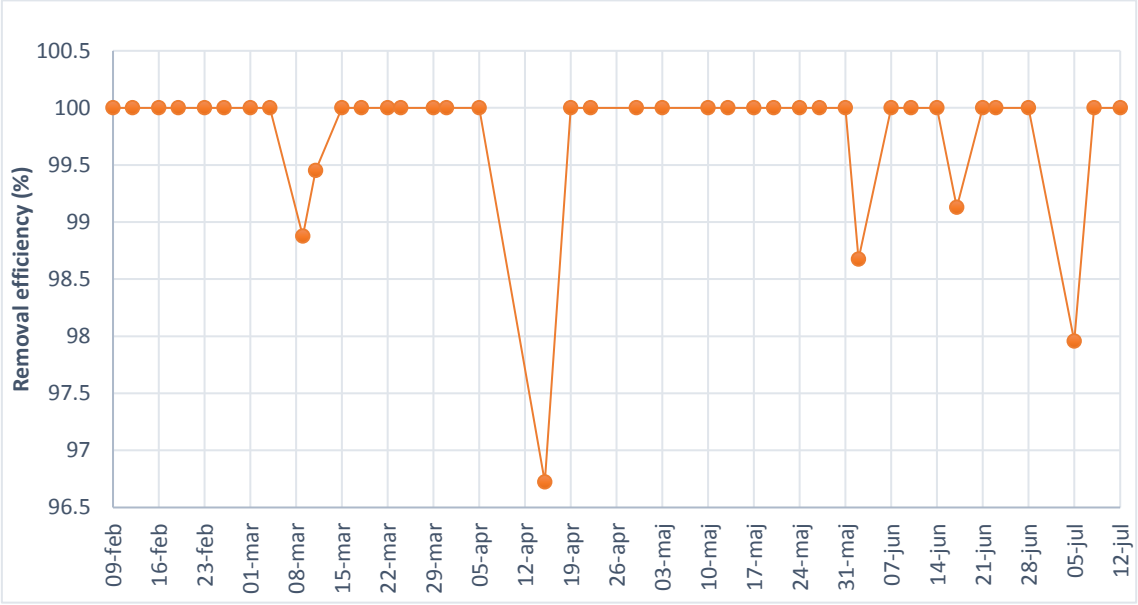

Figure 0-22. Acetate removal efficiency for R3

As shown in Figure 0-19 and Figure 0-22, the acetate removal efficiencies for both reactors reached a value close to 100% in just a few days from the stat-up, also the changes of the removal efficiencies over the operation time were almost negligible. This rapid and high organic removal efficiency indicates that the microorganisms in both reactors could

fully adapt to the new environment, (Zhao, et al., 2016). de-Kreuk at al., (2005) have also obtained almost 100% of COD removal efficiency by using aerobic granular sludge (de Kreuk, et al., 2005).

For R3, during the period February 16th to March 11th, the DOC removal efficiency was decreased slowly and then recovered back to its previous level. Zhao et al., (2016) have discussed that this reduction in removing organic carbon is related to the morphological changes in the sludge flocs during granulation (Zhao, et al., 2016).

4a.1.2.3. Nutrient removal

4a.1.3.1. Nitrogen removal

An important aim of the study was to simultaneously achieve granulation and nutrient removal. Figure 0-23 to Figure 0-26 show the detailed results for nitrogen removal efficiencies. The ammonium concentration in the influent was approximately 115 mg/L. It is important to note that some amount of nitrogen and phosphorous were removed from the system by sludge wasting. These values for nitrogen and phosphorus is approximately 12.2 mg and 2.3 mg per 100 mg of TSS respectively.

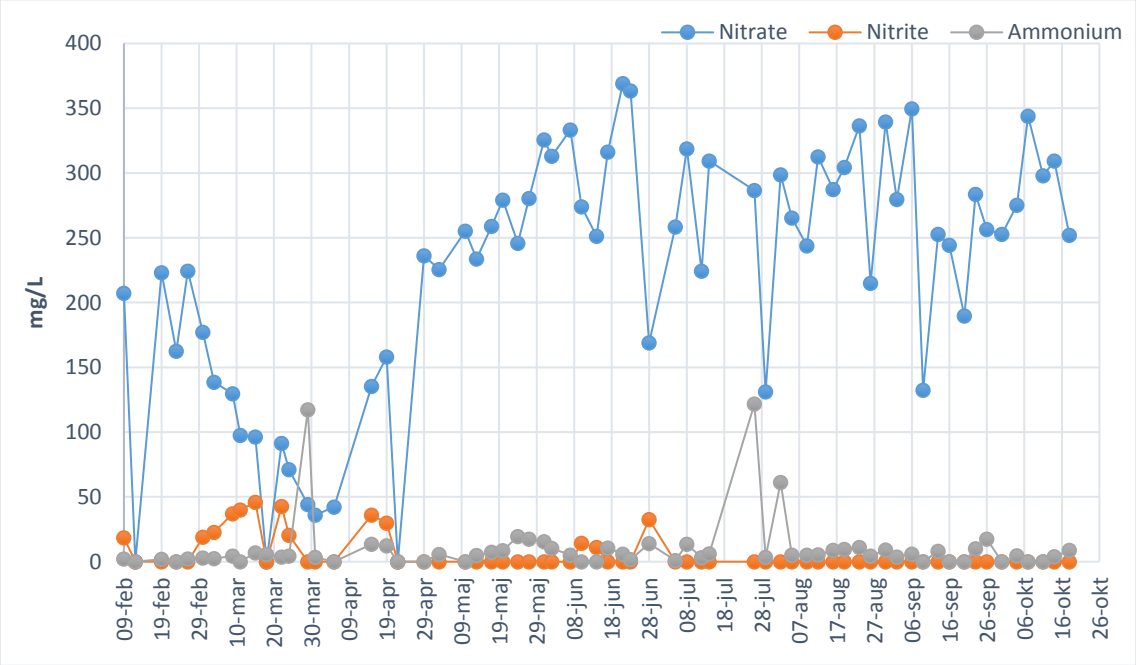

Figure 0-23. Ammonium, nitrate and nitrite concentration in the effluent from R2

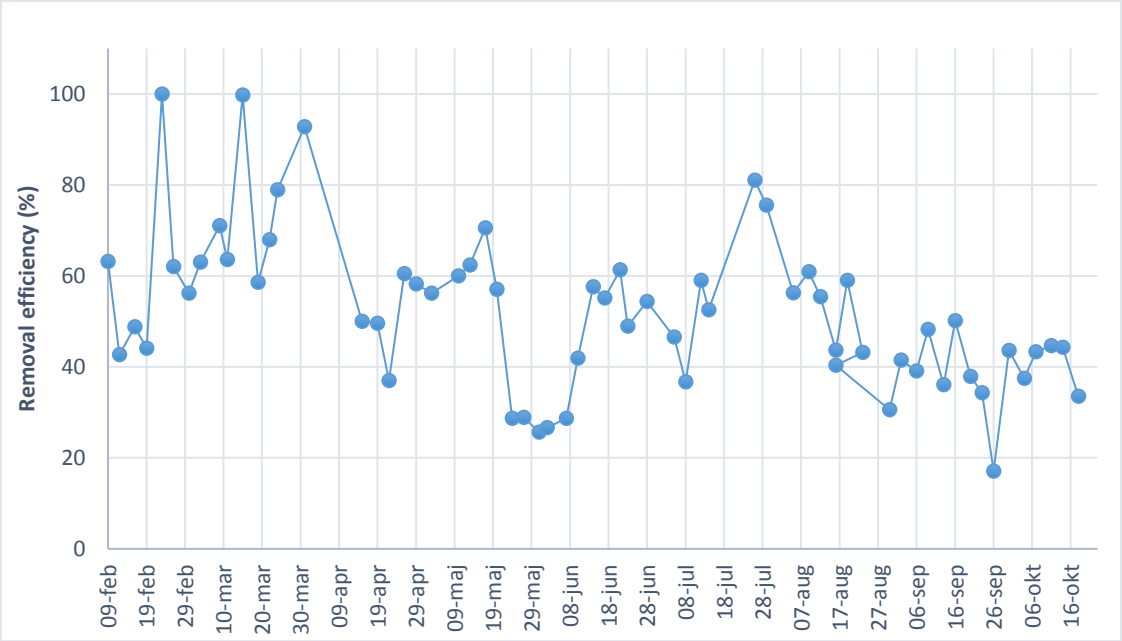

Figure 0-24. Total nitrogen removal efficiency for R2

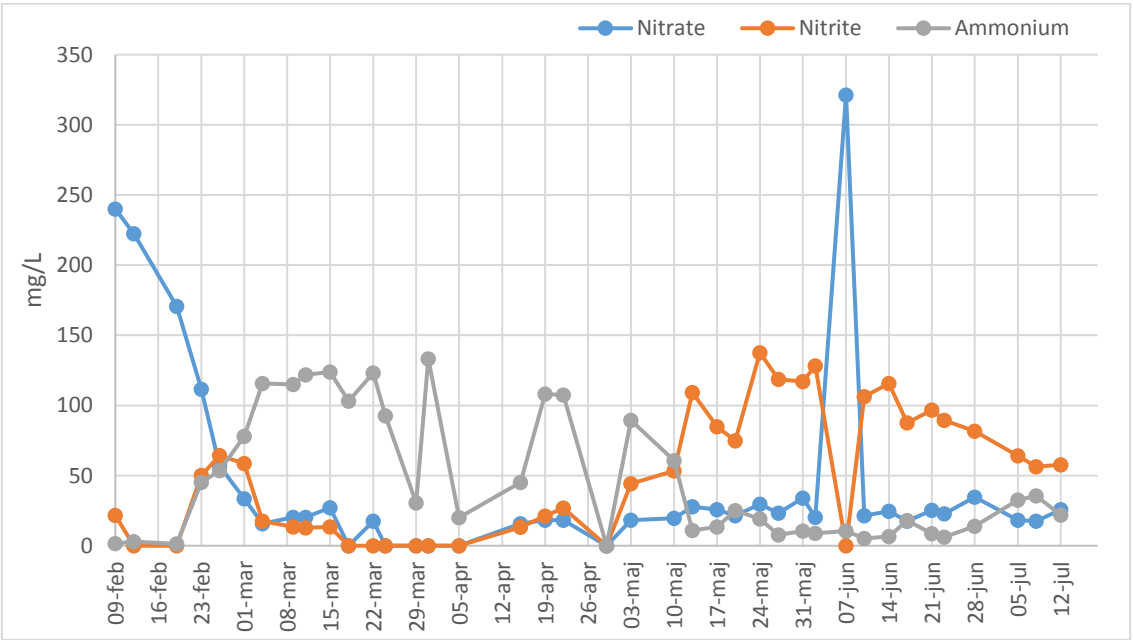

Figure 0-25. Ammonium, nitrate and nitrite concentration in the effluent from R3

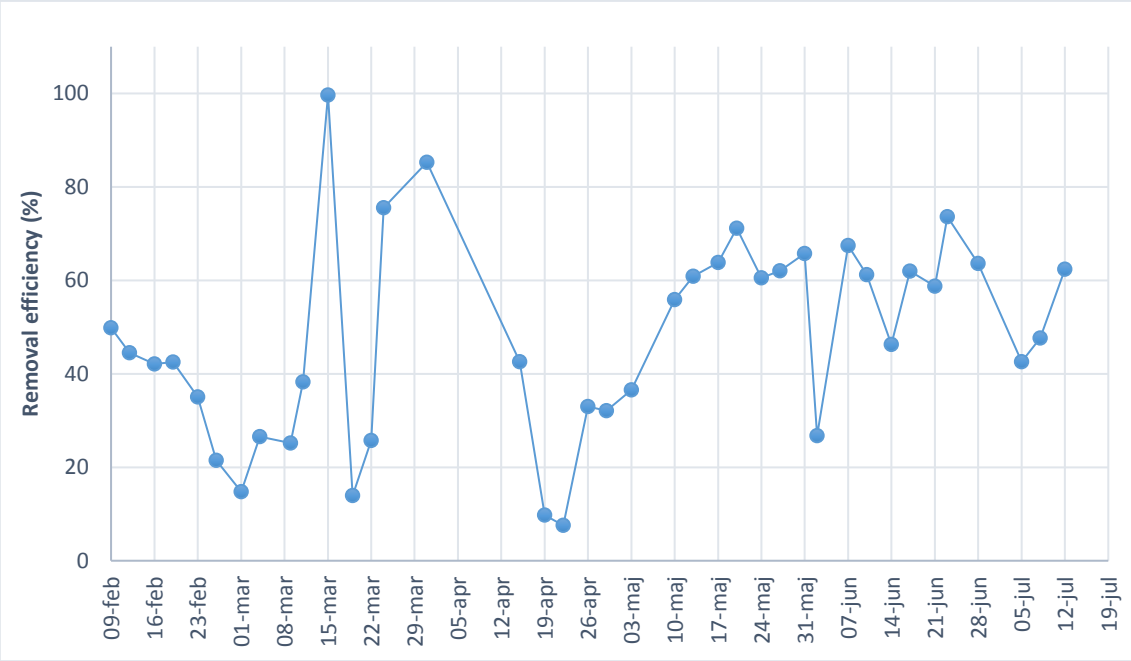

Figure 0-26. Total nitrogen removal efficiency for R3

According to Figure 0-24, it seems that the nitrogen removal efficiency increased in R2 from the beginning of the operation and reached the value of 100% on March 15th. However, it underwent a fluctuating trend until July when it stabilized at the value around 50%. More detailed look on Figure 0-23, reveals that in this reactor, nitrite and ammonium were almost removed while nitrate was in an elevated concentration. Regarding Eqs. (1) to (3), during nitrification, the nitrate concentration increases and during denitrification it decreases. Therefore, it can be concluded that in this reactor nitrification was proceeding while denitrification did not take place sufficiently especially from 29th of April when the nitrate concentration began to increase. Also, approximately 13.4 % of the total nitrogen removal is due to sludge wasting.

In granulated reactor, as it is clear in Figure 0-25, ammonium was in an elevated concentration during the first 3 months of operation. This indicates that nitrification and also denitrification in this reactor were insufficient.

Finally, on May, ammonium removal happened in this reactor. However, the concentration of nitrite was high and nitrate was low which is the sign of incomplete denitrification from May 2016. Figure 0-26 shows that total nitrogen removal in granulated reactor was decreasing to the minimum of 15% during the first three weeks of

operation. It can be suggested that the changes of settling time and biomass washout during this period have caused this significant reduction in nitrogen removal efficiency. Basin et al., (2012) have faced the same trend by removal of half of the biomass in the reactor (Bassin, et al., 2012). The average TN removal efficiency in this reactor over the operation time was 48 % in which 5% was due to sludge wasting.

According to Figure 0-24 and Figure 0-26, it looks like the granular sludge had better performance during the latter half of the experiment.

4a.1.3.2. Phosphorous removal

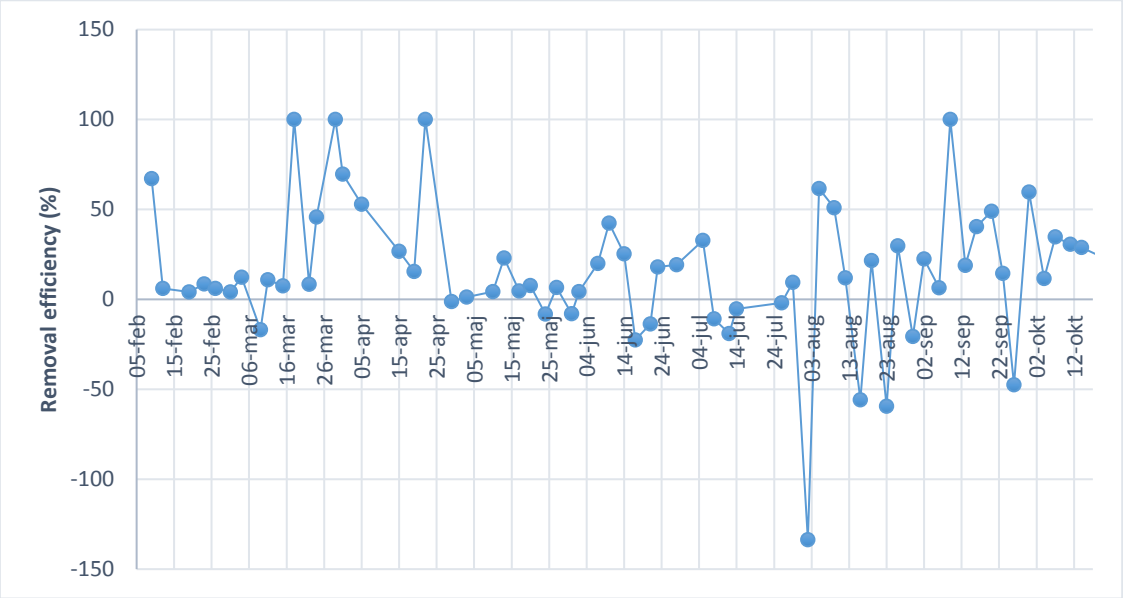

Figure 0-27. Phosphate removal efficiency for R2

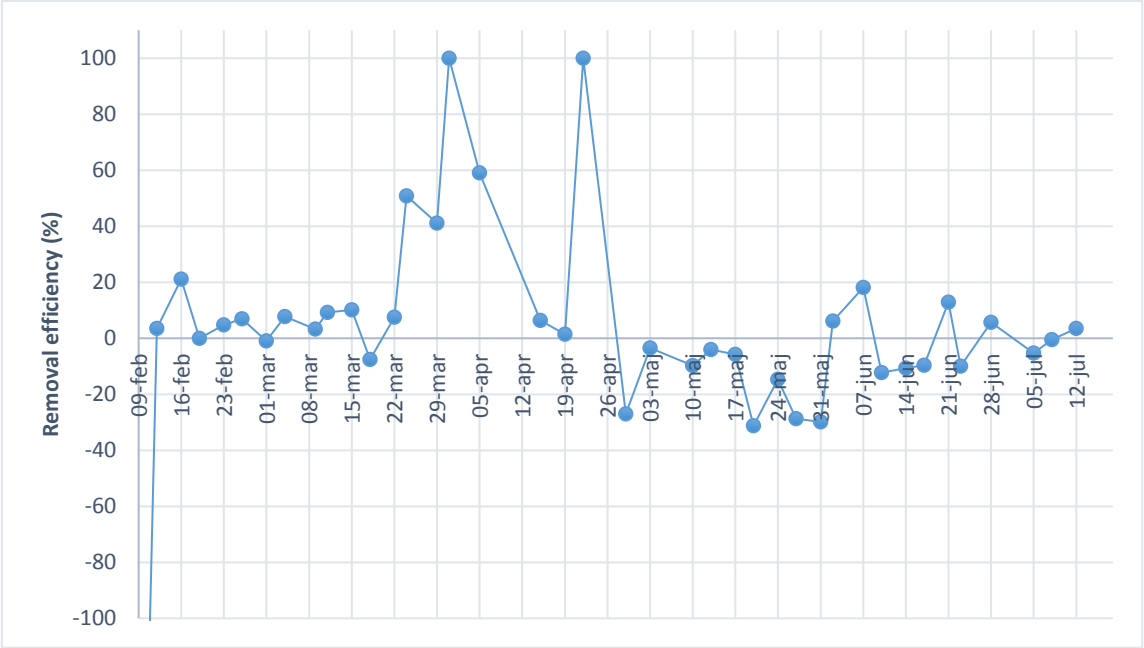

Figure 0-28. Phosphate removal efficiency for R3

As shown in Figure 0-27 and Figure 0-28, the phosphate removal efficiencies for the two reactors were fluctuating and were not stabilized over the operation time.

From March 16th to April 25th floccular sludge showed reasonable performance and it even obtained 100% phosphate removal during this period.

According to Figure 0-28, from the beginning of the experiment until March 18th, granular sludge had low phosphate removal efficiency, followed by a dramatic increase from March 18th to April 5th. Then it underwent a sudden drop to even below zero and could not recover back to its previous trend. One possible reason for this sudden drop in removing phosphate is the size of granules. From the beginning of the operation to the end of April, the sizes of the granules were normal and therefore, the oxygen could easily penetrate deep into the granules and the biological processes could easily take place. From April, as previously mentioned, giant and over- sized fluffy granules (the average diameter of 50mm) were formed in the reactor. In this situation, oxygen could not transport deep into the granules, thus; the phosphate uptake rate started to decrease. From June to the end of operation, the reactor performance was not promising in removing phosphate.

4a.1.3. Cycle analysis

The first cycle analysis was performed on R2 and R3 on June 14th. The samples were taken out from the reactors according to the procedure in section 3a.7.3. Later on, the samples were analysed for DOC and some of the major anions and cations. Figure 0-29 and Figure 0-30 illustrate the results for R2 and R3 respectively.

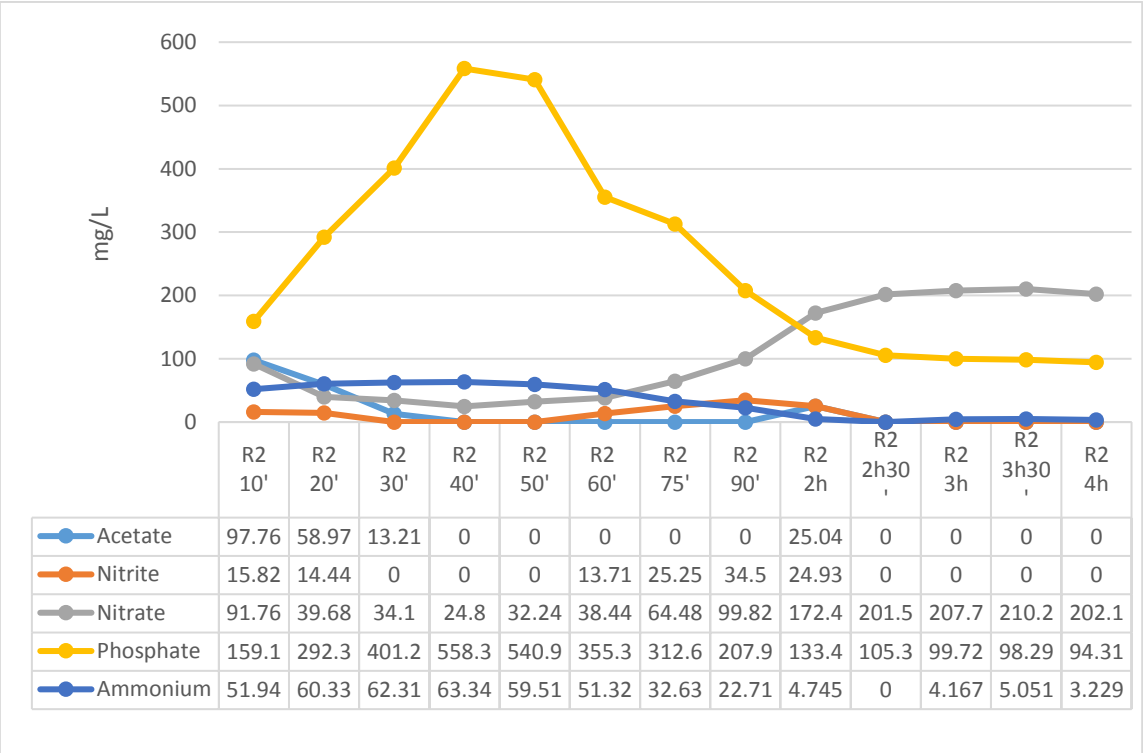

	R2 10'	R2 20'	R2 30'	R2 40'	R2 50'	R2 60'	R2 75'	R2 90'	R2 2h	R2 2h30'	R2 3h	R2 3h30'	R2 4h
Acetate	97.76	58.97	13.21	0	0	0	0	0	25.04	0	0	0	0
Nitrite	15.82	14.44	0	0	0	13.71	25.25	34.5	24.93	0	0	0	0
Nitrate	91.76	39.68	34.1	24.8	32.24	38.44	64.48	99.82	172.4	201.5	207.7	210.2	202.1
Phosphate	159.1	292.3	401.2	558.3	540.9	355.3	312.6	207.9	133.4	105.3	99.72	98.29	94.31
Ammonium	51.94	60.33	62.31	63.34	59.51	51.32	32.63	22.71	4.745	0	4.167	5.051	3.229

Figure 0-29. Cycle analysis for R2 (aeration was started at 60' and turned off at 3h23')

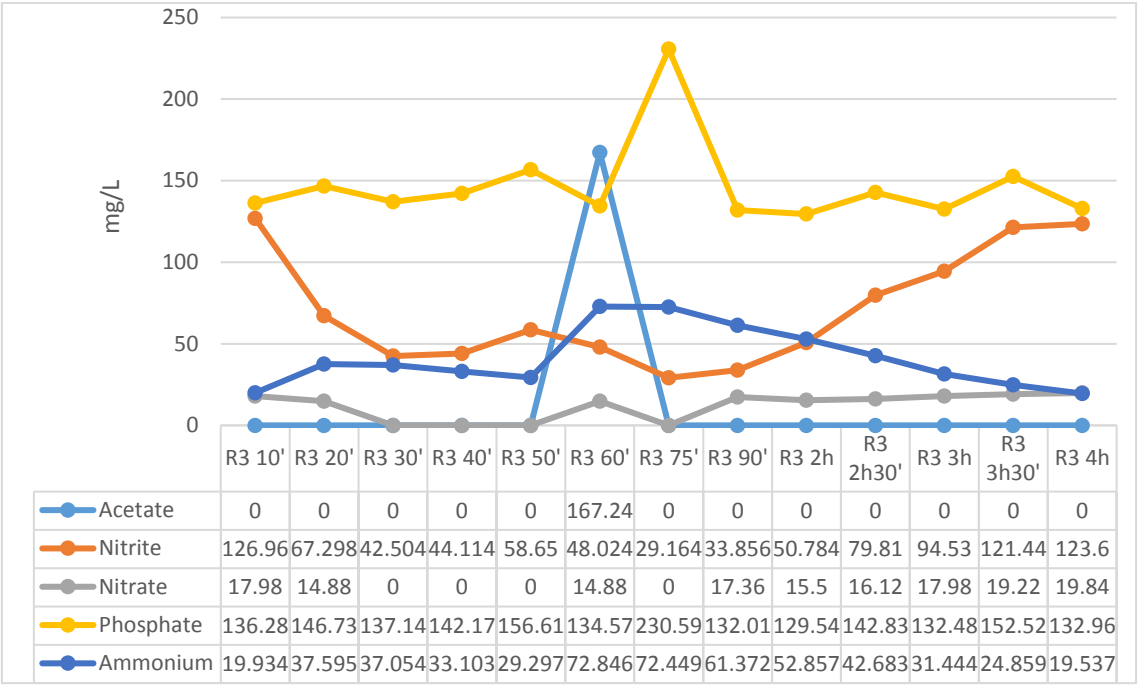

	R3 10'	R3 20'	R3 30'	R3 40'	R3 50'	R3 60'	R3 75'	R3 90'	R3 2h	R3 2h30'	R3 3h	R3 3h30'	R3 4h
Acetate	0	0	0	0	0	167.24	0	0	0	0	0	0	0
Nitrite	126.96	67.298	42.504	44.114	58.65	48.024	29.164	33.856	50.784	79.81	94.53	121.44	123.6
Nitrate	17.98	14.88	0	0	0	14.88	0	17.36	15.5	16.12	17.98	19.22	19.84
Phosphate	136.28	146.73	137.14	142.17	156.61	134.57	230.59	132.01	129.54	142.83	132.48	152.52	132.96
Ammonium	19.934	37.595	37.054	33.103	29.297	72.846	72.449	61.372	52.857	42.683	31.444	24.859	19.537

Figure 0-30. Cycle analysis for R3 (aeration was started at 60' and turned off at 3h51')

In both reactors, acetate was consumed during the feed phase and completely removed shortly after the feeding period, especially for R3 which it consumed immediately. Therefore, the microorganisms were living with no external carbon source for a long period. This trend supports the fact that in simultaneous denitrification and enhanced biological phosphorous removal there is a direct competition between denitrifies and PAOs for the available COD. Under such situation, either phosphate removal or denitrification might be disrupted (Lochmatter, et al., 2014). This trend is in agreement with the finding of Aulenta et al. (Aulenta, et al., 2003).

Phosphate was released in R2 while the acetate was consumed during the anoxic phase in both reactors. Once the acetate was consumed completely and the reactors entered the aerobic phase, the phosphate started to be taken up. However, the rate of phosphate consumption is much lower than that of acetate. Therefore, the microorganisms lived most of the time with the presence of phosphate. Comparison of the phosphate concentration in R2 and R3 shows that R3 had higher phosphate uptake rate. This is probably due to the higher nitrite concentration in this reactor as nitrite acts as an electron acceptor in the denitrification reaction and denitrifies the PAOs. Although there is no clear proof in the literature about the effect of nitrite on phosphate uptake rate during the

anoxic phase, however, there are some studies that showed the effect of nitrite supply on phosphate uptake rate during anoxic phase (Lee, et al., 2001). In addition, nitrate inhibits PAOs. Thus, there is PAOs in R2 but not in R3

As it is observed from the diagrams above, at the end of the cycle, nitrite and nitrate were present in the reactor. This leads to the anoxic condition in the next feeding phase, therefore, a part of carbon source will be consumed by denitrifies, leaving less carbon for the PAOs leading to a lower phosphate removal efficiency in the following cycle (Lochmatter, et al., 2014). de-Kreuk et al., (2007) have suggested that, one possible solution to decrease the nitrate concentration at the end of the aeration phase is to provide the reactor with extra anoxic phase at the end of aeration phase, i.e. to stop the aeration.

During the aerobic phase, as it is observed from the graph, ammonium in both reactors were oxidized to nitrite and finally to nitrate. Therefore, ammonium experienced a decreasing trend. For R2, ammonium oxidized to nitrite and that is why a short increase is seen at the beginning of the aeration phase. Next, nitrite oxidized to nitrate and removed thoroughly and no nitrite remained in the reactor. At the end of the cycle, only nitrate was remained in the reactor. The overall nitrogen removal efficiency in this reactor was almost 57%.

In contrast, in R3, much nitrite and ammonium remained at the end of aeration phase. The overall nitrogen removal in this reactor was approximately 47%. The overall nitrogen removal efficiency was higher in R2, but R3 performed better in regards to denitrification. The TOC and TN results from this cycle study are provided in Appendix Ⅱ.

4a.2. Second run

The second run was initiated on July 5th 2016 and all the reactors (R1, R2 and R3) were in operation. R1 and R3 were inoculated with the new seed sludge and R2 was in operation from the previous run. R1 was run for 108 days, until October 18th 2016 and R3 for 43 days, until September 9th 2016. Since all the results form R2 were presented and discussed in section 4a.1., this section deals only with the results for R1 and R3.

As previously mentioned, for obtaining aerobic granules in the desired reactor, here R3, the settling time must be shortened. Therefore, setting time in R3 were decreased

gradually until it reached the value of two minutes after 19 days from the start-up. Figure 0-31 shows the changes of settling time for the reactors. Also, some microscopic image of R1 and R3 are provided below. See Figure 0-32 to Figure 0-34.

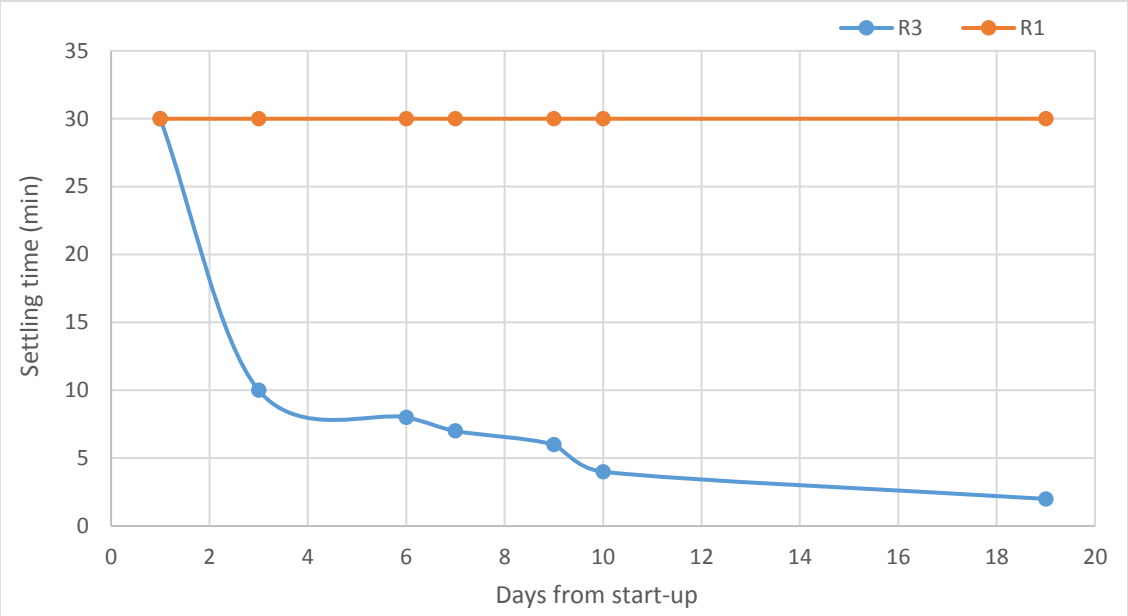

Figure 0-31. Changes of settling time for R1 and R3 during the first 19 days of operation

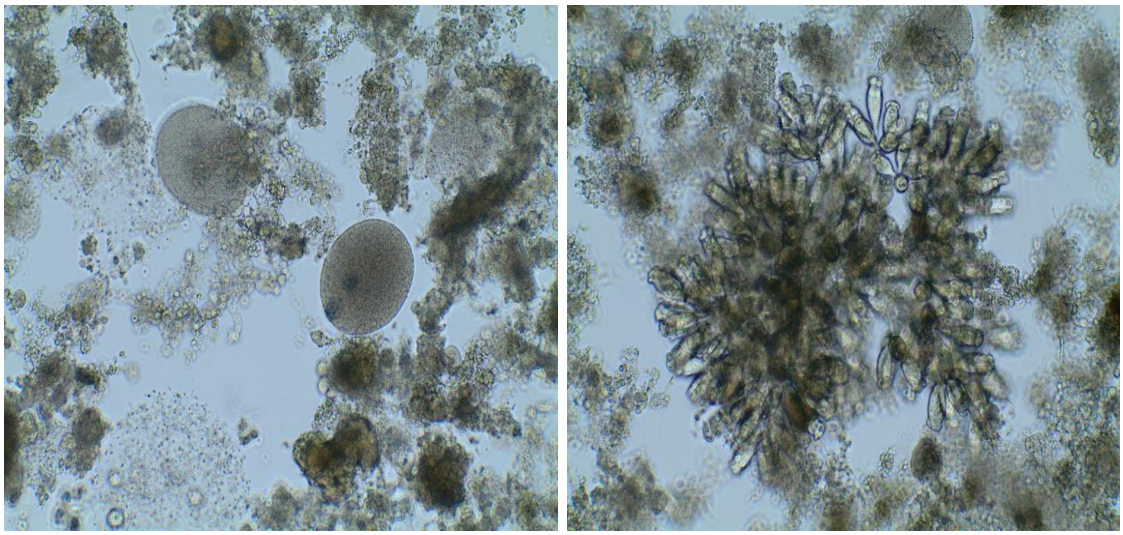

Figure 0-32. Microscopic image of R1 after 21 days from inoculation

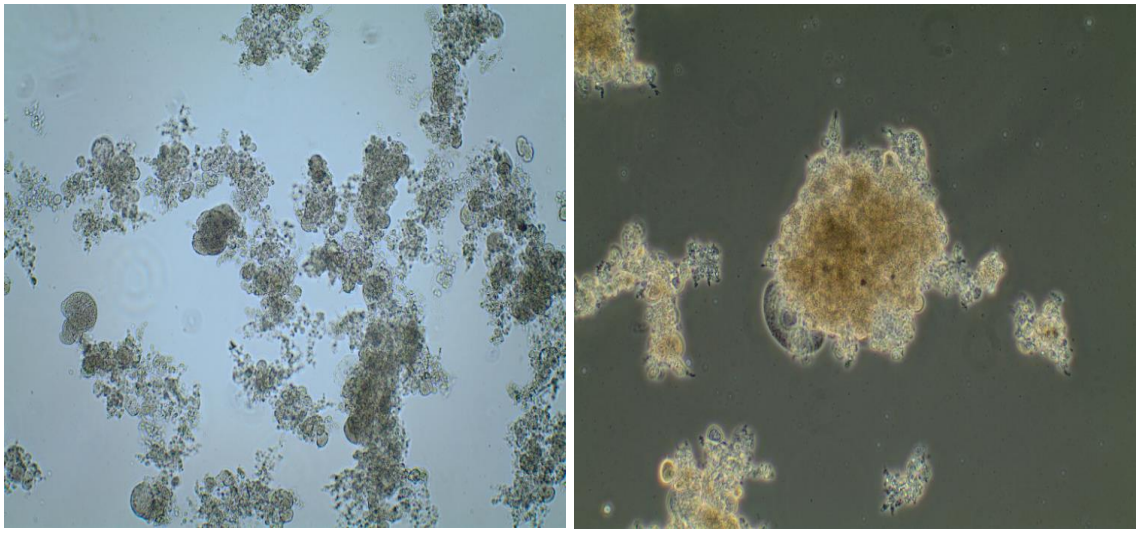

Figure 0-33. Microscopic image from R3 after 7 days from inoculation

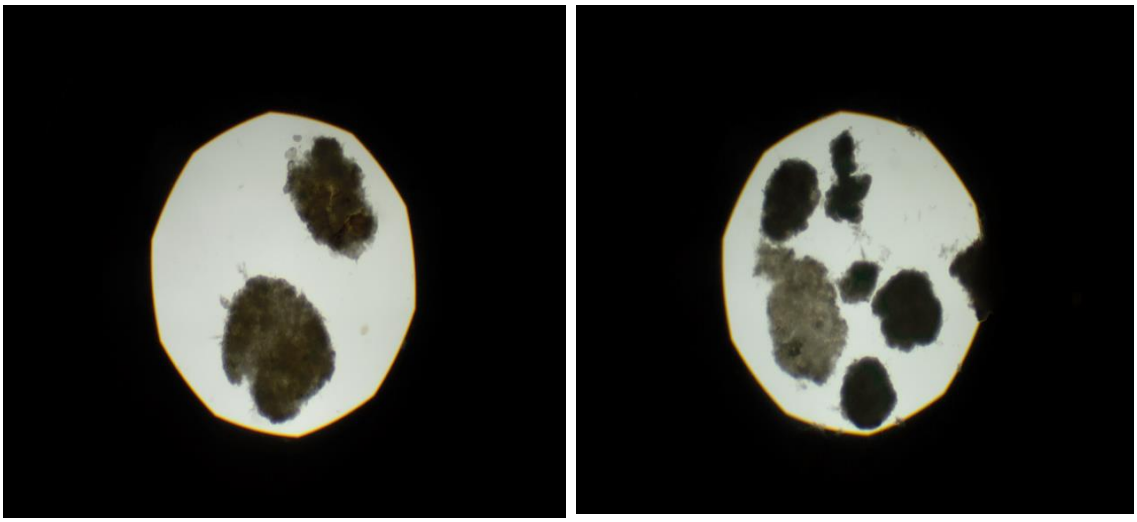

Figure 0-34. Microscopic image from R3 after 15 days (left) and 21 days (right) from inoculation

4a.2.1. Sludge analysis

The MLSS and MLVSS concentration in R1 and R3 are illustrated in Figure 0-35 and Figure 0-37 respectively. Changes of MLVSS/MLSS over time for the reactors are provided in Figure 0-36 and Figure 0-38.

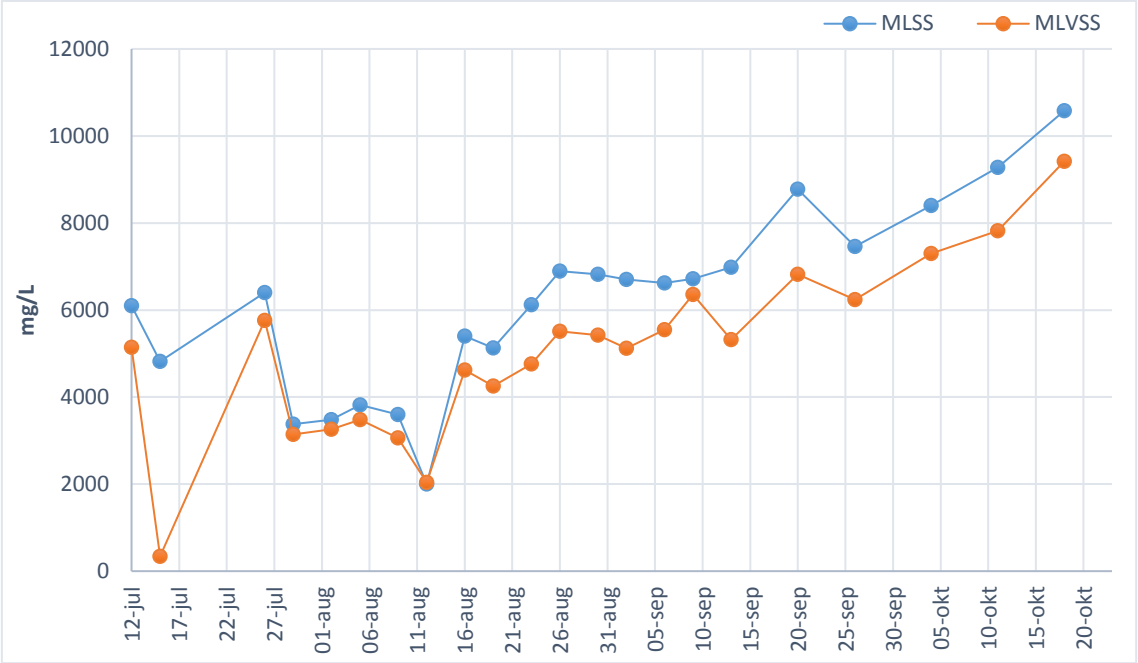

Figure 0-35. MLSS and MLVSS concentration in R1

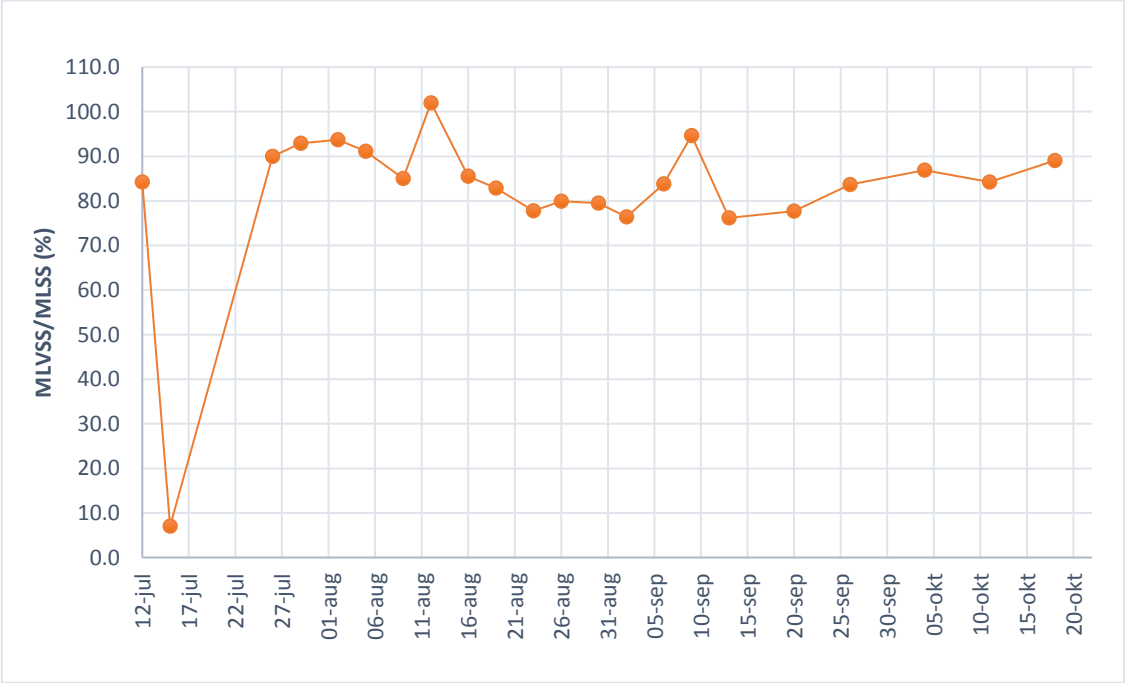

Figure 0-36. Changes of MLVSS/MLSS ratio for R1

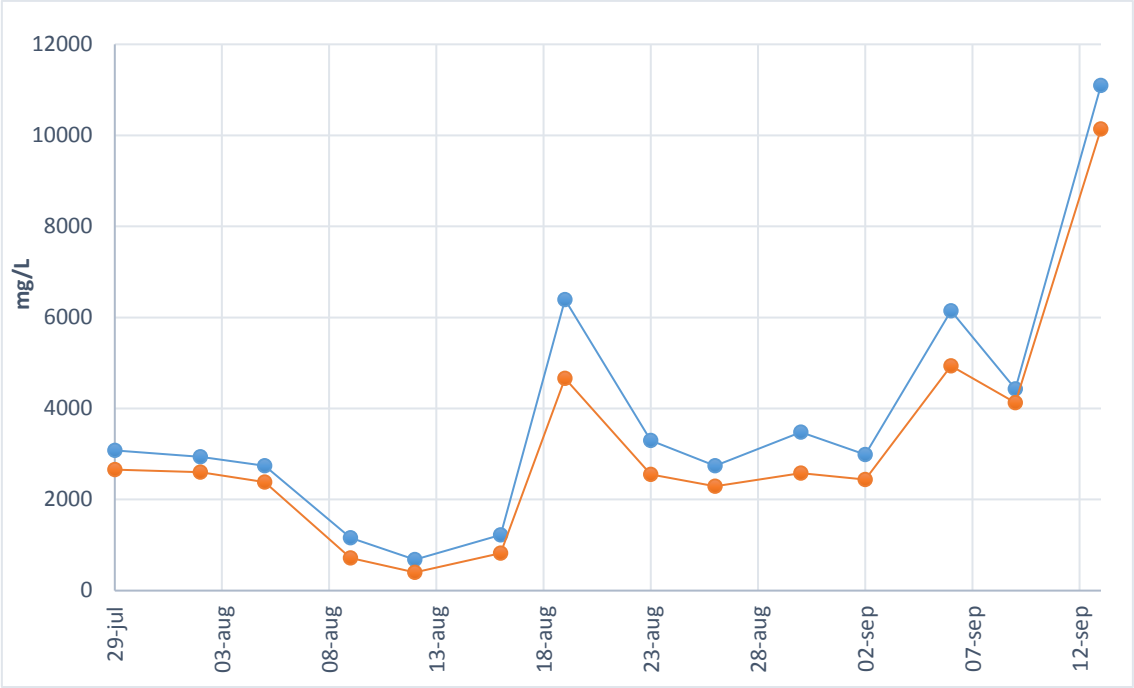

Figure 0-37. MLSS and MLVSS concentration in R3

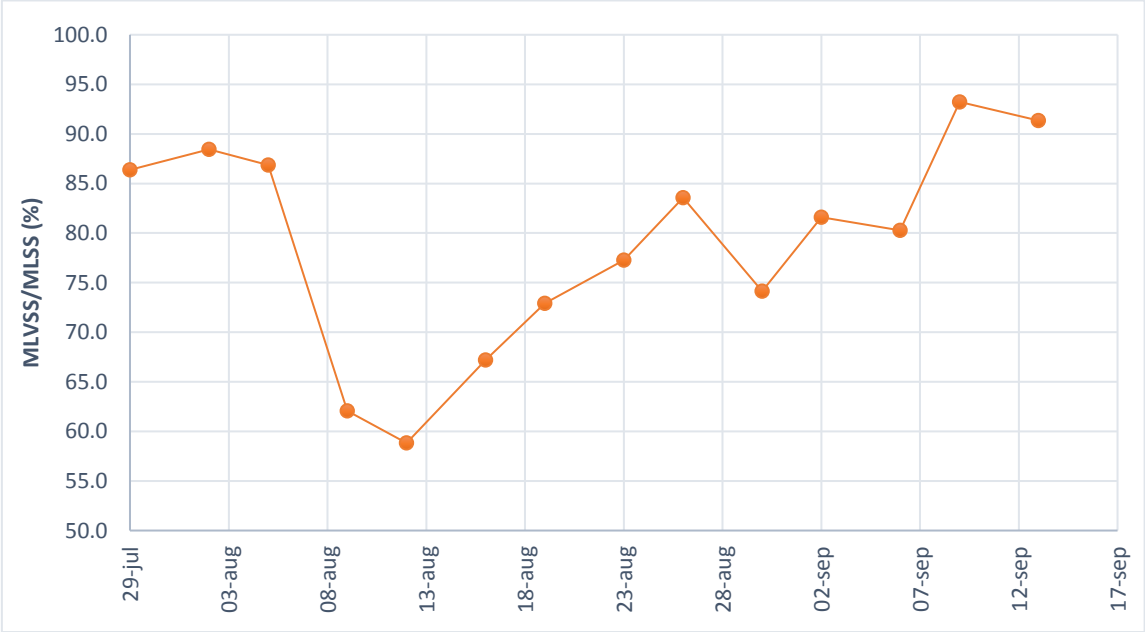

Figure 0-38. Changes of MLVSS/MLSS ratio for R3

The MLSS concentration of the seed sludge on the day of inoculation was 2720 mg/L. According to Figure 0-35, only one week after inoculation, the MLSS concentration in R1 reached 6100 mg/L. During the next four weeks, the MLSS decreased until it reached to the minimum of 2000 mg/L on August. 12th, Therefore, it is expected to observe an increase in SS concentration in the effluent during this period, see Figure 0-39.

From 12th of August, the reactor performance became stable for 3 weeks at the average MLSS of 5000 mg/L. From then, the biomass concentration in the reactor continued to increase and reached the maximum of 10580 mg/L on October18th. As it is observed, during the last five weeks, the reactor's performance has not stabilized and this is usually the sign of inadequate or non-regular sludge removal. However, high concentration of biomass in the reactor would be beneficial for organic matter removal and would improve the capacity of the reactor to resistance against shock loadings (Tay, et al., 2002).

MLVSS in the reactor had also similar trend as MLSS. The MLVSS/MLSS ratio was almost 85% on the beginning of the experiment and it increased to almost 100% on August12th. Then it stabilizes at the average of around 85%. The increase in MLVSS/MLSS ratio is the sign of new biomass formation and the values for this reactor is in agreement with the references (Tchobanoglous, et al., 2004).

In reactor 3, the MLSS and MLVSS had also similar trend. The MLSS on the beginning of the operation was around 3000 mg/L, however, it faced a sharp decrease to the minimum of 400 mg/L due to reduction of settling time and severe biomass washout on 14th of August. After this period, the biomass started to increase in the reactor and reached the value of 6400 mg/L on August 19th. After this period, the biomass concentration in the reactor began to stabilize around the value of 3500 mg/L until 7th of September. Again, after this time the biomass concentration in the reactor started to increase and reached the maximum of 11000 mg/L.

For this reactor, the MLVSS/MLSS ratio was almost 85% at the beginning of inoculation. However, after a sharp decrease to the minimum of 55% on August12th, it increased to the value close to 90%. The reason for the sharp reduction of MLVSS/MLSS are due to some error or accumulation of inorganic material from the feed.

4a.2.2. Supernatant (effluent) analysis

4a.2.2.1. Total Suspended Solids and Volatile Suspended Solids

The TSS and VSS in the supernatant from R1 and R3 are illustrated in Figure 0-39 and Figure 0-40. The VSS/TSS ratio for the supernatant from the aforementioned reactors and provided in Figure 0-41 and Figure 0-42.

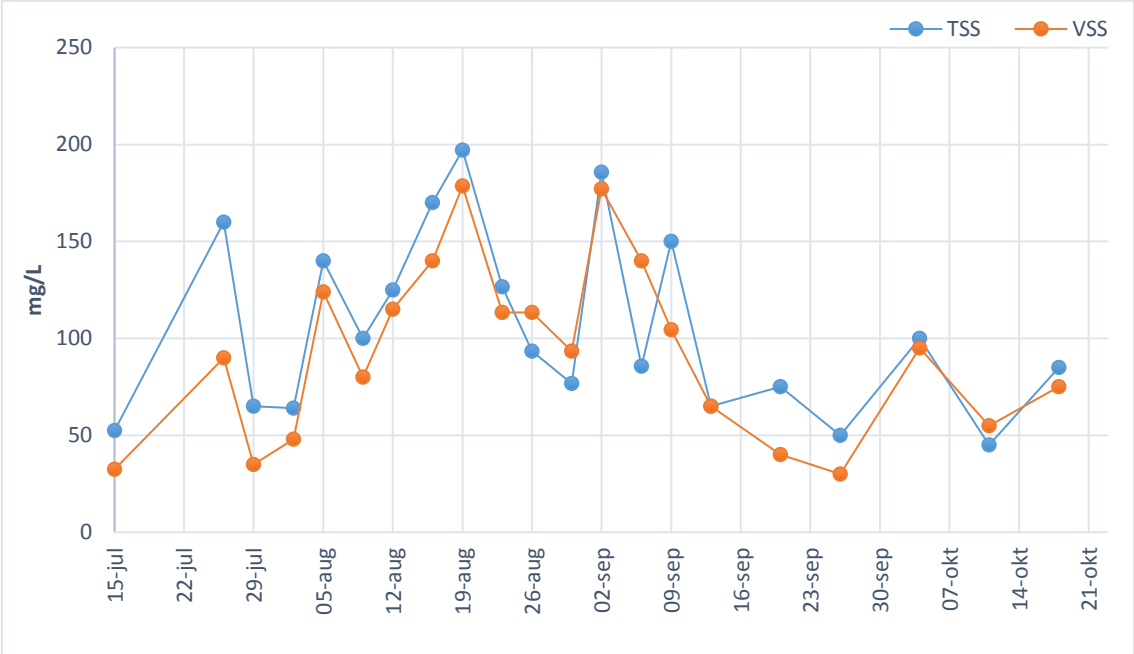

Figure 0-39. TSS and VSS of the supernatant from R1

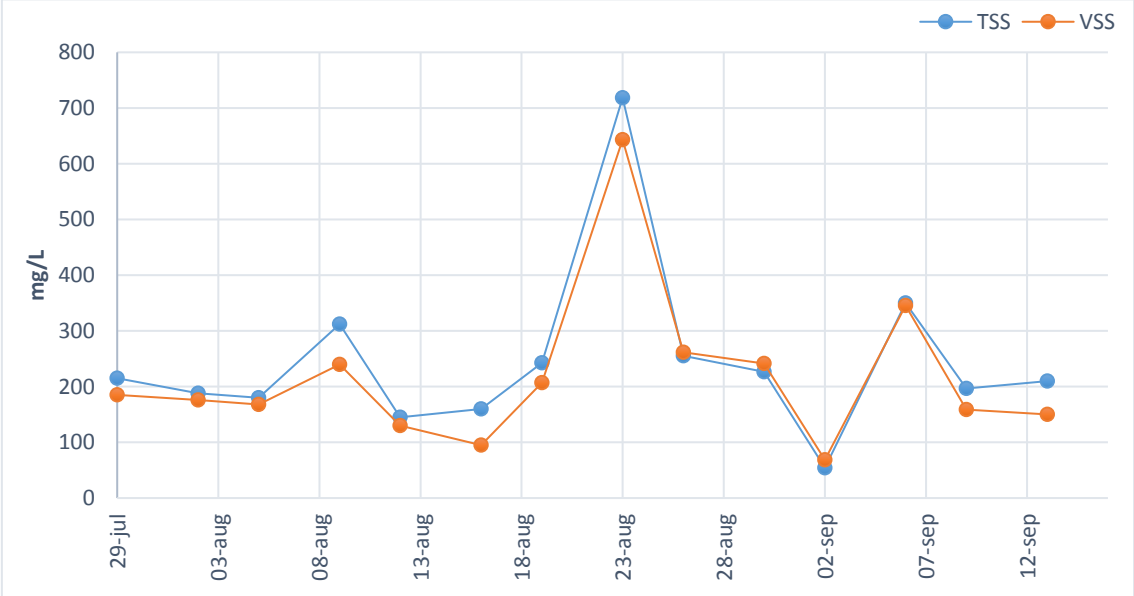

Figure 0-40. TSS and VSS of the supernatant from R3

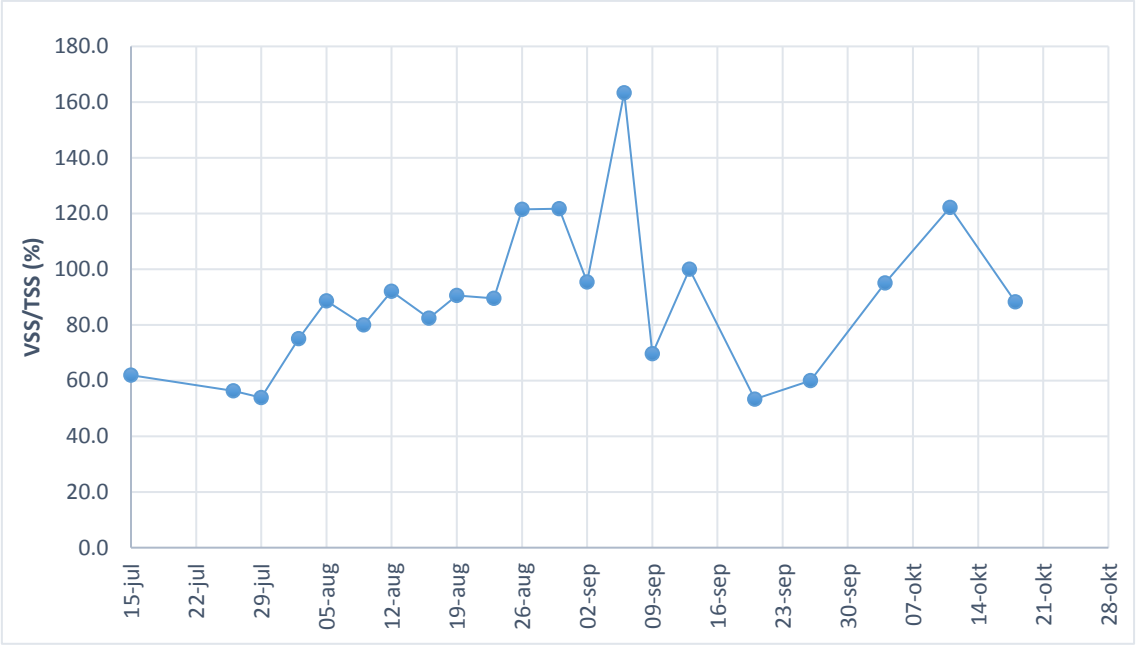

Figure 0-41. VSS/TSS ratio for the supernatant from R1

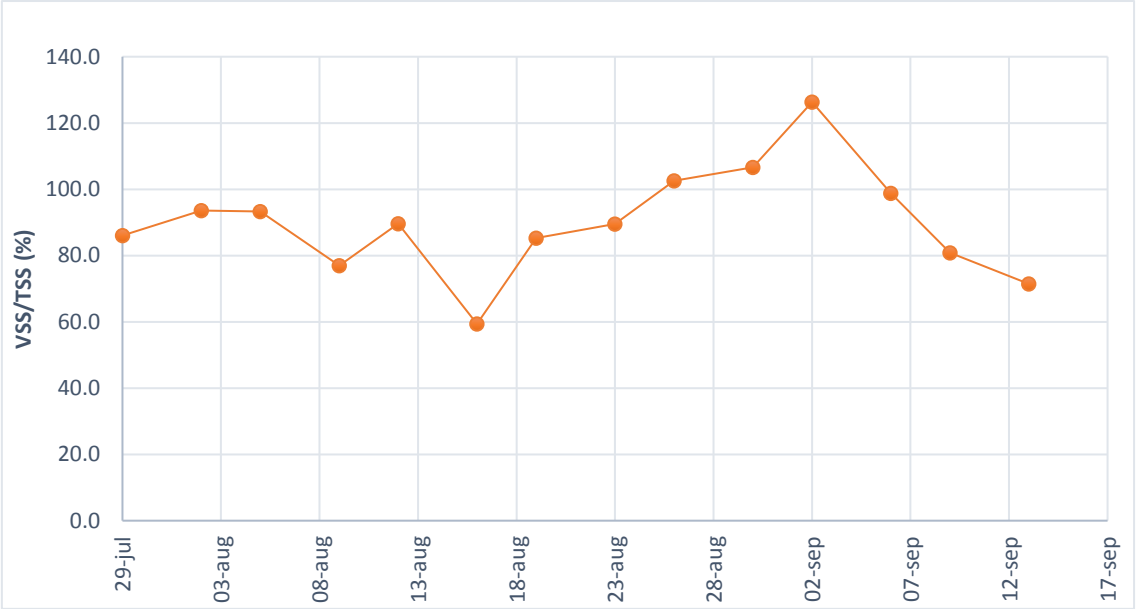

Figure 0-42. VSS/TSS ratio for the supernatant from R3

According to Figure 0-39, the SS concentration in the effluent from R1 at the beginning of the operation was 50 mg/L. From that time until late August, the SS concentration in the reactor underwent an increase trend and touched the maximum of 200 mg/L on

August19th. A possible reason for this increase maybe due to the new environment for the biomass. After this time, the reactor performance improved and as a result, SS concentration decreased in the effluent and reached the value around 75 mg/L at the end of the operation. However, according to the limitation set by EU directive, the effluent from this reactor needs further treatment prior discharging to the environment.

In Reactor 3, as shown in Figure 0-40, the SS concentration in the effluent was around200 mg/L at the beginning of inoculation and gradually increased to 700 mg/L in 23rd of August. This increasing trend is due to the biomass washout. After that, the SS concentration dropped to the minimum of 70 mg/L on 2nd of September and began to stabilize for the rest of the operation at the average value of 200 mg/L. By comparing the performance of the two reactors in removing SS it can be said that granular sludge had a more stable performance than floccular sludge but at lower efficiency with higher concentrations of suspended solids in the effluent.

4a.2.2.2. Organic Carbon

The reactors' performance in removing organic matter, here acetate, are depicted in Figure 0-43 to Figure 0-46.

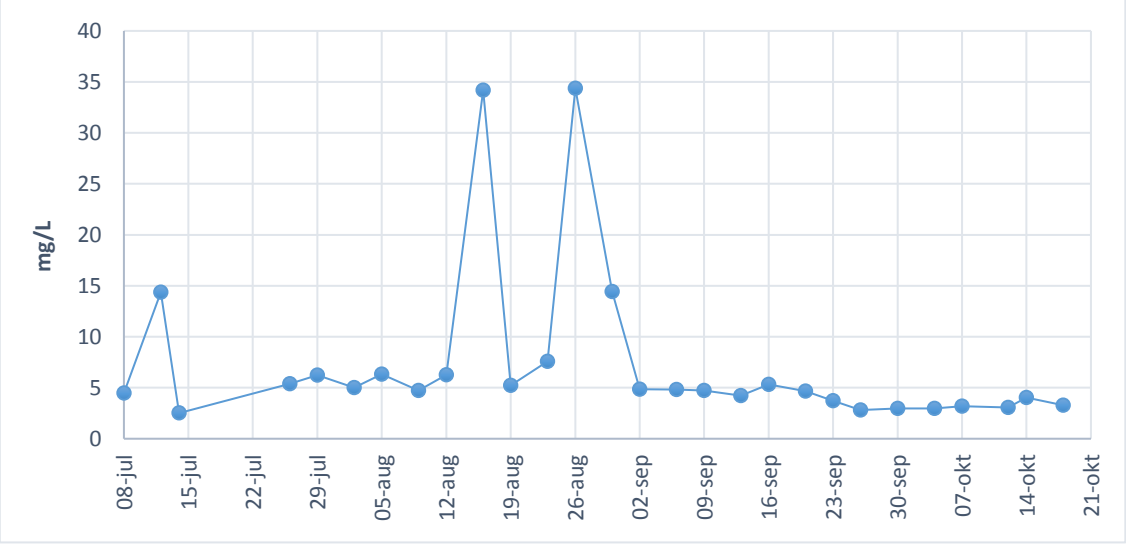

Figure 0-43. DOC concentration in the effluent from R1

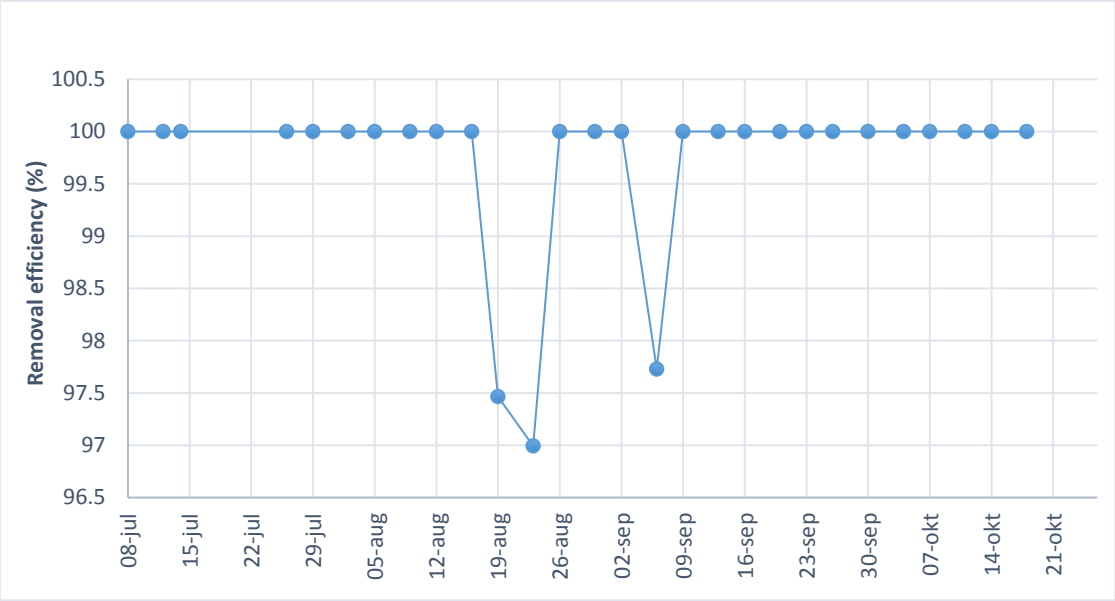

Figure 0-44. Acetate removal efficiency for R1

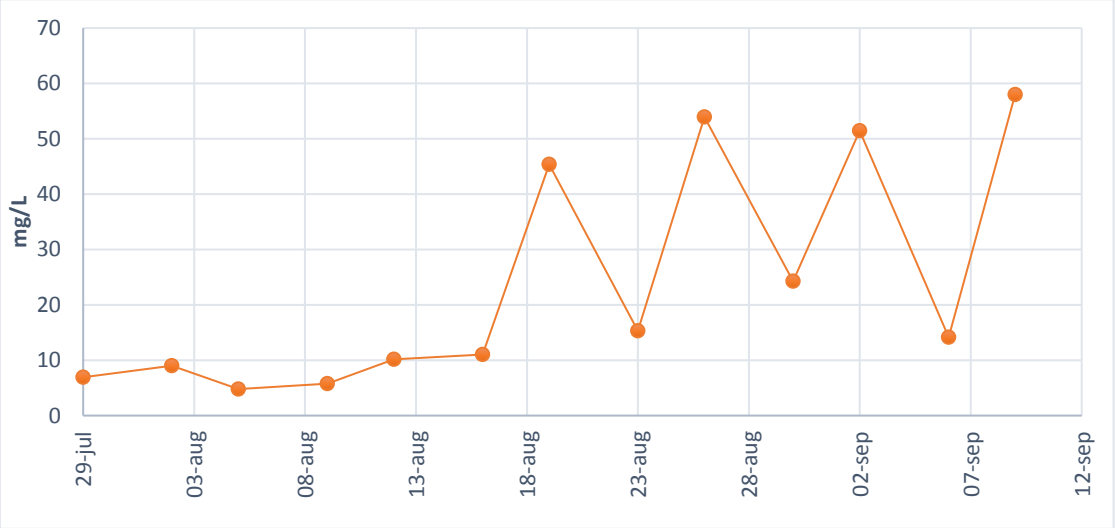

Figure 0-45. DOC concentration in the effluent from R3

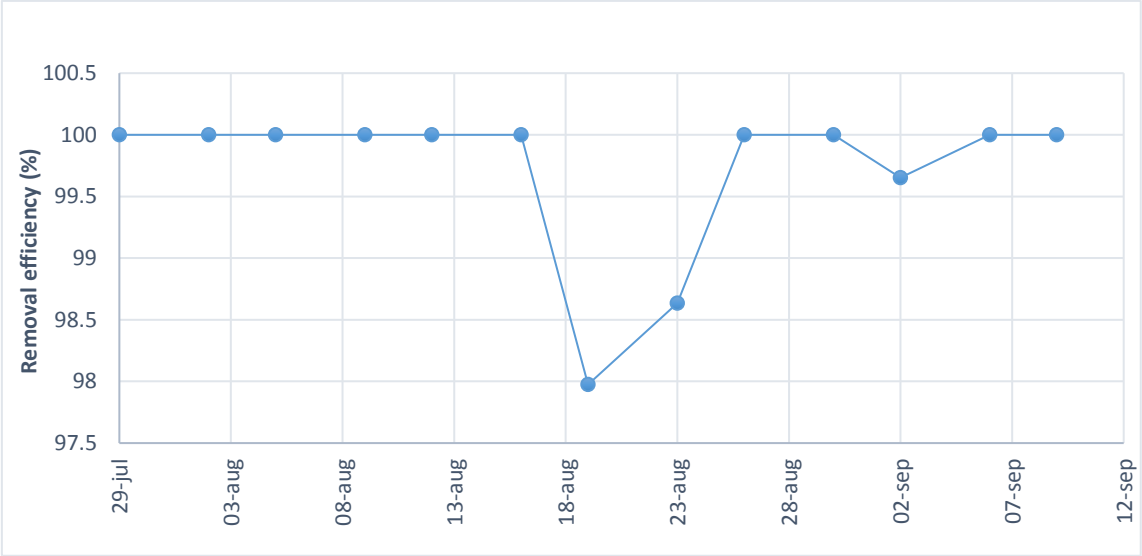

Figure 0-46. Acetate removal efficiency for R3

According to Figure 0-43, reactor 1, which was operating with floccular sludge, had 5 mg/L of DOC at the beginning of the operation and stabilized within the two weeks of operation. There are a few times that the DOC concentration in the effluent were elevated and reached the maximum of 35 mg/L. however, apart from these picks, the DOC concentration in the effluent were below 5 mg/L and the reactors operation were quite stable.

Reactor 3, Figure 0-45, had 10 mg/L of DOC at the beginning of operation and started to decrease until 12th of August. But unlike R1, the performance of this reactor did not stabilize during the rest of operation and it was fluctuating a lot. Finally, on 9th of September it reached to the maximum of 60 mg/L.

According to Figure 0-44 and Figure 0-46, both of the reactors showed excellent performance in removing organic matter from the early stages of operation (above 97%). Moreover, their performances were stable and uniform. These results are consistent with the findings of Tay et al (2010).

4a.2.2.3. Nutrient removal

4a.2.2.3.1. Nitrogen removal

The performance of the reactors in removing TN, ammonium, nitrite and nitrate are depicted in Figure 0-47to Figure 0-50. The concentrations of ammonium in the influent was approximately nitrate and nitrite in the feed stream were 115 mg/L.

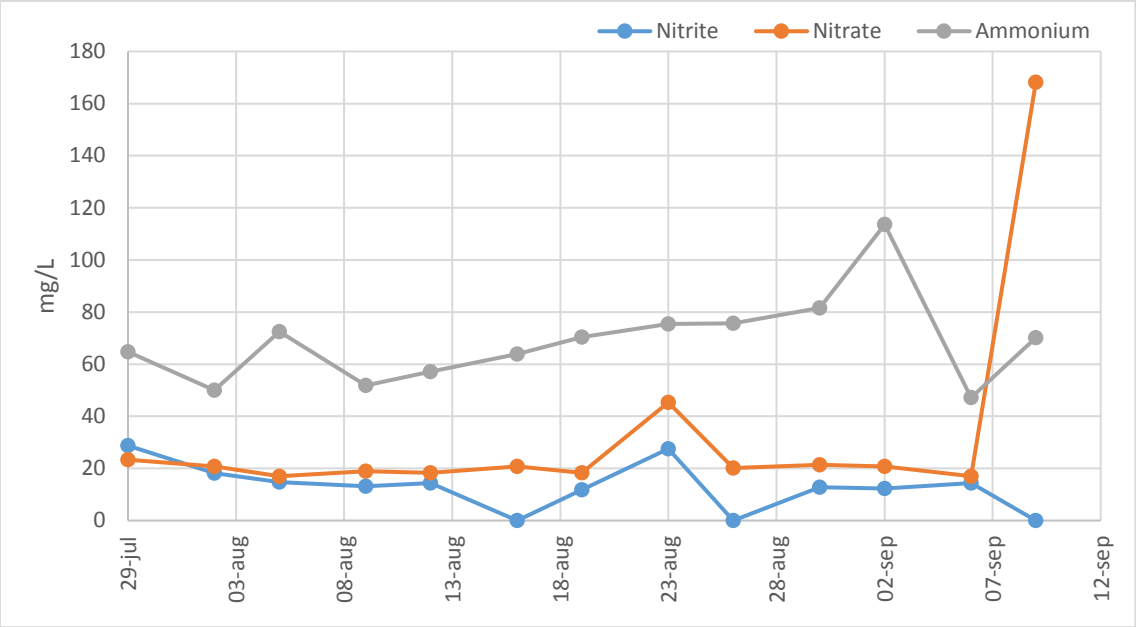

Figure 0-47. Ammonium, nitrite and nitrate concentration in the effluent from R3

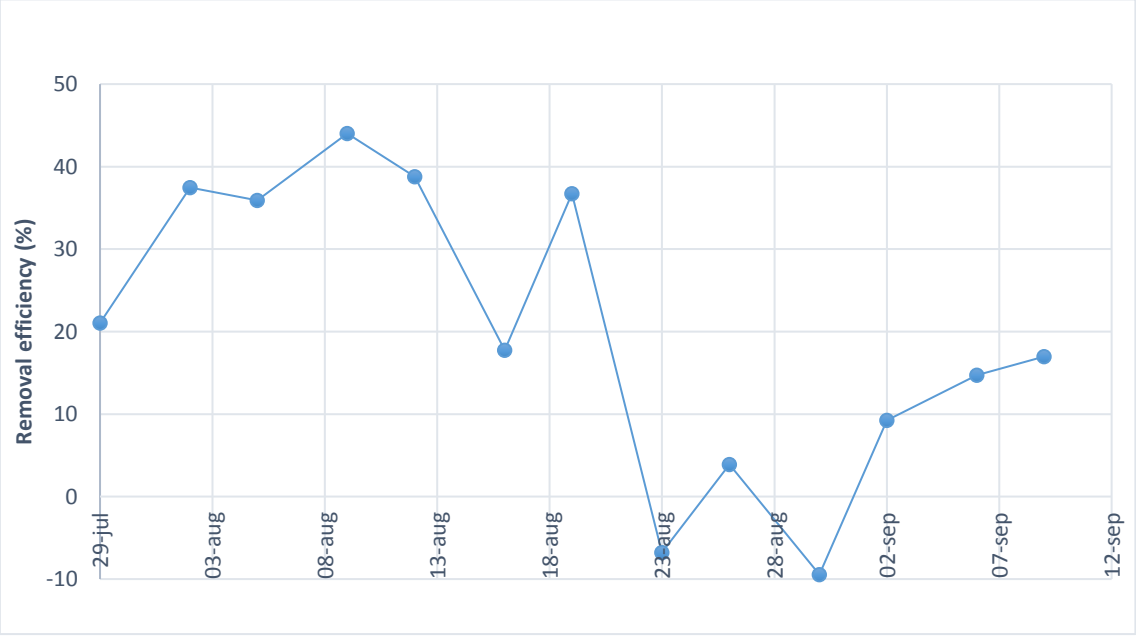

Figure 0-48. Total nitrogen removal efficiency for R3

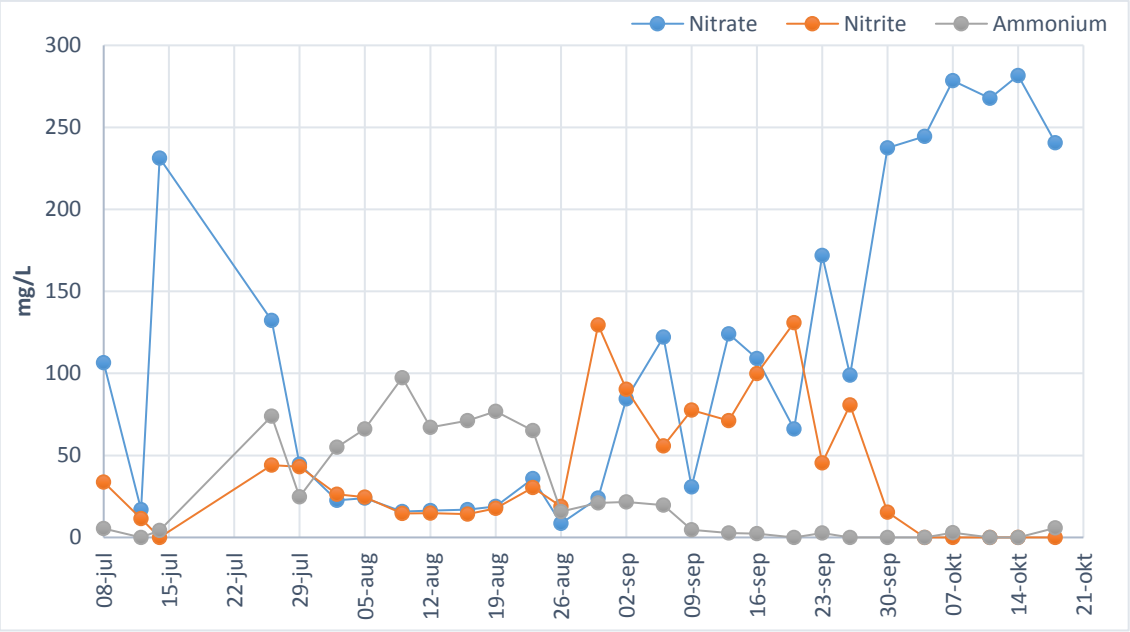

Figure 0-49. Ammonium, nitrite and nitrate concentration in the effluent from R1

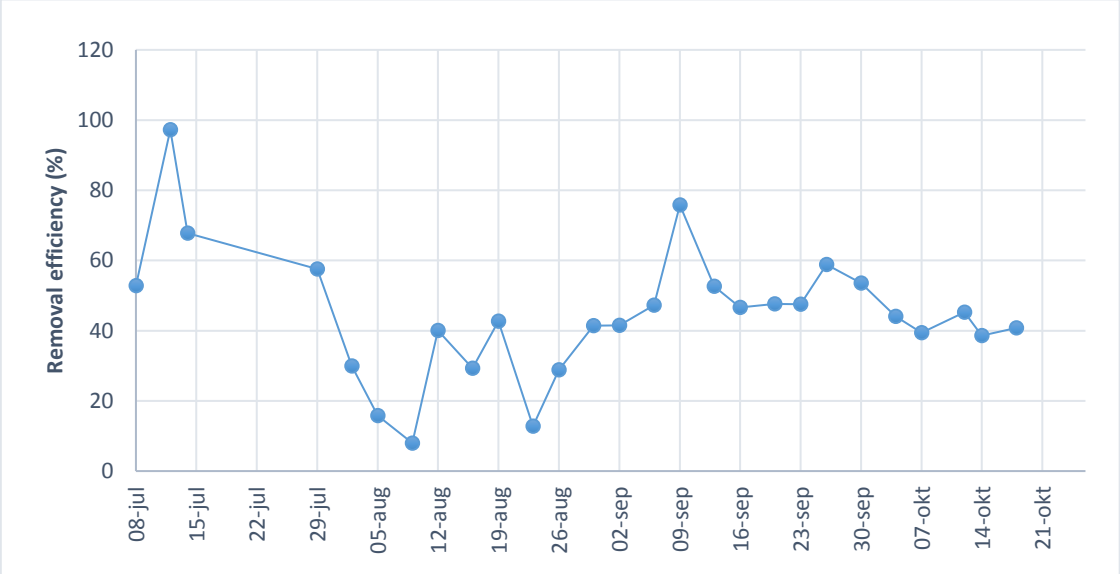

Figure 0-50. Total nitrogen removal efficiency for R1

As shown in Figure 0-47, in R3, ammonium concentration in the effluent from the reactor and at the beginning of the operation was approximately 65 mg/L, however, according to the results, it seems that no ammonium oxidation has happened in this reactor and the ammonium concentration was remained almost constant. This indicates that no

nitrification has happened in the reactor. Nitrate and nitrite have undergone almost a similar trend except for the end of the operation when there was a slight nitrate accumulation in the reactor. For this reactor, TN removal efficiency was 20 % at the beginning of the operation, but while the aerobic granules were forming, denitrification was also enhancing in the reactor, resulted in increase in TN removal efficiency. After only 10 days from the inoculation, on August 9th, the reactor reached its maximum performance with 45% removal of total nitrogen. From that time, reactor performance started to decrease and reached the minimum of minus 10 % on August 30th. This negative value and the elevated ammonium concentration in the reactor at this period, indicate that ammonium was not being oxidized and was remained in the reactors from successive cycles. The reasons for the impaired nitrification is (are) unknown, however, inhibition of nitrifiers due to some operational factors such as low pH and temperature, and low depth of DO are proved in various studies (Bao, et al., 2009).

According to Figure 0-49 and Figure 0-50 in reactor1, the concentration of ammonium was high and underwent an increase trend followed by a sharp drop until September 9th. Then ammonium concentration dropped to the negligible value for the rest of the operation. The reduction in ammonium concentration is the sign of nitrification. During the first week of operation, nitrite and nitrate concentration decreased which indicate that denitrification was proceeding in the reactor and total nitrogen removal touched the maximum of 100 %. From July 15th to July 26th, nitrite, nitrate concentration increased, resulting in a sharp reduction in total nitrogen removal efficiency during this period. After this period, the reactor performance in removing total nitrogen improved and stabilized at the average of around 45%.

From the results, it can be concluded that granulated reactor had more fluctuating trend and lower performance in removing total nitrogen in comparison to flocculated. Also by comparing the TN removal efficiency of granular sludge in the second run with that of the first run, it is observed that granular sludge in the first run had better performance in removing nitrate, nitrite and consequently higher TN removal efficiency. The reason for that is mainly due to the granules' size. As the diameter of the aerobic granular sludge increases, it forms a certain anaerobic area in the inner part of the granule, which will improve the denitrification process, therefore, the TN removal rate can be improved.

4a.2.2.3.2. Phosphate Removal

The phosphate removal efficiencies of the operating reactors are depicted in Figure 0-51 and Figure 0-52.

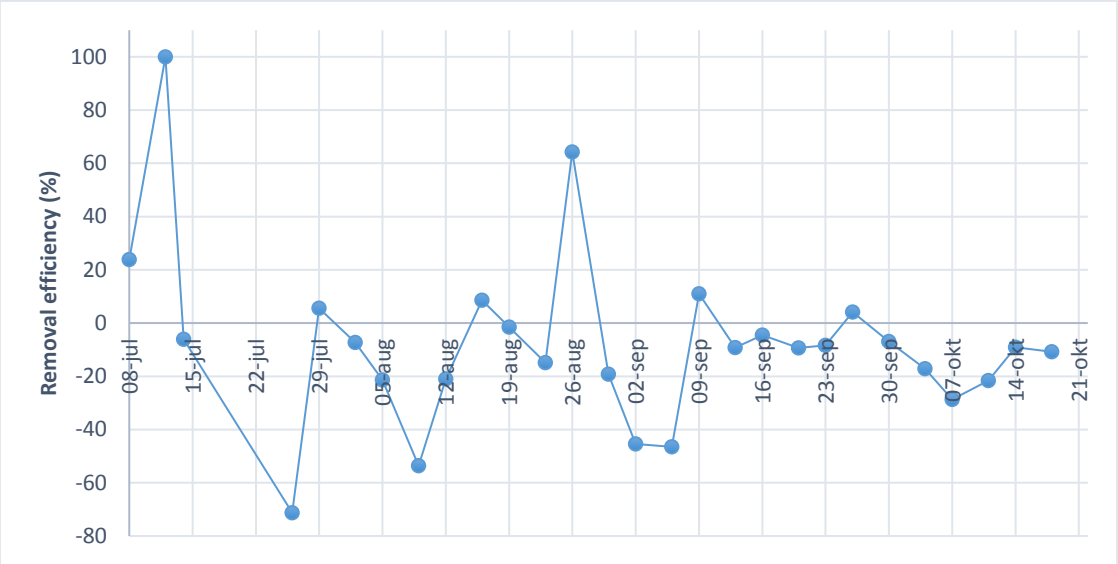

Figure 0-51. Phosphate removal efficiency for R1

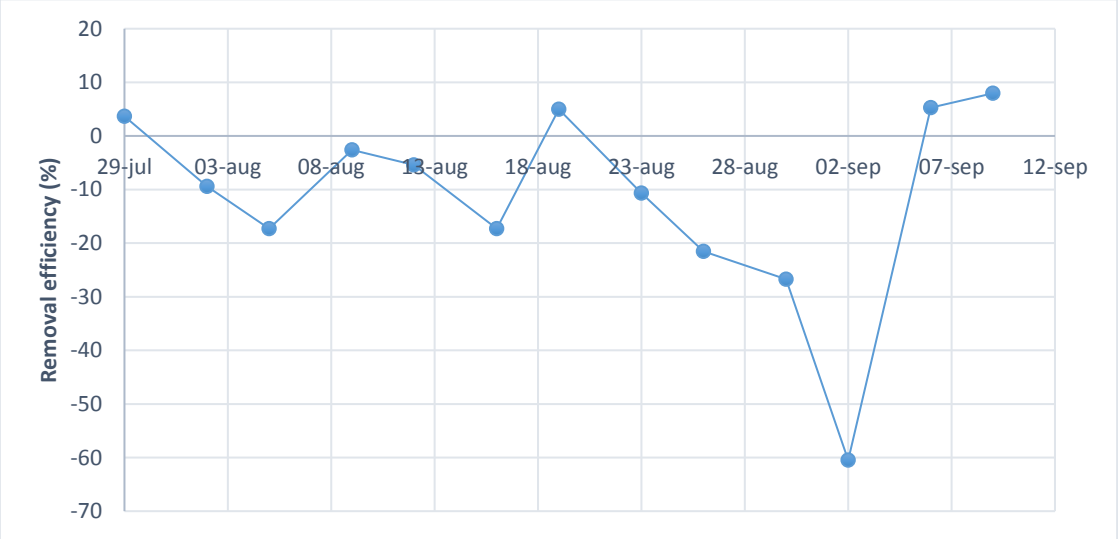

Figure 0-52. Phosphate Removal efficiency for R3

As it is clear from the graphs, phosphate removal has taken place in both reactors to some extent but in general the performance was not stable over the operation time. The average phosphate removal efficiency for flocculated reactor, R1, is minus 7.5% and for

granulated reactor it is minus 11.5%. The negative value means, the phosphate release in the system during the anoxic phase but it has not been taken up during the aerobic phase.

4a.2.3. Cycle Analysis

A cycle measurement was conducted in this run to show the typical reactors' performance during one cycle of operation.

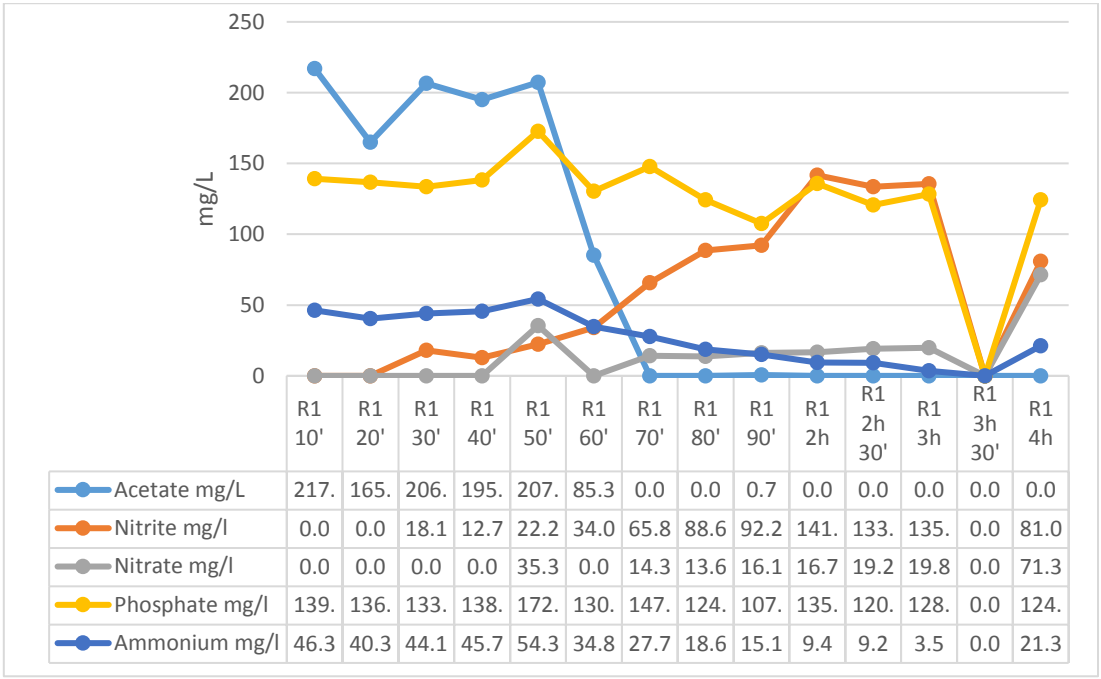

	R1 10'	R1 20'	R1 30'	R1 40'	R1 50'	R1 60'	R1 70'	R1 80'	R1 90'	R1 2h	R1 2h 30'	R1 3h	R1 3h 30'	R1 4h
Acetate mg/L	217.	165.	206.	195.	207.	85.3	0.0	0.0	0.7	0.0	0.0	0.0	0.0	0.0
Nitrite mg/l	0.0	0.0	18.1	12.7	22.2	34.0	65.8	88.6	92.2	141.	133.	135.	0.0	81.0
Nitrate mg/l	0.0	0.0	0.0	0.0	35.3	0.0	14.3	13.6	16.1	16.7	19.2	19.8	0.0	71.3
Phosphate mg/l	139.	136.	133.	138.	172.	130.	147.	124.	107.	135.	120.	128.	0.0	124.
Ammonium mg/l	46.3	40.3	44.1	45.7	54.3	34.8	27.7	18.6	15.1	9.4	9.2	3.5	0.0	21.3

Figure 0-53. cycle study for R1(aeration was started at 60' and turned off at 3h23')

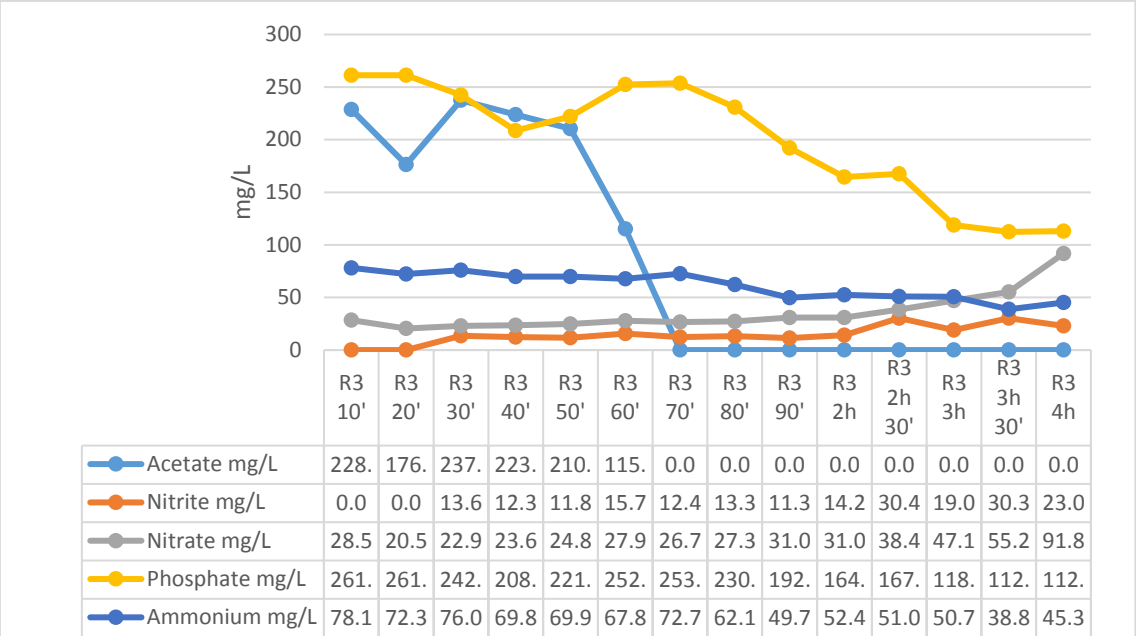

	R3 10'	R3 20'	R3 30'	R3 40'	R3 50'	R3 60'	R3 70'	R3 80'	R3 90'	R3 2h	R3 2h 30'	R3 3h	R3 3h 30'	R3 4h
Acetate mg/L	228.	176.	237.	223.	210.	115.	0.0	0.0	0.0	0.0	0.0	0.0	0.0	0.0
Nitrite mg/L	0.0	0.0	13.6	12.3	11.8	15.7	12.4	13.3	11.3	14.2	30.4	19.0	30.3	23.0
Nitrate mg/L	28.5	20.5	22.9	23.6	24.8	27.9	26.7	27.3	31.0	31.0	38.4	47.1	55.2	91.8
Phosphate mg/L	261.	261.	242.	208.	221.	252.	253.	230.	192.	164.	167.	118.	112.	112.
Ammonium mg/L	78.1	72.3	76.0	69.8	69.9	67.8	72.7	62.1	49.7	52.4	51.0	50.7	38.8	45.3

Figure 0-54. cycle analysis for R3 (aeration was started at 60' and turned off at 3h51')

The reactors during the whole experiment, were working under alternating anaerobic feeding phase with phosphate presence, anoxic phase and aeration phase to encourage the slow growth microorganisms such as PAOs and to promote biological phosphorus removal.

According to Figure 0-53 and Figure 0-54, acetate concentration started to decrease once the feeding phase was completed. The reason for this reduction is because of denitrifies and PAOs which taken up acetate. However, not all the acetate was converted into PHAs. Therefore, once the reactor entered the aeration phase, considerable amount of acetate remained. However, acetate was quickly consumed by heterotrophs.

During the feeding phase and anoxic phase, phosphate was released to the liquid and during the aerobic phase phosphate was taken up by PAOs and converted into cell-internal polyphosphate at a very slow rate.

By comparing the phosphate concentration in R1 and R3one can observe that granulated reactor had higher phosphate concentration during the aeration phase though they were fed with similar feed stream composition. The reason is due to the fact that some substrate

such as acetate can penetrate into deeper layer of the granules which results in phosphate release and PHB formation during the aeration phase (Bao, et al., 2009).

It is observed in the reactors that during the aeration phase, when there was no organic compound present in the reactors, ammonium was decreased while nitrate was increased This due to the oxidation of ammonium to nitrite and further to nitrate by AOBs and NOBs and the ability of these bacteria to grow independent of organic compounds (Winkler, 2012).

The summary of the reactors' performance during the whole experiment are reported in Table 0-1

Table 0-1. Overall reactors' performance

	First run		**Second run**	
Removal efficiency	R2 (295 days) Floccular sludge	R3 (162 days) Granular sludge	R1 (108 days) Floccular sludge	R3 (43 days) Granular sludge
Acetate	99%	99%	99.7%	99.7%
TN	52%	48%	45%	20%
Phosphate	16%	-0.01%	-7.7%	-11.5%

4a.3. pH records

As previously mentioned, the pH in the reactors were continuously recorded using a certain software and portable electrodes. Examples of a 9-day, and a single-cycle pH recording are provided in **Error! Reference source not found.** and Figure 0-55.

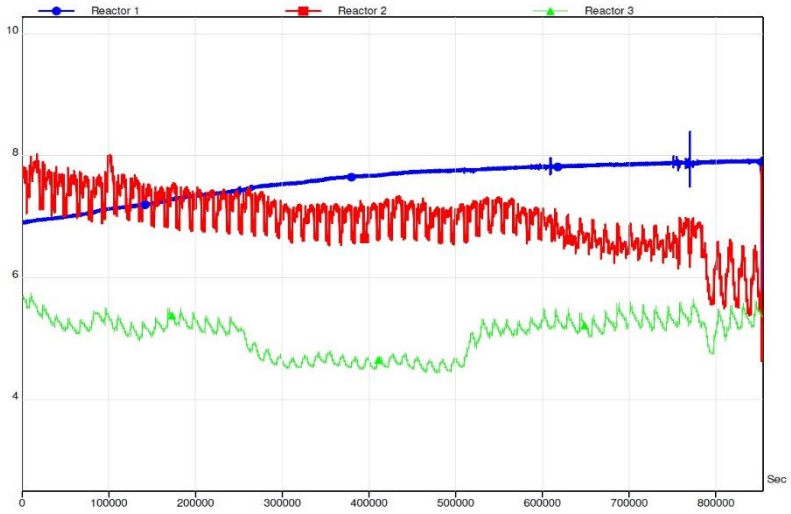

Figure 0-55. A 9 days pH recording

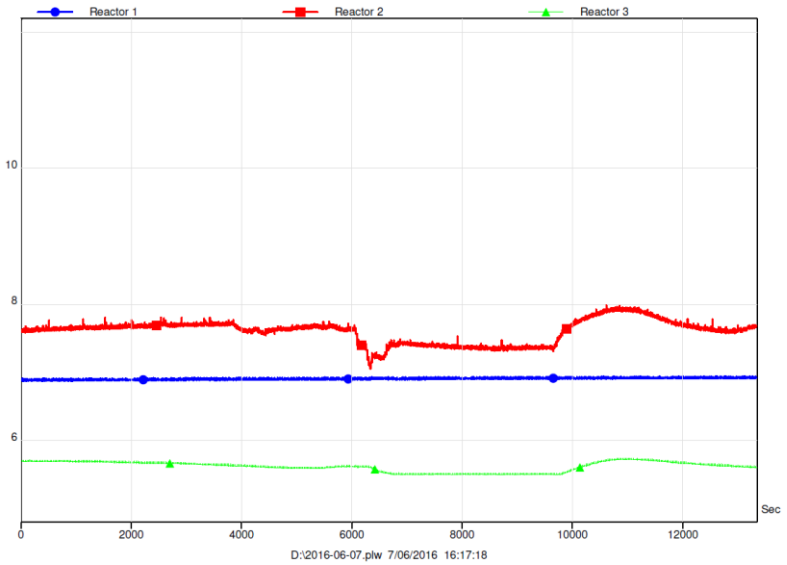

Figure 0-55. A single-cycle pH recording

As it is observed from the graphs above, the pH changes in the reactors did not follow the same pattern. In Figure 0-55 where a one cycle profile is shown, the pH in granulated reactor (R3) was lower than the other two. Also, the pH is not the same for floccular (R1) and semi-floccular sludge (R2) as well.

Figure 0-55 shows that the pH in the reactors changes with the time. Usually during the anaerobic phase, the pH is dropped due to fermentation processes and production of some other compounds. In contrast, during the aerobic phase, the pH in increased mainly due to CO_2 stripping.

b) Membrane filtration

As previously mentioned, the aim of the following filtration tests is to compare the filtration characteristics of floccular and aerobic granular sludge and the supernatant of these two reactors. Therefore, this section is dedicated to the laboratory experiments, results and discussion for the filtration tests. It is important to note that all the filtration tests in this work have been performed on the sludge and the effluents from R2 and R3 operating during the first run (February-July 2016).

The following section is delivered into three parts. The first part is related to the results for cake layer resistance measurement, the second part is related to the filtration of the effluent from the reactors and the third part is related to the filtration of kaolin suspension through the dynamic membrane.

4b.1. Cake layer resistance

The cake layer resistance of the sludge from reactor 2 and rector 3 were measured and the obtained results are presented and discussed below.

4b.1.1. Floccular sludge

4b.1.1.1. First trial

The first trial to measure the cake layer resistance of the floccular sludge, R2, was attempted on April 18th and 19th. The detailed information about flux and TMP for each of the graphs below can be found in Appendix Ⅲ. Some preliminary results are presented in Appendix V.

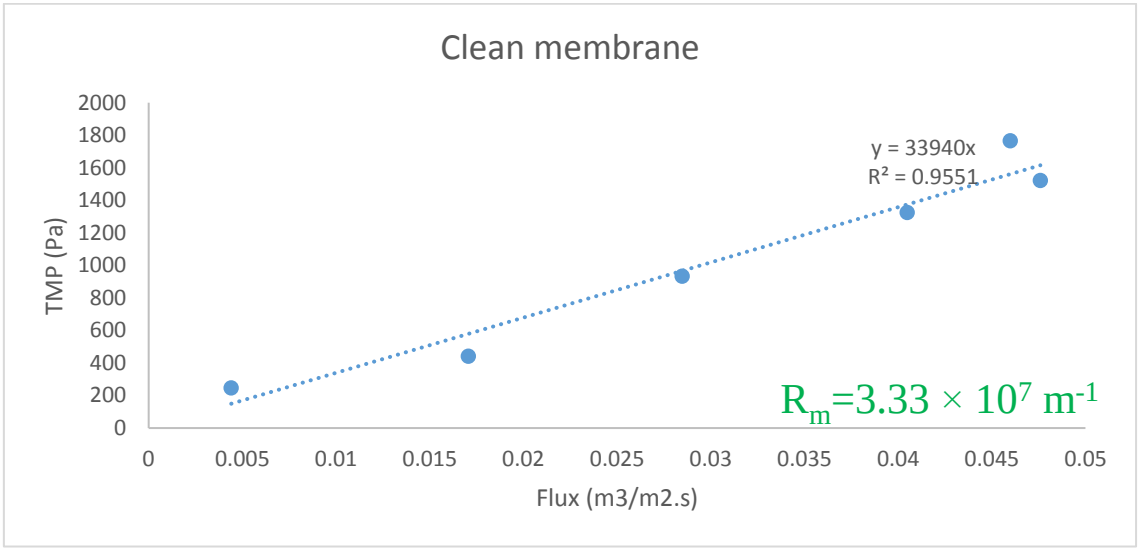
Clean membrane
TMP (Pa)
Flux (m3/m2.s)
y = 33940x
R² = 0.9551
$R_m=3.33 \times 10^7\ m^{-1}$

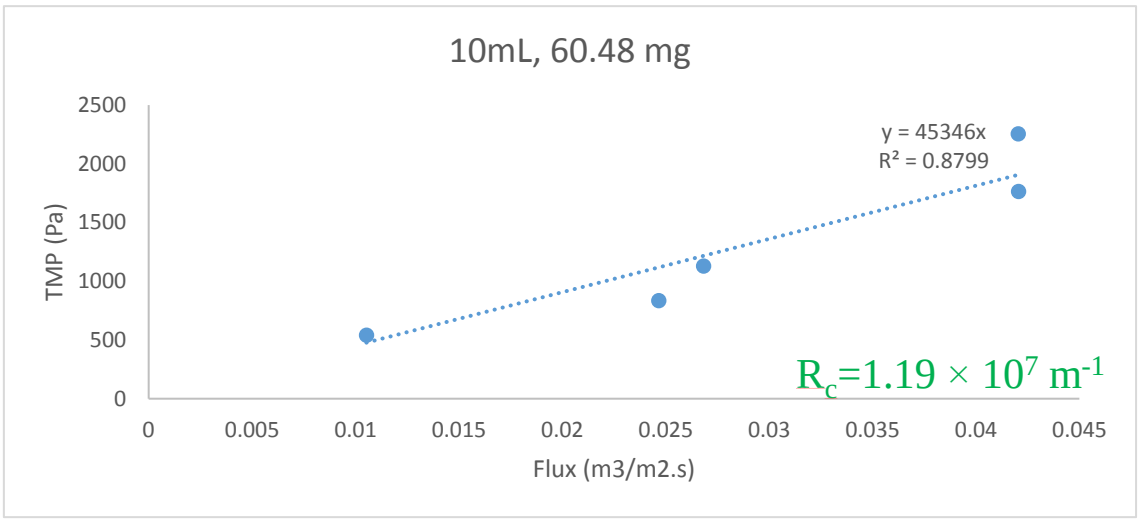
10mL, 60.48 mg
TMP (Pa)
Flux (m3/m2.s)
y = 45346x
R² = 0.8799
$R_c=1.19 \times 10^7\ m^{-1}$

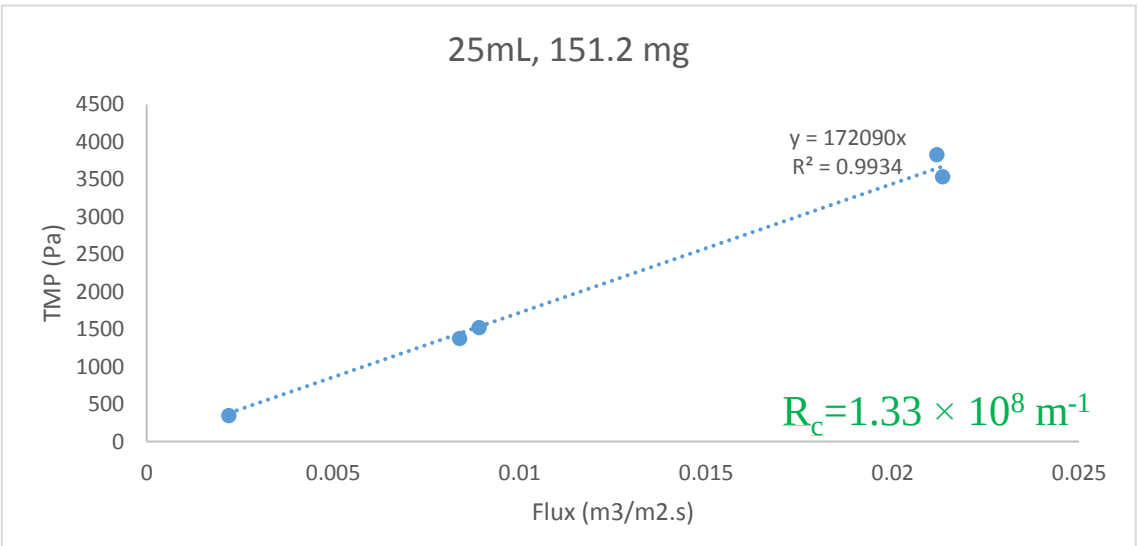
25mL, 151.2 mg
TMP (Pa)
Flux (m3/m2.s)
y = 172090x
R² = 0.9934
$R_c=1.33 \times 10^8\ m^{-1}$

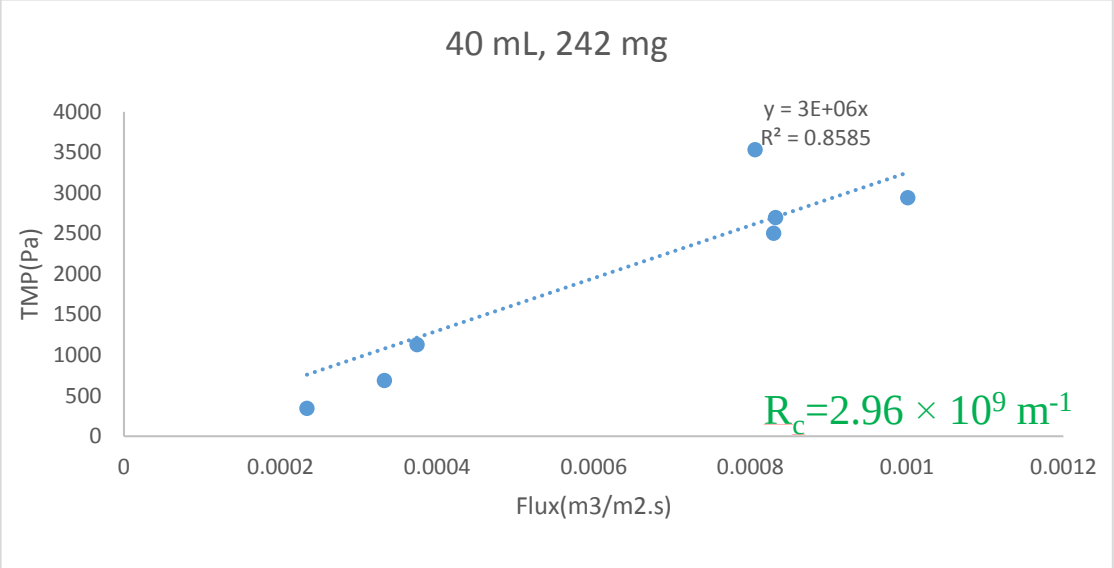
40 mL, 242 mg
y = 3E+06x
R² = 0.8585
TMP(Pa)
4000
3500
3000
2500
2000
1500
1000
500
0
0
0.0002
0.0004
0.0006
0.0008
0.001
0.0012
Flux(m3/m2.s)
$R_c=2.96 \times 10^9\ m^{-1}$

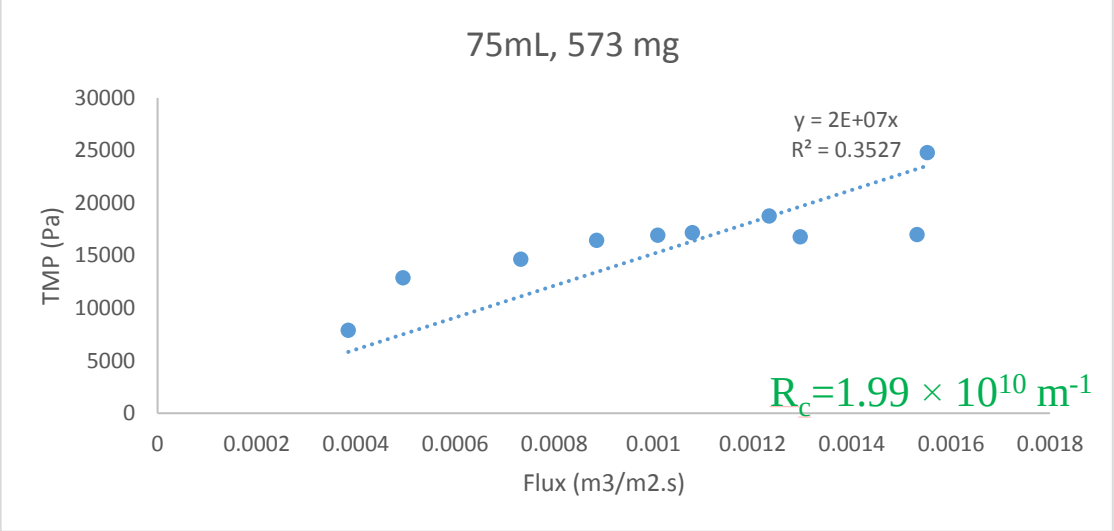
75mL, 573 mg
y = 2E+07x
R² = 0.3527
TMP (Pa)
30000
25000
20000
15000
10000
5000
0
0
0.0002
0.0004
0.0006
0.0008
0.001
0.0012
0.0014
0.0016
0.0018
Flux (m3/m2.s)
$R_c=1.99 \times 10^{10}\ m^{-1}$

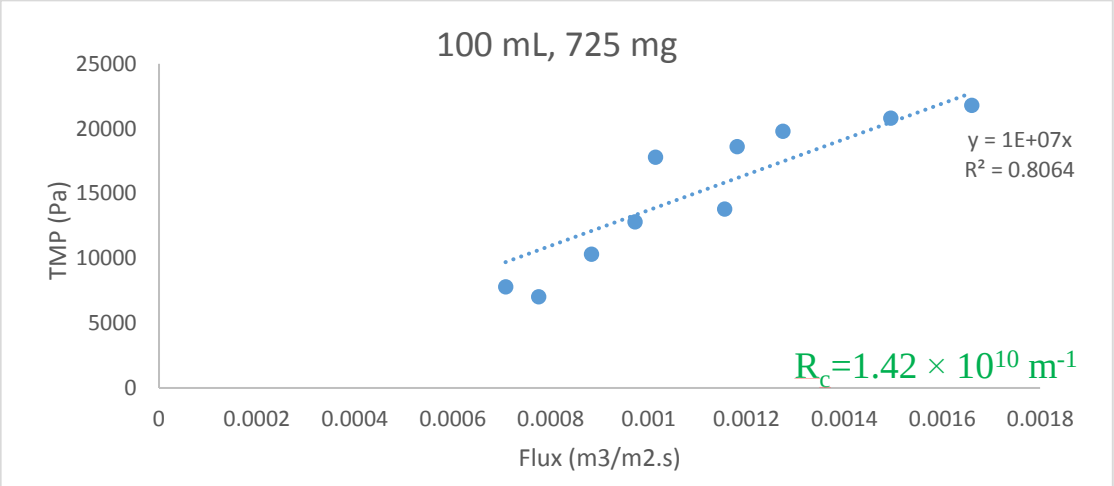
100 mL, 725 mg
y = 1E+07x
R² = 0.8064
TMP (Pa)
25000
20000
15000
10000
5000
0
0
0.0002
0.0004
0.0006
0.0008
0.001
0.0012
0.0014
0.0016
0.0018
Flux (m3/m2.s)
$R_c=1.42 \times 10^{10}\ m^{-1}$

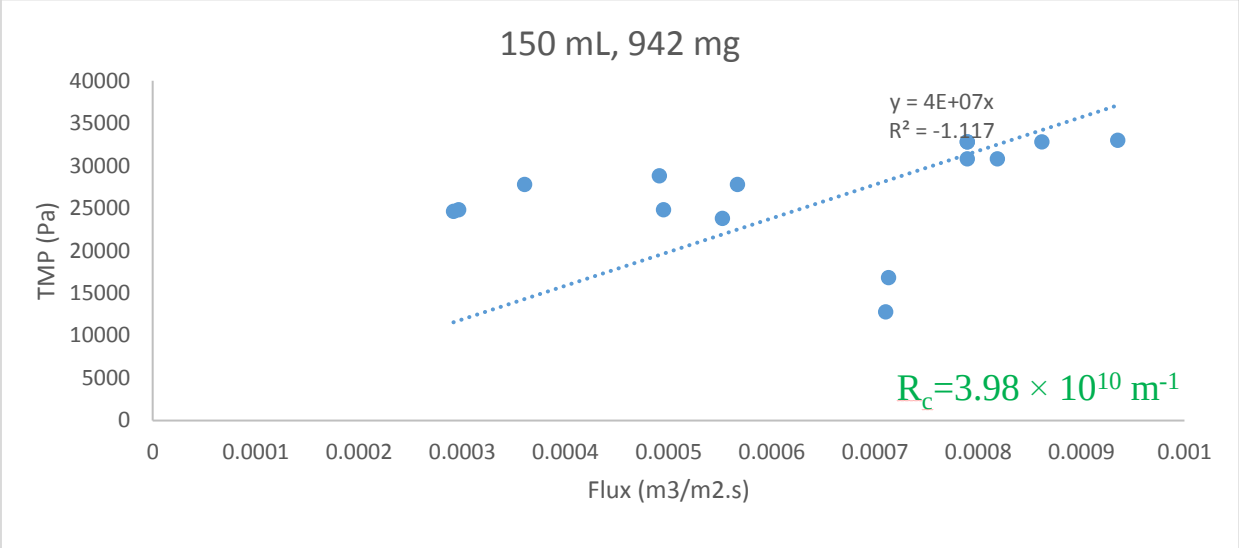

Figure 0-56. TMP vs Flux for clean membrane and for different amount for sludge from R2 (first trial'9

The summary of the results is listed in Table 0-2 and is depicted in Figure 0-57. It is important to note that when the first trial was done, the sludge in reactor 2 was in floccular form and it easily attached to the surface of the membrane.

Table 0-2. Total and cake layer resistance of the sludge from R2, first trial

Sludge amount per square meter of membrane area (gr/m^2)	Total resistance (m^{-1})	Cake layer resistance contribution (%)
16	4.52×10^7	26.5
40	17.17×10^7	80.63
64	299.4×10^7	98.8
151	1996×10^7	99.8
191	998×10^7	99.6
247	3992×10^7	99.9
419	9980×10^7	99.9

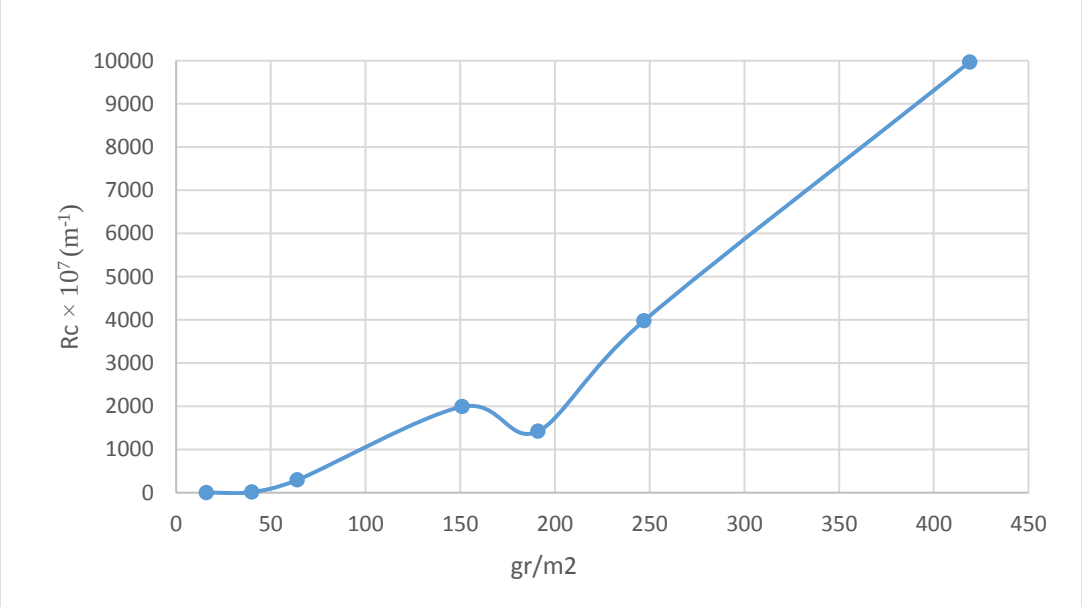

Figure 0-57. Cake layer resistance for sludge per square meter of the membrane for R2 at first trail

For all the above tests except for the last four (75, 100, 150, and 300 mL), the pressure gradient across the mesh were reflected by water head difference. For the last three, a suction pump was installed and the TMP were recorded by a pressure gauge. According to the results presented in Figure 0-56, the membrane intrinsic resistance was 3.33×10^7 m^{-1}. This value seems to be reasonable in comparison to other similar studies (Li, et al., 2012).

The cake layer resistance was determined based on the corresponding fitted line, though for some of the tests the R squared were negative. The negative R squared means that the fitted line did not follow the trend of the data and that fits the data worse than the horizontal line. Also, as it is observed from Table 0-2, there is a direct relation between the amount of sludge on the membrane and the cake layer resistance contribution. Li et al., (2012) have found almost 86% contribution of the cake layer on an 80 µm nylon mesh in a dead end membrane filtration. During the experiments, the biomass was effectively retained by the nylon mesh and attached to the surface of the membrane. In addition, the water level above the membrane produced enough pressure to prevent the cake layer from detachment. As it is clear from Figure 0-57, for the last three measurements, there were a sharp increase in TMP and also poor correlations between the TMP and the permeate flux. These are possibly due to the addition of the suction pump and also due to the large amount of sludge on the membrane surface.

4b.1.1.2. Second trial

The second trial was performed on June 20th. Similar to the first trial, the cake layer resistance of the sludge layer was measured at different amounts. The obtained results are presented as follows.

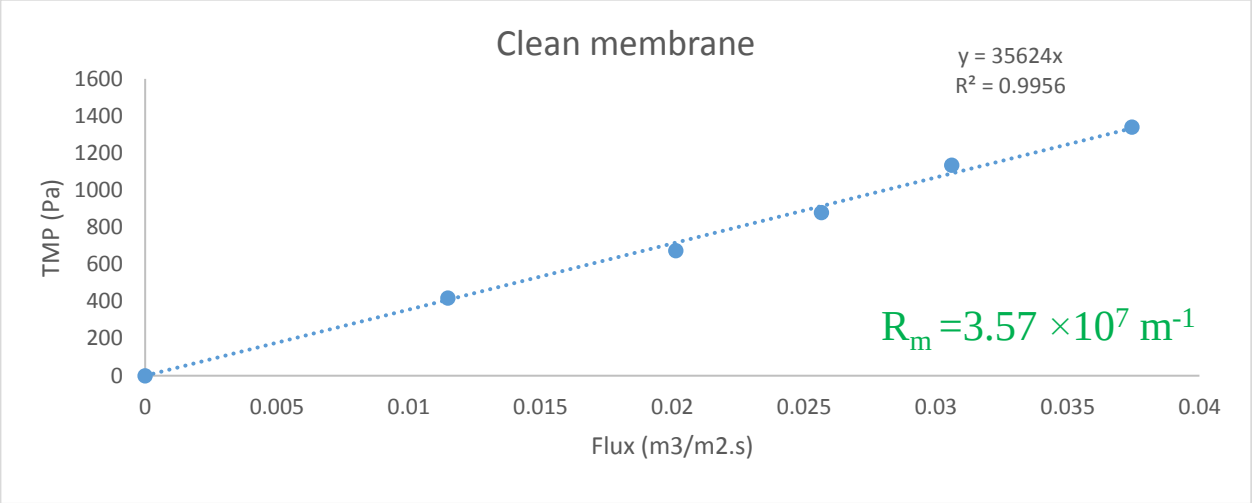

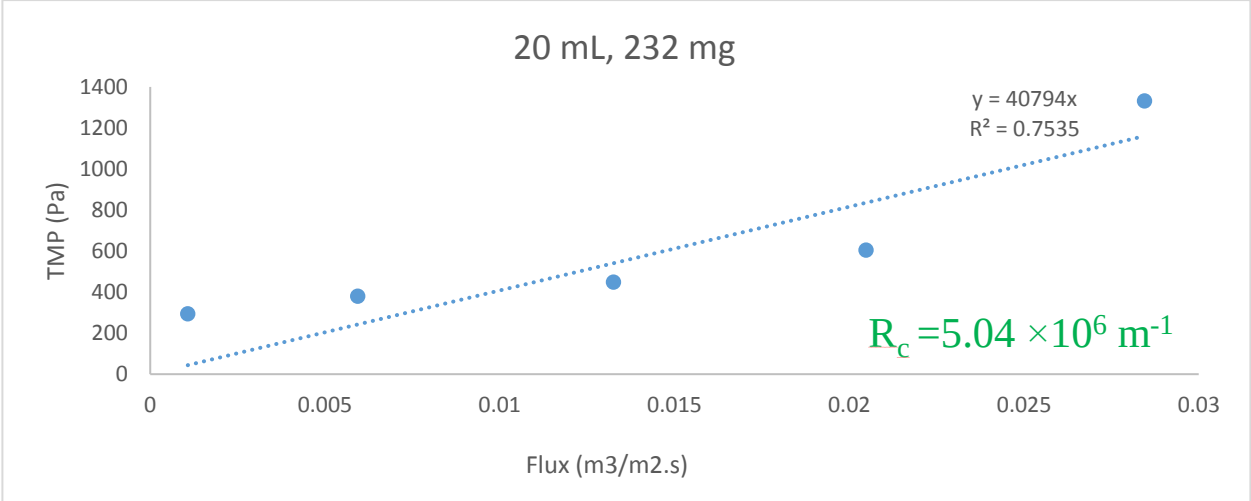

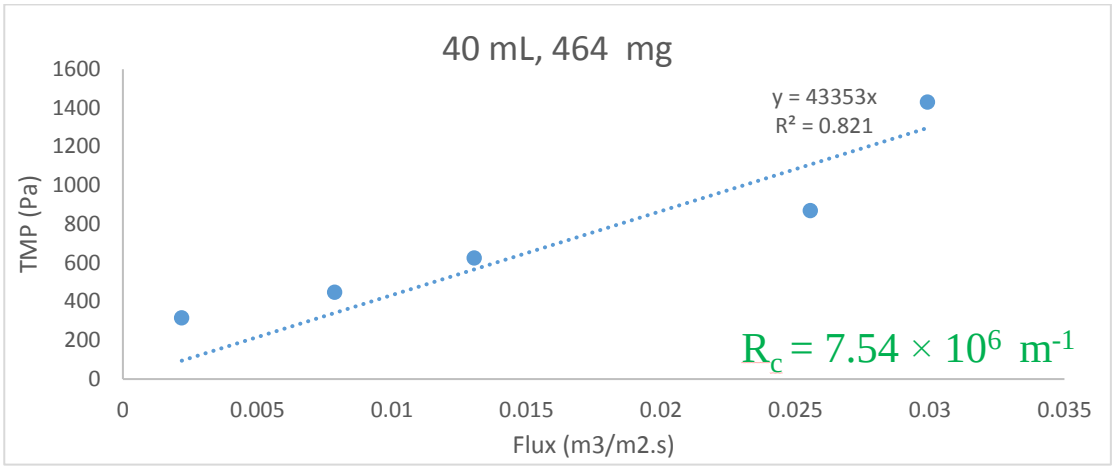
40 mL, 464 mg
y = 43353x
R² = 0.821
TMP (Pa)
Flux (m3/m2.s)
$R_c = 7.54 \times 10^6\ m^{-1}$

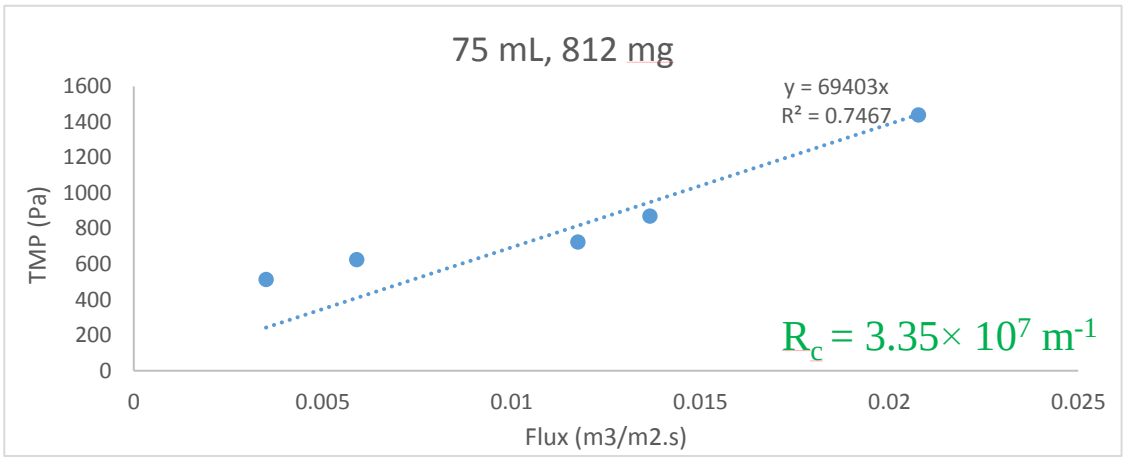
75 mL, 812 mg
y = 69403x
R² = 0.7467
TMP (Pa)
Flux (m3/m2.s)
$R_c = 3.35 \times 10^7\ m^{-1}$

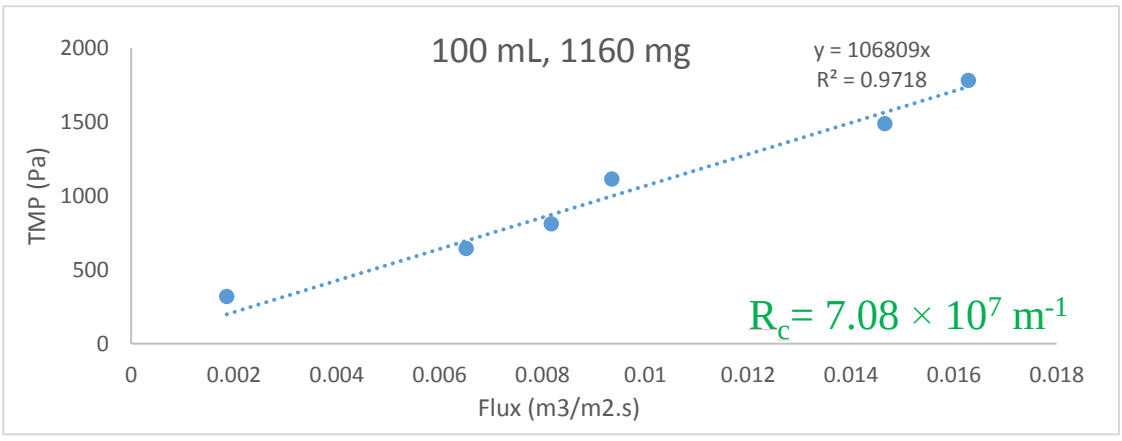
100 mL, 1160 mg
y = 106809x
R² = 0.9718
TMP (Pa)
Flux (m3/m2.s)
$R_c = 7.08 \times 10^7\ m^{-1}$

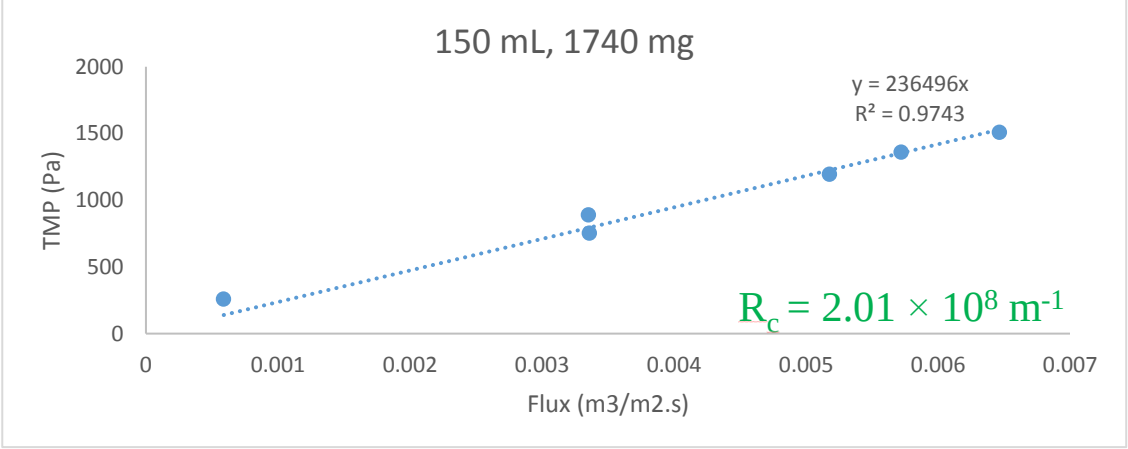
150 mL, 1740 mg
y = 236496x
R² = 0.9743
TMP (Pa)
Flux (m3/m2.s)
$R_c = 2.01 \times 10^8\ m^{-1}$

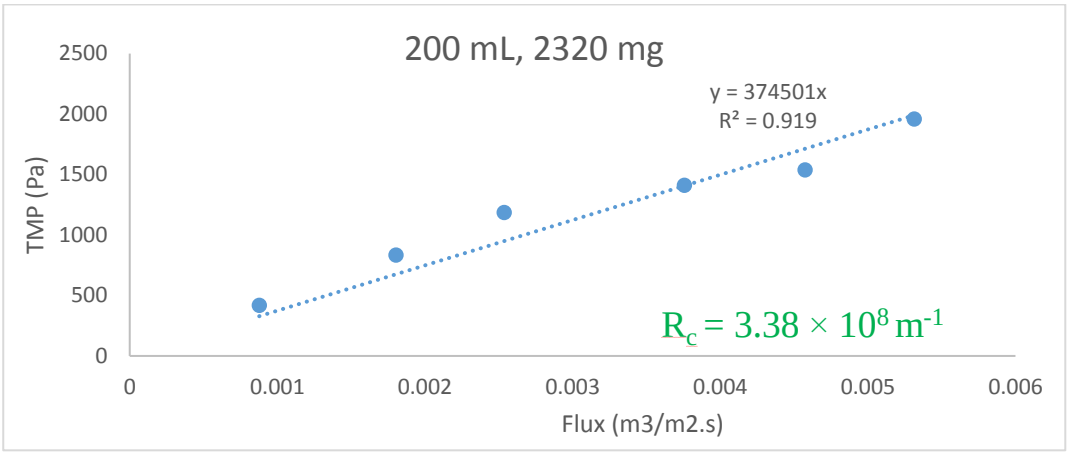
200 mL, 2320 mg
y = 374501x
R² = 0.919
TMP (Pa)
2500
2000
1500
1000
500
0
0
0.001
0.002
0.003
0.004
0.005
0.006
Flux (m3/m2.s)
$R_c = 3.38 \times 10^8\ m^{-1}$

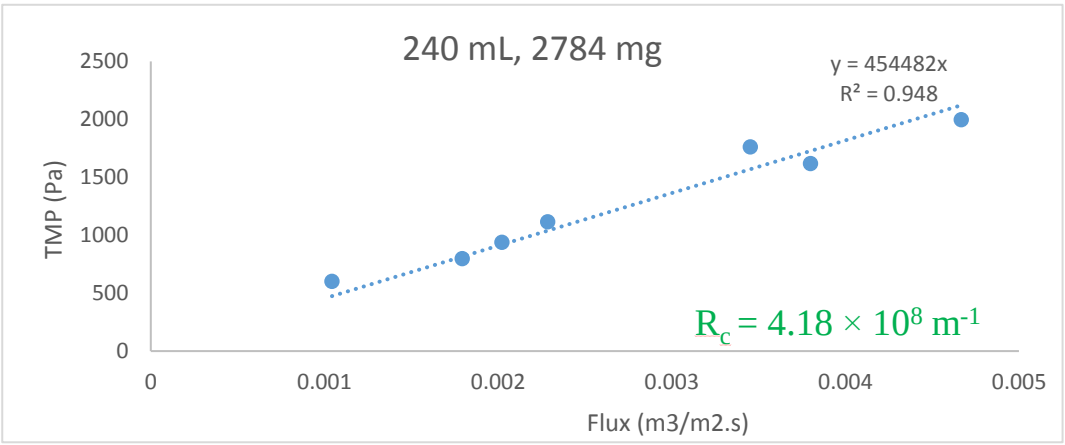
240 mL, 2784 mg
y = 454482x
R² = 0.948
TMP (Pa)
2500
2000
1500
1000
500
0
0
0.001
0.002
0.003
0.004
0.005
Flux (m3/m2.s)
$R_c = 4.18 \times 10^8\ m^{-1}$

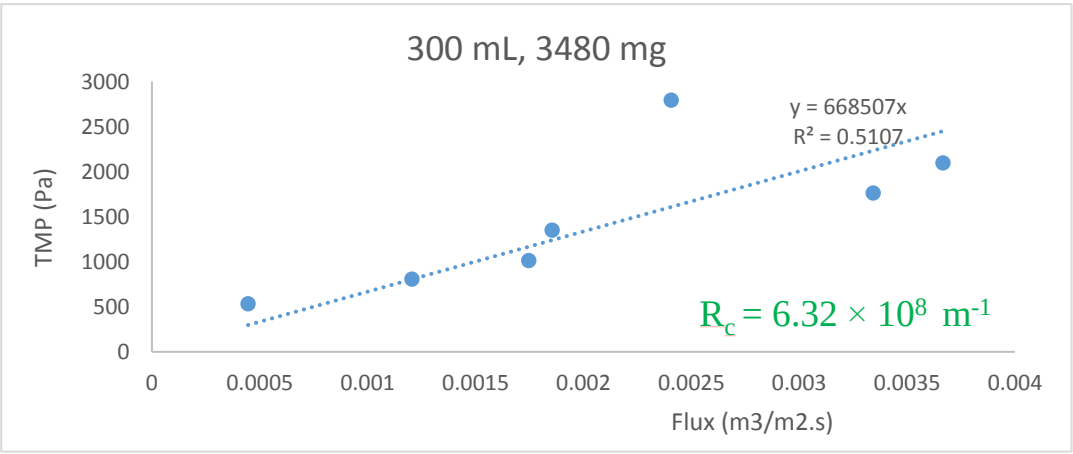
300 mL, 3480 mg
y = 668507x
R² = 0.5107
TMP (Pa)
3000
2500
2000
1500
1000
500
0
0
0.0005
0.001
0.0015
0.002
0.0025
0.003
0.0035
0.004
Flux (m3/m2.s)
$R_c = 6.32 \times 10^8\ m^{-1}$

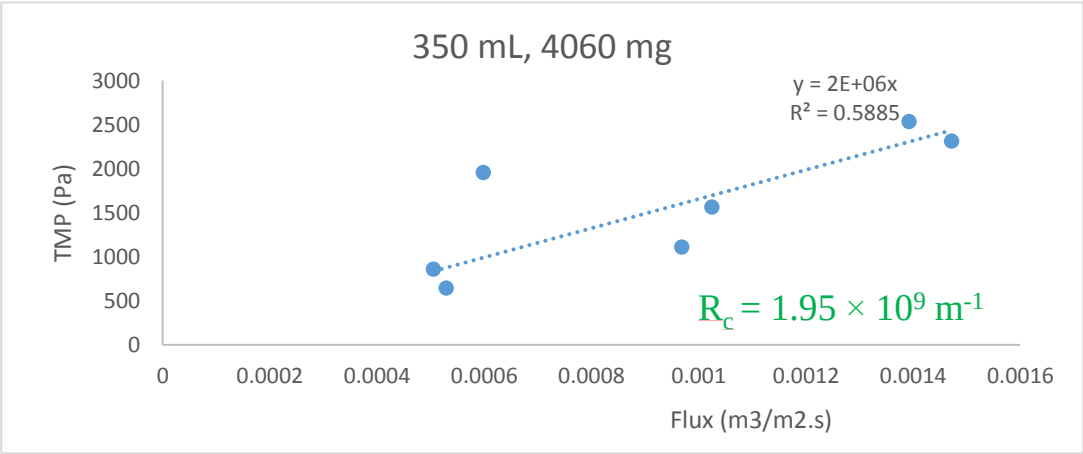
350 mL, 4060 mg
y = 2E+06x
R² = 0.5885
TMP (Pa)
3000
2500
2000
1500
1000
500
0
0
0.0002
0.0004
0.0006
0.0008
0.001
0.0012
0.0014
0.0016
Flux (m3/m2.s)
$R_c = 1.95 \times 10^9\ m^{-1}$

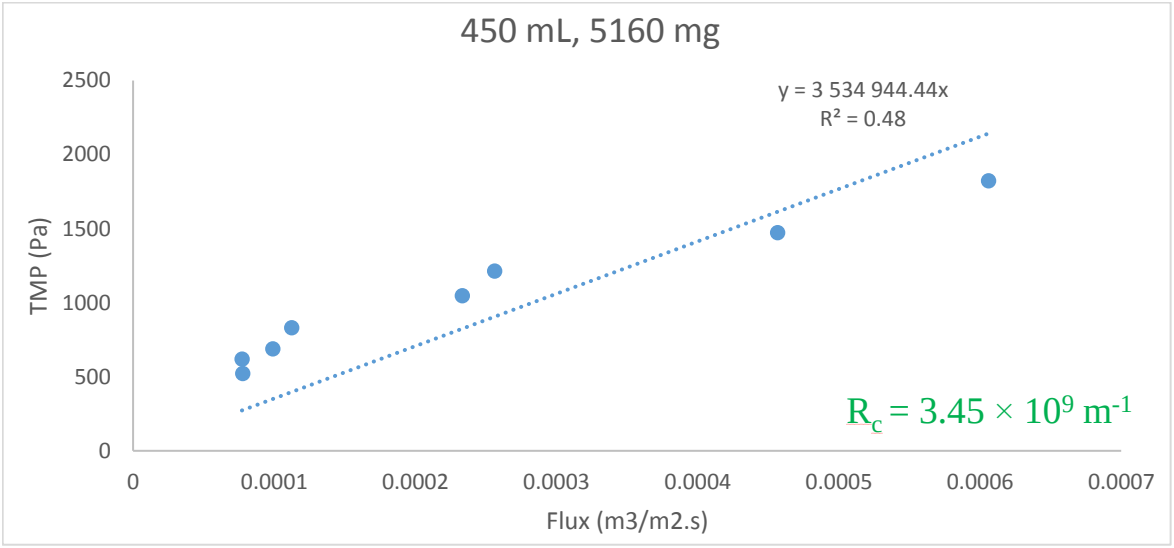

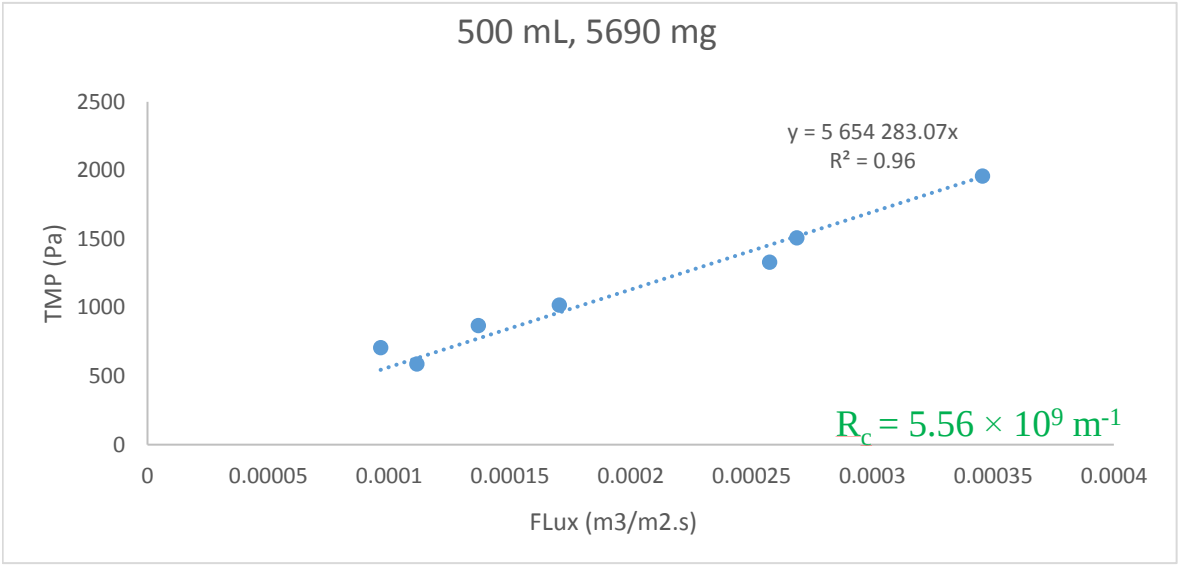

Figure 0-58. TMP vs Flux for clean membrane and for different amount of sludge from R2 (second trial)

Table 0-3. Total and cake layer resistance of the sludge from R2, second trial

Sludge amount per square meter of membrane area (gr/m^2)	Total resistance (m^{-1})	Cake layer resistance contribution (%)
61.05	4×10^7	12.6
122	4.3×10^7	17.5
229	6.9×10^7	48
305.25	10.6×10^7	66.4
456	23.6×10^7	87.7

610.5	37.4×10^7	90.4
763	45.3×10^7	92.7
915.7	66.7×10^7	94.7
1068	199.6×10^7	97.7
1373	352.7×10^7	97.8
1525.7	564.3×10^7	98.5

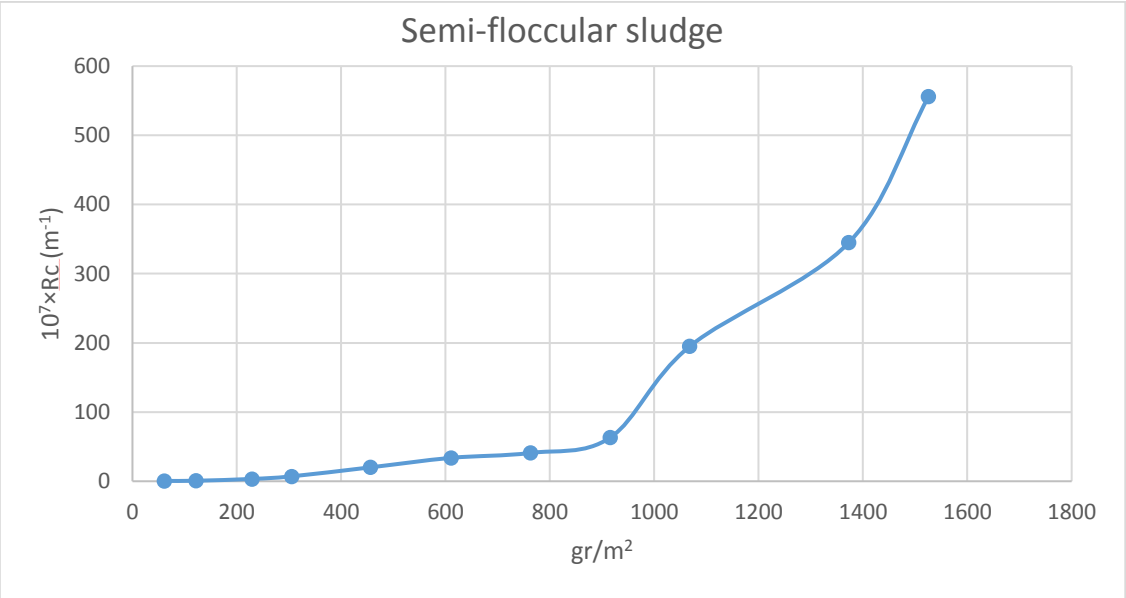

Figure 0-59. Cake layer resistance for sludge from R2 per square meter of the membrane (second trial)

The second trial was performed a few months after the first trial. During this trial, the sludge in R2 had become semi-flocculated and the morphology of it had changed. Therefore, it is expected to observe different behaviour from the first trial. These differences for example might be in deposition pattern and cake layer formation, filtration resistance, and fouling properties (Liang, et al., 2013).

As it is observed from Table 0-3 and Figure 0-59, while the thickness of the sludge layer on the membrane surface was increasing, the contribution of the cake layer resistance on total hydraulic resistance was also increasing. By comparing the first and the second trial, it can be concluded that the semi-flocculated sludge had an order of magnitude lower hydraulic resistance than the normal flocculated sludge. This can be because of the more porous structure and canals existing in the cake layer formed by semi-floccular sludge.

During the second trial, there were some difficultly in attachment of the sludge particles to the membrane surface while during the first trial when the sludge was completely in floccular from, they easily formed a compact layer on the membrane surface. The reason for tendency of floccular sludge to attach on the membrane surface can be due to the higher EPS and moisture content of this type of sludge.

4b.1.2. Granular sludge

4b.1.2.1. First trial

The experiments to measure the cake layer resistance for granular sludge were also conducted twice. The first run was done on April 25th and the second run was performed on June 27th.

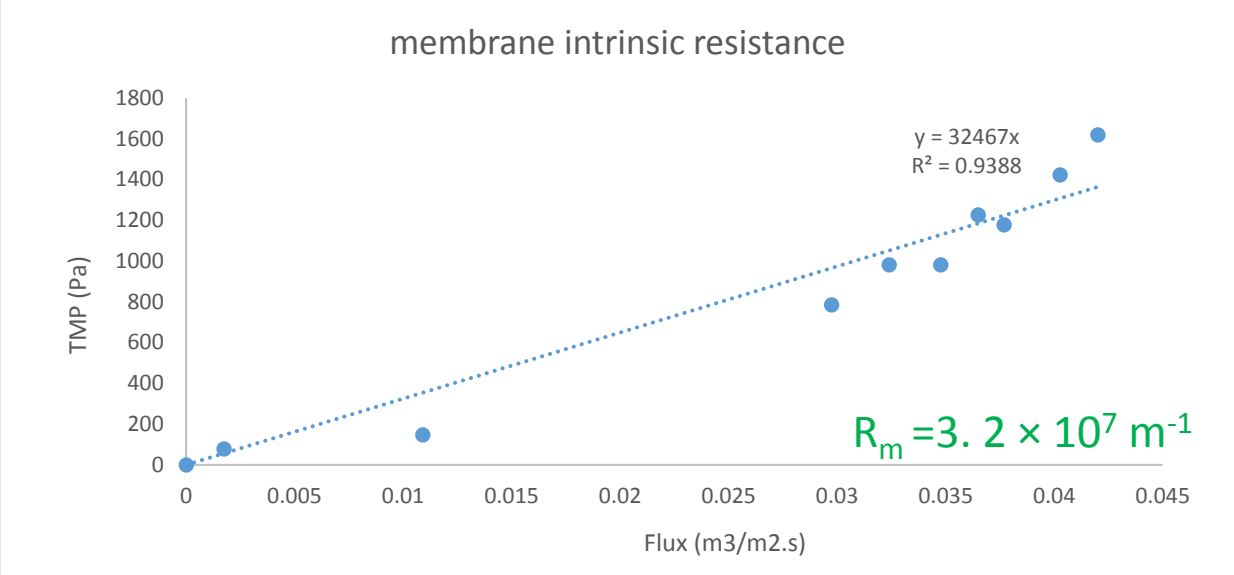
membrane intrinsic resistance
y = 32467x
R² = 0.9388
TMP (Pa)
Flux (m3/m2.s)
$R_m = 3.2 \times 10^7\ m^{-1}$

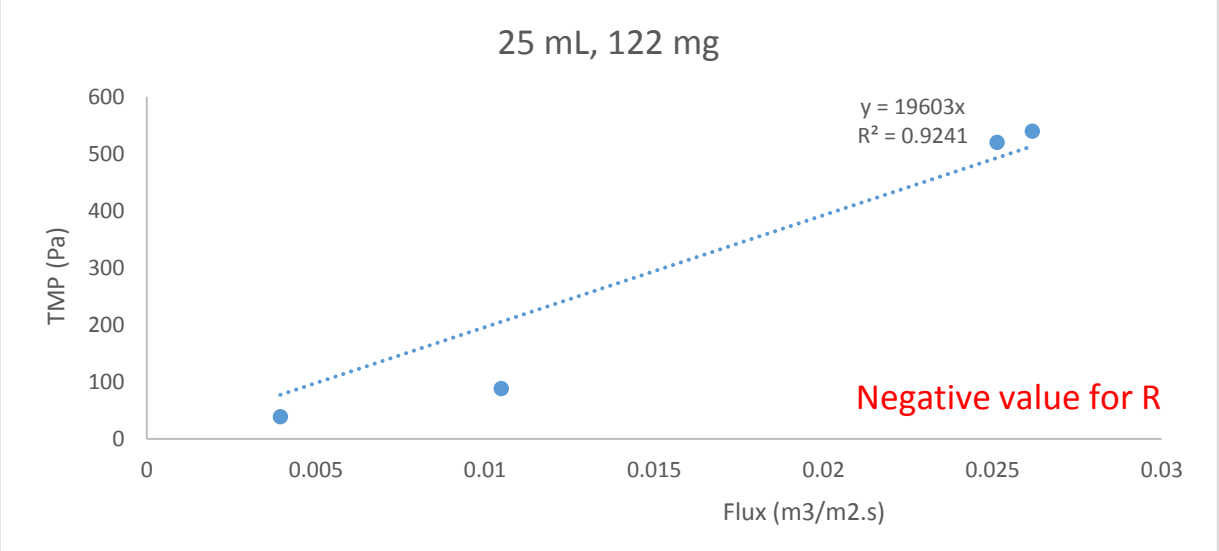
25 mL, 122 mg
y = 19603x
R² = 0.9241
TMP (Pa)
Flux (m3/m2.s)
Negative value for R

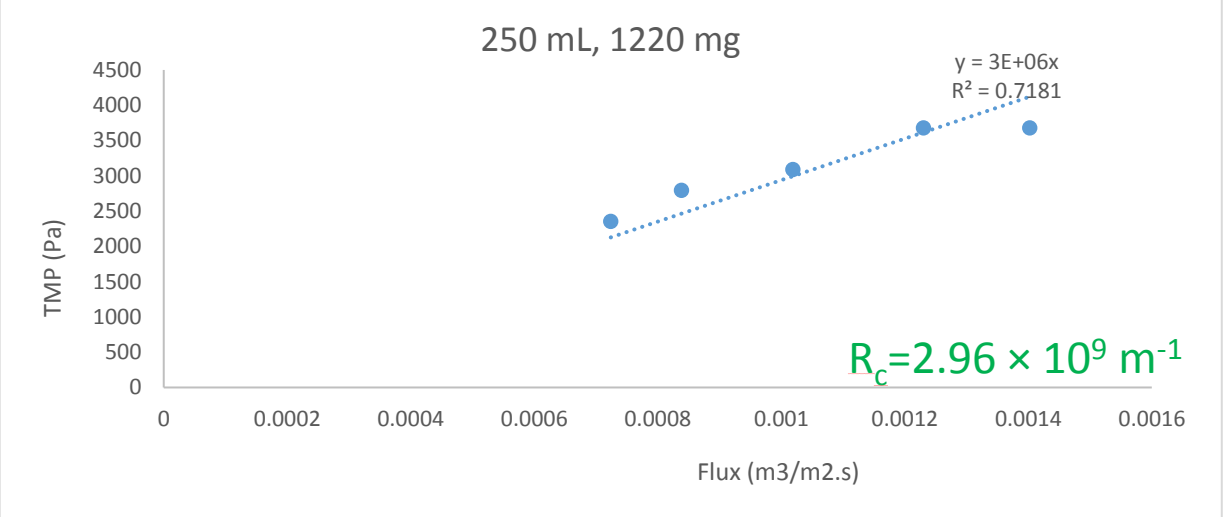
250 mL, 1220 mg
y = 3E+06x
R² = 0.7181
TMP (Pa)
Flux (m3/m2.s)
$R_c = 2.96 \times 10^9\ m^{-1}$

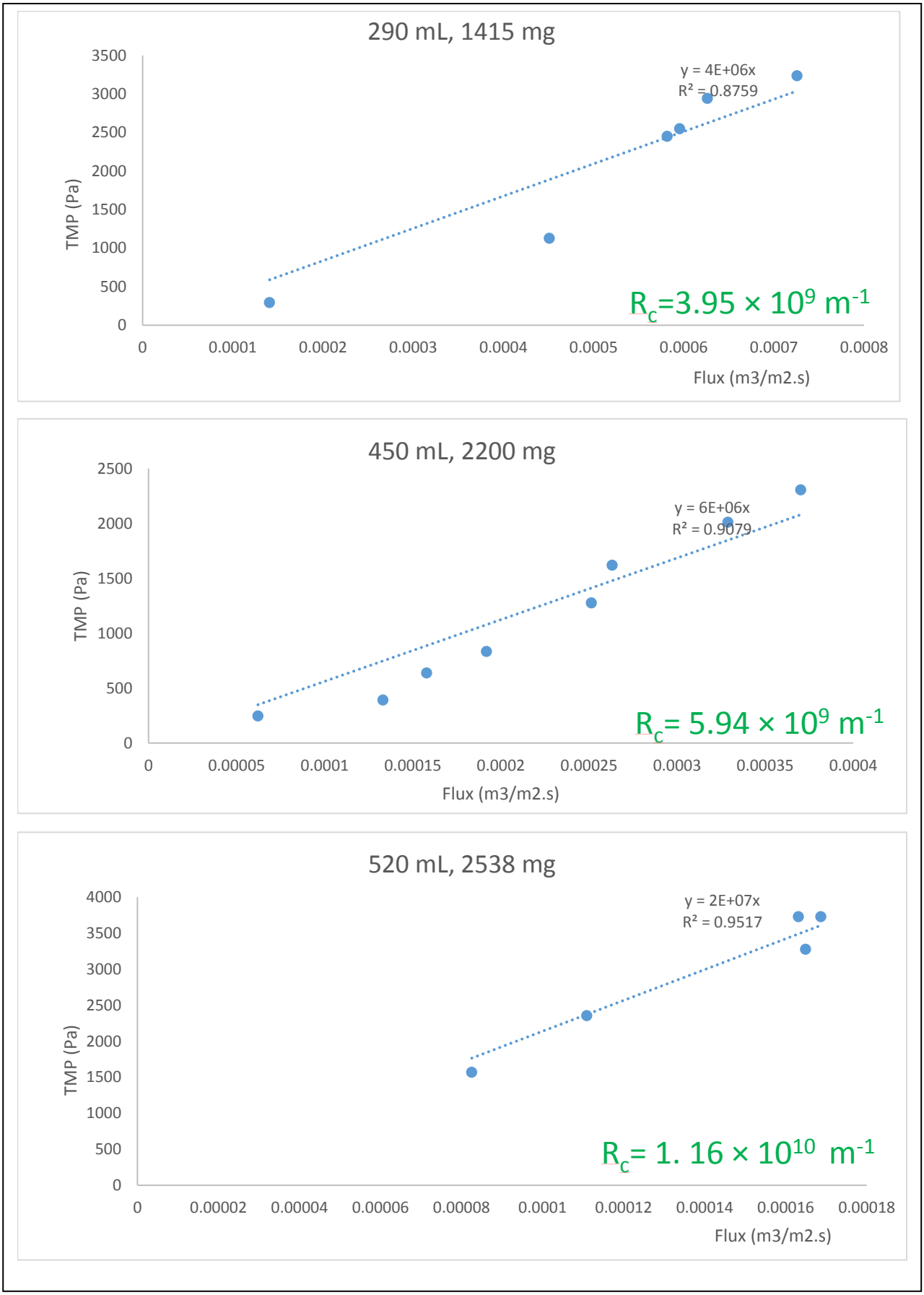
290 mL, 1415 mg
y = 4E+06x
R² = 0.8759
TMP (Pa)
Flux (m3/m2.s)
R_c=3.95 × 10^9 m^{-1}
450 mL, 2200 mg
y = 6E+06x
R² = 0.9079
TMP (Pa)
Flux (m3/m2.s)
R_c= 5.94 × 10^9 m^{-1}
520 mL, 2538 mg
y = 2E+07x
R² = 0.9517
TMP (Pa)
Flux (m3/m2.s)
R_c= 1. 16 × 10^{10} m^{-1}

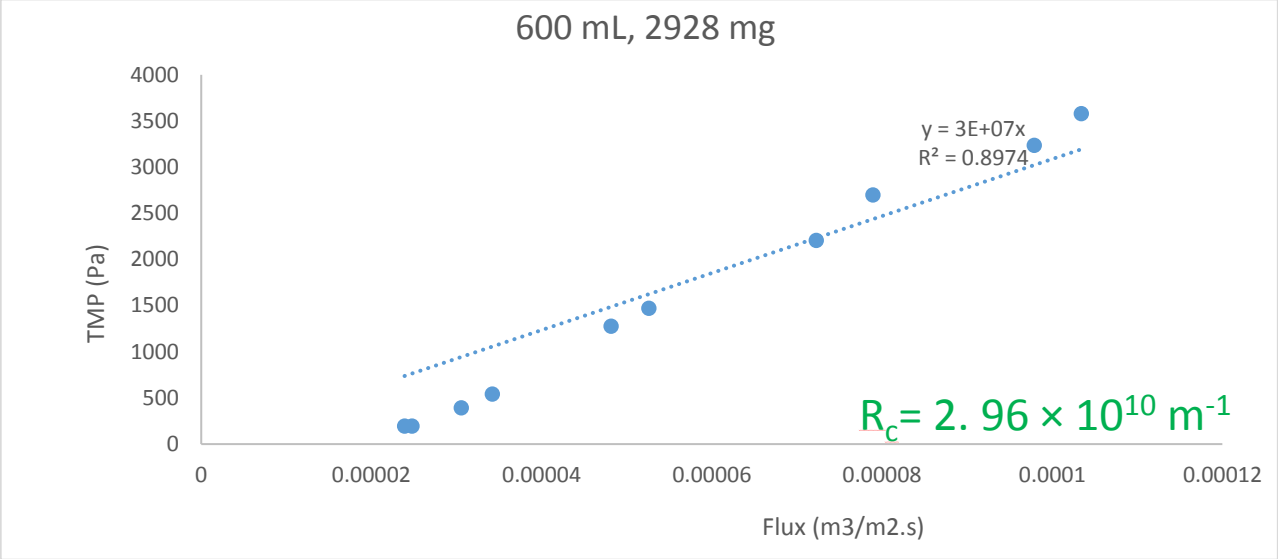
600 mL, 2928 mg
y = 3E+07x
R² = 0.8974
TMP (Pa)
Flux (m3/m2.s)
R_c= 2. 96 × 10^{10} m^{-1}

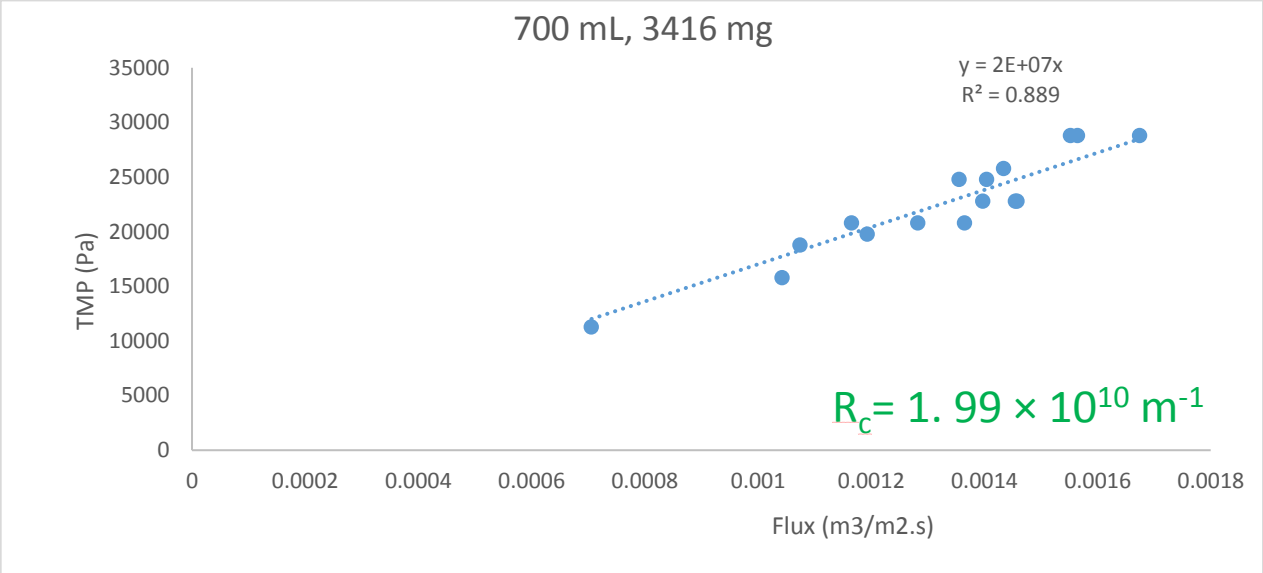
700 mL, 3416 mg
y = 2E+07x
R² = 0.889
TMP (Pa)
Flux (m3/m2.s)
R_c= 1. 99 × 10^{10} m^{-1}

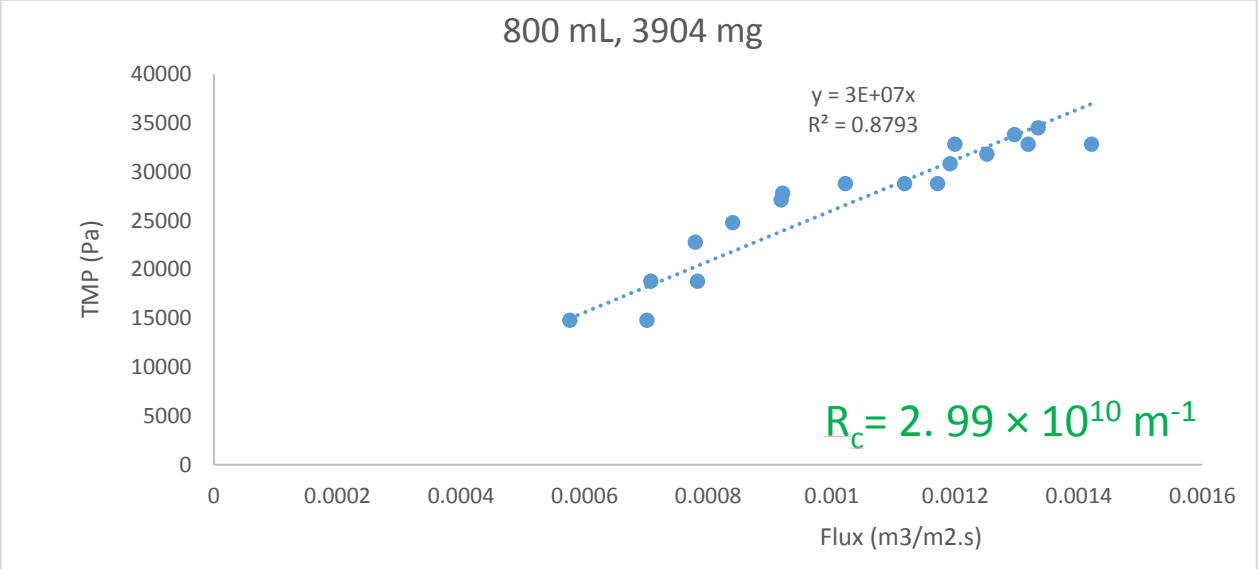
800 mL, 3904 mg
y = 3E+07x
R² = 0.8793
TMP (Pa)
Flux (m3/m2.s)
R_c= 2. 99 × 10^{10} m^{-1}

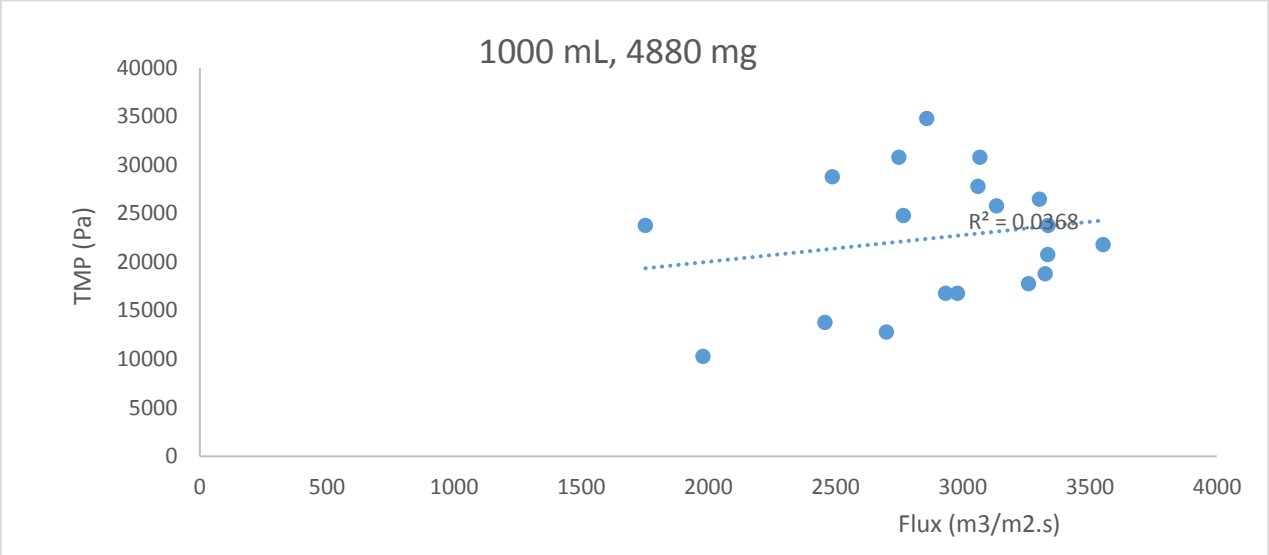

Figure 0-60. TMP vs Flux for clean membrane and for different amount of sludge from R3 (first trial)

Table 0-4. Total and cake layer resistance of the sludge R3, first trial

Sludge amount per square meter of membrane area (gr/m^2)	Total resistance (m^{-1})	Cake layer resistance contribution (%)
32.10	0	0
321.05	299.40×10^7	98.9
372.36	399.2×10^7	99.2
580	$598.8. \times 10^7$	99.4
670	1996×10^7	99.8
770	2994×10^7	99.8
900	1996×10^7	99.8
1027	2994×10^7	99.8

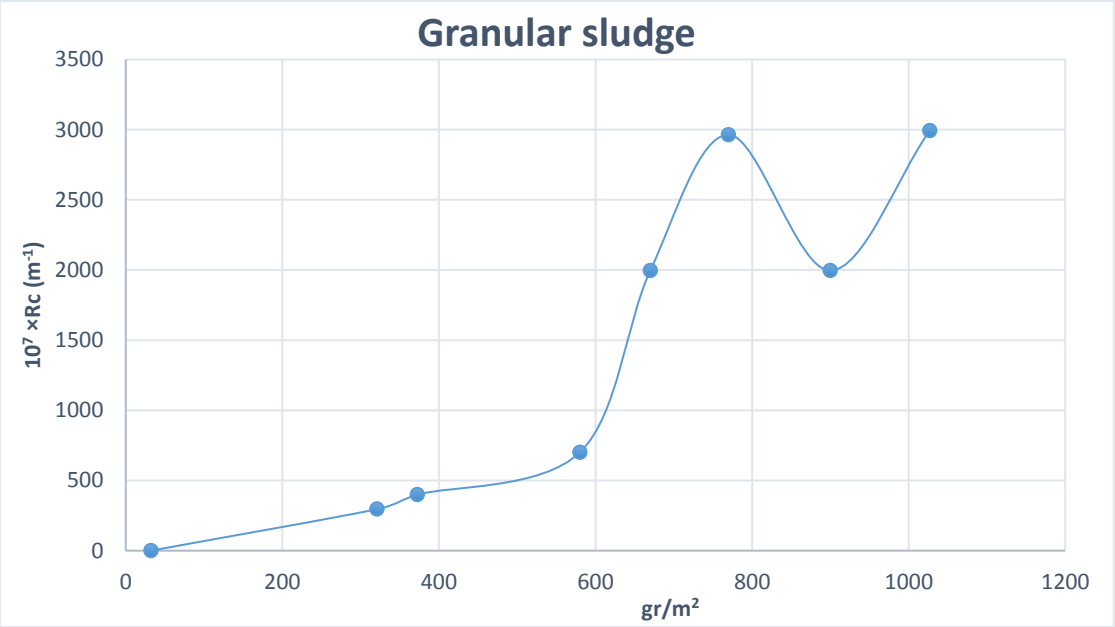

Figure 0-61. Cake layer resistance for sludge from R3 per square meter of the membrane (first trial)

4b.1.2.2. Second trial

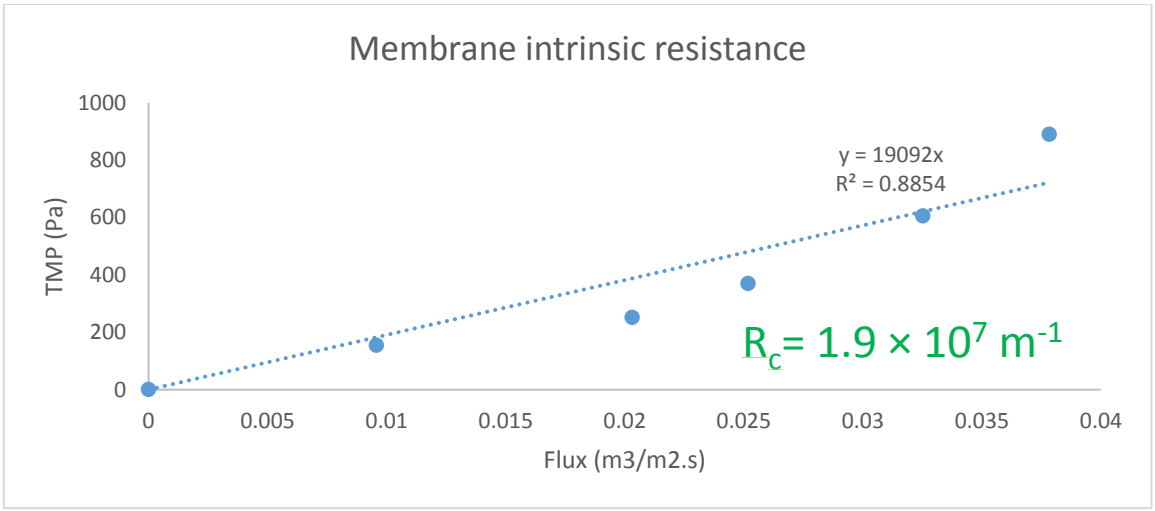

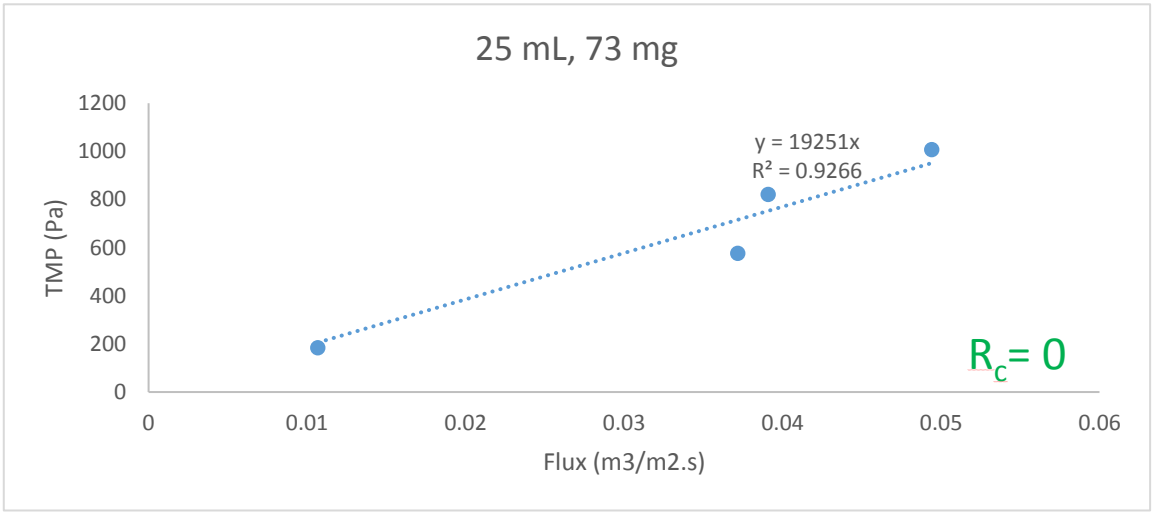

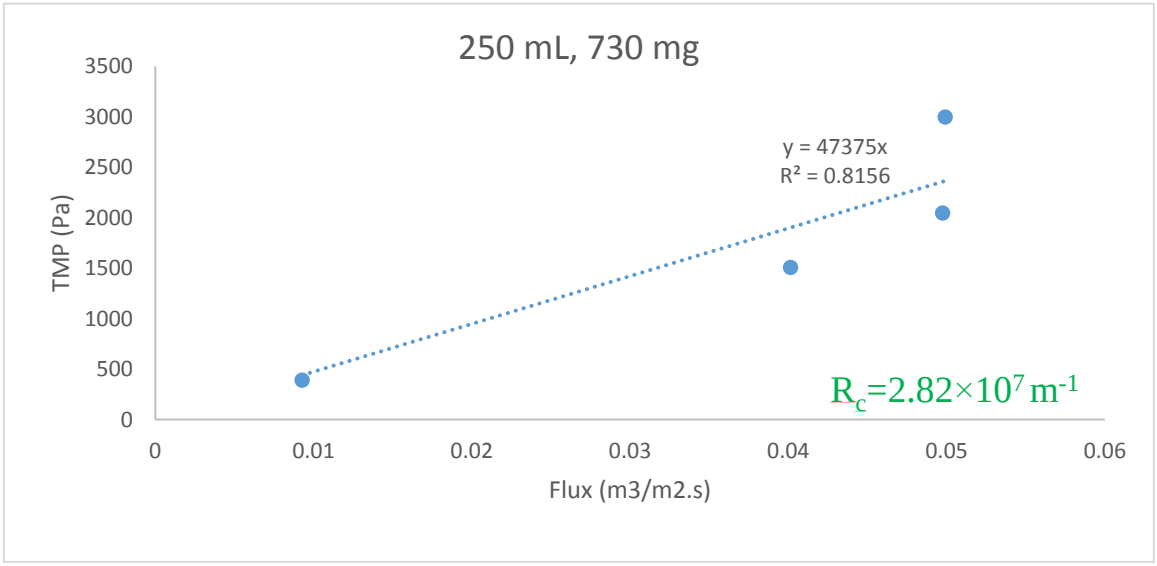

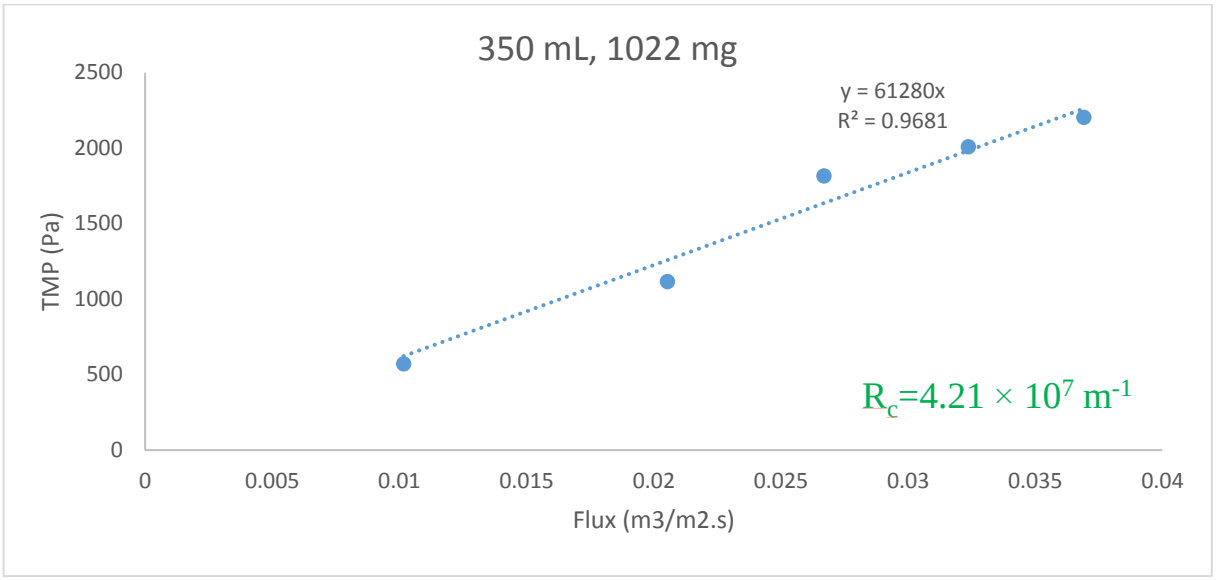
350 mL, 1022 mg
y = 61280x
R² = 0.9681
TMP (Pa)
2500
2000
1500
1000
500
0
0
0.005
0.01
0.015
0.02
0.025
0.03
0.035
0.04
Flux (m3/m2.s)
R_c=4.21 × 10^7 m^{-1}

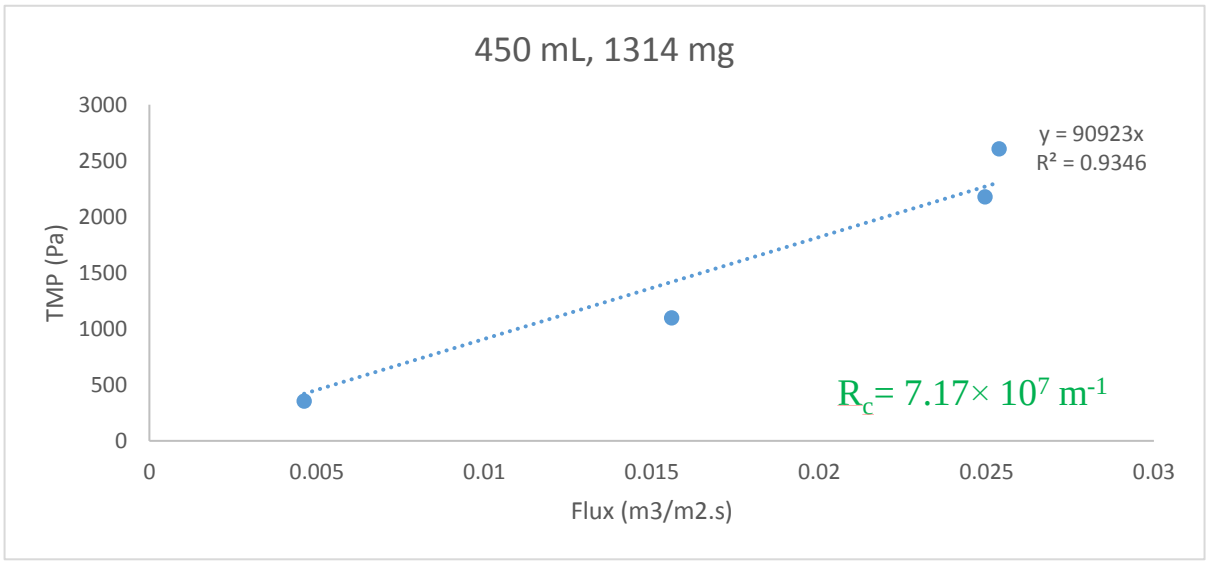
450 mL, 1314 mg
y = 90923x
R² = 0.9346
TMP (Pa)
3000
2500
2000
1500
1000
500
0
0
0.005
0.01
0.015
0.02
0.025
0.03
Flux (m3/m2.s)
R_c= 7.17× 10^7 m^{-1}

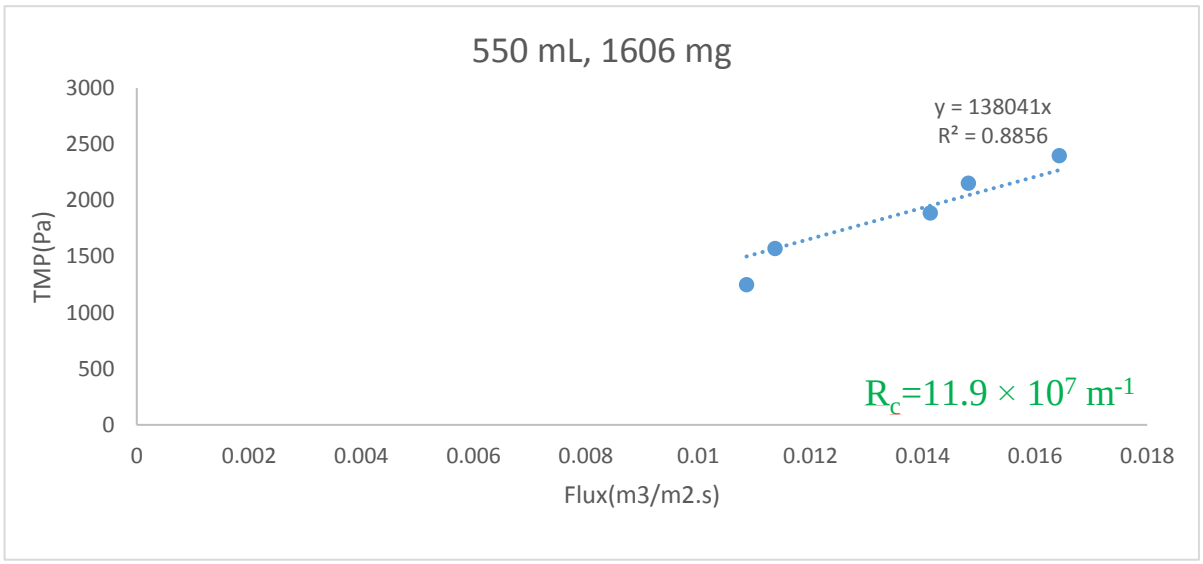
550 mL, 1606 mg
y = 138041x
R² = 0.8856
TMP(Pa)
3000
2500
2000
1500
1000
500
0
0
0.002
0.004
0.006
0.008
0.01
0.012
0.014
0.016
0.018
Flux(m3/m2.s)
R_c=11.9 × 10^7 m^{-1}

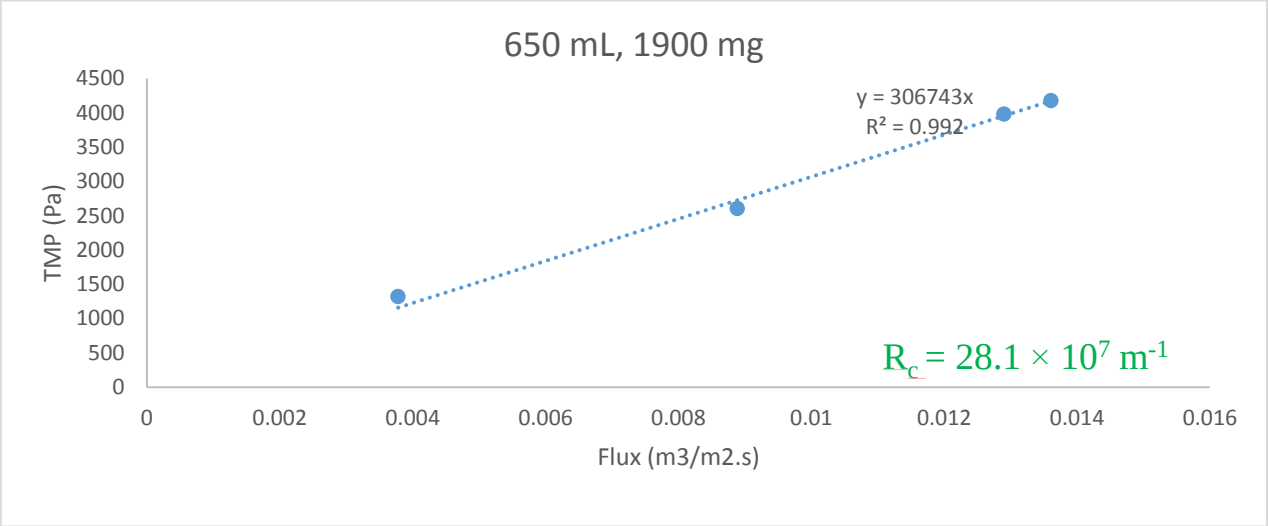

Figure 0-62. TMP vs flux for different cake layer amount for sludge from R3, second trial

Table 0-5. Total and cake layer resistance of the sludge R3, second trial

Sludge amount per square meter of membrane area (gr/m^2)	Total resistance (m^{-1})	Cake layer resistance contribution (%)
19.2	1.92×10^7	0
192.1	4.73×10^7	59
270	6.12×10^7	68.9
374	9.07×10^7	79
425	13.77×10^7	86.25
247	30.61×10^7	93.8

According to Table 0-5 and Figure 0-62, the total membrane resistance for the lower amounts of granules applied, was lower than membrane intrinsic resistance which is not possible. This is maybe due to the shape and structure of the aerobic granules. They had a round shape and big diameter and at low amount they could hardly deposit on the membrane surface. The same as previous results, the cake layer was the main resistance component of the total hydraulic resistance.

By comparing the resistance of granular sludge and floccular sludge, it is clear that floccular sludge had greater tendency to deposit on the membrane surface than that of granular sludge. In other words, the cake layer formed by the granular sludge has a more porous structure. Therefore, from the results, it can be concluded that, sludge characteristics such as particle size shape, and structure have great influence on the cake layer resistance. It has previously been found that, the smaller the particles deposited on the membrane surface, the greater the resistance (Jun, et al., 2007). However, it should be pointed out that the results obtained from this work, is reflecting only the short-term operation and not the long term operation.

4b.2. Dynamic membrane formation

In order to investigate the formation and performance of dynamic membrane, the supernatant form R2 and R3 (operating in the first run) were collected and then filtered through the membrane. The rejection of sludge flocs by nylon mesh and dynamic membrane were assessed by measuring turbidity of the permeate at regular time intervals. In other words, the performance of dynamic membrane was assessed by analysing the permeate quality in terms of turbidity and TSS.

4b.2.1. Filtration of the supernatant from R2 (Floccular sludge)

On May 30th, the supernatant from successive cycles were collected and then filtered through the mesh filter. The main aims of this set of experiments were to investigate the possibility of dynamic membrane formation on top of the 100 µm mesh filter and the performance of it in rejecting suspended solids. The SS rejection was evaluated by measuring turbidity at regular time intervals.

The feed stream characteristics, experiment duration and some other specifications are listed in Table 0-6 and Figure 0-63.

Table 0-6. Filtration of supernatant from floccular sludge, R2

Experiment Specification	
Influent TSS (mg/L)	78.33
Influent Turbidity (FAU)	29
Total volume of filtered liquid (L)	10

Max Flux (LMH)	4556
Min Flux (LMH)	981
Duration (min)	205
Minimum turbidity (FAU)	7
Maximum turbidity (FAU)	19
Average turbidity removal	55 %

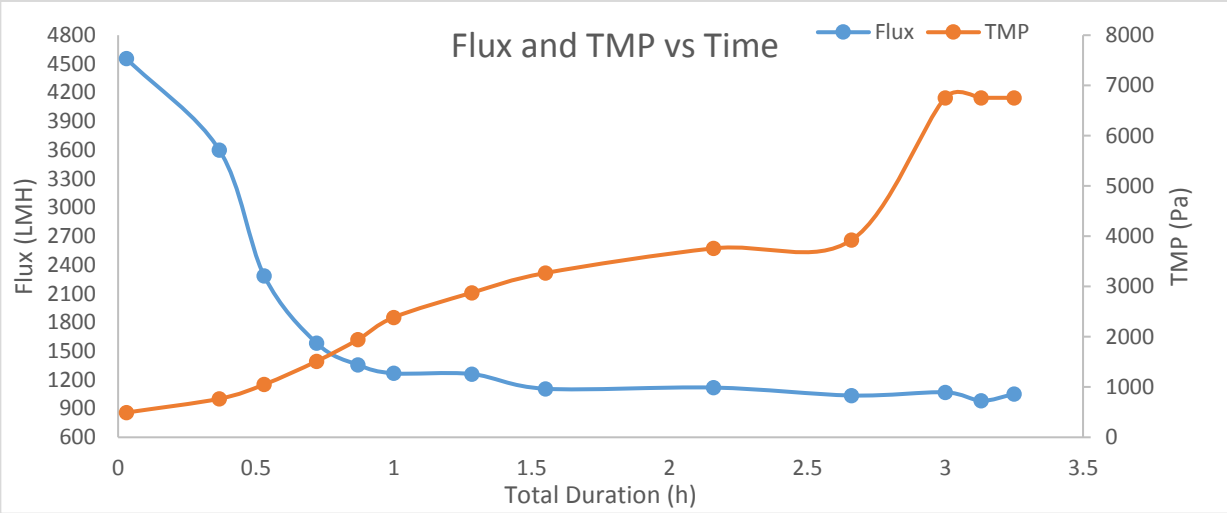

Figure 0-63. Filtration characteristics of the Supernatant from R2

4b.2.2. Filtration of the supernatant from R3 (granular sludge)

On June 3rd, the supernatant from successive cycles were collected and then filtered through the mesh filter. The feed stream characteristics and some other specifications are listed in Table 0-7 and the results are depicted in Figure 0-64.

Table 0-7. Filtration of supernatant from granular sludge, R3

Experiment Specification	
TSS (mg/L)	198
Initial TOC	17.83
Turbidity (FAU)	83
Total volume of filtered liquid (L)	16
Max flux (LMH)	7620
Min flux (LMH)	281

Duration (min)	380
Minimum turbidity (FAU)	3
Maximum turbidity (FAU)	11
Average turbidity removal (%)	92
Average TOC removal (%)	77.5

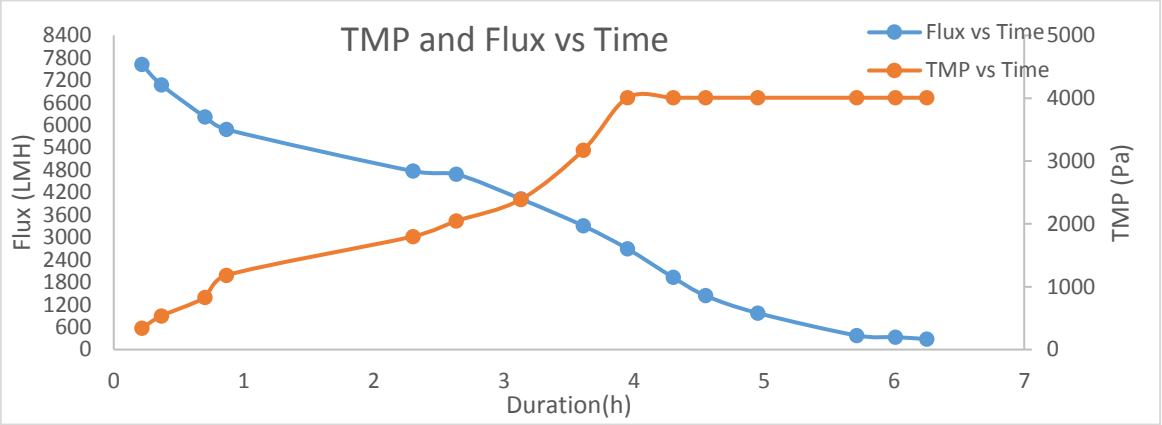

Figure 0-64. Filtration characteristics of supernatant from R3

The results proved the successful formation of dynamic membrane for both of the reactors. In-situ deposited coarser particles on the surface of the membrane played a key role in rejection of finer particles. Some researchers have also found similar results (Wang, et al., 2012). According to results above, it is concluded that the dynamic membrane formed by the supernatant from granulated reactor had better performance in rejection of suspended solids and also it provided almost two times higher permeate flux than that of flocculated reactor. The total hydraulic resistance from R3 is two times higher than R2 which is probably due to the higher amount of SS in the run with the granular sludge.

4b.3. Adsorption capacity

In order to investigate the adsorption capacity of the cake layer formed by the sludge, kaolin suspension was used. The experiment procedure is explained in section 3b.2.3. The experiments were run in two parts, the first part was performed on pure membrane without addition of sludge and the second part was performed by addition of sludge to form a cake layer. Below the results for the first part is given.

4b.3.1. Kaolin suspension

As it was explained in section 3b.2.3., the relationship between the kaolin concentration and absorbance at 400 nm wavelength was determined. Table 0-8 summarizes the results and Figure 0-65 shows the calibration curve. Based on Beer's law, there is a linear and straightforward relationship between concentration and absorbance. Therefore, the best-fit line was fitted and the equation of that line was used as a baseline for calculating the unknown kaolin concentration. Eq. (11), shows the equation of that linear line.

Table 0-8. Kaolin concentration vs absorbance at 400nm

Concentration (mg/L)	Absorbance at 400 nm
100	0.298
200	0.609
250	0.857
500	1.151
600	1.326
1000	1.925

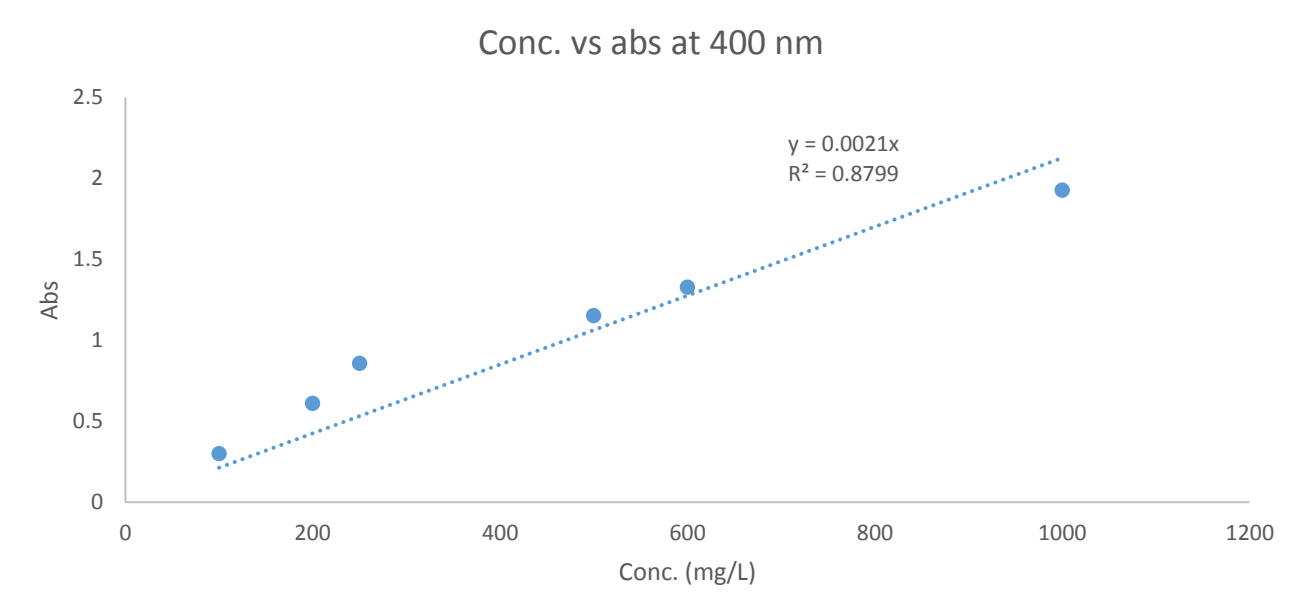

Figure 0-65. Calibration curve for kaolin suspension at 400 nm

$$C = \frac{\text{Abs}}{0.0021} \qquad \text{Eq (11)}$$

Where C is the concentration in mg/L and Abs is the absorbance of the sample at 400 nm wavelength which can be determined using spectrophotometer.

On June 20th, the kaolin suspension with the concentration of 600 mg/L was prepared and filtered through the clean membrane. At regular time intervals samples were taken at the effluent from the filter column. Then by using Eq. (11) the unknown concentration of the samples at the effluent port were determined. Figure 0-66 shows the results for the experiment with kaolin and clean membrane.

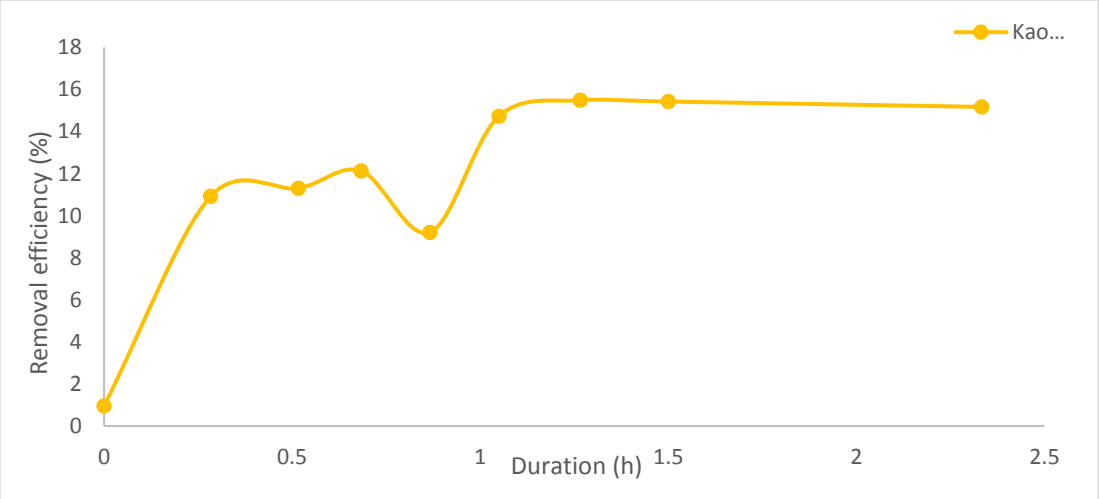

Figure 0-66. Removal efficiency of kaolin suspension through clean membrane

4b.3.2. Kaolin suspension and cake layer from R2 and R3

On July 12th and 13th, 800 (2540 mg) and 900 (6000 mg) mL of the sludge from R3 and R2 were collected respectively. They were passed through the membrane to form a cake layer. Then the concentrated kaolin solution was prepared with the concentration of 724 mg/L and 615 mg/L respectively. It was passed through the cake layer and samples were taken at the effluent port and the absorbance of them were measured. Removal efficiencies were calculated over the operation time, see Figure 0-67 and Figure 0-68.

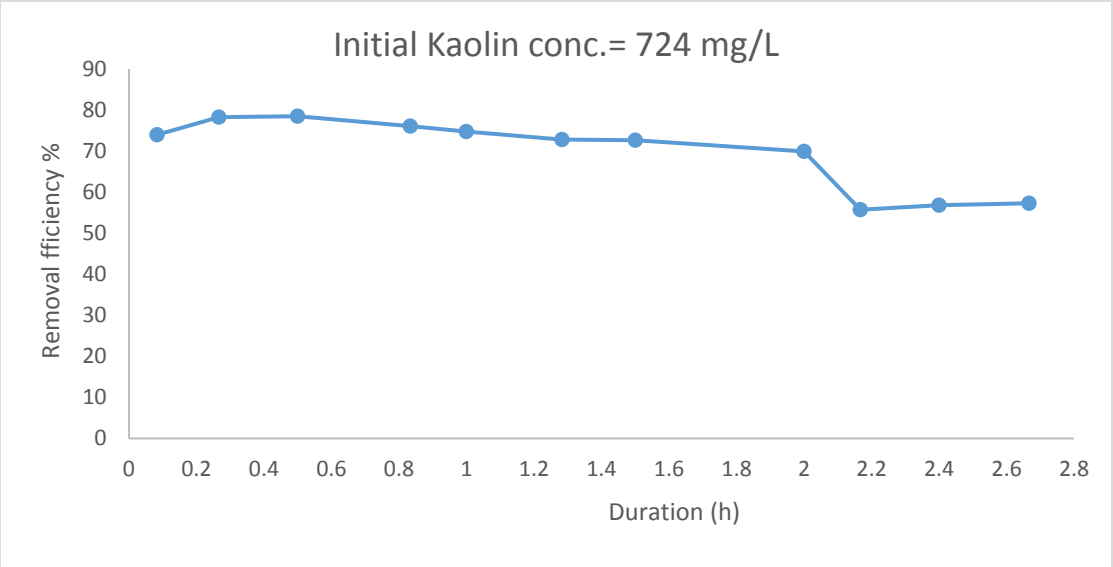

Figure 0-67. Kaolin removal efficiencies with cake layer from R3

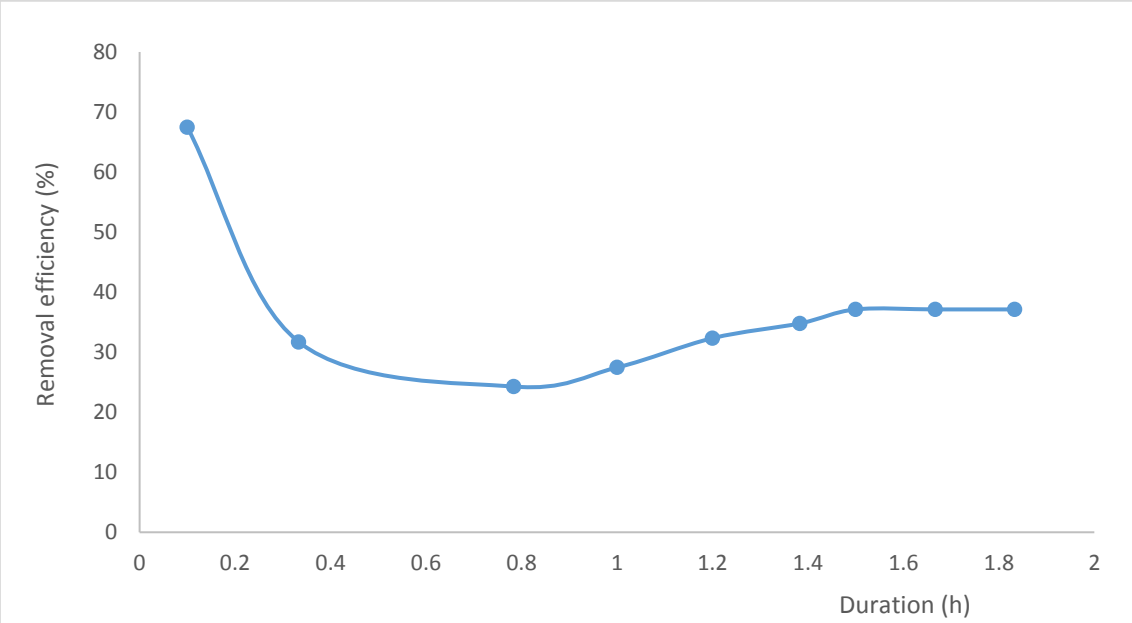

Figure 0-68. Kaolin removal efficiencies with cake layer from R2

According to the figures above, aerobic granular sludge has shown higher adsorption capacity. The net kaolin removal efficiency for cake layer from R3 is 42% while that of R2 was 22%. The higher removal capacity of R3 is due to high surface area per volume of bio-mass of granules (de-Kreuk & van-Loosdrecht, 2004).

Chapter5: Conclusions

The following chapter present a conclusion for the main findings attained from the experiments. This chapter is structured in two sections. The first one is dedicated to the aerobic granulation technology while the second covered the membrane filtration part.

5.1. Aerobic granulation technology

The results obtained from the experiments run over one year in WET lab and on 3 laboratory scale SBRs, proved the possibility of the aerobic granules formation under the organic loading rate of 2 kg COD/(m^3.d) and with the COD:N:P ratios of 20:3:1. However, due to over-growth of filamentous organisms, over-sized granules were observed in R3 during the first run.

In terms of the reactors' performance in treating wastewater, all the reactors (floccular and granular) showed great performance in removing organic matter. TN removal efficiencies for all the reactors were not as high as acetate removal efficiencies. The best performance in TN removal belongs to R2 which was in operation with floccular ans semi-granular sludge.

All the reactors performed poorly in removing phosphate and even in R3 and R1 the phosphate removal efficiencies were negative. The reason(s) behind it (are) still unknown. But, in general, there are several parameters contributing to removing phosphorous, such as organic loading rate and availability of organic carbon in the system. In this work, the carbon source was consumed immediately after the feeding phase was commenced, leaving no extra organic carbon for biological phosphorous removal. The overall reactors' performance during the whole experiment were provided in Table 0-1.

5.2. Dynamic membrane technology

In this work, a cake layer was successfully formed by both types of sludge on a 100 µm nylon mesh filter. The results have demonstrated that the cake layer resistance dominated the filtration process in short-term operation and the mesh filter itself did not play a significant role for filtration.

Cake layer resistance and its development are closely associated with the operating conditions, such as sludge concentration and its morphology. In this work, floccular sludge had the highest and granular sludge had the lowest cake layer resistance due to more porous structure. Though in this project the formation time was not investigated, it can be concluded that the larger particle size favours fast cake-layer formation and lower filtration resistance. Also, the results from the two trials on floccular and semi-floccular sludge showed different properties of the sludge and consequently different behaviour in filtration characteristics.

The dynamic membrane formed by supernatant from granular sludge had higher performance in SS rejection and granular sludge also had higher adsorption capacity than that of floccular sludge. This is probably due to bigger particle size in the supernatant from R3 which could be more effectively rejected by the dynamic membrane and the membrane itself.

5.3. Future Works

Although dynamic membrane filtration technology is proved to be effective in producing high quality effluent with low SS concentration, the mechanisms behind it are still unknown. To date there are numbers of studies conducted on the possibility of cake layer formation and its performance on solids rejection, but the number of studies focusing on the underlying principles of cake layer and also gel layer formation are not sufficient. On the other hand, for obtaining an in-depth knowledge of this technology it is important and beneficial to use a well-designed experimental set up in parallel to a mathematical model. Moreover, the bio-cake development is closely associated with the operating conditions, such as sludge concentration and characteristics, transmembrane pressure (TMP) and

hydrodynamics, and the properties of filter material itself. Therefore, it is recommended to standardize the operating conditions before initiation of the tests,

This work was carried out with synthetic wastewater which cannot fully evaluate the performance with the real wastewater. Therefore, it is highly recommended to conduct research as similar as possible to the real wastewater and also with more emphasis on the formation mechanisms and fouling properties. Also for obtaining more realistic results, using more accurate apparatus for measuring permeate flux and TMP is essential.

The following research questions can be regarded as a new direction for future works.

1- What are the mechanisms behind cake layer formation and gel layer formation?
2- What are the composition and structure of the DM formed on the surface and interspace of the membrane filter?
3- What are the effects of sludge properties i.e., sludge particle size distribution, hydrophobicity, viscosity and EPS content on bio cake layer formation and fouling properties?
4- How will the dynamic membrane formation and performance be if a real wastewater is used?
5- What are the mechanism of fouling?
6- What are the effect of membrane pore size (finer membrane) on filtration characteristics of the sludge?
7- What are the effects of important operational parameters such as aeration and agitation on formation and performance of dynamic membrane?

References

Campos, J. L., Figueroa, M., Mosquera-Corral, A. & Méndez , . R., 2009. Aerobic sludge granulation: state-of-the-art. *International Journal of Environmental Engineering,* 1(2).

Abdullah, N., Ujang, Z. & Yahya, A., 2011. Aerobic granular sludge formation for high strength agro-based wastewater treatment. *Bioresource Technology,* Volume 102, pp. 6778-6781.

Adav, S. S. & Lee, D.-J., 2008. Extraction of extracellular polymeric substances from aerobic granule with compact interior structure. *Hazardous Materials,* Volume 154, pp. 1120-1126.

Adav, S. S., Lee, D.-J. & Tay, J.-H., 2008. Extracellular polymeric substances and structural stability of aerobic granule. *Water Research,* Volume 42, pp. 1644-1650.

Ahmed, Z. et al., 2007. Effects of sludge retention time on membrane fouling and microbial community structure in a membrane bioreactor. *Membrane Science,* Volume 287, pp. 211-218.

Allhands, M. N., 2005. *Removing Solids with Automatic Self-Cleaning Filters.* Houston, Texas, THE 15TH ANNUAL PRODUCED WATER SEMINAR.

APHA, 1995. *Standard Methods for the Examination of Water and Wastewater, 19th ed,* Washington D.C.: American Public Health Association, American Water Works Association, Water Environment Federation.

Aulenta, F. et al., 2003. Effect of periodic feeding in sequencing batch reactor on substrate uptake and storage rates by a pure culture of Amaricoccus kaplicensis. *Water Research,* Volume 37, pp. 2764-2772.

Awang, N. A. & Shaaban, M. G., 2016. Effect of reactor height/diameter ratio and organic loading rate on formation of aerobic granular sludge in sewage treatment. *Intenational Biodeterioration and Biodegradation,* Volume 112, pp. 1-11.

Bao, R. et al., 2009. Aerobic granules formation and nutrients removal characteristics in sequencing batch airlift reactor (SBAR) at low temperature. *Hazardous Material,* Volume 168, pp. 1334-1340.

Basile, A., Cassano, A. & Rastogi, N. K., 2015. *Advances in Membrane Technologies for Water Treatment. Materials, Processes and Applications.* United Kingdom: Woodhead Publishing.

Bassin, J. P., Dezotti, M. & Van Loosdrecht, M., 2012. Simultaneous Nitrogen and Phosphate removal in Aerobic Granular Sludge Reactors Operated at Different Temperatures. *Water Research,* Volume 46, pp. 3805-3816.

Bathe, S., de Kreuk, M. K., McSwain, B. S. & Schwarzenbeck, N., 2005. *Aerobic Granular Sludge.* First ed. Germany: International Water Association. IWA.

Bhave, R. R., 1996. Cross-Flow Filtration. In: *Fermentation and Biochemical Engineering Handbook; Principles, Process Design, and Equipment.* s.l.:William Andrew, pp. 27-347.

Bindhu, B. K. & Madhu, G., 2013. Influence of Organic Loading Rates on Aerobic Granulation Process for the Treatment of Wastewater. *Clean Energy Technologies,* 1(2), pp. 84-86.

Buetehorn, S. et al., 2011. NMR imaging of local cumulative permeate flux and local cake growth in submerged microfiltration processes. *Membrane Science,* 371(1-2), pp. 52-64.

Castro-Barros, C. M., 2013. *Guidelines for granular sludge reactor design,* s.l.: SANITAS.

Chu, H., Dong, B., Zhang, Y. & Zhou, X., 2012. Gravity filtration performances of the bio-diatomite dynamic membrane reactor for slightly polluted surface water purification. *Water Science and Technology,* 66(5), pp. 1139-1146.

Chu, H. et al., 2014. Dynamic membrane bioreactor for wastewater treatment:Operation, critical flux, and dynamic membrane structure. *Journal of Membrane Science,* Volume 450, pp. 265-271.

Chu, L. & Li, S., 2006. Filtration Capability nd Operational Characteristics of Dynamic Membrane Bioreactor for Municipal Wastewater Treatment. *Separation Purification Technology,* Volume 51, pp. 173-179.

Cicek, N., 2002. *Membrane Bioreactors in the Treatment of Wastewater Generated from Agricultural Industries and Activities,* Saskatchewan: University of Manitoba.

Crittenden, J. C. et al., 2012. *Water Treatment: Principles and Design.* 3rd ed. s.l.:John Wiley & Sons, Inc.

de Amorim, M. P. & Ramos, L. R. A., 2006. Control of irreversible fouling by application of dynamic membranes. *Desalination,* 192(1-2), pp. 63-67.

de Bruin, L. M. et al., 2004. Aerobic granular sludge technology: an alternative to activated sludge?. *Water Science and Technology,* 49(11-12), pp. 1-7.

de-Kreuk, M. K., Heijnen, J. J. & Van Loosdrecht, M. M., 2005. Simultaneous COD, Nitrogen,and Phosphate Removal by Aerobic Granular Sludge. *Biotechnology and Bioengineering,* 90(6), pp. 761-769.

de-Kreuk, M. & van-Loosdrecht, M. V., 2004. Selection of Slow Growing Organisms as a Means for Aerobic Granular Sludge Stability. *Water Science and Technology,* 49(11-12), pp. 9-17.

Duan, W. et al., 2011. Effect of sludge retention time on characteristics of dynamic membrane in sequencing bioreactors. *Water Science Technology,* 63(10), pp. 2316-2323.

EBS, 2016. *Environmental Business Specialists.* [Online]
Available at: http://www.ebsbiowizard.com/2011/01/mixed-liquor-volatile-suspended-solids-mlvss-mlss/
[Accessed 20 11 2016].

EC, 1991. *Council Directive 91/271/EEC of 21 May 1991 concerning urban waste-water treatment,* s.l.: EUR-Lex.

Ersahin, M. E., Ozgun, H., Dereli, R. K. & Lier, J. V., 2012. A review on dynamic membrane filtration: Materials, applications and future perspectives. *Bioresource Technology,* Volume 122, pp. 196-206.

Ersahin, M. E., Ozgun, H., Tao, Y. & Lier, J. B. v., 2014. Applicability of dynamic membrane technology in anaerobic membrane bioreactors. *Water Research,* Volume 48, pp. 420-429.

Ersahin, M. . E., Ozgun, H. & van Lier, J. B., 2013. Effect of Support Material Properties on Dynamic Membrane Filtration Performance. *Separation Science and Technology,* Volume 48, pp. 2263-2269.

Ersan, Y. C. & Erguder, T. H., 2014. The effect of seed sludge type on aerobic granulation via anoxic–aerobic operation. *Environmental Technology,* 35(23), pp. 2928-2939.

Evenblij, H., 2006. *Filtration Characteristics in Membrane Bioreactors,* s.l.: s.n.

Fan, B. & Huang, X., 2002. Characteristics of a self-forming dynamic membrane coupled with a bioreactor for municipal wastewater treatment. *Environmental Science Technology,* 36(23), pp. 5245-5251.

Field, R., 2010. Fundamentals of Fouling. *Membrane for Water Treatment.*

Fuchs, W. et al., 2005. Influence of operational conditions on the performance of a mesh filter activated sludge process. *Water Research,* Volume 39, pp. 803-810.

Gao, D., Liu, L., Liang, H. & Wu, W.-M., 2011. Aerobic granular sludge: characterization, mechanism of granulation and application to wastewater treatment. *Critical Reviews in Biotechnology,* 31(2), pp. 137-152.

Grenier, A., Meireles, M., Aimar, P. & Carvin, P., 2008. Analysing Flux Decline in Dead-End Filtration. *Chemical Engineering Research and Design,* Volume 86, pp. 1281-1293.

Groves, G. R. et al., 1983. Dynamic Membrane Ultrafiltration and Hyperfiltration for the Treatment of Industrial Effluents for Water Reuse. *Desalination,* Volume 47, pp. 305-312.

Gupta, N., Jana, N. & Majumder, C. B., 2008. Submerged Membrane Bioreactor System for Municipal Wastewater Treatment Process: An Overview. *Indian Journal of Chemical Technology,* Volume 15, pp. 604-612.

Helness, H., 2007. *Biological phosphorus removal in a moving bed biofilm reactor,* Trondheim: Norwegian University of Science and Technology, NTNU.

Hong, H. et al., 2014. Fouling mechanisms of gel layer in a submerged membrane bioreactor. *Bioresource Technology,* Volume 166, pp. 295-302.

Huang, T. et al., 2013. A Comparative Study of Aerobic Granule and Activated Sludge Based Dynamic Membrane Reactors for Wastewater Treatment. *Bioprocessing and Biotechniques,* 3(2).

IWA, 2013. *The Intenational Water Association, Sequencing Batch Reactor.* [Online] Available at: http://www.iwapublishing.com/news/sequencing-batch-reactor [Accessed 28 10 2016].

Janczukowicz, W., Szewczyk, M., Krzemieniewski, M. & Pesta, J., 2001. Settling Properties of Activated Sludge from a Sequencing Batch Reactor (SBR). *Environmental Studies,* 10(1), pp. 15-20.

Jiang, T., Kennedy, M., Vanrolleghem, P. A. & Schippers, J. C., 2008. *Controlling membrane pore blocking and filter cake build-up in side-stream MBR systems,* s.l.: s.n.

Jing-Feng, W. et al., 2012. Comparison and Analysis of Membrane Fouling between Flocculent Sludge Membrane Bioreactor and Granular Sludge Membrane Bioreactor. *PlosOne,* 7(7).

Jun, Z. et al., 2007. Comparison of membrane fouling during short-term filtration of aerobic granular sludge and activated sludge. *Journal of Environmental Science,* Volume 19, pp. 1281-1286.

Kennedy, K. J. & Lentz, E. M., 2000. Treatment of Landfill Leachate Using Sequensing Batch and Continuous Flow Upflow Anaerobic Sludge Blanket (UASB) Reactors. *Water Research,* 34(14), pp. 3640-3656.

Kiso, Y. et al., 2000. Wastewater treatment performance of a filtration bio-reactor equipped with a mesh as a filter material. *Water Research,* 34(17), pp. 4143-4150.

Kiso, Y. et al., 2005. Coupling of sequencing batch reactor and mesh filtration:Operational parameters and wastewater treatment performance. *Water Research,* Volume 39, pp. 4887-4898.

Konczak, B., Karcz, J. & Miksch, K., 2014. Influence of Calcium, Magnesium, and Iron Ions on Aerobic Granulation. *Applied Biochemistry and Biotechnology,* 174(8), pp. 2910-2918.

Kong, Y., Liu, Y.-Q., Tay, J.-H. & Zhu, J., 2009. Aerobic Granulation in Sequencing Batch Reactors With Different Reactor Height/Diameter Ratios. *Enzyme and Microbial Technology,* 45(5), pp. 379-383.

Kreuk, M. d. & Loosdrecht, M. V., 2006. Formation of Aerobic Granules With Domestic Sewage. *Environmental Engineering,* Volume 132, pp. 694-697.

Lee, D. S., Joen, C. O. & Park, J. M., 2001. Biological Nitrogen REmoval With Enhanced Phosphate Uptake in a Sequencing Batch Reactor Using Single Sludge System. *Water Research,* 35(16), pp. 3968-3976.

Lee, J., Ahn, W.-Y. & Lee, C.-H., 2001. Comparison of the filtration characteristics between attached and suspended growth microorganisms in submerged membrane bioreactor. *Water Research,* 35(10), pp. 2435-2445.

Leong, J., Rezania , B. & Mavinic, D. S., 2016. Aerobic granulation utilizing fermented municipal wastewater under low pH and alkalinity conditions in a sequencing batch reactor. *Environmental Technology,* 37(1), pp. 55-63.

Liang, S. et al., 2013. Effect of sludge properties on the filtration characteristics of self-forming dynamic membranes (SFDMs) in aerobic bioreactors: Formation time, filtration resistance, and fouling propensity. *Membrane Science,* Volume 436, pp. 186-194.

Li, J. et al., 2014. Aerobic Sludge Granulation in a Full-Scale Sequencing Batch Reactor. *BioMed Research International,* Volume 2014, p. 12 pages.

Li, J. et al., 2015. Accelerating Aerobic Sludge Granulation by Adding Dry Sewage Sludge Micropowder in Sequencing Batch Reactors. *International Journal of Environmental Research and Public Health,* Volume 12, pp. 10056-10065.

Liu, L., Gao, D.-W., Zhang, M. & Fu, Y., 2010. Comparison of Ca2+ and Mg2+ enhancing aerobic granulation in SBR. *Journal of Hazardous Materials,* Volume 181, pp. 382-387.

Liu, Q. S., Tay, J.-H. & Liu, Y., 2003. Substrate concentration-independent aerobic granulation in sequential aerobic sludge blanket reactor. *Environmental Technology,* 24(10), pp. 1235-1242.

Liu, Y. & Tay, J.-H., 2002. The essential role of hydrodynamic shear force in the formation of biofilm and granular sludge. *Water Research,* 36(7), pp. 1653-1665.

Liu, Y. & Tay, J.-H., 2004. State of the art of biogranulation technology for wastewater treatment. *Biotechnology Advances,* Volume 22, pp. 533-563.

Li, W.-W.et al., 2012. A dead-end filtration method to rapidly and quantitatively evaluate the fouling resistance of nylon mesh for membrane bioreactors. *Separation and Purification Technology,* Volume 89, pp. 107-111.

Lochmatter, S., Maillard, . J. & Holliger, C., 2014. Nitrogen Removal over Nitrite by Aeration Control in Aerobic Granular Sludge Sequencing Batch Reactors. *Environmental Research and Public Health,* Volume 11, pp. 6955-6978.

McSwain, B. S., Irvine, R. L. & Wilderer, P. A., 2004. The effect of intermittent feeding on aerobic granule structure. *Water Science and Technology,* 49(11), pp. pp 19-22.

Meng, F. G. et al., 2005. Cake layer morphology in microfiltration of activated sludge wastewater based on fractal analysis. *Separation and Purification Technology,* 44(3), pp. 250-257.

Mesquita, D. P., Amaral, A. L. & Ferreira, E. C., 2011. *Quantitativeimage analysis for sludge volume index and total suspended solids prediction in activated sludge system disturbances.* Lisbon, 11th International Chemical and Biological Engineering Conference, Portugal, pp. 426-427.

Mosquera-Corral, A., de Kreuk, M. K., Heijnen, J. J. & Van Loosdrecht, M. M., 2005. Effects of oxygen concentration on N-removal in an aerobic granular sludge reactor. *Water Research,* Volume 39, pp. 2676-2686.

Motosic, M., Vukovic , M., Curlin, M. & Mijatovic, I., 2008. Fouling of Hallow Fibre Submerged Membrane During Long Term Filtration of Activated Sludge. *Desalination,* Volume 219, pp. 57-65.

Moy, B. -p. et al., 2002. High organic loading influences the physical characteristics of aerobic granules sludge. *Letters in Applied Microbiology,* Volume 34, pp. 407-412.

NEIWPCC, 2005. *Sequencing Batch Reactor Design and Operational Considerations,* New England: New England Interstate Water Pollution Control Commission.

Ni, B. J., 2012. In: *Formation, Characterization and Mathematical Modeling of the Aerobic Granular Sludge.* Brisbane: Springer, pp. 5-6.

Oh, J. H., no date. *Fundamental and application of aerobic granulation technology for wastewater treatment,* s.l.: s.n.

Pabby, A. K., Rizvi, S. S. H. & Sastre, A. M., 2008. *Handbook of Membrane Separations: Chemical, Pharmaceutical, Food, and Biotechnological Applications.* s.l.:CRC Press; Taylor and Francis Group.

Park, C., 2007. *Extracellular Polymeric Substances in Activated Sludge Flocs: Extraction, Identification, and Investigation of Their Link with Cations and Fate in Sludge Digestion,* Virginia: s.n.

Pennsylvania Department of Environmental Protection, n.d. *Drinking Water Operator Certification Training Module 19:Membrane Filtration,* Pennsylvania: Bureau of Water Supply and Wastewater Management, Department of Environmental Protection.

Persson, G., 2015. *High-loaded Activated Sludge Effects of Different Aeration Strategies at Sjölunda WWTP,* Lund: Lund University.

Poostchi, A. A. et al., 2015. Formation of pre-coating dynamic membrane on mesh filter by cross-flow filtration of PAC–water suspension in a bioreactor: experimental and modeling. *Desalination and Water Treatment,* 55(1), pp. 17-27.

Qin, L., Tay, J.-H. & Liu, Y., 2004. Selection pressure is a driving force of aerobic granulation in sequencing batch reactors. *Process Biochemistry,* Volume 39, pp. 579-584.

Radjenovic, J. et al., 2008. Membrane Bioreactor (MBR) as an Advanced Wastewater Treatment Technology. *Environmental Chemistry,* Volume 5, pp. 37-101.

Rocktäschel, T. et al., 2015. Influence of the granulation grade on the concentration of suspended solids in the effluent of a pilot scale sequencing batch reactor operated with aerobic granular sludge. *Separation and Purifiction Technology,* Volume 142, pp. 234-241.

Royal HaskoningDHV, 2013. *The Natural Way of Treating Wastewater,* The Netherlands: Nereda Company.

Sam, S. B. & Dulekgurgen, E., 2015. Characterization of exopolysaccharides from floccular and aerobic granular activated sludge as alginate-like-exoPS. *Desalination and Water Treatment,* pp. 1-12.

Sathasivan, A., 2014. *Biological Phosphorus Removal Processes for Wastewater Treatment.* [Online]
Available at: https://www.eolss.net/Sample-Chapters/C07/E6-144-10.pdf
[Accessed 2 11 2016].

Seo, G. T. et al., 2002. Non-Woven fabric filter separation activated sludge reactor for domestic wastewater reclamation. *Water Science and Technology,* 47(1), pp. 133-138.

Shan, H., 2004. *Membrane Fouling During the Microfiltration of Primary and Secondary Wastewater Treatment Plant Effluents,* s.l.: University of Pittsburgh.

Soltanzadeh, S., Shayegan, J. & Jalali, S., 2015. Effect of pH on Aerobic Granulation and Treatment Performance in Sequencing Batch Reactors. *Chemical Technology and Engineering,* 38(5), pp. 851-858.

Stypka, A., 1998. *Factors Influencing Sludge Settling Parameters and Solids Flux in the Activated Sludge Process; A Literature Review,* Stockholm: Kungl Tekniska Högskolan.

Szabo, E. et al., 2016. Effects of Wash-Out Dynamics on Nitrifying Bacteria in Aerobic Granular Sludge During Start-Up at Gradually Decreased Settling Time. *Water,* 8(5), p. 172.

Tay, J.-H., Liu, Q. S. & Liu, Y., 2001a. Microscopic observation of aerobic granulation in sequential aerobic sludge blanket reactor. *Applied Microbiology,* Volume 91, pp. 168-175.

Tay, J.-H., Liu, Q. S. & Liu, Y., 2001b. The role of cellular polysaccharides in the formation and stability of aerobic granules. *Letters in Applied Microbiology,* Volume 33, pp. 222-226.

Tay, J.-H., Liu, Q. S. & Liu, Y., 2001c. The effects of shear force on the formation, structure and metabolism of aerobic granules. *Applied Microbial Biotechnology,* Volume 57, pp. 227-233.

Tay, J.-H., Liu, Q. S. & Liu, Y., 2002. Characteristics of Aerobic Granules Grown on Glucose and Acetate in Sequential Aerobic Sludge Blanket Reactors. *Environmental Technology,* 23(8), pp. 931-936.

Tay, J.-H., Pan, S., He, Y. & Tay, S. T. L., 2004. Effect of Organic Loading Rate on Aerobic Granulation. I: Reactor Performance. *Environmental Engineering,* 130(10), pp. 1094-1101.

Tay, J.-H.et al., 2006. *Biogranulation Technologies for Wastewater Treatment: Microbial Granules.* 1st ed. s.l.:Elsevier Ltd.

Tchobanoglous, G., Burton, F. L. & Stensel, H., 2004. *Wastewater engineering: Treatment and reuse.* 5th ed. Boston: McGraw-Hill.

Toh, S. K., Tay, J.-H., Moy, B. Y.-P. & Ivanov, V., 2002. Size-effect on the physical characteristics of the aerobic granule in a SBR. *Applied Microbial Biotechnology,* Volume 60, pp. 687-696.

US EPA, 1999. *Wastewater Technology Fact Sheet: Sequencing Batch Reactors,* Washington, D.C.: U.S. Environmental Protection Agency.

US EPA, 2001. *Low-Pressure Membrane Filtration for Phatogen Removal: Applications, Implementations and Regulatory Issues,* s.l.: United States Environmental Protection Agency, Office of Water.

US EPA, 2005. *Membrane Filtration Guidance Manual,* Cincinnati: United States Environmental Protection Agency , Office of Ground Water and Drinking Water.

Val del Rio, A. et al., 2013. Effects of the cycle distribution on the performance of SBRs with aerobic granular biomass. *Environmental Technoogy,* 34(11), pp. 1463-1472.

van-Loosdrecht, M. M. et al., 1995. Biofilm structures. *Water Science and Technology,* 32(8), pp. 35-43.

Vigneswaran, S., Sundaravadivel, M. & Chaudhary, D. S., n.d. *Sequencing Batch Reactors: Principles, Design/Operation and Case Studies,* s.l.: s.n.

Waltz, K. H., 2009. *Simultaneous Nitrification and Denitrification of Wastewater Using a Silicon Membrane Bioreactor,* California, US: California Polytechnic State University.

Wang, J.-Y., Chou, K.-S. & Lee, C.-J., 1998. Dead-End Flow Filtration of Solid Suspension in Polymer Fluid through an Active Kaolin Dynamic Membrane. *Separation Science and Technology,* 33(16).

Wang, Y.-K., Sheng, G.-P., Li, W.-W. & Yu, H.-Q., 2012. A pilot investigation into membrane bioreactor using mesh filter. *Bioresource Technology,* Volume 122, pp. 17-21.

Wang, Z.-W., Liu, Y. & Tay, J.-H., 2005. Distribution of EPS and cell surface hydrophobicity in aerobic granules. *Applied Microbiology and Biotechnology,* Volume 69:469.

Wilen, B.-M., 1995. *Effect of Different Parameters on Settling Properties of Activated Sludge,* Göteborg: Chalmers University of Technology.

Wilf, M., 2007. *Membrane Types and Factors Affecting Membrane Performance,* s.l.: Stanford University.

Winkler, M.-K. H., 2012. *Magic Granules,* Delft: Technnische Universiteit Delft.

Wisconsin Department of Natural Resources, 2009. *Introduction to Phosphorus Removal Study Guide,* Wisconsin: Wisconsin Department of Natural Resources.

Wu, J. & He, C., 2012. Effect of cyclic aeration on fouling in submerged membrane bioreactor for wastewater treatment. *Water Research,* 46(11), pp. 3507-3515.

Wu, Y., Huang, X. & Zuo, W., n.d. *Effect of Mesh Pore Size on Performance of a Self-forming Dynamic Membrane Coupled Bioreactor for Domestic Wastewater Treatment,* China: s.n.

Wu, Y., Huang, X., Wen, X. & Chen, F., 2005. Function of dynamic membrane in self-forming dynamic membrane coupled bioreactor. *Water Science Technology,* 51(6-7), pp. 107-114.

Xiao, F., Yang, S. F. & Li, X. Y., 2008. Physical and hydrodynamic properties of aerobic granules produced in sequencing batch reactors. *Separation and Purification Technology,* Volume 63, pp. 634-641.

Xuan, W. et al., 2010. The EPS characteristics of sludge in an aerobic granule membrane bioreactor. *Bioresource Tehnology,* Volume 10, pp. 8046-8050.

Xu-Jiang, Y., Dodds, J. & Leclerc, D., 1995. Cake Characteristics in Crossflow and Dead-End Microfiltration. *Filtration and Separation,* pp. 795-798.

Yamagiwa, K., Ohmae, Y., Dahlan, M. H. & Ohkawa, A., 1991. Activated Sludge Treatment of Small-Scale Wastewater by a Plunging Liquid Jet Bioreactor with Cross-Flow Filtration. *Bioresource Technology,* Volume 37, pp. 215-222.

Yamagiwa, K., Oohira, Y. & Ohkawa, A., 1994. Performance evaluation of a plunging liquid jet bioreactor with crossflow filtration for small-scale treatment of domestic wastewater. *Bioresource Technology,* 50(2), pp. 131-138.

Yu, H. et al., 2016. Effect of solid retention time on membrane fouling in membrane bioreactor: from the perspective of quorum sensing and quorum quenching. *Applied Microbiology and Biotechnology,* 100(18), pp. 7887-7897.

Zedda, M., Heidlberger, A. & Neugebauer, E., n.d. *Membrane Processes-Review-.* [Online] Available at: https://www.uni-due.de/imperia/md/content/water-science/membrane_processes.pdf
[Accessed 29 10 2016].

Zhang, Y. et al., 2014. Characteristics of dynamic membrane filtration: structure, operation mechanisms, and cost analysis. *Chinese Science Bulletin,* 59(3), pp. 247-260.

Zhao, X. et al., 2016. Decreasing effect and mechanism of moisture content of sludge biomass by granulation process. *Environmental Technology,* 37(2), pp. 192-201.

Zheng, X. et al., 2010. Effect of Copper(II) on the characteristics of aerobic Granules. *Advanced Material Research,* Volume 113-117, pp. 71-75.

Zhu, Z., Zhou, Y., Li, X. & Chen, J., 2006. Characteristics of aerobic granular sludge membrane bioreactor for wastewater treatment. *Water Resource and Environmental Protection,* 27(1), pp. 57-62.

Zita, A. & Hermansson, M., 1996. *Effects of Bacterial Cell Surface Structures and Hydrophobicity on Attachment to Activated Sludge Flocs.* Gothenburg, s.n.

Zita, A. & Hermansson, M., 1997. Effects of Bacterial Cell Surface Structures and Hydrophobicity on Attachment to Activated Sludge Flocs. *Applied and Environmental Microbiology,* 63(3), pp. 1168-1170.

Attachments

7-1. Appendix I- Settling time alteration

Settling time alteration plant for aerobic granulation was done based on step wise settling time reduction. More detailed information can be fine in the tables below.

Table 0-1. Settling time alteration plan for R3 in the first run

Date of alteration	Settling time (min)
2016.02.02	30
2016.02.03	25
2016.02.05	20
2016.02.06	15
2016.02.08	10
2016.02.10	8
2016.02.11	6
2016.02.15	4
2016.02.18	3
2016.02.22	2

Table 0-2. Settling time alteration plan for R3 in the second run

Date of alteration	Settling time (min)
2016.07.27	30
2016.07.29	10
2016.08.01	8
2016.08.02	7
2016.08.04	6
2016.08.05	4
2016.08.14	2

7-2. Appendix Ⅱ- Cycle studies

The results for the two cycle studies are provided below. **Error! Reference source not found.** and **Error! Reference source not found.**, shows the TOC, TN, IC and TC changes over one cycle of the operation for R2 and R3 respectively.

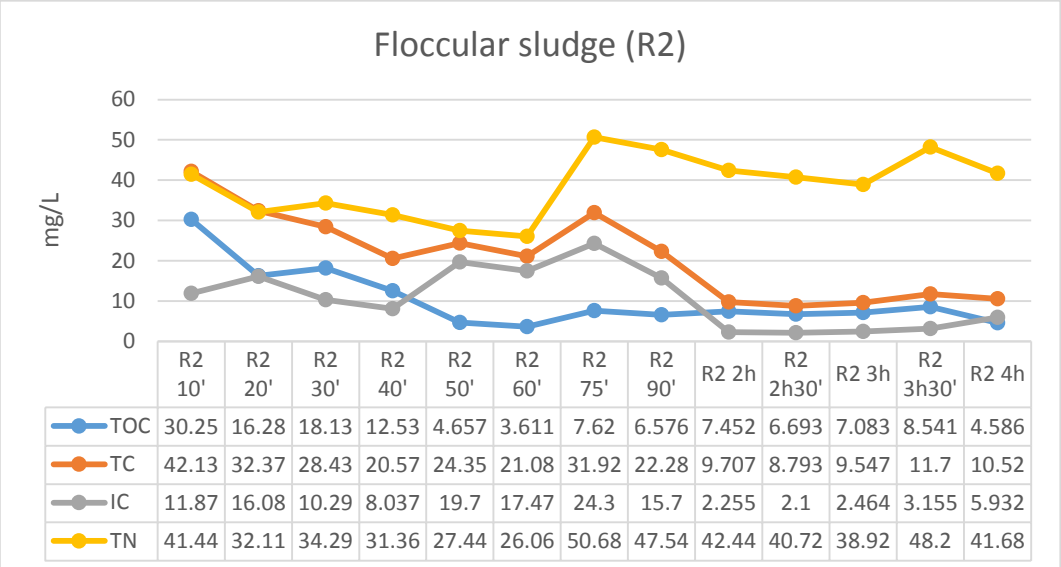

	R2 10'	R2 20'	R2 30'	R2 40'	R2 50'	R2 60'	R2 75'	R2 90'	R2 2h	R2 2h30'	R2 3h	R2 3h30'	R2 4h
TOC	30.25	16.28	18.13	12.53	4.657	3.611	7.62	6.576	7.452	6.693	7.083	8.541	4.586
TC	42.13	32.37	28.43	20.57	24.35	21.08	31.92	22.28	9.707	8.793	9.547	11.7	10.52
IC	11.87	16.08	10.29	8.037	19.7	17.47	24.3	15.7	2.255	2.1	2.464	3.155	5.932
TN	41.44	32.11	34.29	31.36	27.44	26.06	50.68	47.54	42.44	40.72	38.92	48.2	41.68

Figure 0-1. Cycle study for R2 during the first run

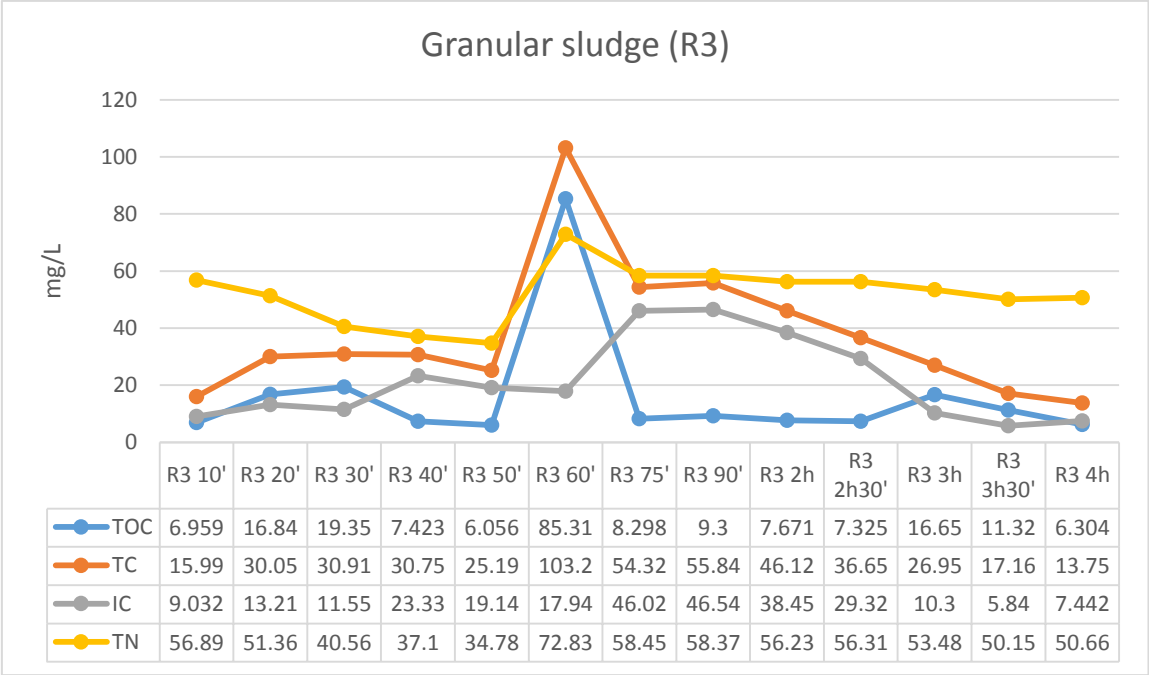

	R3 10'	R3 20'	R3 30'	R3 40'	R3 50'	R3 60'	R3 75'	R3 90'	R3 2h	R3 2h30'	R3 3h	R3 3h30'	R3 4h
TOC	6.959	16.84	19.35	7.423	6.056	85.31	8.298	9.3	7.671	7.325	16.65	11.32	6.304
TC	15.99	30.05	30.91	30.75	25.19	103.2	54.32	55.84	46.12	36.65	26.95	17.16	13.75
IC	9.032	13.21	11.55	23.33	19.14	17.94	46.02	46.54	38.45	29.32	10.3	5.84	7.442
TN	56.89	51.36	40.56	37.1	34.78	72.83	58.45	58.37	56.23	56.31	53.48	50.15	50.66

Figure 0-2. Cycle study for R3 during the first run

The same cycle study performed during the second run on R1 and R3. The results are presented in **Error! Reference source not found.** and **Error! Reference source not found.**.

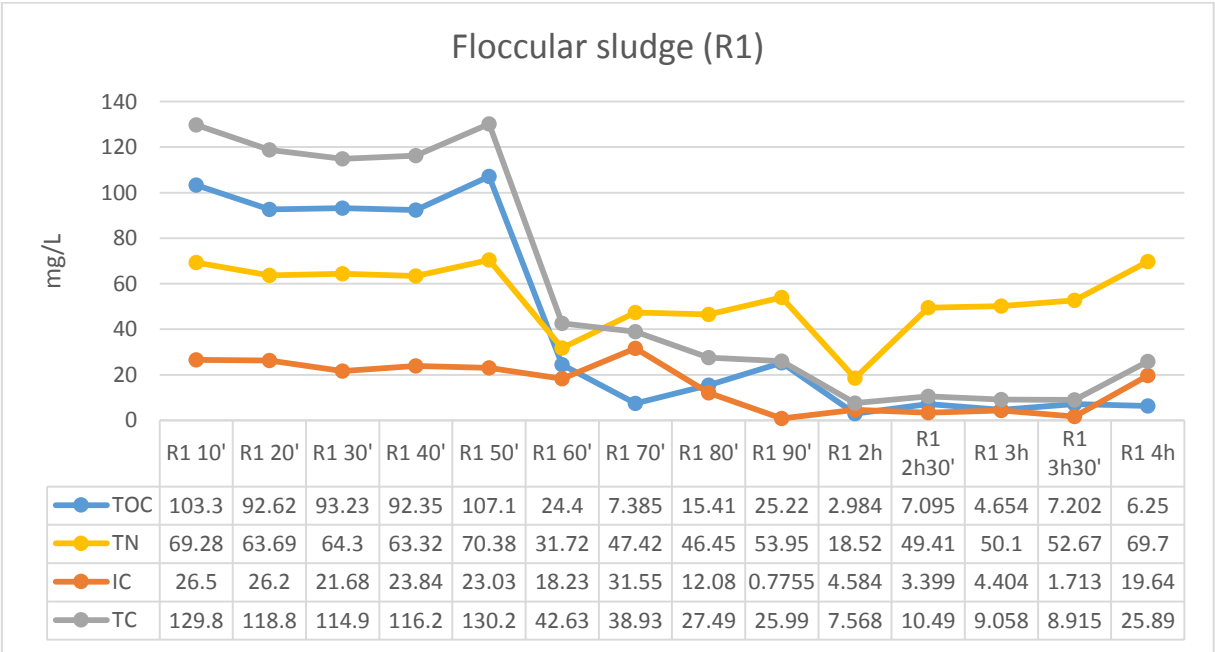

	R1 10'	R1 20'	R1 30'	R1 40'	R1 50'	R1 60'	R1 70'	R1 80'	R1 90'	R1 2h	R1 2h30'	R1 3h	R1 3h30'	R1 4h
TOC	103.3	92.62	93.23	92.35	107.1	24.4	7.385	15.41	25.22	2.984	7.095	4.654	7.202	6.25
TN	69.28	63.69	64.3	63.32	70.38	31.72	47.42	46.45	53.95	18.52	49.41	50.1	52.67	69.7
IC	26.5	26.2	21.68	23.84	23.03	18.23	31.55	12.08	0.7755	4.584	3.399	4.404	1.713	19.64
TC	129.8	118.8	114.9	116.2	130.2	42.63	38.93	27.49	25.99	7.568	10.49	9.058	8.915	25.89

Figure 0-3. Cycle study for R1 during the second run (aeration was started at 60' and turned off at 3h23')

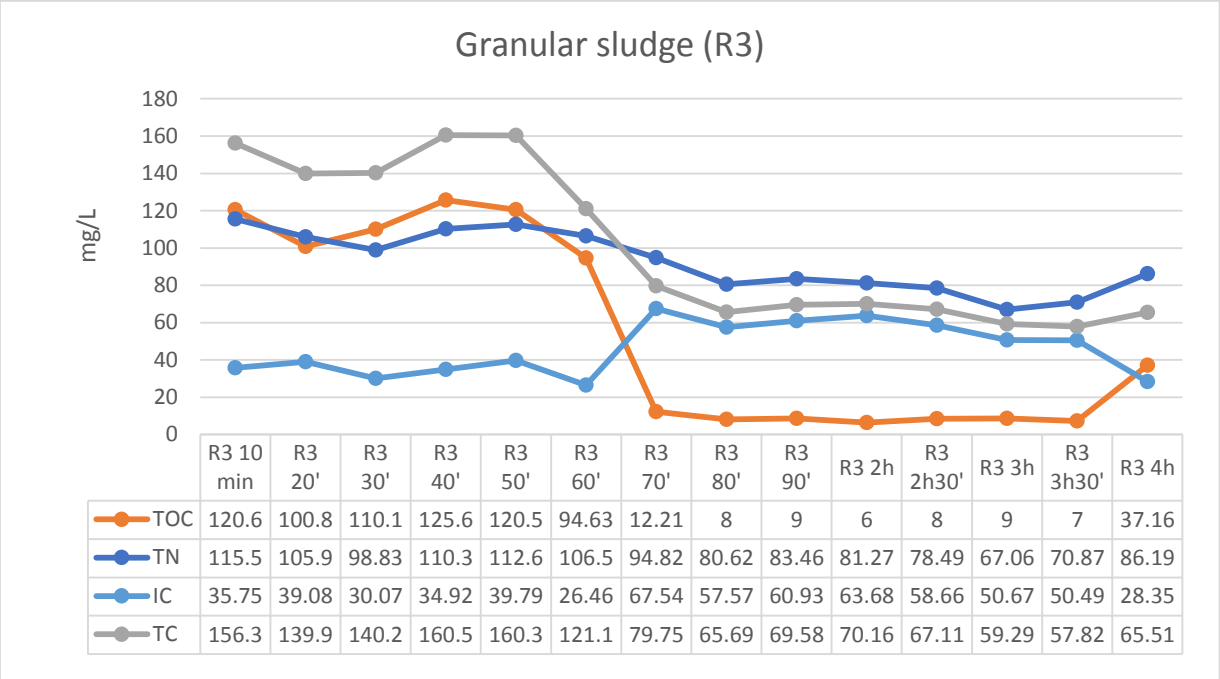

	R3 10 min	R3 20'	R3 30'	R3 40'	R3 50'	R3 60'	R3 70'	R3 80'	R3 90'	R3 2h	R3 2h30'	R3 3h	R3 3h30'	R3 4h
TOC	120.6	100.8	110.1	125.6	120.5	94.63	12.21	8	9	6	8	9	7	37.16
TN	115.5	105.9	98.83	110.3	112.6	106.5	94.82	80.62	83.46	81.27	78.49	67.06	70.87	86.19
IC	35.75	39.08	30.07	34.92	39.79	26.46	67.54	57.57	60.93	63.68	58.66	50.67	50.49	28.35
TC	156.3	139.9	140.2	160.5	160.3	121.1	79.75	65.69	69.58	70.16	67.11	59.29	57.82	65.51

Figure 0-4. Cycle study for R3 during the second run

7-3. Appendix III- TMP vs flux records of floccular sludge (R2), first trial

Table 0-3. TMP and flux for clean membrane

ΔH (cm)	Flow(mL/s)	TMP (Pa)	Flux ($m^3/m^2.s$)
4.5	64.810	441.450	0.017
9.5	108.20	931.950	0.028
13.5	153.840	1324.350	0.040
15.5	180.850	1520.550	0.048
2.5	16.744	245.250	0.004
18	174.760	1765.800	0.046

Table 0-4. TMP and flux for 10 mL (60.48 mg) of sludge R2

ΔH (cm)	Flow (mL/s)	TMP (Pa)	Flux ($m^3/m^2.s$)
5.5	40	539.550	0.011
11.5	101.98	1128.150	0.027

8.5	93.75	833.850	0.025
18	159.81	1765.800	0.042
23	159.79	2256.300	0.042

Table 0-5. TMP and flux for 25 mL (151.2 mg) of sludge R2

ΔH (cm)	**Flow (mL/s)**	**TMP (Pa)**	**Flux ($m^3/m^2.s$)**
14	31.88	1373.400	0.008
15.5	33.87	1520.550	0.009
36	81.11	3531.600	0.021
39	80.51	3825.900	0.021
3.5	8.37	343.350	0.002

Table 0-6. TMP and flux for 40 mL (242 mg) of sludge R2

ΔH (cm)	**Flow (mL/s)**	**TMP (Pa)**	**Flux ($m^3/m^2.s$)**
3.5	8.88	343.350	0.002
7	12.64	686.700	0.003
11.5	14.22	1128.150	0.004
36	30.64	3531.600	0.008
25.5	31.53	2501.550	0.008
27.5	31.63	2697.750	0.008
30	38.05	2943	0.010

Table 0-7. TMP and flux for 75 mL (573 mg) of sludge R2 with suction pump and pressure gauge

water level above the membrane (cm)	**Flow (mL/s)**	**Pressure gauge (mbar)**	**TMP (kPa)**	**Flux ($m^3/m^2.s$)**
29.5	1.461	50	7.895	0.0004
29.5	1.881	100	12.895	0.0005
30	3.833	140	16.943	0.0010
32.5	4.098	140	17.188	0.0011

38.5	4.687	150	18.777	0.0012
28.5	4.924	140	16.796	0.0013
28.5	5.821	142	16.996	0.0015
28.5	5.900	220	24.796	0.0015
27	2.782	120	14.649	0.0007
25	3.365	140	16.452	0.0009

Table 0-8. TMP and flux for 100 mL (725 mg) of sludge R2 with suction pump and pressure gauge

water level above the membrane (cm)	**Flow (mL/s)**	**Pressure gauge (mbar)**	**TMP (kPa)**	**Flux ($m^3/m^2.s$)**
39	2.946	32	7.026	0.0008
28.5	2.690	50	7.796	0.0007
28.5	3.358	75	10.296	0.0009
28.5	3.694	100	12.796	0.0009
28.5	4.391	110	13.796	0.001
28.5	3.853	150	17.796	0.001
28.5	4.488	158	18.596	0.001
28.5	4.844	170	19.796	0.001
28.5	5.681	180	20.796	0.001
28.5	6.310	190	21.796	0.002

Table 0-9. TMP and flux for 150 mL (942 mg) of sludge R2 with suction pump and pressure gauge

water level above the membrane (cm)	**Flow (mL/s)**	**Pressure gauge (mbar)**	**TMP (kPa)**	**Flux ($m^3/m^2.s$)**
28.5	1.11	218	24.596	0.0003
28.5	1.13	220	24.796	0.0003
28.5	1.37	250	27.796	0.0003
28.5	2.70	100	12.796	0.0007

28.5	2.71	140	16.796	0.0007
28.5	2.10	210	23.796	0.0006
28.5	1.88	220	24.796	0.0005
28.5	2.15	250	27.796	0.0006
28.5	1.87	260	28.796	0.0005
28.5	3	280	30796	0.0008
28.5	3.11	280	30.796	0.0008
28.5	3	300	32.796	0.0008
28.5	3	300	32.796	0.0008
28.5	3.28	300	32.796	0.0009
28.5	3.56	302	32.996	0.0009

Table 0-10. TMP and flux for 300 mL of sludge R2 with suction pump and pressure gauge

water level above the membrane (cm)	**Flow (mL/s)**	**Pressure gauge (mbar)**	**TMP (kPa)**	**Flux ($m^3/m^2.s$)**
28.5	0.457	340	36.796	0.0001
28.5	0.550	360	38.796	0.0001
28.5	0.600	360	38.796	0.0001
28.5	0.920	360	38.796	0.0002
28.5	1.212	365	39.296	0.0003
28.5	1.266	390	41.796	0.0003
28.5	1.250	390	41.796	0.0003
28.5	1.440	400	42.796	0.0004

7-4. Appendix Ⅳ- TMP vs flux records of floccular sludge (R2), second trial

Table 0-11. TMP and flux for measuring membrane intrinsic resistance

ΔH (cm)	**Flow (mL/s)**	**TMP (Pa)**	**Flux ($m^3/m^2.s$)**
0	0	0	0
6.87	76.527	673.947	0.020
13.67	142.270	1341.027	0.037
8.97	97.514	879.957	0.026

4.27	43.649	418.887	0.011
11.57	116.292	1135.017	0.0306

Table 0-12. TMP and flux for 20 mL (232 mg) of sludge R2

ΔH (cm)	Flow (mL/s)	TMP (Pa)	Flux ($m^3/m^2.s$)
3	4.082	294.300	0.001
3.87	22.556	379.647	0.006
4.57	50.378	448.317	0.013
6.17	77.821	605.277	0.020
13.57	108.108	1331.217	0.029
15.37	137.931	1507.797	0.036

Table 0-13. TMP and flux for 40 mL (464 mg) of sludge R2

ΔH (cm)	Flow (mL/s)	TMP (pa)	Flux ($m^3/m^2.s$)
3.22	8.31	315.882	0.002
4.57	29.90	448.317	0.008
6.37	49.63	624.897	0.013
8.87	97.08	870.147	0.025
14.57	113.64	1429.317	0.030

Table 0-14. TMP and flux for 75 mL (812 mg) of sludge R2

ΔH (cm)	Flow (mL/s)	TMP (Pa)	Flux ($m^3/m^2.s$)
5.22	13.30	512.082	0.003
6.37	22.42	624.897	0.006
7.37	44.66	722.997	0.011
8.87	51.91	870.147	0.014
14.67	78.95	1439.127	0.021

Table 0-15. TMP and flux for 100 mL (1160 mg) of sludge R2

ΔH (cm)	Flow (mL/s)	TMP (Pa)	Flux ($m^3/m^2.s$)
6.57	24.764	644.517	0.007

8.27	31.056	811.287	0.008
15.17	55.690	1488.177	0.015
18.15	61.881	1780.515	0.016
3.25	7.059	318.825	0.002
11.35	35.519	1113.435	0.009

Table 0-16. TMP and flux for 150 mL (1740 mg) of sludge R2

ΔH (cm)	Flow (mL/s)	TMP (Pa)	Flux ($m^3/m^2.s$)
2.64	2.24	258.984	0.0006
7.67	12.77	752.427	0.0033
9.07	12.74	889.767	0.0033
12.17	19.68	1193.877	0.0051
13.87	21.74	1360.647	0.0057
15.37	24.57	1507.797	0.0064

Table 0-17. TMP and flux for 200 mL (2320 mg) of sludge R2

ΔH (cm)	Flow (mL/s)	TMP (Pa)	Flux ($m^3/m^2.s$)
8.50	6.85	833.850	0.0018
4.25	3.33	416.925	0.0009
12.07	9.63	1184.067	0.0025
14.37	14.27	1409.697	0.0037
15.67	17.38	1537.227	0.0046
19.97	20.19	1959.057	0.0053

Table 0-18. TMP and flux for 240 mL (2784 mg) of sludge R2

ΔH (cm)	Flow (mL/s)	TMP (Pa)	Flux ($m^3/m^2.s$)
9.57	7.68	938.817	0.0020
11.37	8.68	1115.400	0.0023
17.97	13.12	1762.857	0.0034
6.15	3.96	603.315	0.0010
16.5	14.43	1619	0.0038
8.15	6.82	799.515	0.0018

20.35	17.73	1996.335	0.0046

Table 0-19. TMP and flux for 300mL (3480 mg) of sludge R2

ΔH (cm)	Flow (mL/s)	TMP (Pa)	Flux ($m^3/m^2.s$)
8.21	4.58	805.401	0.0012
10.31	6.64	1011.411	0.0017
13.77	7.05	1350.837	0.0018
17.97	12.71	1762.857	0.0033
21.37	13.94	2096.397	0.0037
28.47	9.15	2792.907	0.0024
5.45	1.69	534.645	0.0004

Table 0-20. TMP and flux for 350 mL (4060 mg) of sludge R2

ΔH (cm)	Flow (mL/s)	TMP (Pa)	Flux ($m^3/m^2.s$)
8.77	1.92	860.337	0.0005
15.97	3.89	1566.657	0.0010
23.57	5.59	2312.217	0.0014
25.84	5.29	2534.904	0.0014
6.57	2.01	644.517	0.0005
11.33	3.68	1111.473	0.0009
19.97	2.27	1959.057	0.0006

Table 0-21. TMP and flux for 450 mL (5160 mg) of sludge R2

ΔH (cm)	Flow (mL/s)	TMP (Pa)	Flux ($m^3/m^2.s$)
5.31	0.29	520.911	7.7E-05
6.31	0.29	619.011	7.70E-05
7.01	0.37	687.681	9.9E-05
8.47	0.42	830.907	0.0001
10.67	0.89	1046.727	0.0002
12.37	0.97	1213.497	0.0002
15	1.73	1471.500	0.0004

18.57	2.30	1821.717	0.0006

Table 0-22. TMP and flux for 500 mL (5960 mg) of sludge R2

ΔH (cm)	Flow (mL/s)	TMP (Pa)	Flux ($m^3/m^2.s$)
6.01	0.42	589.581	0.0001
7.21	0.36	707.301	9.7E-05
8.87	0.52	870.147	0.0001
10.37	0.65	1017.297	0.0002
13.57	0.98	1331.217	0.0002
15.37	1.02	1507.797	0.0002
19.97	1.31	1959.057	0.0003

7-5. Appendix V- TMP vs flux records of floccular sludge(R2), not promising results

The below results were considered poor since theR^2 was either close to zero or negative. These tests were conducted April 14th 2016.

Table 0-23. TMP and flux for measuring membrane intrinsic resistance

ΔH (cm)	Flow (ml/s)	TMP (Pa)	Flux ($m^3/m^2.s$)
6.5	54.85	637.65	0.014
12	100	1177.2	0.026
17.5	127.06	1716.75	0.033
4.5	30.14	441.45	0.008

Table 0-24. TMP and flux for 50 mL (174 mg) of sludge R2

ΔH (cm)	Flow(ml/s)	TMP (Pa)	Flux ($m^3/m^2.s$)
40	5.16	3924	0.0010
42	3.66	4120.200	0.0009
40	3.33	3924	0.0009
22.5	0.76	2207.250	0.0002
34.8	0.53	3413.880	0.0001

39	0.46	3826	0.0001
40	0.30	3924	7.9E-05
39	0.18	3826	4.8E-05

Table 0-25. TMP and flux for 100 ml (348 mg) of sludge R2

water level above the membrane (cm)	Flow (mL/s)	Pressure gauge (mbar)	TMP (kPa)	Flux ($m^3/m^2.s$)
29.5	3.20	320	34.894	0.0008
29.5	3.70	340	36.894	0.0009
29.5	3.17	300	32.894	0.0008
29.5	1.81	280	30.894	0.0004
29.5	2.12	300	32.894	0.0005
29.5	4.50	360	38.894	0.0011

Table 0-26. TMP and flux for 125 mL (425 mg) of sludge, R2

water level above membrane (cm)	Flow (mL/s)	Pressure gauge (mbar)	TMP (kPa)	Flux ($m^3/m^2.s$)
55.5	3	220	27.445	0.0008
55.5	2.60	280	33.445	0.0007
55.5	2.91	300	35.445	0.0007
55.5	3.10	330	38.445	0.0008

7-6. Appendix VI- TMP vs flux records of granular sludge (R3), first trial

Table 0-27. TMP and flux for measuring membrane intrinsic resistance

ΔH (cm)	Flow (mL/s)	TMP (Pa)	Flux ($m^3/m^2.s$)
1.5	41.44	147.150	0.011

12.5	138.73	1226.25	0.036
8	113.05	784.800	0.029
10	132.15	981	0.035
12	143.27	1177.200	0.038
16.5	159.68	1618.650	0.042
14.5	153.04	1422.450	0.040
10	123.10	981	0.032
0.8	6.63	78.480	0.002
0	0	0	0

Table 0-28. TMP and flux for 25 mL (122 mg) of sludge, R3

ΔH (cm)	Flow (mL/s)	TMP (Pa)	Flux (m3/m2.s)
0.4	15	39.240	0.004
0.9	39.81	88.290	0.010
5.5	99.46	539.550	0.026
5.3	95.51	519.930	0.025

Table 0-29. TMP and flux for 250 mL (1220 mg) of sludge, R3

ΔH (cm)	Flow (mL/s)	TMP (Pa)	Flux (m3/m2.s)
37.5	5.33	3678.750	0.0014
37.5	4.67	3678.750	0.0012
31.5	3.87	3090.150	0.0010
28.5	3.19	2795.850	0.0008
24	2.75	2354.400	0.0007
22.5	1.88	2207.250	0.0005

Table 0-30. TMP and flux for 290 mL (1415 mg) of sludge, R3

ΔH (cm)	Flow(mL/s)	TMP (Pa)	Flux ($m^3/m^2.s$)
3	0.53	294.300	0.0001
11.5	1.71	1128.150	0.0004
25	2.21	2452.500	0.0006

26	2.26	2550.600	0.0006
30	2.38	2943	0.0006
33	2.76	3237.300	7.3E-07

Table 0-31. TMP and flux for 450 mL (2200 mg) of sludge, R3

ΔH (cm)	Flow (mL/s)	TMP (Pa)	Flux ($m^3/m^2.s$)
2.5	0.24	245.250	6.2E-05
4	0.50	392.400	0.0001
6.5	0.60	637.650	0.0001
8.5	0.73	833.850	0.0002
13	0.95	1275.300	0.0002
16.5	1	1618.650	0.0002
20.5	1.25	2011.050	0.0003
23.5	1.41	2305.350	0.0004
30	1.50	2943	0.0004
38	1.58	3728	0.0004
38	1.58	3728	0.0004
38	1.34	3728	0.0003

Table 0-32. TMP and flux for 520 mL (2538 mg) of sludge, R3

ΔH (cm)	Flow (mL/s)	TMP (kPa)	Flux ($m^3/m^2.s$)
16	0.31	1.570	8.3E-05
24	0.42	2.354	0.0001
33.4	0.63	3.276	0.0002
38	0.64	3.728	0.0002
38	0.62	3.728	0.0001

Table 0-33. TMP and flux for 600 mL (2928 mg) of sludge, R3

ΔH (cm)	Flow (mL/s)	TMP (Pa)	Flux ($m^3/m^2.s$)
2	90.80	196.200	0.024
2	94.11	196.200	0.024

4	116.80	392.400	0.030
5.5	130	539.550	0.034
13	183	1275.300	0.048
15	200	1471.500	0.052
22.5	274	2207.250	0.072
27.5	300	2697.750	0.079
33	372	3237.300	0.098
36.5	393	3580.650	0.103

Table 0-34. TMP and flux for 700 mL (3416 mg) of sludge, R3

water level above membrane (cm)	**Flow (mL/s)**	**Pressure gauge (mbar)**	**TMP (kPa)**	**Flux ($m^3/m^2.s$)**
28.5	2.68	85	11.296	0.0007
28.5	3.96	130	15.796	0.0010
28.5	4.08	160	18.796	0.0010
28.5	4.53	170	19.796	0.0012
28.5	4.43	180	20.796	0.0012
28.5	4.87	180	20.796	0.0013
28.5	5.19	180	20.796	0.0013
28.5	5.53	200	22.796	0.0014
28.5	5.54	200	22.796	0.0014
28.5	5.31	200	22.796	0.0014
28.5	5.15	220	24.796	0.0013
28.5	5.33	220	24.796	0.0014
28.5	5.45	230	25.796	0.0014
28.5	6.36	260	28.796	0.0016
28.5	5.94	260	28.796	0.0015
28.5	5.90	260	28.796	0.0015

Table 0-35. TMP and flux for 800 mL (3904 mg) of sludge, R3

water level above membrane (cm)	Flow (mL/s)	Pressure gauge (mbar)	TMP (kPa)	Flux ($m^3/m^2.s$)
28.5	2.66	120	14.700	0.0007
28.5	2.19	120	14.796	0.0005
28.5	2.69	160	18.796	0.0007
28.5	2.98	160	18.796	0.0008
28.5	2.96	200	22.796	0.0008
28.5	3.19	220	24.796	0.0008
28.5	3.50	250	27.796	0.0009
28.5	3.49	243	27.096	0.0009
28.5	3.88	260	28.796	0.0010
28.5	4.45	260	28.796	0.0011
28.5	4.25	260	28.796	0.0011
28.5	4.53	280	30.796	0.0012
28.5	4.56	300	32.796	0.0012
28.5	4.76	290	31.796	0.0012
28.5	5.01	300	32.796	0.0013
28.5	4.92	310	33.796	0.0013
28.5	5.07	317	34.496	0.0013
28.5	5.40	300	32.796	0.0014

Table 0-36. TMP and flux for 1000 mL (4880 mg) of sludge, R3

water level above membrane (cm)	Flow (mL/s)	Pressure gauge (mbar)	TMP (kPa)	Flux ($m^3/m^2.s$)
28.5	2.09	75	10.296	0.0005
28.5	2.85	100	12.796	0.0008
28.5	2.59	110	13.796	0.0007
28.5	3.09	140	16.796	0.0008
28.5	3.15	140	16.796	0.0008

28.5	3.44	150	17.796	0.0009
28.5	3.51	160	18.796	0.0009
28.5	3.52	180	20.796	0.0009
28.5	3.75	190	21.796	0.0009
28.5	1.85	210	23.796	0.0005
28.5	3.52	210	23.796	0.0009
28.5	2.92	220	24.796	0.0008
28.5	3.31	230	25.796	0.0009
28.5	3.49	237	26.496	0.0009
28.5	2.62	260	28.796	0.0007
28.5	3.23	250	27.796	0.0009
28.5	2.90	280	30.796	0.0007
28.5	3.24	280	30.796	0.0008
28.5	3.02	320	34.796	0.0008

7-7. Appendix VII- TMP vs flux records of granular sludge (R3), second trial

Table 0-37. TMP and flux for measuring membrane intrinsic resistance

ΔH (cm)	Flow (mL/s)	TMP (Pa)	Flux ($m^3/m^2.s$)
3.77	95.69	369.837	0.0252
6.17	123.59	605.277	0.0325
9.07	143.75	889.767	0.0378
1.57	36.36	154.017	0.0096
2.57	77.20	252.117	0.0203
0	0	0	0

Table 0-38. TMP and flux for 25 mL (73 mg) of sludge, R3

ΔH (cm)	Flow (mL/s)	TMP (Pa)	Flux ($m^3/m^2.s$)
1.87	40.56	183.447	0.0106
5.87	141.30	575.847	0.0372
8.37	148.57	821.097	0.0390
10.27	187.82	1007.487	0.0494

Table 0-39. TMP and flux for 250 mL (730 mg) of sludge, R3

ΔH (cm)	Flow (mL/s)	TMP (Pa)	Flux ($m^3/m^2.s$)
15.37	152.54	1507.797	0.0401
30.57	189.66	2998.917	0.0499
20.87	189.04	2047.347	0.0497
3.97	35.18	389.457	0.0092

Table 0-40. TMP and flux for 350 mL (1022 mg) of sludge, R3

ΔH (cm)	Flow (mL/s)	TMP (Pa)	Flux ($m^3/m^2.s$)
22.47	140.25	2204.307	0.0369
20.47	123	2008.107	0.0323
18.50	101.42	1814.850	0.0267
5.82	38.61	570.942	0.0101
11.37	78.02	1115.397	0.0205

Table 0-41. TMP and flux for 450 mL (1314 mg) of sludge, R3

ΔH (cm)	Flow (mL/s)	TMP (Pa)	Flux ($m^3/m^2.s$)
3.62	17.55	355.122	0.0046
11.19	59.28	1097.739	0.0156
22.19	94.83	2176.839	0.0250
26.57	96.41	2606.517	0.0253

Table 0-42. TMP and flux for 550 mL (1606 mg) of sludge, R3

ΔH (cm)	Flow (mL/s)	TMP (kPa)	Flux ($m^3/m^2.s$)
19.22	53.70	1.885	0.0141
21.92	56.29	2.150	0.0148
24.42	62.44	2.395	0.0164
12.72	41.28	1.247	0.0108
16	43.21	1.569	0.0113

Table 0-43. TMP and flux for 650 mL (1900 mg) of sludge, R3

ΔH (cm)	Flow (mL/s)	TMP (kPa)	Flux ($m^3/m^2.s$)
13.52	14.37	1.326	0.0038
40.62	49.02	3.984	0.0129
42.62	51.72	4.181	0.0136
26.57	33.77	2.606	0.0088

7-8. Appendix Ⅷ Dynamic membrane development for supernatant from R2

To develop a dynamic membrane several tests were performed on the supernatant from the reactors. All the results are presented below.

Table 0-44. TMP and flux for measuring membrane intrinsic resistance

ΔH (cm)	Flow (mL/s)	TMP (Pa)	Flux ($m^3/m^2.s$)
0	0	0	0
1.37	20.67	134.397	0.0054
2.37	61.80	232.497	0.0162
9.87	97.56	968.247	0.0257
2.17	50.45	212.877	0.0132
4.87	74.96	477.747	0.0197
14.37	185.47	1409.697	0.0488

Table 0-45. Filtration of supernatant from R2, first trial May 20th

Duration (h)	Flow (mL/s)	ΔH water (cm)	Turbidity (Fau)	TMP (Pa)	Flux ($m^3/m^2.s$)	TSS (mg/L)
0.066	1.29	2.02	10	198.162	0.0003	48
0.167	1.21	2.04	17	200.124	0.0003	43.3
0.33	1.07	4.82	20	472.842	0.0003	40
0.5	1.04	6.70	20	657.270	0.0002	36.6
0.74	1.01	11	20	1079.100	0.0002	32
0.85	0.96	16	23	1569.600	0.0002	26.6
1	0.97	20.50	22	2011.050	0.0002	50
1.21	0.81	24.30	25	2383.830	0.0002	63.3

1.4	0.70	29.30	22	2874.330	0.0001	50
1.65	0.73	33.30	21	3266.730	0.0002	50
1.77	0.72	35	21	3433.500	0.0002	N.A.

Table 0-46. Experiment's specifications, first trial May 20th

Inlet TSS (mg/L)	Turbidity (Fau)	Total volume of filtered (L)	Max flux (LMH)	Min flux (LMH)	Average turbidity removal	Total duration (min)
86.6	30	6	1226	664	33%	107

Table 0-47. Filtration of supernatant from R2, second trial May 24th

Duration (h)	Flow (mL/s)	ΔH water (cm)	Turbidity (Fau)	TMP(kPa)	Flux ($m^3/m^2.s$)	TSS (mg/L)
0.03	1.34	5.55	14	0.544	0.0004	40
0.25	1.35	6.05	16	0.593	0.0004	53.3
0.5	1.26	7.05	17	0.691	0.0003	36.6
0.75	1.14	8.82	15	0.865	0.0003	46.6
0.87	1.01	9.72	12	0.953	0.0003	50
1.25	0.59	13.52	20	1.326	0.0002	negative value
1.48	0.19	20.52	18	2.013	5.2E-05	40
1.77	0.10	28.02	20	2.748	2.7E-05	negative value
2.33	0.10	41.32	12	4.053	2.8E-05	40

Table 0-48. Experiment's specifications, second trial May 24th

Inlet TSS (mg/L)	Turbidity (Fau)	Total volume of filtered (L)	Max flux (LMH)	Min flux (LMH)	Average turbidity removal	Total duration (min)
216.6	84	11	1280	97.523	81%	153

Table 0-49. Filtration of supernatant from R2, third trial May 30th

Duration (h)	Flow (mL/s)	ΔH water (cm)	Turbidity (Fau)	TMP(kPa)	Flux ($m^3/m^2.s$)	TSS (mg/L)

0.03	4.81	5.02	9	0.492	0.0012	26.67
0.36	3.80	7.82	7	0.767	0.0010	53.3
0.53	2.41	10.72	12	1.051	0.0006	32
0.72	1.67	15.42	13	1.512	0.0004	35
0.87	1.43	19.82	12	1.944	0.0003	32
1	1.34	24.32	13	2.385	0.0003	37.7
1.28	1.33	29.32	12	2.876	0.0003	33.3
1.55	1.17	33.32	13	3.268	0.0003	34
2.16	1.18	38.32	13	3.759	0.0003	34
2.66	1.09	40	13	3.924	0.0003	34
3	1.13	40.82	17	6.754	0.0003	42.2
3.13	1.03	40.82	18	6.754	0.0003	51.1
3.25	1.11	40.82	19	6.754	0.0003	40

The experiment's specifications for this trial (May 30th) was presented in the section 4b.2.1.

7-9. Appendix IX- Dynamic membrane development for supernatant from R3

Table 0-50. Filtration of supernatant from R3, first trial, May 11th

Duration (h)	**Flow (mL/s)**	**ΔH water (cm)**	**Turbidity (Fau)**	**TMP (kPa)**	**Flux ($m^3/m^2.s$)**
0.16	1.12	27	1	2.648	0.0003
0.25	1.17	27	0	2.648	0.0003
0.28	1.28	27	3	2.648	0.0003
0.35	1.18	27	2	2.648	0.0003
0.36	1.19	27	1	2.648	0.0003
0.45	1.17	27	0	2.648	0.0003
0.55	1.09	27	1	2.648	0.0003
0.73	1.27	27	2	2.648	0.0003
0.91	1.28	27	3	2.648	0.0003
1	1.20	27	1	2.648	0.0003
1.11	1.13	27	0	2.648	0.0003

1.25	1.11	27	0	2.648	0.0003
1.50	1.11	27	0	2.648	0.0003
1.66	1.09	27	0	2.648	0.0003
1.83	1.19	27	0	2.648	0.0003

Table 0-51. Experiment's specifications, first trial, May 11th

Inlet TSS (mg/L)	Turbidity (Fau)	Total volume of filtered (L)	Max flux (LMH)	Min flux (LMH)	Average turbidity removal	Total duration (min)
125	37	8.23	1218	1031	98%	110

Table 0-52. Filtration of supernatant from R3, second trial, May 13th

Duration (h)	Flow (mL/s)	ΔH water (cm)	Turbidity (Fau)	TMP (Pa)	Flux ($m^3/m^2.s$)
0.16	2.22	1	8	98.100	0.0006
0.20	1.93	1	4	98.100	0.0005
0.36	1.58	1	4	98.100	0.0004
0.43	1.61	1	4	98.100	0.0004
0.55	1.61	1	7	98.100	0.0004
0.78	1.54	1	9	98.100	0.0004
1	1.66	1.20	2	117.720	0.0004
1.25	1.58	1.50	2	147.150	0.0004
1.50	1.60	1.50	3	147.150	0.0004
1.65	1.66	1.50	1	147.150	0.0004
1.80	1.51	1.50	1	147.150	0.0004
1.95	1.58	1.50	2	147.150	0.0004
2	1.55	1.50	1	147.150	0.0004
2.28	1.57	1.50	2	147.150	0.0004
2.43	1.43	1.80	2	176.580	0.0003
2.55	1.48	1.80	1	176.580	0.0004
2.68	1.46	2	3	196.200	0.0004
2.80	1.65	2.30	0	225.630	0.0004

Table 0-53. Experiment's specifications, second trial, May 13th

Inlet TSS (mg/L)	Turbidity (Fau)	Total volume of filtered (L)	Max flux (LMH)	Min flux (LMH)	Average turbidity removal	Total duration (min)
45	18	13	2105	975	93%	168

Table 0-54. Filtration of supernatant from R3, third trial, May 17th

Duration (h)	Flow (mL/s)	ΔH water (cm)	Turbidity (Fau)	TMP (Pa)	Flux ($m^3/m^2.s$)
0.20	1.80	1	1	98.100	0.0004
0.32	2.01	1	4	98.100	0.0005
0.39	1.83	1	4	98.100	0.0005
0.50	1.96	1.20	5	117.720	0.0005
0.80	1.80	1.80	4	176.580	0.0005
1	1.78	1.80	3	176.580	0.0004
1.10	2.02	1.80	2	176.580	0.0005
1.20	1.72	1.80	4	176.580	0.0004
1.55	1.62	2.80	1	274.680	0.0004
1.71	1.81	2.80	1	274.680	0.0005
2	1.57	2.80	2	274.680	0.0004
2.18	1.51	2.80	3	274.680	0.0004
2.42	1.58	3.30	1	323.730	0.0004
2.70	1.79	4.30	3	421.830	0.0005
2.95	1.79	4.70	2	461.070	0.0005
3.10	1.61	5	0	490.500	0.0004
3.30	1.37	5.30	1	519.930	0.0004
3.45	1.40	5.30	0	519.930	0.0004
3.95	1.46	5.50	2	539.550	0.0004
4.10	1.34	5.90	1	578.790	0.0004
4.45	1.29	5.90	1	578.790	0.0003
4.80	1.28	5.90	3	578.790	0.0003
4.95	1.24	6.55	3	642.555	0.0003

5.10	1.38	7.55	3	740.655	0.0004
5.20	1.33	8.45	3	828.945	0.0004

Table 0-55. Experiment's specifications, third trial, May 17th

Inlet TSS (mg/L)	Turbidity (Fau)	Total volume of filtered (L)	Max flux (LMH)	Min flux (LMH)	Average turbidity removal	Total duration (min)
50	23	25	1913	1178	91%	312

The forth run was performed on June 3rd. prior to running the experiment, membrane was replaced with the new one. And the membrane intrinsic resistance was measured again. In the following tables the obtained results and experiment's specification are reported.

Table 0-56. TMP and flux for measuring membrane intrinsic resistance, fourth trial, June 3rd

ΔH (cm)	Flow (mL/s)	TMP (kPa)	Flux ($m^3/m^2.s$)
0	0	0	0
4.07	88.46	0.399	0.0232
9.87	126.10	0.968	0.0332
1.27	48.26	0.124	0.0127
5.97	100	0.585	0.0263
9.17	125.30	0.899	0.0330

Table 0-57. Filtration of supernatant from R3, fourth trial, June 3rd

Duration (h)	Flow (mL/s)	ΔH water (cm)	Turbidity (Fau)	TMP(kPa)	Flux ($m^3/m^2.s$)
0.21	1.42	2.15	5	0.210	0.0004
0.36	1.40	2.24	6	0.219	0.0004
0.53	1.38	2.37	5	0.232	0.0004
0.70	1.34	3.08	6	0.302	0.0004
0.86	1.41	3.65	3	0.358	0.0004

2.63	1.31	8.85	4	0.868	0.0003
3.13	1.12	10.35	4	1.015	0.0003
3.61	0.92	17.35	3	1.702	0.0002
3.95	0.75	20.73	3	2.033	0.0002
4.30	0.53	21.45	5	2.104	0.0001
4.55	0.40	30.65	5	3.006	0.0001
4.95	0.27	36	4	3.531	7.2E-05
5.71	0.13	40.23	3	3.946	3.4E-05
6.01	0.11	40.64	3	3.986	2.8E-05

Table 0-58. Experiment's specifications, fourth trial, June 3rd

Inlet TSS (mg/L)	**Turbidity (Fau)**	**Total volume of filtered (L)**	**Max flux (LMH)**	**Min flux (LMH)**	**Average turbidity removal**	**Total duration (min)**
N.A	36	14	1345	104	88%	380

Table 0-59. Filtration of supernatant from R3, fifth trial, June 7th

Duration (h)	**Flow (mL/s)**	**ΔH water (cm)**	**Turbidity (Fau)**	**TMP (kPa)**	**T.S.S (mg/L)**	**TOC (mg/L)**	**Flux ($m^3/m^2.s$)**
0.21	8.04	3.45	9	0.338	10.9	3.29	0.0021
0.36	7.47	5.45	11	0.534	29	3.97	0.0019
0.70	6.57	8.45	10	0.828	16.36	4.70	0.0017
0.86	6.21	12.05	11	1.182	14.55	N.A.	0.0016
2.30	5.04	18.35	8	1.800	14.54	3.90	0.0013
2.63	4.95	20.85	5	2.045	10.9	4.34	0.0013
3.13	4.25	24.35	6	2.388	16.36	4.59	0.0011
3.61	3.49	32.35	4	3.173	0	3.87	0.0009
3.95	2.84	40.85	4	4.007	18	3.27	0.0007
4.30	2.04	40.85	5	4.007	20	3.30	0.0005
4.55	1.52	40.85	7	4.007	30.90	3.55	0.0004
4.95	1.03	40.85	4	4.007	21.80	3.23	0.0002

5.71	0.40	40.85	5	4.007	8.80	4.40	0.0001
6.01	0.35	40.85	4	4.007	0	3.59	9.2E-05
6.25	0.30	40.85	3	4.007	20	4.86	7.8E-05

Table 0-60. Experiment's specifications, fifth trial, June 7th

Inlet TSS (mg/L)	**Inlet TOC (mg/L)**	**Turbidity (Fau)**	**Total volume of filtered (L)**	**Max flux (LMH)**	**Min flux (LMH)**	**Average turbidity removal**	**Average TOC removal**	**Total duration (min)**
198.18	17.83	83	16	7621	281.2	92%	77.5%	380